UNIVERSITÀ DEGLI STUDI DI MILANO

Graduate School of Animal Health and Production:
Science, Technology and Biotechnologies

Department of Veterinary Science and Public Health (DIVET)

PhD Course in Biotechnologies Applied to Veterinary and
Animal Husbandry Sciences
(Cycle XXV)

Doctoral Thesis

Analysis of microRNAs and genic polymorphisms in the diagnosis of neoplastic and transmissible diseases in dogs

(Vet/06)

Dr. Francesca ALBONICO
Nr. R08625

Tutor: Dr. Michele MORTARINO

Coordinator: Prof. Fulvio GANDOLFI

Academic Year 2011-2012

SUMMARY

ABBREVIATIONS

ABC: activated B-cell like;

AGO: argonaute protein;

ALL: acute lymphoblastic leukemia;

AML: acute myeloid leukemia;

APC: antigen-presenting cell;

APL: acute promyelocytic leukemia;

ATP: adenosine triphosphate;

CCND1: cyclin D1;

CLL: chronic lymphocytic leukemia;

CLP: common lymphoid progenitor;

CML: chronic myeloid leukemia;

CMP: common myeloid progenitor;

CT: threshold cycle;

DLBCL: diffuse large B-cell lymphoma;

DNA: Deoxyribonucleic acid;

dsDNA: DNA double-stranded;

dsRNA: RNA double-stranded;

eIF: eukaryotic initiation factor;

ErP: erythroid progenitor;

Exp-5: exportin 5;

GFP: green fluorescent protein;

GMP: granulocyte-macrophage progenitor;

GTP: guanosine triphosphate;

HL: Hodgkin lymphoma;

hnRNPs: Heterogeneous nuclear ribonucleoproteins;

HOX: Homeobox;

HRM: high resolution melting;

IRES: Internal robosome entry site;

LT-HSC: long-term hematopoietic stem cell;

MCL: mantle cell lymphoma;

MEP: megakaryocyte-erythroid progenitor;

MHC: major histocompatibility complex;

miRBase: microRNA database;

miRNA: microRNA;

miRNP: microRNA ribonucleoprotein complex;

MkP: megakaryocyte progenitor;

MM: multiple myeloma;

MP: multipotent progenitors;

MRE: microRNA recognition element;

mRNA: Messenger RNA;

NHL: non hodgkin's lymphoma;

NK: natural killer;

OG: oncogenes;

ORF: Open reading frame;

PAZ: Piwi-argonaute-zwille;

PCR: Polymerase Chain Reaction;

qRT-PCR : Quantitative reverse transcriptase PCR;

RISC: RNA-Induced Silencing Complex;

RBC: red blood cells;

RNA: Ribonucleic acid;

RNAi: RNA interference;

RNAse: Ribonuclease;

rRNA: Ribosomal ribonucleic acid;

RT: retrotranscription;

siRNA: Short interfering RNA;

STHSC: short-term hematopoietic stem cell;

TCl-1: S-cell leukemia／lymphoma 1;

TSG: tumor suppressor gene;

UTR: UnTraslated Region;

VBA: Visual basic application

Chapter 1:

Analysis of microRNAs in canine hematopoietic malignancies for diagnostic purposes

1.1 AIM OF THE WORK

MicroRNAs (miRNAs) are a new class of small non-coding RNAs involved in the negative regulation of gene expression. In humans, it has been shown that miRNAs play a key role in the modulation of the innate immune response and in the regulation of normal and neoplastic hematopoiesis. The expression profile of these molecules varies in the different stages of differentiation of the hematopoietic system cellular components and any alteration of these processes is directly associated with dysregulation of one or more miRNAs. At this regard, in human medicine, the miRNA expression profiles are used for the classification of hematopoietic tumors, and other types of cancer, for diagnostic and prognostic purposes. The frequency and nature of some of these tumors are similar in dogs and humans. In dog, the studies of hemato-oncology performed to date have shown that the currently used methodologies are not always able to obtain comprehensive information about the staging, grading, immunophenotyping and prognosis. This makes miRNAs very attractive as new potential diagnostic and prognostic markers allowing better subclassification of these tumors in dogs. It should be considered that dogs are affected by spontaneous hematopoietic and immunological disorders resembling those affecting humans. This opens the possibility that some evolutionarily conserved miRNAs may play a role in the pathogenesis of, for example, canine lymphomas and leukemias, as reported in humans.

The purpose of the study undertaken in this project was to examine, using real time RT-PCR, the expression profile of a panel of miRNAs in some hematological malignancies of the dog, such as chronic lymphocytic leukemia (CLL), lymph node lymphoma and splenic lymphoma, in relation to their non cancer tissues. Panels of miRNAs, already known in humans because of their importance in hematopoietic malignancies, have been selected for investigation, according to the information available in the literature and databases, and to their level of conservation in the canine genome. As a preliminary step, for each studied

canine neoplasia, an accurate validation of suitable candidate endogenous control genes for normalization of miRNA expression levels in normal and neoplastic lymphoid tissues was made. This was performed by means of real time RT-PCR followed by statistical analysis using the algorithms NormFinder and geNorm. The results of this study confirm that in dogs, as already shown in humans, there is differential expression of some miRNAs in various hematologic malignancies, suggesting the potential utility of miRNA monitoring as a new diagnostic strategy in canine hematopoietic malignancies. At this regard, it should be underlined that in dogs is often difficult to obtain a sufficient number of fresh clinical samples to perform large diagnostic studies. From here the need arises to carry out studies of retrospective nature based on appropriately validated methods of analysis that make possible to analyze archival samples, such as paraffin-embedded tissues or cytological smears on glass slides. With regard to miRNAs, analysis procedures of cytological smears are not currently available in the literature, and only a little number of studies using tissue samples fixed in formalin and embedded in paraffine have been published, with no reference to canine tumours. Therefore, one of the goals of this study was to develop a methodology for extraction and analysis of miRNAs from smears of aspirated lymph node (for the study of lymph node lymphoma) and peripheral blood (for the study of CLL) and from tissue sections fixed in formalin and included in paraffin (for the study of splenic lymphoma). The results obtained during this study confirm the possibility to analyze miRNAs for retrospective studies starting from such archival samples, as the data obtained from these samples are comparable to those obtained from fresh samples. This reinforces the potential utility of miRNA monitoring in the diagnosis of canine hematopoietic malignancies.

1.2 INTRODUCTION

1.2.1 microRNAs

MicroRNAs (miRNAs) are a class of short (approximately 21-22 nucleotides) noncoding RNAs that are involved in gene expression negative regulation through sequence-specific base pairing to target mRNAs, usually in their 3'-UTR part, resulting in translational repression or mRNA degradation and gene silencing (Bartel D.P. 2004). Each miRNA can control hundreds of gene targets, and different miRNAs can regulate the same target mRNA. Most miRNAs are widely expressed in several tissues and organs, whereas a limited number are restricted to certain cell types reflecting the diversity in cellular phenotypes and as such suggest a role in tissue differentiation and maintenance. Due to their abundant presence and far-reaching potential, miRNAs have been reported to be involved in a variety of functions, including developmental transitions, neuronal patterning, apoptosis, adipogenesis metabolism and hematopoiesis in different organisms (Singh S.K. et al 2008).

1.2.2 miRNAs: history

MiRNAs were first discovered in 1993 by Victor Ambros, Rosalind Lee and Rhonda Feinbaum during a study regarding the nematode *Caenorhabditis elegans* (*C. elegans*) development (Lee R.C. and Ambros V., 1993). This study discovered that the *lin-14* gene was able to be regulated by a short RNA product from *lin-4* gene. Indeed, *lin-4* gene encoded for a 61 nucleotide precursor RNA that accrued to a 22 nucleotide mature RNA, containing sequences partially complementary to multiple sequences in the 3' UTR of the lin-14 mRNA. This complementarity was sufficient and necessary to inhibit the translation of lin-14 mRNA. Retrospectively, this was the first miRNA identified, even though Ambros et al. speculated that it was a nematode idiosyncrasy. Later, in XXI Century, when

let-7 (phylogenetically conserved beyond nematodes) was discovered to be able to repress *lin-41*, *lin-14*, *lin28*, *lin42* and *daf12* mRNA during the developmental stages of *C. elegans*, became apparent that the short non-coding RNA identified in 1993 was part of a wider phenomenon (Singh S.K. et al, 2008; Reinhart B.J. et al 2000; Pasquinelli A.E. et al 2000). Since then, over 4000 miRNAs have been discovered in all studied eukaryotes including mammals, fungi and plants.

1.2.3 miRNAs: biogenesis and mechanism of action

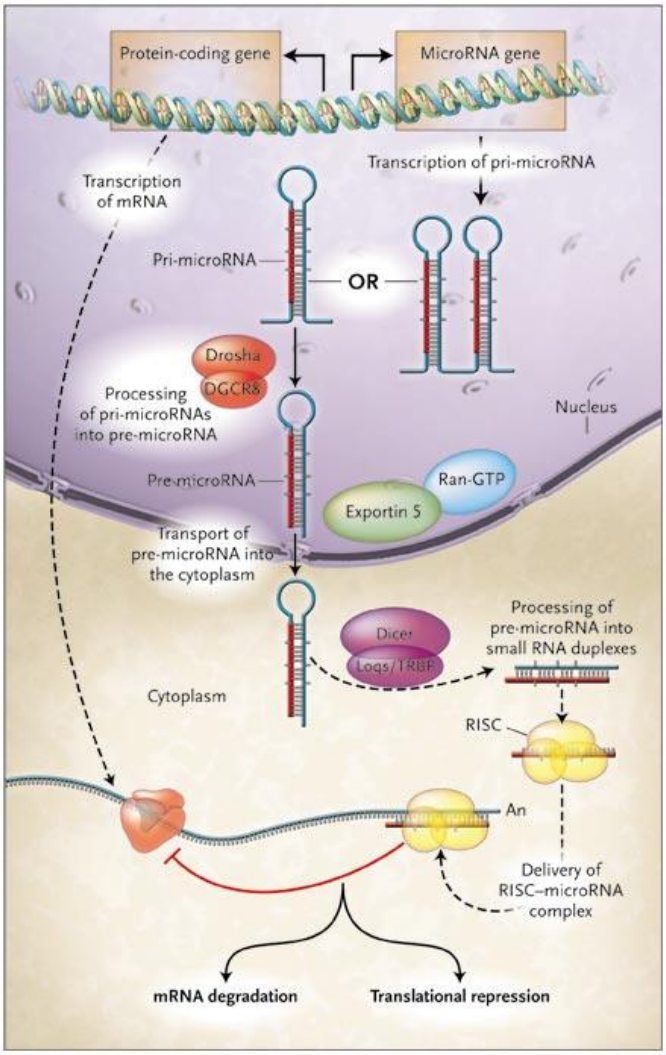

Figure 1. miRNA biogenesys (Chen C.Z. 2005)

miRNA biogenesis includes miRNA transcription in the nucleus, the export of miRNAs from the nucleus to the cytoplasm, and subsequent processing and maturation in the cytoplasm (Figure 1) (Singh S.K. et al, 2008). In many cases, the transcription of miRNA genes is mediated by **RNA polymerase II (Pol II)**, resulting in long **primary miRNA (pri-miRNA)** transcripts, although a cluster of human miRNAs interspersed within Alu elements in Chromosome 19 have recently been shown to utilize RNA Polymerase III for their transcription (Cai X et al, 2004; Erson A. E. et al, 2008; Liu X et al, 2008). Moreover, viral miRNAs transcribed by pol III were identified, raising the possibility that some endogenously encoded miRNAs may utilitize this polymerase (Pfeffer S. et al, 2005).

Many miRNA genes tend to be in close proximity to other miRNAs, and are transcribed as polycistronic transcripts (Lee Y et al, 2002). According to the genomic region that a miRNA resides in, miRNAs can be grouped into several categories: intronic miRNAs in protein-coding genes, exonic miRNAs in non-coding genes and intronic miRNAs in non-coding genes (Rodriguez A et al, 2004; Lee Y et al, 2004; Liu X et al, 2008). As illustrated in Figure 2, pri-miRNAs exist in several configurations. One or more miRNAs may be found within a single pri-miRNA. Many pri-miRNAs are long, unspliced transcripts. Alternatively, pri-miRNAs may be spliced with the miRNA hairpin located in an intron, exon, or the 3' UTR. These spliced host transcripts often encode proteins, although many lack of identifiable coding potential (Rodriguez A et al, 2004).

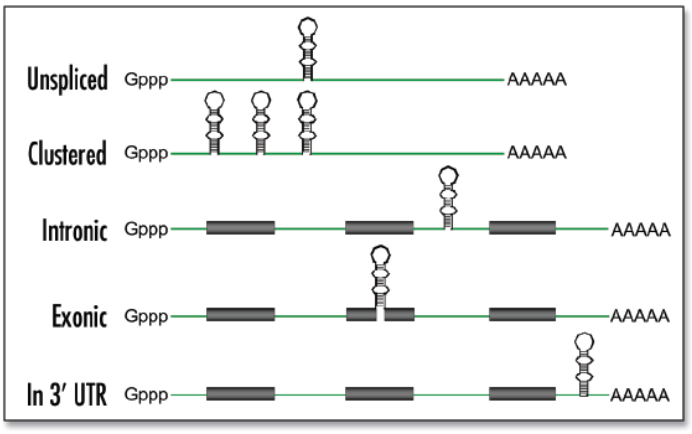

Figure 2. Structures of primary miRNA transcripts (pri-miRNAs)
(Mendell J.T. 2005)

A typical monocistronic pri-miRNA is composed of a doublestranded stem of ~33 base pairs, a terminal loop and two flanking unstructured single-stranded segments (Figure 2) (Lee Y et al, 2002; Liu X et al, 2008). The generation of **precursor miRNA (pre-miRNA)** from the pri-miRNA transcript takes place in the nucleus through the action of the **microprocessor complex**, composed of the RNase III enzyme **Drosha** and the **double-stranded RNA-binding domain (dsRBD)** protein **DiGeorge syndrome critical region gene 8** (**DGCR8**), into 70– 80 nucleotide pre-miRNAs (Figure 1)(Lee Y et al, 2003; Denli A.M et al, 2004; Gregory R.I. et al, 2004; Singh S.K. et al, 2008). This process is known as **cropping**: during this step Drosha liberates the double-stranded stem from the remainder of the pri-miRNA by cleaving proximal and distal of the stem, and thus generates a pre-miRNA that has a 5' monophosphate and a 3'2-nt hydroxyl overhang (Lee Y et al, 2003; Liu X et al, 2008). Cleavage of a pri-miRNA by microprocessor begins with DGCR8 recognizing the ssRNAdsRNA junction typical of a pri-miRNA (Han J. et al, 2004). Drosha is brought close to its substrate through interaction with DGCR8 and cleaves the stem of a pri-miRNA ~11 nt away from the two singlestranded segments (Han J. et al, 2006). The precision of Drosha–DGCR8 cleavage is very important for miRNA maturation. Any shift in the position of the Drosha cut, even by a single nucleotide on the primiRNA, will affect the position of Dicer cleavage. A shift in the Dicer cleavage site could result in different 5'-ends and 3'-ends in the mature miRNA, resulting in different affinity for the mRNA target (Singh S.k. et al, 2008). Although microprocessor is already sufficient for conversion of a pri-miRNA into a pre-miRNAs in vitro, cleavage of pri-miRNA in vivo does not depend on Drosha and DGCR8 only, but also on other accessory proteins, such as the RNA binding protein hnRNP A1 and the p68 and p72 RNA helicases (Liu X et al, 2008). There is evidence that pre-miRNAs can be produced without having to undergo the microprocessor machinery if they are directly spliced from the introns in which they reside (Figure 3) (Okamura et al., 2007; Ruby et al., 2007). These miRNAs are called **mirtrons** and have traditionally been thought to only exist in *Drosphila* and *C. elegans*. However, mammalian

mirtons that even show conservation between species have recently been discovered (Berezikov et al., 2007).

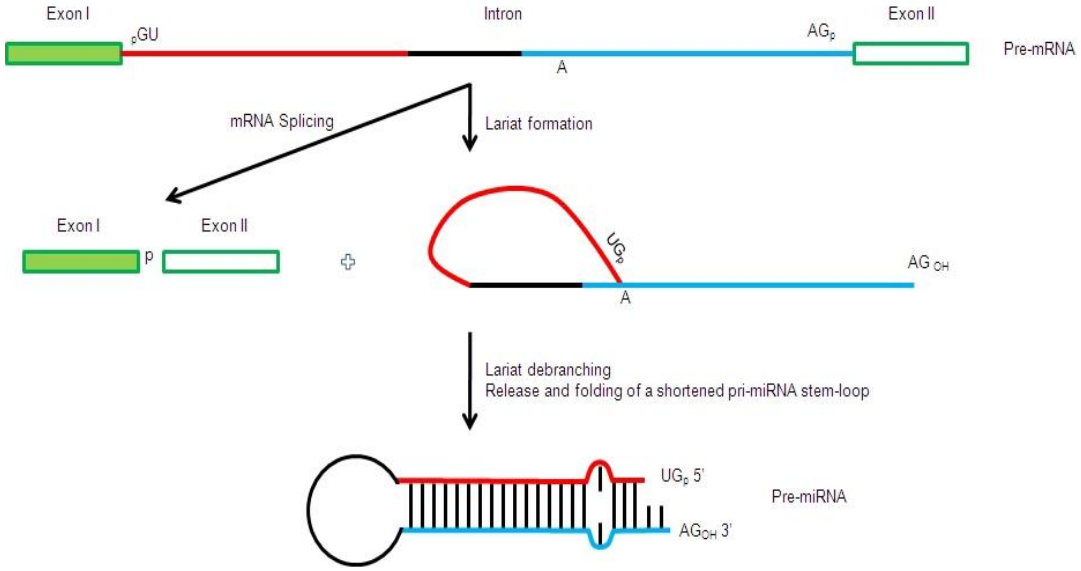

Figure 3. splicing mirtrons (Lages E. et al, 2012)

Pre-miRNAs are exported to the cytoplasm from the nucleus by **exportin-5 (Exp-5)** in the presence of Ran-GTP as a cofactor (Fig. 1) (Lund E et al, 2004; Bohnsack M.T. et al, 2004; Singh S.K. et al, 2008). The nuclear membrane protein exportin 5 recognises the 2 nucleotide overhang on the 3' end of the pre-miRNA (Zeng and Cullen, 2004) and then transports it into the cytoplasm using ran-guanine triphosphatase (Ran-GTP) which is hydrolyzed in Ran-GDP. The role of Exp-5 in nucleocytoplasmic transport was verified by using RNA interference (RNAi). In the event of Exp-5 depletion by RNAi, the level of mature miRNAs goes down but pre-miRNA does not accumulate in the nucleus. The lack of accumulation could be due to instability of pre-miRNA. This suggests the possibility that interaction of pre-miRNA with Exp-5 is required for the stability of pre-miRNA (S.K. et al, 2008).

In the cytoplasm the pre-miRNAs are processed into a short RNA duplex, termed miRNA duplex, by RNase III enzyme **Dicer** (Figures 1 and 4) (Liu X et al, 2008; Singh et al, 2008). Dicer cleavage ends with the release of an imperfect miRNA:miRNA duplex around 20-25 nucleotides in size containing the mature

miRNA strand and its opposite complementary miRNA strand. Both arms of the pre-miRNA stem loop structures are imperfectly paired, containing G:U wobble pairs and single nucleotide insertions. These imperfections cause one strand of the duplex to be less stably paired at its 5'-end (Seitz H and Zamore PD 2006).

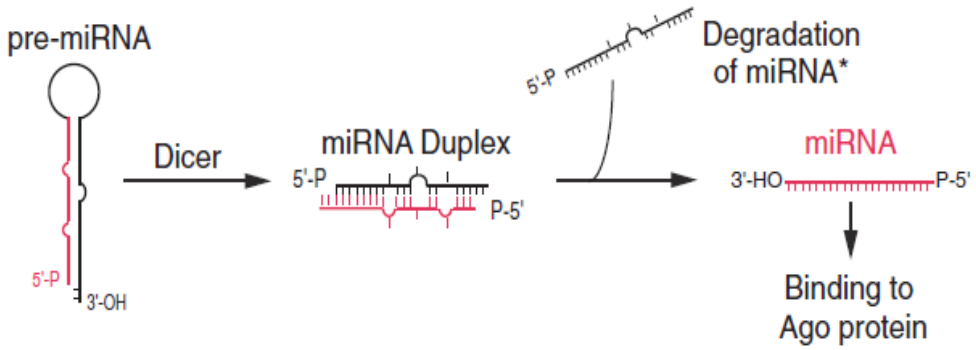

Figure 4. Precursor miRNA (Pre-miRNA) processing (Liu X. et al, 2008)

After processing with Dicer, miRNA duplex interacts with the **RNA Induced Silencing (RISC)** loading apparatus. RISC is an RNA–protein complex that mediates the effect of inhibition of target mRNA by the action of miRNAs. The miRNA duplex loaded into RISC is first carried out to give the mature miRNA single-stranded, which represents the biologically active form; the unwinding of the duplex strands starts at the ends with the lowest thermodynamic stability. The relative stabilities of the base pairs at the 5'-ends of two strands determine the fate of the strand (Schwarz D.S. et al, 2003). In general, the miRNA strand which has its 5'-terminus at the lowest thermodynamic stability, acts as the mature miRNA, **guide strand**, and the other strand, **passenger strand**, is degraded. However, a report has shown that both strands could be coaccumulated as miRNA pairs in some tissues, and subjected to strand selection in other tissues (Ro S. et al 2007). Mature miRNAs are incorporated into the effector complexes, known as miRNP (microRNA ribonucleoprotein), mirgonaute, or **miRISC**, which is composed of Dicer, transactivating response RNA binding protein (TRBP) and protein **Argonaute 2 (Ago 2)** (Figure 1 and 5)(Singh et al, 2008).

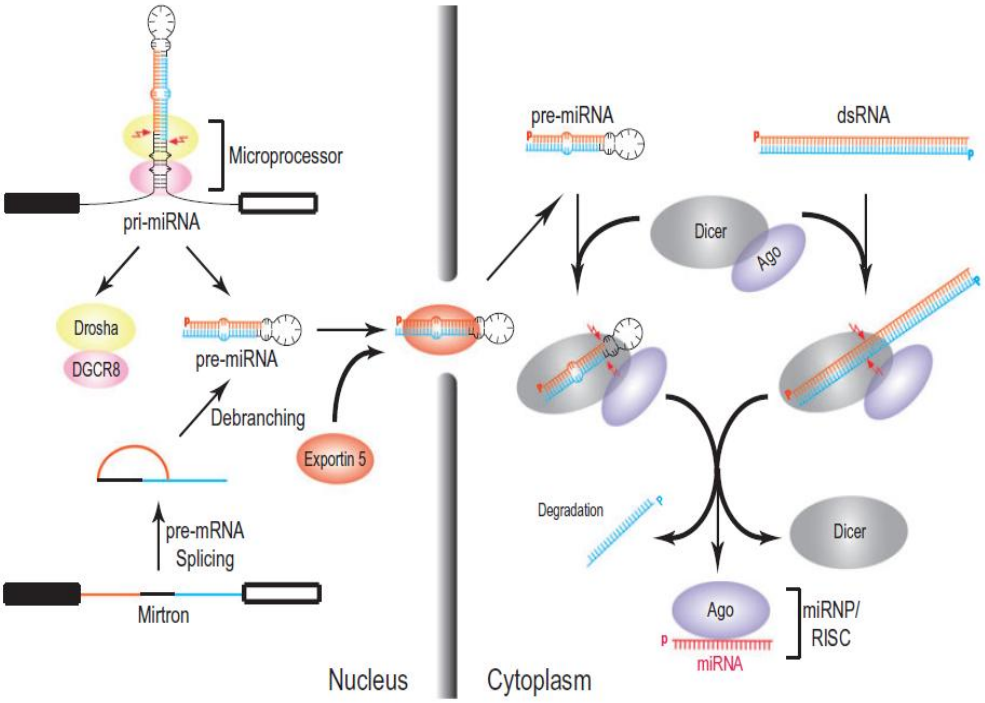

Figure 5. miRNA processing (Liu X. et al, 2008).

The Argonaute family includes different proteins, each containing characteristic domains termed **PAZ** and **PIWI**. The Argonaute family can be phylogenetically divided into two protein families: **Ago** and **Piwi**, depending on similarities to Arabidopsis AGO1 and Drosophila Piwi proteins, respectively (Carmell M.A. et al, 2002). miRNAs bind Ago proteins whereas Piwi proteins bind a newly discovered class of small RNAs known as piwi-interacting RNAs (piRNAs), which are almost exclusively expressed in the germline (Aravin A.A. et al, 2007; Kim V.N. 2006). The miRNA/Ago ribonucleoprotein that is formed represents the core component of the effector complexes that mediate miRNA function and is known as miRNP (Mourelatos Z. et al, 2002). It is important to note that, in 4 mammalian argonaute proteins, only Ago2 has endonucleolytic (also known as slicer) ability and is the only argonaute necessary for RNA silencing, whereas the others are involved in translational repression (Meister et al., 2004).

miRNAs base-pair with **miRNA recognition elements (MREs)** located in their mRNA targets (typically in the 3' untranslated region—3'UTR) and deposit their bound Ago proteins onto mRNA targets. The result is **translational repression** of the targeted mRNA, often followed by mRNA **destibilization or endonucleolytic cleavage** of the targeted mRNA. The exact molecular function is dependent upon how extensive the complementarity of the miRNA is with its mRNA target and which Ago protein is deposited on the mRNA target. If a miRNA, bound to Ago2, pairs with extensive complementarity with a cognate mRNA target, then the mRNA is cleaved at a position across from nucleotides 10 and 11 of the miRNA, while the miRNA remains intact (Figure 6) (Elbashir S.M. et al, 2001; Hutvagner G. and Zamore P.D. 2002; Liu J et al, 2004; Liu X et al, 2008). This cleavage event produces 5'-phosphate and 3'-hydroxyl terminal products, characteristic of other RNase H-like enzymes (Martinez J. and Tuschl T. 2004, Schwarz et al, 2004). The target mRNA is subsequently degraded via routine cellular pathways (Figure 6).

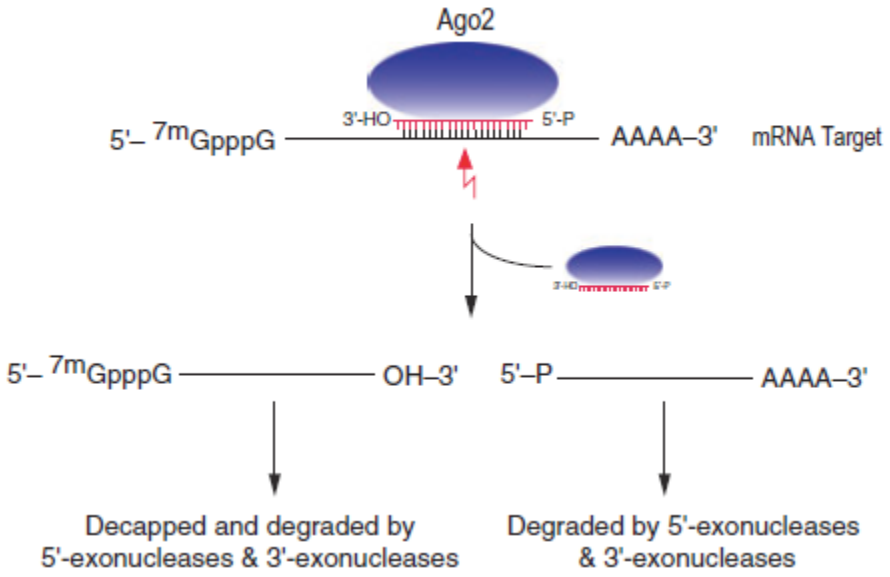

Figure 6. Target RNA cleavage by Ago2-containing miRNP (Liu X et al, 2008).

mRNA target cleavage by miRNAs is the major mechanism of regulation by plant miRNAs (Dugas D.V. and Bartel B. 2004, Llave C et al, 2002). In animals, however, there are very few examples of miRNAs that regulate their mRNA targets by cleavage (Yekta S. et al, 2004); rather, the predominant silencing mode of animal

miRNAs is to repress the translation of their mRNA targets and/or to destabilize them without endonucleolytic cleavage (Figure 7B) (Ambros V. 2004; Filipowicz W. 2005). The vast majority of animal miRNAs base-pair with imperfect complementarity with their mRNA targets. Experimental and bioinformatics approaches have shown that the most important determinant of target RNA recognition by a miRNA is perfect or near-perfect complementarity between the proximal (5') region of the miRNA (nucleotides 2–8) and the mRNA, also known as the "**seed**" **region** or the "nucleus" (Figure 6A) (Doench J.G. and Sharp P.A. 2004; Kiriakidou M. et al, 2004; Lai E.C. 2002; Rajewsky N. and Socci N.D. 2004; Liu X et al, 2008). The miRNAs sharing common seed sequences are grouped into miRNA families. These miRNAs possibly have overlapping targets and are considered to be redundant (Hwang H.W. et al, 2007).

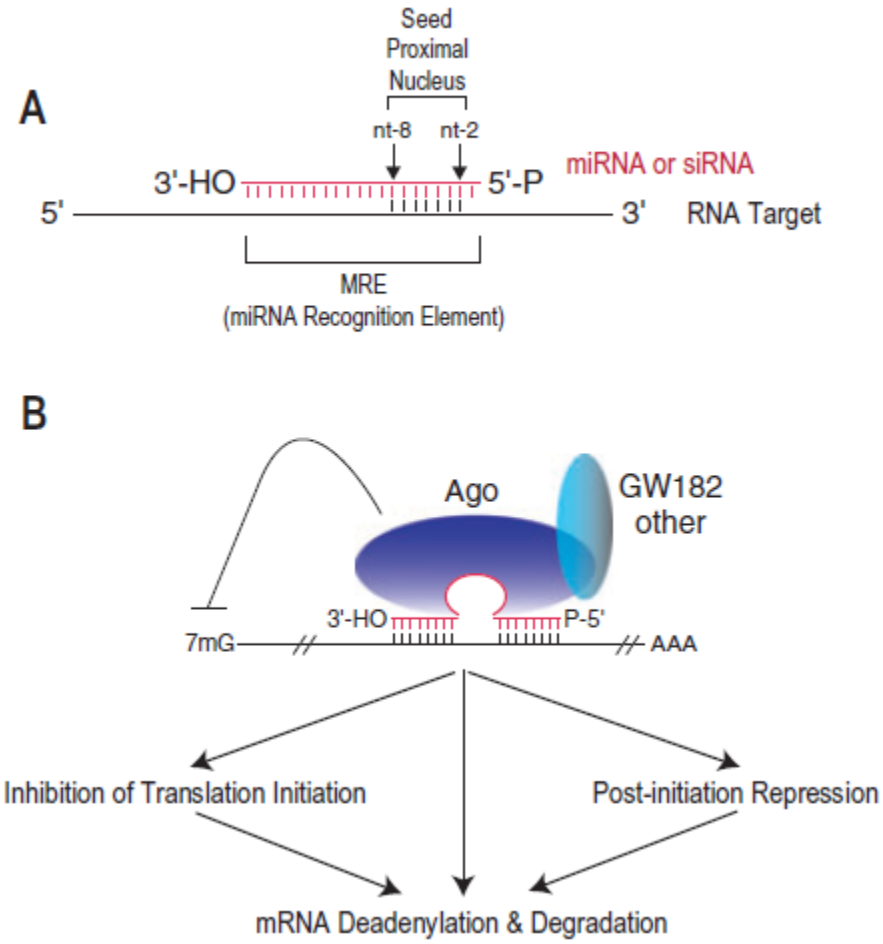

Figure 7. Principles of miRNA binding to target RNA (Liu X et al, 2008).

Recent reports have demonstrated that mRNA subjected to miRNA repression accumulates in **P-bodies** (Teixeira D. et al, 2005). P-bodies have been reported as the sites for decapping and degradation of mRNAs. P-bodies include the Dcp1p ⁄ Dcp2p, activators of decapping, Dhh1p (referred to as RCK in mammals), Pat1p, Lsm1-7p, Edc3p and the 5'–3'-exonuclease Xrn1p. The decapping process exposes the transcript to degradation by the 5' 3'-exonuclease Xrn1p. Alternatively, transcripts can be degraded in the 3' 5' direction following deadenylation in exosomes, by a conserved complex of 3'-to-5'- exonucleases (Singh S.K. et al, 2008). P-bodies contain untranslated mRNAs and can serve as sites of mRNA degradation. This suggests that RISC proteins direct the mRNA to P-bodies, possibly for storage. So, the P-bodies do not just degrade mRNA, but also temporarily sequester them away from the translation machinery (Singh S.K. et al, 2008).

1.2.4 miRNAs: target prediction and validation

To delineate the function of any specific miRNA is necessary the target identification (Mendell J.T. 2005). In plants, target identification is greatly simplified because of the perfect complementarity between miRNAs and their mRNAs target. Instead, in *C. elegans*, *Drosophila* and mammals the target identification is more difficult because miRNAs and their mRNAs target are not perfectly complementary (Ambros V. 2004). Based on the interaction between lin-4 and its mRNA target lin-14 in *C. elegans* (Figure 8), it is generally believed that miRNAs bind one or several partially complementary sites in mRNA target 3' UTR (LeeR.C. et al, 1993), and the region of base-pairing in miRNA 5' end is considered the most critical. Specifically, miRNA nucleotides 2-8 form the "seed" region and many current target prediction algorithms operate a searching for complementarity with this sequence (John B. et al, 2004; Lewis B.P. et al, 2003).

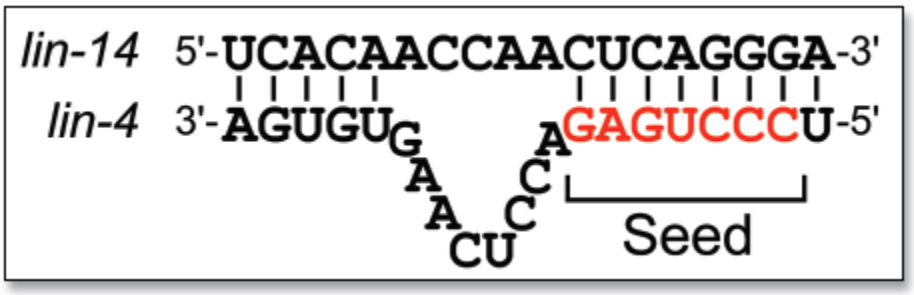

Figure 8. miRNA recognition of target mRNAs (Mendell J.T. 2005)

A recent study identified many putative miRNA targets by searching for seed sequence complementarity that was conserved in several vertebrate genomes. That study predicted that up to 30% of human transcripts are regulated by miRNAs (Lewis B.P. et al, 2005). Additional studies have now demonstrated that base-pairing between the 3' end of a miRNA and a target without a strong seed match can also induce silencing (Brennecke J. et al, 2005). Therefore, the computational prediction of miRNA targets depends on rules that have been built on a small number of known interactions between some miRNAs and their targets, which were then generalized in search of the entire genome.

Starting from three animal miRNAs, lin-4, let-7 and Bantam, with experimentally validated target known, the group of Stark A. et al. screened the entire *Drosophila* genome on the basis of three criteria:

- perfectly complementary, or G-U pairing, between the target 3'-UTR and the first 8 nucleotides of the miRNA
- formation of structurally and thermodynamically favored heteroduplex between miRNA and its putative target,
- evolutionarily conserved miRNA target sites, between *Drosophila melanogaster* and *D. pseudoobscura*

To experimentally validate the potential target, GFP reporter gene was fused upstream the 3'UTR of the predicted target and the expression of GFP in "WING DISC" with and without overexpression of the corresponding miRNA was examined. (Stark A. et al. 2003).

The research group of Burge et al., instead, developed the **TargetScan algorithm** to predict miRNA targets in vertebrates, on the basis of complementarity with the miRNA-target (particularly in 5'-miRNA region) and the evolutionary conservation among vertebrates. 29% of their predicted targets have unknown functions, while 71% have different functions, such as DNA binding, transcriptional regulation, signal transduction and kinase activity. Subsequently, they experimentally validated 11 predicted target, using a HeLa cells line, with luciferase fused to the 3'-UTR of the target predicted, as a reporter system.
Although the prediction success rate in the entire genome is difficult to determine, these studies constitute an important step toward understanding the animals miRNAs function (Lewis B.P. et al, 2005).

While computational prediction of miRNA targets has advanced rapidly, still few mammalian targets have been verified through direct experimentation (Mendell J.T. 2005). These studies are critical not only for understanding miRNA function, but also for refining and improving target prediction algorithms. Two main approaches are utilized to targets validation. The most common method involves the generation of plasmids containing the target mRNA 3' UTR fused to a reporter gene, such as luciferase (Lewis B.P. et al, 2003). Paired constructs are generated with mutations in the miRNA binding sites. When these reporters are expressed in cell lines expressing the miRNA of interest, the mutant construct exhibits enhanced expression since the miRNAs can no longer bind. This method is experimentally tractable and allows direct definition of the miRNA binding sites. However, like all reporter assays, these experiments do not recapitulate the precise context of the miRNA recognition sites nor do they reproduce endogenous expression levels. Thus, these experiments must be interpreted with caution (Mendell J.T. 2005). Another strategy utilizes a recently described method to inhibit the function of miRNAs in cell lines. 2'-O-methyl oligoribonucleotides that are complementary to miRNAs act as sequence-specific competitive inhibitors of miRNA function (Meistell G. et al, 2004; Hutvagner G et al, 2004). Thus, transfection of cells with these antisense reagents allows direct

examination of endogenous target mRNA and protein levels in the presence and absence of functional miRNAs. These studies more reliably demonstrate in vivo regulation of a target by a miRNA, but they do not provide proof that the regulation is direct. Ideally, both reporter assays and analysis of endogenous miRNA function with antisense oligos should be performed to establish a miRNA-target interaction (Mendell J.T. 2005). The development of methodologies that would allow direct demonstration of a miRNA-target mRNA interaction in vivo, perhaps utilizing crosslinking and immunoprecipitation in a manner analogous to chromatin immunoprecipitation, would significantly advance these efforts (Mendell J.T. 2005).

1.2.5 miRNAs database

The **microRNA Registry** was created in 2003 with the purpose of to provide an archive, in an organized and understandable way, of all published miRNA sequences, in order to facilitate the development of the computational approach to predict miRNA genes and targets and to avoid, given the high rate of miRNAs gene discovery, unexpected overlap of identical miRNA denominated in a different way (Griffiths-Jones S. 2004).

The **miRBase database**, dated 2007, comes from an expansion of the miRNA Registry, and encompasses both the nomenclature of genes and sequence data. It has three main functions:

1. miRBase Registry. It provides an independent service of names assignment for new miRNA genes, prior to publication

2. miRBase Sequences. It provides sequence data, annotations, bibliographic references and links to other resources, for all published miRNAs. The database (Version 10.0) contains more than 5000 sequences for 58 species. A number of access for both strands of the precursor and the mature sequence is assigned, in order to be able to trace the origin of the sequence (Griffiths-Jones, S. 2008). Figure 9 shows an example of miRBase Target screen.

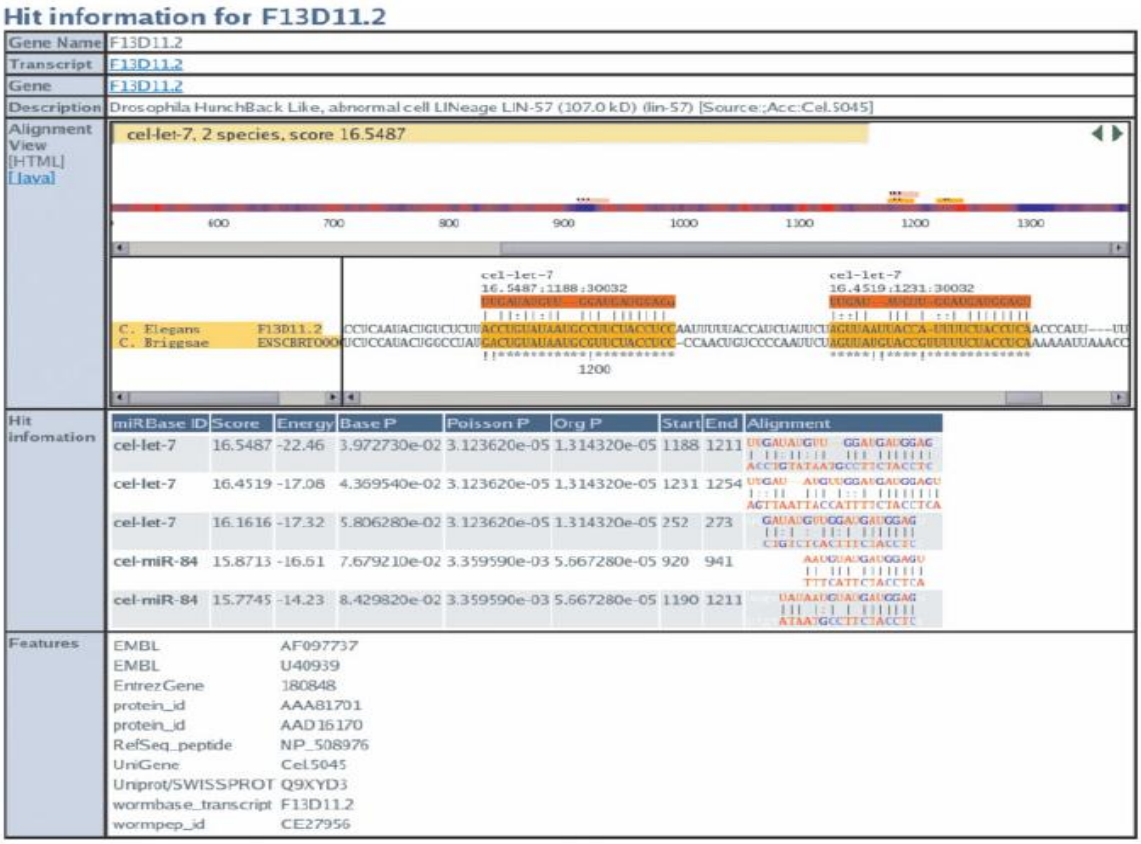

Figure 9. Example of miRBase Target screen (from Griffiths-Jones S., 2006).

3. miRBase Targets. It provides an automated system for predicting the targets of all miRNAs from animals. The current version of the database v5 includes more than 500000 target transcripts for all miRNAs in 24 species using the Miranda algorithm (John B. et al. 2005)

The main objective of the miRBase Registry is to assign unique names to the different miRNAs. For every miRNAs is assigned a numerical identifier based on sequence similarity. Homologues miRNAs in different organisms receive the same name. The name depends on the sequence of the mature miRNA and not on the precursor sequence.

The scheme of the nomenclature is as follows:

1. the name of the miRNA contains three or four letters of the species, as prefix and suffix number. For example, hsa-miR-212

2. mature sequences identical, but originating from different loci in an organism, have the same name with a numerical suffix (mir-6-1 and mir-6-2)

3. to sequences that vary by one or two nucleotides, is given a letter suffix (miR-181a and miR-181b)

4. to genes of miRNAs in plants are given a structured name such as *ath-MIR166a*. the letter as a suffix describes mature miRNA derived from related but different loci

5. the names of the viral miRNAs are conventionally related to the locus from which are derived, such as EBV-mir-BART1 derived from the Epstein Barr virus BART to the locus (Griffiths-Jones, S. 2008).

Figure 10 shows an example of screen miRBase.

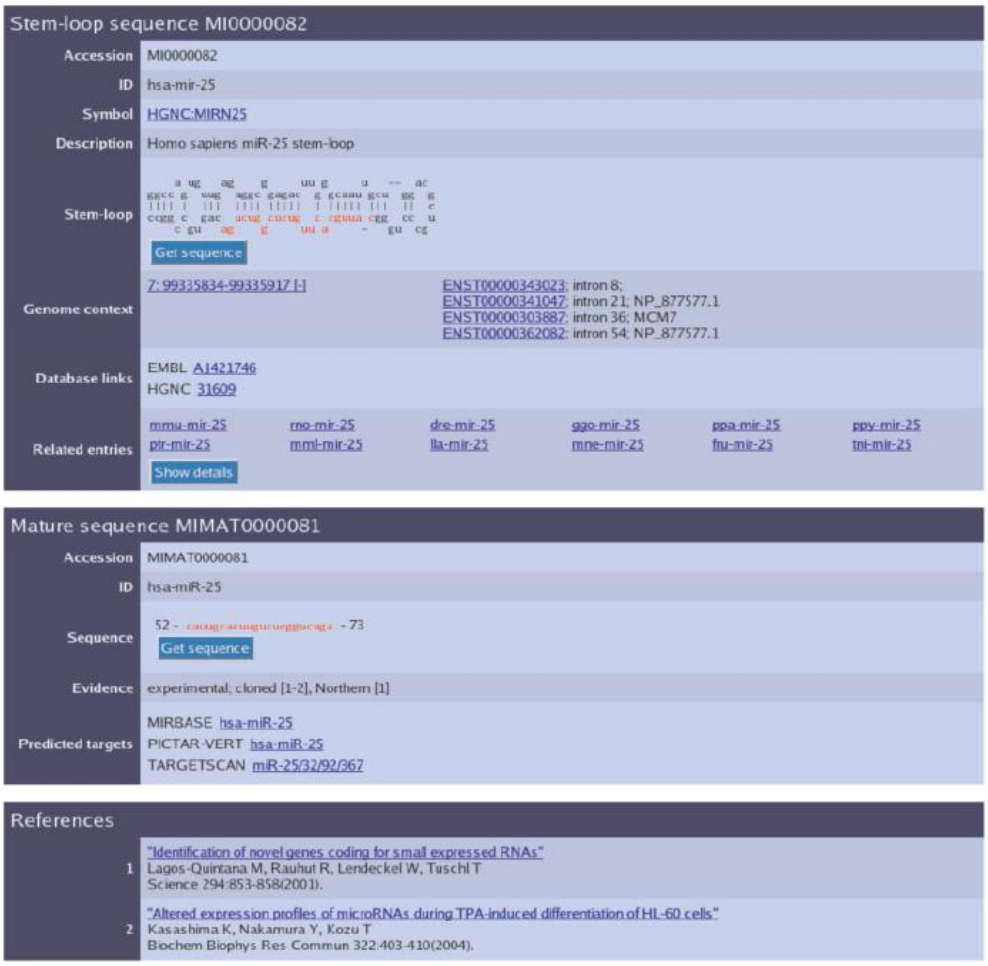

Figure 10. Example of miRBase screen (from Griffiths-Jones S., 2006).

All miRNAs present in the database have been mapped for their coordinates within the genome. The groups of miRNA sequences are highlighted within the genome and can be defined and retrieved in block (Griffiths-Jones, S. 2008). Furthermore, the overlap between miRNAs sequences, transcripts, proteins and noncoding sequences are noted (http://microrna.sanger.ac.uk/).

1.2.6 miRNAs expression studies

miRNAs expression was initially determined using a cloning strategy (Chen C.Z. et al, 2004), while the techniques most commonly applied nowadays are: Northern blotting, quantitative reverse transcriptase-polymerase chain reaction (RT-PCR) or microarray technology. However, these high throughput methods should be used with caution, especially miRNA microarrays, because irreproducible results may be obtained, for instance due to large differences in individual optimal hybridization temperatures of the probes. Quantitative RT-PCR specific for mature miRNAs seems to provide more accurate results and is currently considered the golden standard method (Chen C. et al, 2005; Kluiver J. et al, 2006).

Northern blot analysis is a well-established technique for studying messenger RNA expression and was soon adapted to detect miRNAs in cells or tissues (Lee R.C. et al. 1993; Valoczi A. et al, 2004). Subsequently, conventional **DNA microarray technology** was modified to form miRNA microarrays, allowing the simultaneously detection of multiple miRNAs across various samples (Miska E.A. et al, 2004; Nelson P.T. et al, 2004; Thomson J.M. et al, 2004; Castoldi M. et al, 2006). Lu et al. developed a novel microarray strategy to improve probe specificity, which is critical due to the short nature of mature miRNAs. They performed hybridization in solution using polystyrene capture beads that are coupled to oligonucleotide probes complementary to the miRNAs of interest. The hybrid solutions are then analyzed using a multicolor flow cytometer that measure bead color, denoting miRNA identity, and label intensity, denoting miRNA abundance (Lu J. et al, 2005). In parallel to microarray platforms,

commercial assays for **quantitative reverse transcriptase polymerase chain reaction (RT-PCR)** have become available. These allow the analysis of miRNAs in small tissue samples or even single cells (Tang F. et al, 2006). RT-PCR is currently the choosen technique to quantify the expression profiles of individual miRNAs in a wide variety of cell types and pathological situations. In 2005, the group of Chen et al. has developed a new **TaqMan-based real-time quantification** of miRNAs that includes two steps: stem–loop RT and realtime PCR. Stem–loop RT primers bind to at the 3' portion of miRNA molecules and are reverse transcribed with the reverse transcriptase enzyme. Then, RT product is quantified using conventional TaqMan PCR that includes miRNA-specific forward primer, reverse primer and a dye-labeled TaqMan probes. The purpose of tailed forward primer at 5' is to increase its melting temperature (Tm) depending on the sequence composition of miRNA molecules (Figure 11) (Chen C. et al. 2005).

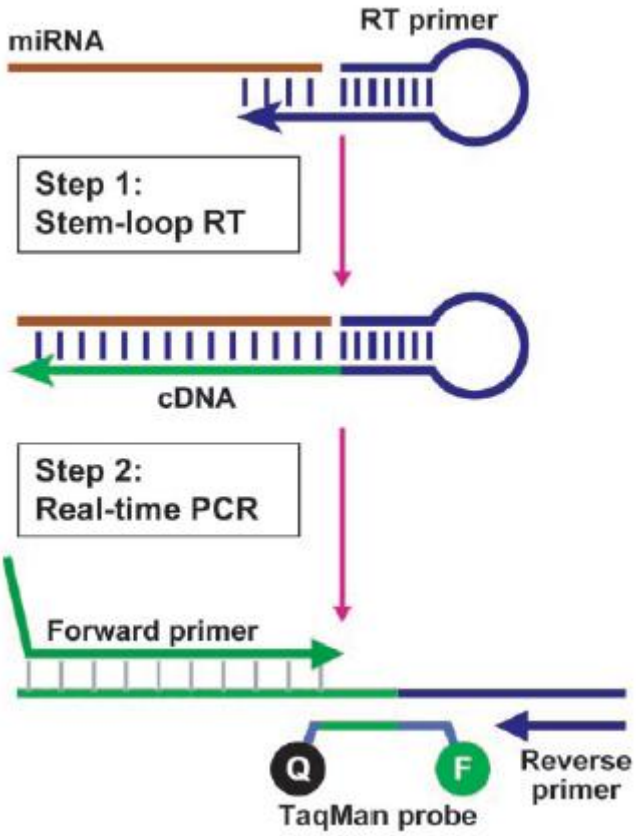

Figure 11. TaqMan-based real-time quantification (Chen C. et al. 2005).

Housekeeping selection for qRT-PCR

The quantitative Real-Time PCR (qRT-PCR) is used to evaluate gene expression, and requires the same type of normalization of traditional methods of mRNA quantifying (Vandesompele J. et al. 2002). In gene expression analysis, there are several variables that must be kept controlled, as the amount of starting material, enzymatic efficiencies and differences between tissues or cells in the activity transcriptional overall. In order to normalize these variables different strategies are used, including controlled conditions for reproducible RNA extraction and standardization of the number of transcribed genes compared to the number of cells contained in the sample, even though an accurate count of the cells is often compromised, for example starting from tissues. Another method of normalization is to use the amount of total RNA. The major problem of this method depends on the fact that most of the RNA is rRNA and therefore it is not always is representative of the mRNA fraction (Vandesompele J. et al. 2002). Until now, the standardization system most commonly used to normalize the mRNA fraction is utilize an internal control gene. This internal control, also called housekeeping gene, must shoes a stable level expression, i.e. not to vary in tissues or cells under investigation or in response to experimental treatments. This ideal condition is actually not achievable in practice, since the literature shows that there are no universal control genes, and the expression of the housekeeping genes can considerably vary in different conditions. The choice of the gene and the number of housekeeping depends on the tissue or on the cell type examined (Warrington JA et al. 2000). Vandesompele, in 2002, has done an extensive evaluation of 10 housekeeping genes commonly used in 13 different human tissues and described a procedure to calculate the factor of normalization based on more control genes to obtain a normalization of gene expression data more accurate and realistic. Among the candidate genes, are selected genes belonging to different functional classes, which allows to significantly reduce the possibility that they can be co-regulated. The level of expression of these internal control genes must be determined in a sufficient number of representative samples of the study that you want to lead (Vandesompele J. et al. 2002). It is

generally accepted that the levels of gene expression can be normalized through an internal control gene stable and accurately selected. However, in order to validate the presumed stable expression of the control gene any nonspecific variation must be eliminated. Therefore the study in question has developed a measurement of the gene stability to determine the stability of expression of the control genes based on not normalized expression levels. This measurement is based on the principle that the expression ratio between two ideal internal control genes is identical in all samples, regardless of the experimental conditions and the cell type. Consequently, the variation of the relationship of expression between two authentic housekeeping reflects the fact that one or both the genes are not expressed constantly; the increase of the variation of the ratio corresponds to a decrease in the stability of expression. For each control gene candidate is determined the variation "pairwise" (two by two) with all other control genes in the form of standard deviation of the ratios of expression transformed into logarithmic scale; the result is defined as the measure **M** of the genetic stability of internal control as the average pairwise variation of a particular gene compared to all other control genes candidates. M genes with lowest expression values are more stable. Assuming that the control genes are not co-regulated, the gradual exclusion of the gene with the highest value of M gives rise to a combination of the 2 constitutively expressed housekeeping genes that have the most stable expression in the samples tested. For this purpose has been created a Visual Basic Application (VBA) for Excel, called **geNorm**, freely available for use, which automatically calculates the M value of gene expression stability for all control genes in a given set of samples. The program allows the elimination of housekeeping genes with worst performance (highest M value) and recalculates the new M value for the remaining genes. Furthermore the systematic variation is calculated in the form of pairwise variation, V, for repeated experiments of RT-PCR on the same gene that reflects the variations of pipetting, enzymatic and inherent to the machine. The work of Vandesompele et al. has shown that, to accurately measure the levels of expression is required normalization with more housekeeping genes rather than just one. Consequently

is necessary to calculate a normalization factor based on the expression levels of housekeeping genes with the best performance. For an accurate calculation of the average of the control genes, Vandesompele et al. proposed to use the geometric mean instead of the arithmetic mean that allows a better control of the extreme values and the differences between quantities of different genes. The number of genes used to calculate the geometric mean is a compromise between precision and practical considerations; fact becomes impractical to use, for example, eight genes control when you must study few target genes or when it has a reduced amount of RNA available. In general, then, using a minimum of 3 most stable control genes with a gradual increase in the number of genes based on the improvement generated (Vandesompele J. et al. 2002).

Another approach for the selection of housekeeping genes is based on the work of Andersen et al. in 2004. This approach involves the application of a mathematical model to describe the expression values measured by qRT-PCR, divide the analysis of the various sub-groups of samples, estimate the variations of expression between the different groups and within the same group and calculate the "stability value" M candidate gene (Andersen C.L. et al., 2004). The group of Andersen created a VBA for Microsoft Excel, called **NormFinder**, freely available for use, which automatically calculates the stability of M for all genes standardization candidates and tested in a set of pilot samples. The authors suggest that the approach based on NormFinder, which takes account of the groups of samples and the direct estimation of the variation of expression, provides a more accurate measurement and solid stability of gene expression than the approach comparative two by two (geNorm). geNorm, basically, sort the genes according to the similarity of their expression profiles. Assuming a situation in which the set of samples is composed by two sub-groups in which all but one of the candidates have differences between the groups, in this case the optimal candidate with no differences between the groups in the approach geNorm could be excluded prematurely, while in NormFinder approach would be presented with the value of M less than the other candidates. Furthermore, the ranking of genes assigned on the basis of the similarity of their expression

profiles is problematic if there are co-regulated genes between the candidates that will tend to show expression profiles similar and therefore, regardless from their actual stability of expression, will be selected as the pair more stable (Andersen C.L. et al., 2004). These considerations suggest that the optimal strategy for the choice of the housekeeping genes consists in analyze the expression data with both methods (geNorm and NormFinder) that can mutually cross the results obtained.

1.2.7 miRNAs and cancer

To date, over 1000 miRNAs have been identified in animal genomes through cloning and bioinformatics approaches. Although the biological roles of only a small fraction of identified miRNAs have been elucidated, in mammals these miRNAs regulate processes essential to cell growth, embryogenesis, stem cell maintenance, hematopoietic cell differentiation, and brain development (Lagos-Quintana M. et al, 2003; Alvarez-Garcia I. and Miska E.A. 2005; Kloosterman W.P. and Plasterk R.H. 2006; Bartel D.P. 2009; Liu J. et al, 2011). Since Croce‘s research group first reported the link between the abnormal expression of miRNAs and cancer in 2002 (Calin G.A. et al, 2002), more and more studies have shown that many miRNAs take part in the progressions of various cancers, including tumor growth, differentiation, adhesion, apoptosis, invasion, and metastasis (Calin G.A. et al, 2004; Calin G.A. et al, 2006; Gaur A. et al, 2007). Moreover, several miRNAs were shown to be located at fragile sites or at genomic sites that are altered in cancer (Calin G.A. et al, 2004). Specific miRNAs were shown to be underexpressed and map to regions that are frequently deleted, whereas others were reported to be overexpressed and map at regions that are frequently amplified in cancer (Calin G.A. et al, 2002; Johnson S.M. et al, 2005; He L. et al, 2005; Tagawa H. et al, 2005). miRNA profiling experiments have revealed that many miRNAs are abnormally expressed in clinical cancer samples. In addition, in in vitro and in vivo models, these abnormal expressions have been pointed out to be closely related to various biological behaviors of cancers (Lu J.

et al, 2005; Sassen S. et al, 2008; Liu J. et al, 2011). Thus, alterations of miRNAs expression may promote tumor formation by modulating the functional expression of critical genes involved in tumor development and progression (Wiemer E.A. 2007).

1.2.8 miRNAs in hematopoiesis

Hematopoiesis is regulated by miRNAs. Various miRNAs are up-regulated at specific stages during hematopoietic development and the functional relevance of miRNAs has been proven at many different stages of lineage specification. Knockout of specific miRNAs can produce dramatic phenotypes leading to severe hematopoietic defects. Furthermore, several studies demonstrated that specific miRNAs are differentially expressed in hematopoietic stem cells. However, the emerging picture is extremely complex due to differences between species, cell type dependent variation in miRNA expression and differential expression of diverse target genes that are involved in various regulatory networks. There is also evidence that miRNAs play a role in cellular aging or in the inter-cellular crosstalk between hematopoietic cells and their microenvironment. The field is rapidly evolving due to new profiling tools and deep sequencing technology. In human, the miRNAs expression profiles are of diagnostic relevance for classification of different diseases. Recent reports on the generation of induced pluripotent stem cells with miRNAs have fuelled the hope that specific miRNAs and culture conditions facilitate directed differentiation or culture expansion of the hematopoietic stem cell pool (Bissels U. et al, 2012).

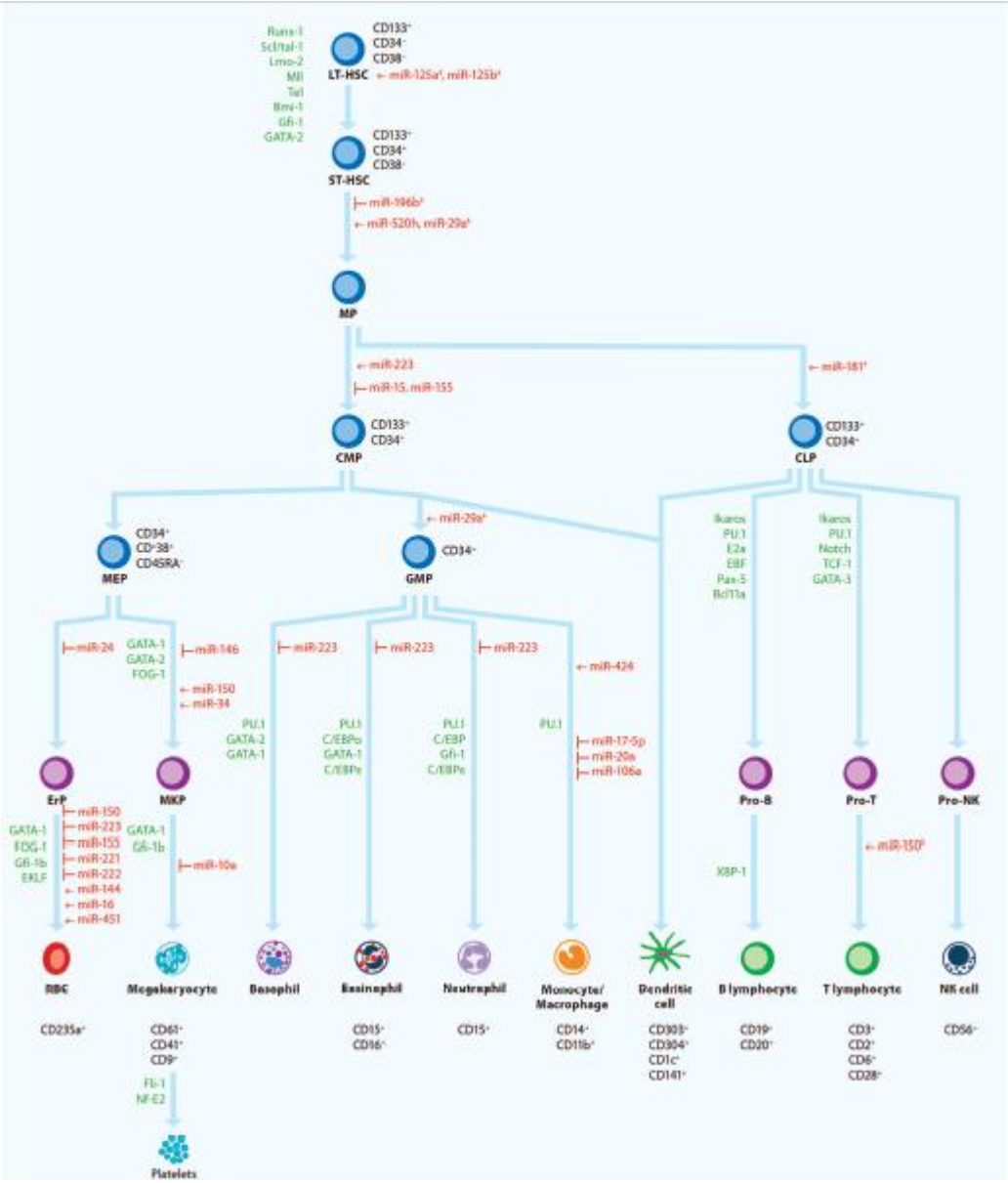

Figure 12. Role of miRNAs in hematopoietic development (Bissels U. et al, 2012). These miRNAs were mainly identified using *in vitro* assays with human cells - only those miRNAs labeled with ‡ were identified in the murine system.
Some transcription factors are demonstrated in green according to Orkin and Zon 2008.

MiRNA expression in normal hematopoiesis has been studied in murine and human hematopoietic tissue by several groups. It has been shown that these non-coding RNAs play critical roles in almost every stage of hematopoiesis (Table 1, Figure 12).

miRNA	**Function**
miR-150	Controls B- and T- cell differentiation Expressed in mature B cells and T cells Blocks transition from pro-B to pre-B cells Down-regulates C-MYB
miR-155	Controls B- and T- cell differentiation Controls germinal center reaction ↑ in activated T cells Reduces erythroid, myeloid and megakaryocytic differentiation
miR-221 and miR-222	Block erythroid differentiation by targeting c-KIT
miR-181a	B- and T-cell differentiation ↑ in murine B-cell lineage Blocks differentiation of human progenitor cells
miR-223	↑ in myeloid lineage Up-regulates granulopoiesus Down-regulates erytropoiesis
miR-142	↑ B and myeloid lineage
miR-146	Blocks lymphoid differentiation ↑ in murine Th1 cells
miR-10a, miR-126, miR-106, miR-10b, miR-17, miR20	↓ in megakaryocyte lineage

Table 1. MiRNA expression in normal hematopoiesis
(from Kluiver J. et al, 2006; Vasilatou D. et al, 2009)

miRNAs in lymphoid differentiation

The first study demonstrating the relation between miRNAs and hematopoiesis was published in 2004. In this study, Chen et al. cloned 150 miRNAs from murine bone marrow and found that three miRNAs (mir-181, mir-223 and mir-142) were preferentially expressed in hematopoietic cells. mir-181 was highly expressed in B-lymphoid cells of murine bone marrow. Its ectopic expression in hematopoietic

stem cells resulted in an increase in the proportion of B-lineage cells in vivo and in vitro. In addition, mir-223 and mir-142 were highly expressed in myeloid lineage (mir-142 in B-lymphoid cells too). However, ectopic expression of these two miRNAs resulted in an increase in the proportion of T cells, but not of B or myeloid cells as it might be expected (Chen C.Z. et al, 2004; Vasilatou D. et al, 2009). On the other hand, Ramkinssoon et al. who studied expression profiles of mir-142, mir-181, mir-223 and mir-155 found differences in expression patterns between human and mouse hematopoietic cells (Ramkinssoon S.H. et al, 2005; Vasilatou D. et al, 2009). A very important miRNA in hematopoiesis is mir-150. It is preferentially expressed in mature, resting T and B cells but not in their progenitors. It is up-regulated during B-cell and T-cell maturation but down-regulated again during further differentiation of naive T cells into Th1 and Th2 cells of murine hematopoietic tissue (Monticelli S. et al, 2005). Ectopic expression of mir-150 in hematopoietic stem cell progenitors reduces mature B-cell levels in the circulation, spleen and lymph nodes with little effect on T-cell or myeloid cell levels. Further experiments provide evidence that mir-150 blocks the transition from pro-B to pre-B cell during B-cell maturation (Zhou B. et al, 2007) probably explaining the way that ectopic expression of this miRNA reduces mature B cells. In addition, TG and knockout (KO) mice models have shown that mir-150 induces the apoptosis of pro-B cells. Moreover, miR-150 was found to target C-MYB, a transcription factor that controls lymphocyte development. As previously mentioned, mir-150 is preferentially expressed in mature B lymphocytes but not in their progenitors. C-MYB, on the other hand, is highly expressed in lymphocyte progenitors and down-regulated in mature cells. Xiao et al. demonstrated, in vivo, an interesting relationship between these expression patterns (Xiao C. et al, 2007). Indeed, miR-150 directly down-regulates C-MYB, by binding to its mRNA and consequently controls its protein expression in a dose-dependent manner. Another important miRNA in lymphoid differentiation is mir-155. It is a product of B-cell integration cluster (BIC) transcript that was first described as a frequent site of integration for the avian leucosis virus (Tam W. et al, 1997). High levels of mir-155 are present in activated B cells and T cells and in

activated monocytes (Fabbri M. et al, 2009). The function of mir-155 has been studied in both TG and KO mice. The first TG mice that specifically over-expressed mir-155 in B cells developed a pre-leukemic pre-B-cell proliferation evident in spleen and bone marrow, followed by a B-cell malignancy (Costinean S. et al, 2006). Two independent groups developed mir-155 KO mice to study the role of mir-155 in B-cell and T-cell differentiation. Thai et al. showed that mir-155 regulates germinal center reaction and T-helper cell differentiation by affecting cytokine production while Rodriguez et al. showed that bic/miR-155 regulates the function of both lymphocytes and dendritic cells leading to defective immune response (Rodriguez A. et al, 2007; Thai T.H. et al, 2007). Finally, Georgantas et al. found 33 miRNAs that were expressed in human stem-progenitor cells (HSPC) from bone marrow and peripheral blood. The authors used bioinformatic techniques to combine these results with HSPC mRNA expression data and with miRNA-mRNA target prediction so as to create a miRNA-mRNA interaction database, the Transcriptome Interaction Database. Then, they formed a model for miRNA control of hematopoiesis. According to this model, mir-181 and mir-128 inhibit differentiation of all hematopoietic lineages while mir-146 inhibits differentiation of multipotent progenitor cell (MPP) into common lymphoid progenitors (CLP) (Georgantas R.W. et al, 2007).

miRNAs in granulocyte and monocyte differentiation

A miRNA that plays an important role in myeloid differentiation is mir-223. Fazi et al. studied myeloid differentiation in acute promyelocytic leukemia (APL) cells and demonstrated that mir-223 up-regulates mouse granulopoiesis in association with the transcription factors negative nuclear factor IA (NFIA) and CCAAT/enhancer binding protein a (CEBPA). Both transcription factors are able to bind to mir-223 promoter. NFIA down-regulates while CEBPA up-regulates mir-223 expression. Treatment of APL cells with retinoic acid (RA) resulted in CEBPA replacement of NFIA, up-regulation of mir-223 and enhanced granulocytic differentiation. Interestingly, mir-223 was found to inhibit translation of NFIA, resulting in a negative-feedback loop that favors granulocytic differentiation (Fazi

F. et al, 2005). However, two recent studies do not confirm the previous results. In the first study, Fukao et al. found that myeloid expression of mir-223 might be specified by the conserved 5' proximal cis-regulatory element where transcription factors PU.1 and C/EBP cooperatively act on. In addition, by studying the APL cell model that was used by Fazi et al., they found that RA induced differentiation of APL cells, repressed PU.1 and resulted in down regulation of mir-223 (Fukao T. et al, 2007). In the second study, Johnnidis et al. found that mir-223 negatively regulates progenitor proliferation and granulocyte differentiation and activation in KO mice. In addition, they showed that miR-223 targets Mef2c, a transcription factor that promotes myeloid progenitor proliferation and that genetic ablation of Mef2c suppresses progenitor expansion and corrects the neutrophilic phenotype in mir-223 null mice (Johnnidis J.B. et al, 2008). Further investigations are required to shed light on the real mechanisms that regulate mir-223 expression. Fontana et al. investigated the role of mir-17-5p, mir-20a and mir-106a in monocytic differentiation and maturation. In unilineage monocytic cultured cells these miRNAs are down-regulated while acute myeloid leukemia 1 (AML1) transcription factor, which promotes M-CSFR transcription (M-CSF receptor), is up-regulated at the protein but not at the mRNA level. Transfection with miR-17-5p, miR-20a and miR-106a caused the opposite results in AML-1 protein expression followed by enhanced blast proliferation and inhibition of monocytic differentiation and maturation. Further experiments confirmed that these miRNAs target AML-1. In addition, AML1 binds the miRNA 17-5p-92 cluster and 106a-92 cluster promoters and inhibits the expression of mir-17-5p-20a-106a as a negative feedback, indicating that monocytopoiesis is controlled by a circuitry involving miR-17-5p, miR-20a, miR-106a, AML-1 and M-CSF (Fontana L. et al, 2007). Finally, according to the earlier mentioned model of Georgantas et al., mir-155, mir-24a and mir-17 may inhibit the differentiation of MPP into common myeloid progenitor (CMP), while mir-16, mir-103 and mir-107 may inhibit the differentiation of CMP into granulocyticmacrophage progenitor (GMP) (Georgantas R.W. et al, 2007). In addition mir-125b supports myelopoiesis but not G-CSF-induced granulocytic

differentiation and it has been suggested that this involves targeting of the c-Jun and Jund pathways (Surdziel E. et al, 20011).

miRNAs in erythroid and megakaryocytic differentiation

There is an increasing interest in the role of miRNAs in erythroid and megakaryocytic differentiation too. mir-221 and mir-222 are down-regulated during erythroid differentiation and maturation. The first eight nucleotides of the 5' sites of these miRNAs (seed region) are identical. This fact indicates that miR-221 and miR-222 can bind to the same target, which is KIT receptor, a key factor for the proliferation control of hematopoietic cells. Down-regulation of mir-221 and mir-222 probably unblocks KIT expression causing the expansion of erythroblasts (Felli N. et al, 2005). In addition, both erythroid and myeloid colony formation are reduced by mir-155 (Georgantas R.W. et al, 2007). Furthermore, it was demonstrated that mir-150 drives megakaryocyte-erythrocyte progenitor (MEP) differentiation towards megakaryocytes at the expense of erythroid cells (Lu J. et al, 2008). Additionally, Bruchova et al. studied miRNA expression in normal and polycythemia vera erythropoiesis. They evaluated 12 miRNAs by quantitative real time PCR (qRT-PCR) in a large number of samples from peripheral blood mononuclear cells, cultured in a three phase liquid system. During normal erythropoiesis, mir-150, mir-155, mir-221 and mir-222 were progressively down-regulated (in agreement with the studies mentioned earlier), mir-451 (which was found to be erythroid specific) and mir-16 (in reticulocytes) were up-regulated while mir-339 and mir-378 showed a biphasic expression pattern (Bruchova H. et al, 2007). Georgantas et al. had also showed that mir-155 blocks both myeloid and erythroid differentiation (Georgantas R.W. et al, 2007), while the study by O'Connel et al. demonstrates the role of mir-155 in erythropoiesis too. In this study, mouse transplanted with MPP cells that over-express mir-155 developed a myeloproliferative disorder with decreased erythroid/megakaryocytic lineage in bone marrow (O'Connell R.M. et al, 2008). Moreover, Dore et al. showed that the transcription factor GATA-1 activates in vivo the transcription of a single pri-miRNA, encoding miR-144 and miR-451.

Zebrafish embryos depleted of mir-451 form erythroid precursors, but their development into mature circulating red blood cells is strongly and specifically impaired. That was not true when mir-144 was silenced, suggesting that mir-451 has a specific role in erythropoiesis (Dore L.C. et al, 2008). Recently, mir-223 was also found to control erythroid differentiation too. Its down-regulation in progenitor and precursor cells of erythroid lineage seems to be necessary for erythroid maturation while the expression levels of mir-223 are inversely related to the levels of LIM–only protein 2 (LMO2, RBNT2), a highly conserved protein that plays in critical role in hematopoietic differentiation. Further experiments demonstrated that mir-233 downregulates LMO2 protein, by binding to its 3'-UTR, and inhibits differentiation and maturation of erythroid cells (Felli N. et al, 2009). MiRNAs seem to be important in megakaryocytic maturation. Garzon et al. performed miRNA expression profiling of in vitro differentiated megakaryocytes derived from CD34+ hematopoietic progenitors. Twenty miRNAs (including mir-10a, mir-126, mir-106, mir-10b, mir-17 and mir-20) were found to be down-regulated. It was also confirmed that miR-130a targets the transcription factor MAFB, which is involved in the activation of the GPIIB promoter (a key protein for platelet physiology) and that miR-10a directly targets HOXA1 in megakaryopoiesis. These two genes are over-expressed during megakaryopoiesis suggesting that down-regulation of miRNAs unblocks their expression (Garzon R. et al, 2006). Moreover, Labbaye et al. studied leukemic cells lines and showed that megakaryopoiesis is controlled by a pathway, in which PZLF transcription factor suppresses mir-146 transcription and thereby activates the SDF-1 receptor CXCR4 (44). Finally, the transcription factor RUNX1 (also known as AML1 protein) is up-regulated during early hematopoiesis and up-regulates mir-27a. During differentiation of megakaryocytic lineage, mir-27a negatively regulates RUNX1 expression forming a feedback loop (Labbaye C. et al, 2008).

1.2.9 miRNA profiling in haematological malignancies in human

MiRNAs expression in hematological malignancies has been extensively studied. There is an increasing number of reports demonstrating a key role of these non-coding RNAs in the pathogenesis and prognosis of hematological malignancies, the most important of which are summarized in Table 2.

	miRNA	Status	Function	Target
Lymphomas				
HL	miR-155	UR	OG	PU.1
	Let-7a	UR	OG	PRDM1/BLIMP-1
	miR-9	UR	OG	PRDM1/BLIMP-1
DLBCL	miR-155	UR in ABC	OG	PU.1, SHIP1
	miR-15a	DR	TSG	BCL-2
	miR-21	UR in ABC	OG	BCL-2
	miR-221	UR in ABC	OG	E2F1
	miR-17-92	UR	OG	
MCL	miR-17-92	UR	OG	E2F1
	miR-16-1	Binding site deleted	TSG	CCND1
Leukemias				
AML	miR-181a	UR in M1, M2 DR in M4, M5	OG/TSG	TCL-1
APL	miR-15a, 16-1	UR*	TSG	BCL-2
	miR-181b	DR		
ALL	miR-17-92	UR	OG	BIM
	miR-128b	UR		
	miR-204	UR		
CLL	miR-15a	DR	TSG	BCL-2
	miR-16-1	DR	TSG	BCL-2
	miR-29b	DR in poor prognosis CLL	TSG	TCL-1
	miR-181b	DR in poor prognosis CLL	TSG	TCL-1
	miR-155	UR	OG	
CML	miR-203	DR	TSG	ABL-1
	miR-17-92	DR	OG	
MM	miR-15a, 16	DR	TSG	

Table 2. miRNAs in hematological malignancies (Vasilatou D. et al, 2009). UR: up-regulated; DR: down-regulated; OG: oncogenes; TSG: tumor suppressor gene

miRNA expression in CLL (chronic lymphocytic leukaemia)

Chronic lymphocytic leukemia (CLL) is the most common leukemia in the Western world, accounting for 30% of all leukemia cases in the US (Byrd J.C. et al, 2004). The del13(q14) is the most common cytogenetic abnormality in CLL and is usually associated with good prognosis (Dohner H. et al, 2000). Hemizygous and/or homozygous loss at 13(q14) occur in more than half CLL cases. Deletions of 13(q14) loci are frequently found in other types of cancers, such as mantle cell lymphoma, multiple myeloma (MM), prostate cancers and pituitary tumors, suggesting that one or more tumor suppressor genes are located in this region (Nicoloso M.S. et al, 2007). However, until recently, several studies had failed to identify the involved gene located in the deleted region. Calin et al. showed that a cluster of two miRNA genes, mir-15a and mir-16-1 (with < 200 bp distance between them), is located exactly in 13(q14) region. These genes are highly expressed in normal CD5+ B-lymphocytes with mir-16-1 being expressed at higher levels than mir-15a. It was also found that both genes are down-regulated or deleted in the majority (68%) of the CLL samples and that down-regulation of mir-15a and mir-16-1 expression correlates with allelic loss at 13q14, suggesting that these two miRNAs may act as tumor suppressors and that their loss contributes to the pathogenesis of CLL (Calin G.A. et al, 2002). However, in a more recent report, down-regulation of mir-15a and mir-16-1 was found only in a small subset of patients. Fulci et al. evaluated 56 patients with the diagnosis of CLL for miRNA profiling using miRNA cloning and qRT-PCR. Low expression of these miRNAs was found in 11.7% of patients by qRT-PCR and in 11.1% by cloning (Fulci V. et al, 2007). These discrepancies may be attributed to the methodological differences between the two studies, namely the northern blot procedure in the first and the miRNA cloning and qRT-PCR in the recent study, the different controls used (CD5+ cells from tonsils in the first and CD5+ cells from cord blood in the latter study), as well as in the different population of patients. More specifically 68% of informative samples displayed loss of heterozygosity (LOH) at the 13q locus in the study by Calin et al., while 26/67 (38.8%) analyzed patients revealed del(13q) by FISH, in the study by Fulci et al.

Thus a significantly lower percentage of patients in the latter study had deletions at the 13q locus accounting perhaps for the lower frequency of mir-15a/mir-16-1 deletions. Moreover, an alternative mechanism of mir-15a and mir-16-1 reduction is germ line mutations. A germ-line mutation in the mir-16-1-mir-15a primary precursor, in association with deletion of the normal allele was detected in two CLL patients. Interestingly, one patient had a family history of CLL and breast cancer (Calin G.A. et al, 2005). In addition, miR-15a and miR-16-1 have been associated with protein expression in CLL. Mostly non-dividing B-CLL cells over-express BCL-2. No mechanism for this aberrant expression has been identified, although the overexpression of bcl-2 may be attributed in the juxtaposition of BCL-2 to immunoglobulin loci, this mechanism refers to < 5% of the CLL cases. Mir-15a and mir-16-1 expression is inversely correlated with BCL-2 protein levels. Although in normal CD5+ lymphoid cells the levels of both miRNAs were high and the BCL-2 protein was expressed at low levels, in the majority of leukemic cells both mir-15 and mir-16 were expressed at low levels and BCL-2 was over-expressed. Further research showed that miR-15a as well as miR-16-1 downregulate BCL-2 at the post-transcriptional stage of expression. The MEG-01 cell line (a leukemia-derived cell line with deletion of one allele and alteration of the other mir-15a and mir-16-1 loci and no expression of miR-15a and miR-16-1) was selected to be transfected by a vector that contains the full mir-15a/16-1 cluster. BCL-2 levels were highly reduced in comparison to WT MEG-01 cells (not transfected) or cells transfected with an empty vector. It was also shown that both miRNAs can affect BCL-2 protein expression separately and that miR-15 and miR-16 regulate BCL-2 expression at the post-transcriptional level (Cimmino A. et al, 2005). These data first and foremost indicate a possible mechanism for BCL-2 aberrant expression and secondly explain how miR-15a and miR-16-1 exert their tumor-suppressing function in CLL. However, in contrast to the previous results, Fulci et al. reported that down-regulation of mir-15 and mir-16 was not followed by significant increase in BCL-2 expression levels. These data do not support the hypothesis that in CLL, the high levels of BCL-2 expression are secondary to a down-regulation of mir-15 and mir-16 (Fulci V. et al, 2007). Two other miRNAs,

miR-29b and miR-181b, act as tumor-suppressors in aggressive CLL by targeting the S-cell leukemia/lymphoma 1 (TCL-1) oncogene. The levels of both miRNAs inversely correlated with levels of TCL-1 in CLL patients (Pekarsky Y. et al, 2006). TCL-1 is a coactivator of AKT, an oncogene that inhibits apoptotic processes and has a critical role in the regulation of many pathways involved in cell survival, proliferation and death. Its high expression is associated with expression of unmutated IgVH and ZAP-70, factors that indicate aggressive CLL (Nicoloso M.S. et al, 2007). Several groups have investigated miRNA expression profiling of CLL. Calin et al., compared miRNA expression in CLL cells vs. normal CD5+ B cells with a microarray chip and confirmed their results with Northern blot and qRT-PCR. Two groups of miRNAs, the first composed of 55 genes and the second of 29 genes, were found to have statistically significant differences in expression levels between normal and malignant cells. Some of them are located in fragile sites, such as mir-183 at FRA7H, mir-190 at FRA12A, mir-24-1 at FRA9D and mir-213 (Calin G.A. et al, 2004). To investigate whether the expression of miRNAs genes is associated with factors that predict the clinical course of CLL (ZAP-70 expression and mutated/unmutated status of IgVH), Calin et al., performed a genome wide miRNA microchip in a large number of CLL patients. By studying 94 samples of CLL, the group demonstrated that there is a signature of 13 miRNA genes (mir-15a, mir-195, mir-221, mir-23b, mir-155, mir-223, mir-29a-2, mir-24-1, mir-29b-2, mir-146, mir-16-1, mir-16-2, mir-29c) that has prognostic value, because the expression levels of the members of the signature correlate with CLL prognostic factors such as ZAP-70 expression and IgVH mutation status (Calin G.A. et al, 2005). Finally, mir-150, mir-223, mir-29b and mir-29c were over-expressed in patients with IgVH mutated cells supporting previous results (Fulci V. et al, 2007).

miRNA expression in Hodgkin's lymphoma

Hodgkin's lymphoma is a paradigm for a curable cancer. This is especially true in early stages and for younger patients. Nevertheless, some patients relapse, and some ultimately die of refractory disease. The malignant cells (Hodgkin–Reed–Sternberg cells) are a minority in the involved lymph node and usually are

surrounded by reactive cells. Most of the malignant cells are derived from B-cells, but have lost the expression of typical B-cell genes and acquired multiple other markers. Multiple signalling pathways are deregulated in Hodgkin–Reed–Sternberg cells, including NF (nuclear factor)-κB, JAK (Janus kinase)/STAT (signal transducer and activator of transcription), Pl3K (phosphoinositide 3-kinase)/Akt, ERK (extracellular-signal-regulated kinase), AP1 (activator protein 1), Notch1 and receptor tyrosine kinases (Kuppers R. 2009; Munker R. and Calin G.A 2011).

There are a few studies referring to miRNAs alterations in Hodgkin's Lymphoma (HL). Kluiver et al., analyzed HL cell lines and tissue samples and detected high levels of BIC and miR-155 in HL (Kluiver J. et al, 2005). Three years later, Navarro et al., analyzed the expression of 157 miRNAs in 49 lymph nodes from classical HL and ten reactive lymph nodes (RLN) by qRT-PCR and revealed three welldefined groups: nodular sclerosis cHL, mixed cellularity cHL and RLNs. They also found a distinctive signature of 25 miRNAs which differentiated cHL from RLNs, and 36 miRNAs that were differentially expressed between nodular sclerosis and mixed cellularity subtypes. Finally, mir-96, mir-128a and mir-128b were found to be selectively down-regulated in cHL with Ebstein Barr virus (EBV) infection, while mir-138 was related with Ann Arbor stage I-II cHL (Navarro A. et al, 2008). These findings indicate different miRNAs expression patterns in different histological subtypes as well as in early stage disease. Recently, Nie et al. showed that PRDM1/Blimp-1, an important regulator in terminal B-cell differentiation, is targeted by miR-9 and let-7a in cultured Hodgkin/Reed-Sternberg (HRS) cells. MiRNA expression profile demonstrated that both miRNAs are highly expressed in Hodgkin/Reed-Sternberg cells, suggesting that mir-9 and let-7a act as oncogenes in HL cells (Nie K. et al, 2008). Navarro et al. described a 25-miRNA signature based on RNA extracted from entire lymph nodes and found that the expression of mir-135a has prognostic relevance (Navarro A. et al, 2009). Patients with low mir-135a expression relapse earlier and have a shorter disease-free survival duration compared with patients with high expression. When the precursor miR-135a was transfected into cell lines derived from Hodgkin's lymphoma, cell growth slowed, and the cells became apoptotic. The authors also

showed that miR-135a targets the JAK2 pathway and that its re-expression leads to a decrease in the anti-apoptotic gene Bcl-XL (Van Vlierberghe P. et al, 2009).

miRNA expression in NHLs (non-Hodgkin's lymphomas)

NHLs are common, especially in elderly patients, and have widely divergent clinical, immunological and molecular presentations. On the basis of these characteristics (aggressive compared with indolent, T-lineage compared with B-lineage), the prognosis and treatment are very different. Because of the divergent immunological, genetic and clinical phenotypes, no universal GEP for all NHLs is feasible (Munker R. and Calin G.A 2011). **Diffuse large B-cell lymphoma (DLBCL)** is the most common type of lymphoma representing nearly 40% of lymphoid malignancies. There are at least two types of DLBCL that have different prognostic value, the **germinal center type (GC)** with a better outcome and **activated B-cell type (ABC)** with worse prognosis (Lawrie C.H. 2007). MiRNA expression in B-cell lymphomas has been studied by several groups. Eis et al. analyzed lymphoma samples and cell lines and found increased levels of miR-155, in DLBCL. Both BIC RNA and miR-155 were quantified in 23 DLBCL samples. BIC RNA levels were elevated from two to tenfold in DLBCL in comparison with normal CD19+ B cells, which were used as normal control. miR-155 levels were increased to even greater extents. Significantly higher levels of miR-155 were detected in the ABC type compared to the GC phenotype. It was also found that the levels of miR-15a were reduced in DLBCL, which shows that the reduction of this miRNA is not specific to CLL. On the other hand, the levels of miR-16 showed no specific pattern of increase or decrease relative to the control B cells (Eis P.S. et al, 2005). In addition, Kluiver et al. also demonstrated that BIC and mir-155 are highly expressed in DLBCL and primary mediastinal lymphomas, but not in other non-HLs (Kluiver J. et al, 2005). Roehle et al., who analyzed the expression of micro-RNAs in DLBCL, follicular lymphoma (FL) and non neoplastic lymph nodes, found that mir-155 was up-regulated in DLBCL as well. Moreover, this group demonstrated that miR-330, miR-17-5p, miR-106a and miR-210 discriminate DLBCL, FL and RLNs (Roehle A. et al, 2008). In agreement with the

previous results, Lawrie et al. showed that ABC and GC subtypes of DLBCL have distinct miRNA expression profile. mir-155, mir-21 and mir-221 are highly expressed in ABC in comparison with GC DLBCL. These miRNAs were over-expressed in clinical cases of DLBCL and FL as well as in DLBCL that had undergone transformation from FL. Univariate and multivariate analysis suggested that mir-21 expression is an independent prognostic indicator in de novo DLBCL and that high expression of this miRNA was associated with a better outcome (Lawrie C.H. et al, 2007). The aforementioned miRNAs (mir-155, mir-21, and mir-221) were compared in serum samples from DLBCL patients to healthy controls. The levels of these micro-RNAs were found to be up-regulated in patients' serum. In addition, high levels of mir-21 in DLBCL patient serum was associated with improved relapse-free survival (Lawrie C.H. et al, 2008). A possible target of miR-155 is the transcription factor PU.1 that is a member of Ets domain-transcription factor family and is required for late differentiation of B cells (John B. et al, 2004). In addition, the mRNA of the transcription factor C/EBPb has a potential target site for miR-155 in its 3'-UTR (Eis P.S. et al, 2005). In addition, a correlation between miR-155 and NF-kB expression has been found in DLBCL cell lines and patient samples (Rai D. et al, 2008). Recently, miR-155 was found to directly target Src homology-2 domain-containing inositol 5-phosphatase 1 (SHIP1), which acts in the PTEN/AKT pathway. miR-155 binds to 3'-UTR of SHIP 1 and down-regulates SHIP 1 in vivo and in vitro. Down-regulation of SHIP 1 by mir-155 resulted in both myeloproliferative and lymphoproliferative disorder indicating a role of this pathway in myeloid and lymphoid cells (Costinean S. et al, 2009; O' Connell R.M. et al, 2009). **Primary effusion lymphoma (PEL)** is a subtype of DLBCL associated with Kaposi sarcoma-associated herpes virus (KSHV) while some of PELs are coinfected by EBV. PEL cells contain two types of miRNAs encoded by either cellular genes or by KSHV or EBV. A 68-miRNA-specific signature was identified containing KSHV and EBV miRNAs. mir-155 was found to be down-regulated in contrast to ABC DLBCL cases (O' Hara A.J. et al, 2008). A recent study associates miRNA expression in DLBCL with immunophenotype, survival and transformation from FL. Lawrie et al.

studied 80 samples of DLBCL and 18 samples from FL with microarrays and found distinct expression patterns between these two lymphomas. Furthermore, miRNAs expression was associated with GC-like and non-GC-like immunophenotypes (supporting previous results), international prognostic index status and event-free survival in cyclophosphamide, doxorubicin, oncovin, prednisone (CHOP) and rituximab-CHOP treated patients (Lawrie C.H. et al, 2009). These data indicate that miRNAs may be used in the future as prognostic and diagnostic tools in DLBCL. High expression of precursor miR-155/BIC RNA was described in pediatric Burkitt's lymphoma (Metzler M. et al, 2004), but not in adult primary cases of the disease (Kluiver J. et al, 2006). Expression of BIC and miR-155 in three latency type III EBV-positive Burkitt's lymphoma cell lines and in all primary posttransplantation lymphoproliferative disorder cases suggests a possible role for EBV latency type III-specific proteins, in the induction of BIC expression (Kluiver J. et al, 2006). **Mantle cell lymphoma (MCL)** represents 5-10% of all non-HLs and has the worst prognosis among B-cell lymphomas. The t(11;14)(q13;q32) is characteristic of MCL and displays the cyclin D1 (CCND1) gene on chromosome 11 downstream to the enhancer region of the IgH gene on chromosome 14 resulting in CCND1 over-expression. Point mutations and genomic deletions in CCND1 create a truncated mRNA and result in increased proliferation and shorter survival (Wiestner A. et al, 2007). Cell lines, with increased ratio of truncated CCND1 have increased total mRNA levels, increased CCND1 protein expression. miR-16 is able to down-regulate CCND1 protein expression (Chen R.W. et al, 2008). However, the truncation of CCND1 mRNA lacks miR-16-1 binding sites within the CCND1 mRNA 3'-UTR and alters miRNA regulation in MCL suggesting a possible role of this miR-16-1 in CCND1 repression (Chen R.W. et al, 2008). The genetic locus 13q31, which is commonly found amplified in many B-cell lymphomas, such as DLBCL, MCL and solid tumors (Lawrie C.H. 2007), encodes the miRNA cluster mir-17-92, which includes mir-17-5p, mir-18a, mir-19a, mir-20a, mir-19-b-1 and mir-92 (He L. et al, 2005). He et al. found that expression of the mir-17-92 cluster components in mice also over-expressing MYC, enhanced lymphomagenesis while each miRNA of the cluster

did not (He L. et al, 2005). In addition, O' Donnell et al. showed that the c-MYC oncogene activates the transcription of the mir-17-92 cluster (O' Donnell K.A. et al, 2005). c-MYC also induces the expression of the transcription factor E2F1 gene, which in turn can induce c-MYC by means of a positive feedback. mir-17-5p and mir-20a (members of the mir-17-92 cluster) directly down-regulate the transcription factor E2F1. By targeting E2F1, members of the mir-17-92 cluster can reduce the reciprocal activation MYC/ E2F1 and control c-MYC-mediated cellular proliferation (O' Donnell K.A. et al, 2005).

miRNA expression in T-cell lymphomas

The role of miRNAs in T-cell lymphomas in human remains unclear. However, the available data suggest a role of miRNAs in the pathogenesis of T-cell lymphomas. Lum et al. found a high density of integrations upstream of the mir-106a miRNA cistron. In tumors containing integration, the primary transcript encoding the mir-106a cistron was over-expressed 5–20-fold compared with control tumors. The mature miR-106a, miR-363 and miR-17-92 were over-expressed too (Lum A.M. et al, 2007). Landais et al. confirmed pri-mir-106-363 over-expression in 46% of human T-cell leukemias tested (Landais S. et al, 2007).

miRNA expression in AML (acute myelogenous leukaemia)

There is an increasing number of publications investigating the role of miRNAs in acute leukemia. Debernardi et al. analyzed the expression of miRNAs in 30 samples from AML patients with normal karyotype. The levels of miR-181a (mentioned earlier as potential inhibitor of differentiation of all human hematopoietic lineages) (Georgantas R.W. et al, 2007) were elevated in M1 or M2 AML, compared with M4 or M5 AML. The elevated expression of mir-181a observed in AML implies its involvement in the leukemic process. Moreover, mRr-10a, miR-10b and miR-196a-1 were found to correlate with HOX gene expression (Debernardi S. et al, 2007). Cell lines treated with the differentiating agent all-trans-RA (ATRA) showed up-regulation of some miRNAs, including few known tumor suppressor miRNAs, such as mir-15a and mir-16-1, members of the

let-7 family and mir-223, mir-342 and mir-107. mir-181 was found to be down-regulated after treatment with ATRA (Garzon R. et al, 2007). Isken et al. analyzed 50 patient samples with AML and 12 control samples for the expression of 154 human miRNAs. The expression level of mir-26a, mir-26b and mir-29b was intermediate between CD34+ cells and normal bone marrow (NBM) samples. There was a significant difference in the expression pattern of mir-23b, mir-34a and the mir-221/mir-222 cluster between AML and controls. Except for mir-23b, all these were up-regulated in AML samples compared to CD34+ and NBM samples. High levels of expression of mir-221/mir-222 cluster promote growth of several cancer cells lines, by inhibiting the expression of CDKN1B, an inhibitor of cell cycle progression and known tumor suppressor. In addition, they secondary affect KIT expression. Finally, mir-181a expression was reduced in samples with French-American-British (FAB) classification M4 and M5 compared to FAB M1 and M2, supporting the results of the aforementioned study by Debernardi et al. (Debernardi S. et al, 2007; Vasilatou D. et al, 2009). More recently, Marcucci et al. studied samples of leukemia cells from adults under the age of 60 years who had cytogenetically normal AML and internal tandem duplication in the fms-related tyrosine kinase 3 gene (FLT3-ITD), a wild type nucleophosmin (NPM1) or both using micro-RNA expression profiling. A signature of 12 miRNAs was associated with clinical outcome. Among them, members of mir-181 family are down-regulated in high risk AML, with their expression levels being inversely correlated with levels of proteins involved in pathways controlled by toll-like receptors and interleukin-1b (Marcucci G. et al, 2008). Moreover, there is evidence of a unique miRNA signature that distinguishes NPMc + AML (AML with NPM1 mutations and cytoplasmic NPM) from unmutated cases. This signature contains mir-10a, mir-10b, let-7 family and mir-29 family. Some of the miRNAs that are down-regulated, are associated with HOX genes indicating that HOX up-regulation in NPMc + AML is attributed, at least in part, to the loss of miRNA regulation (Garzon R., Garofalo M., Martelli M.P. et al, 2008). In 240 AML patient samples with predominantly intermediate and poor cytogenetics, Garzon et al. found miRNA signatures, associated with balanced 11q23 translocation, isolated

trisomy 8 and FLT3-ITD mutations. In addition, miR-199a and miR-191 were found to have a prognostic value, because they were associated with reduced overall and disease-free survival (Garzon R., Volinia S., Liu C.G. et al., 2008).

miRNA expression in ALL (acute lymphocytic leukaemia)

A screening of deregulated miRNAs in acute lymphocytic leukemia (ALL) has been published, providing a list of miRNAs involved in leukemogenesis. The five highly expressed miRNAs in ALL were mir-128b, mir-204, mir-218, mir-331 and mir-181b-1. The most commonly represented miRNA in ALL is mir-128b with a 436, fivefold difference compared to normal CD19+ B cells. The second most highly expressed miRNA in ALL is mir-204. On the contrary, the four miRNAs with the lowest expression levels are mir-135b, mir-132, mir-199s, mir-139 and mir-150. The mir-17-92 cluster was found to be up-regulated in ALL (Zanette D.L. et al, 2007). Taking into consideration that the miR-17-92 antagonizes the expression of the pro-apoptotic protein BIM and favors the survival of B-cell progenitors (Ventura A. et al, 2008), the involvement of miR-17-92 in ALL is not surprising. Finally, Mi et al. performed a large-scale genome wide miRNA expression profile assay and identified 27 miRNAs that are differentially expressed between AML and ALL. Among them, mir-128a and mir-128b are significantly over-expressed, whereas let-7b and mir-223 are significantly down-regulated in ALL compared to AML. In addition, over-expression of mir-128 in ALL was at least partially associated with promoter hypomethylation and not with an amplification of its genomic locus (Mi S. et al, 2007).

1.2.10 miRNAs in dog

It is known that many miRNAs are evolutionarily conserved among different organisms, so it is possible to predict orthologous genes (homologous genes present in different species, originating from gene duplication events and having different functions) of known miRNAs in different species due to the computational predictions (Shahi P. et al. 2006). The sequence similarities between dog and human allow to use primers and probes designed and commonly used in humans for the monitoring of miRNAs in the dog, when the respective sequences are perfectly conserved (Zhou D. et al. 2008). Until the beginning of my PhD program, only a few studies of miRNA in the dog have been reported. Zhou et al., in 2008, identified 357 miRNA candidates by computational prediction, starting from the dog genome, among them, 300 are known miRNA homologs in humans, the remaining 57 are not reported in any animal species. Of these 357 miRNAs, 125 are located in intronic regions of protein-coding genes, of which 75 are in the sense orientation and 50 anti-sense gene with respect to the host, and the other part in UTR, exons in mRNA or in intergenic spaces. Among all these miRNAs dog, 142 are organized into 53 clusters; alignment of the sequences shows that some clusters are formed by miRNA paralogs and others have multiple pairs. In Figure 13 the genes of miRNAs are schematically represented with colored rectangles and miRNA paralogs, in different clusters, have the same color (Zhou D. et al. 2008).

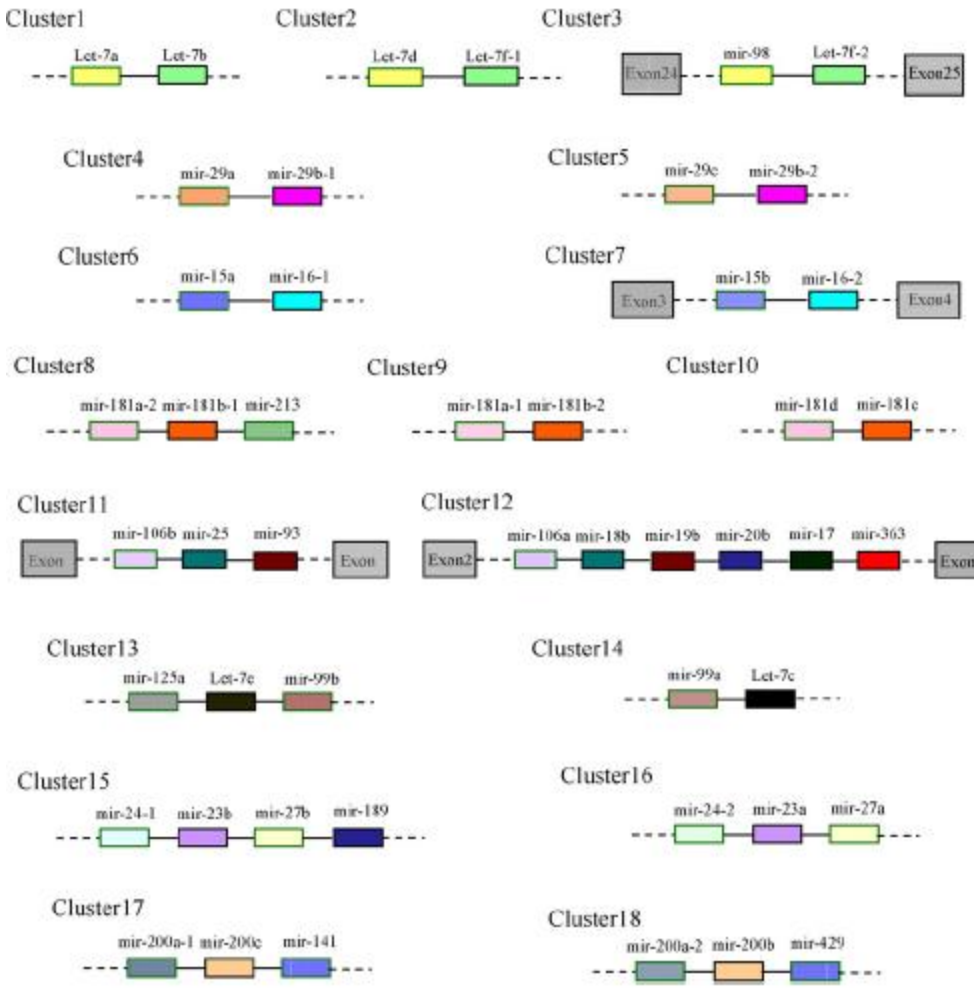

Figure 13. Schematic diagram of miRNA genes in *C. familiaris* (Zhou D. et al. 2008)

Using the sequences of miRNAs currently known in the dog, Zhou et al. analyzed the UTR of protein-coding genes in the genome of dog to identify potential target sites and predicted 865 miRNA target genes. Except for the transcript target 71, with 2 or more target sites, these genes have only one target site in UTRs conserved between dog, human and mouse. The majority of target genes predicted presents a imperfect complementarity with the corresponding miRNA and then it is presumed that are regulated through the repression of translation. Furthermore, it is interesting to note that 28 target genes have sites perfectly complementary to the miRNA, indicating that these miRNAs may work cutting the mRNA (Bentwich I. 2005). In the same study, has been analyzed the

functional annotations distribution of all conserved targets of miRNAs using Gene Ontology (GO) term and has been found that target genes play a wide range of biological functions including transcriptional regulation, stress response, metabolism biochemical processes related to cancer and signal transduction pathways (Bentwich I. 2005). Another study on miRNAs in dogs has been published in 2007by Boggs et al. In this study has been evaluated the expression of a cluster of seven miRNAs (miR-17-3p, miR-17-5p, miR-18, miR-19a, miR-19b, miR92, miR-20). These miRNAs were analyzed in five dog tissues (heart, lung, brain, kidney and liver) by means of qRT-PCR using assays designed on the corresponding human sequences, perfectly preserved in dogs, using the ΔΔCt method (Boggs R.M. et al. 2007). Moreover, in these study the expression data were analyzed by normalization with RNU6B, a small nucleolar RNA, without any assessment of the actual validity of this target as housekeeping under the experimental conditions of interest. Another important work concerning the miRNAs in dog has been published in 2008 by Boggs RM et al. This study was focused on oncomiRNAs, a subclass of miRNAs that includes genes whose expression, or the absence of expression, is associated with cancer (Boggs R.M. et al., 2008). Until the last decade, the domestic dog was little used as a model for the study of several human diseases with genetic components. However, the dog shows marked similarities in genetic and physiological with the man, so that makes him an excellent model for the study and treatment of various inherited diseases. In particular, it was discovered that some miRNAs can function at the same time as oncogenes and tumor suppressor in different types of cancer, therefore, in the work of Boggs et al, the pattern of expression of some miRNAs (miR-15a, miR-16, miR-17-5p, miR-21, miR-29b, miR-125b, miR-145, miR-155, miR-181b, let-7f), which were described in the literature to be associated with breast cancer human, was evaluated. The study showed that these miRNAs in breast cancer follow in dogs the same pattern of expression detected in humans. The genetic similarities observed between the two species indicate that, due to the preservation of the function of these miRNAs, they may target conserved genes in humans and dogs and be involved at the beginning of the

cancerogenesis and metastasis formation (Boggs R.M. et al. 2007). In conclusion, from the analysis of these works it is evident that in dogs a limited number of tissues, not including the hematopoietic tissues, was investigated and a systematic retrospective studies (for example, using samples embedded in paraffin) has not been realized yet. Furthermore, it has not been reported any study with proper validation of housekeeping genes in the different types of canine tissues. In the abovementioned two expression studies, the authors have a priori used as reference gene RNU6B, which cannot be considered a suitable normalizer gene for miRNA expression profiling.

1.2.11 Lymphoma in dog as a model for human

Lymphomas of the dog show histopathological, molecular and clinical features very similar to human non-Hodgkin's lymphoma (NHL). Most subtypes of lymphoma in humans have been recognized as histopathologically identical counterparts in dog, as well as striking similarities in molecular characteristics of the tumor between the two species. In fact, a spontaneous lymphoma in dogs has a clinical presentation, response to chemotherapy and clinical progression similar to the NHL in humans. This makes the dog a good animal model for the study of lymphoma in humans and for the search of new therapeutic agents, since dogs have body size bigger than rodents and genetic characteristics similar to humans, sharing with them the same environment and diet, and above all develop spontaneous tumors (and not artificially induced as usually happens in rodents). Until a short time ago, the use of spontaneous tumors in dogs as a model of human cancer has been limited by the poor availability of reagents and techniques that could be used also in dog. However, recent advances in genomic studies of the dog, including the sequencing of the canine genome, the availability of microarrays, the development of advanced techniques of hybridization and comparative cytogenetics and the development of flow cytometry species-specific, make possible now the use of most of these techniques that were previously used only in humans and in mice (Vail DM. et al,

2000; Kisseberth WC et al, 2007). Dog is a good comparative model for human cancer also due to the fact that it shares with humans the same environment, and therefore it is also chronically exposed to the same environmental pollutants, including carcinogens. It's interesting to note that dog can be even more exposed than humans to toxic and/or carcinogenic substances, because of the close contact with the soil, the surface water potentially contaminated with pesticides or other pollutants, and the greater physical proximity to the discharge of exhaust pipes of motor vehicles. Considering that dog has a half-life shorter than humans, it also has a shorter latency period between exposure to toxic substances and the appearance of the disease. Consequently, dog can play a very useful role of sentinel animal for diseases such as cancer, contributing to the early identification of carcinogens in the environment, the prediction of the risk to humans, and the assessment of the effects on public health. The epidemiological significance of the comparative study of canine cancer for human health has been highlighted by a recent study performed in some areas of the Campania region with a high degree of environmental contamination by carcinogens such as dioxin, showing that dog can anticipate the risk for man to develop cancer in resident population (Marconato et al., 2009).

1.2.12 CLL in dog as a model for human

Chronic lymphocytic leukemia (CLL) is a common hematologic disorder occurring in dogs as well as in humans. In people, CLL is prevalently an indolent B-cell neoplasm caused by the expansion of a subpopulation of CD5-positive B-cells. In dogs, case collections have been reported describing hematologic features and immunophenotype with T-CLL as the most frequent form (Vernau W. and Moore P.F. 1999; Adam F. et al., 2009; Tasca S. et al., 2009). However, some clinical and cytogenetic analogies have been reported between human and canine CLL. In particular, a deletion or the CFA 22q11.2 genomic region, harbouring also the mir-15a/miR-16 cluster, was reported in a case of canine CLL as homologue to the 13q14 deletion in human CLL leading to miR-15a and miR-16

underexpression with pathogenetic and prognostic significance (Calin G.A. et al., 2002; Calin G.A. and Croce C.M. 2002; Breen M. and Modiano J.F. 2008). With regard to the human counterpart, no wide reports are available in dogs as far as prognostic factors for survival are concerned, even if some recent studies have compared canine B-cell and T-cell CLL and found a relationship between immunophenotyping and different prognosis (Williams M.J. et al., 2008; Comazzi S. et al., 2011). The possibility that at least some evolutionary conserved miRNA have a role in the pathogenesis and diagnosis of canine CLL as reported in humans should be thoroughly investigated.

1.2.13 Splenic lymphoma in dog

Splenic neoplasms can be broadly categorized into vascular neoplasms, non angiomatous non lymphomatous sarcomas and lymphomas. In dogs, angiosarcoma is the most common primary splenic tumor, while lymphoma is considered less common (Frey A.J. and Betts C.W., 1977; Spangler W.L. and Culbertson M.R. 1992; ; Day M.J. et al., 1995; Valli V.E. et al., 2006; Christensen N. et al., 2009; Eberle N. et al., 2012). On the contrary, lymphoma represents up to 40% of splenic malignancies in man (Bhatia K. et al, 2007; Kaza R.K. et al., 2010). Splenic lymphoma may be primary or secondary however, primary forms account for 1% or less of all human lymphomas (Bhatia K. et al, 2007; Swerdlow S.H. et al., 2008; Kaza R.K. et al., 2010). These data do not seem clearly available in dogs (Valli V.E. 2007).

In spleen, lymphomas are present as nodular or diffuse lesions (Bhatia K. et al., 2007; Kaza R.K. et al., 2010; Valli V.E. et al, 2006, Valli V.E. 2007). Primary nodular lymphomas have been described in humans (Thieblemont C. et al., 2002; Swerdlow S.H. et al., 2008; Kurtin P.J. 2009) and dogs (Valli V.E. et al 2006; Valli V.E. 2007; Stefanello D. et al., 2011; Flood-Knapik K.E. et al., 2012) as a group of mostly low grade tumors deriving from mature B cell lymphocytes. It has been estimated that 5.3–29% of all lymphomas in dogs are low-grade tumors and are characterized by indolent clinical course, incomplete response to chemotherapy,

but longer survival times compared to aggressive lymphomas (Carter R.F. et al., 1986; Fournell-Fleury C. et al., 1997; Ponce F. et al., 2010). Histopathological subtypes of canine indolent lymphoma include marginal zone lymphoma (MZL), follicular lymphoma (FL) and mantle cell lymphoma (MCL), which are all of B-cell immunophenotype, and T-zone lymphoma (Valli V.E. et al., 2006; Valli V.E. et al., 2011). Canine MZL and MCL develop more frequently in spleen than in lymph nodes (Valli V.E. et al., 2006; Valli V.E. 2007) while primary splenic follicular lymphoma (FL) has been reported but seems rare in both people and dogs (Pittaluga S. et al., 1996; Thieblemont C. et al., 2003; Valli V.E. et al., 2006; Swerdlow S.H. et al., 2008; Mollejo M et al., 2009; Shimizu-Kohno K. et al., 2012; Flood-Knapik K.E. et al., 2012). Diffuse primary splenic lymphomas seem less common than nodular lymphomas in dogs (Valli V.E. 2007) while diffuse sinusoidal splenic invasion by leukemic cells occurs on a regular basis (Workman H.C. and Vernau W. 2003; Vail D.M. and Young K.M. 2007). Primary diffuse splenic lymphomas most commonly reported in man are diffuse red pulp small B cell lymphoma, large B cell lymphoma and, hepatosplenic γ/δ T cell/NK lymphoma and hairy cell leukemia (Issacson P.G. 1997; Swerdlow S.H. et al., 2008; Weidmann E. 2000). With the exception of hairy cell leukemia, lymphomas with a diffuse growth pattern are more aggressive (Weidmann E. 2000; Valli V.E. 2007; Swerdlow S.H. et al., 2008). Diffuse large B cell lymphoma has been reported in dogs and seems to develop in spleen as a multifocal tumor that tends to become diffuse by the time of diagnosis (Valli V.E. 2007) but no data are available on its behaviour. Hepatosplenic lymphoma of γ/δ T cell origin has been described in dogs (Fry M.M. et al., 2003; Cienava E.A. et al., 2004; Keller S.M. et al., 2012). In these dogs primary diffuse involvement of the spleen together with severe splenomegaly are characteristic of this rapidly fatal disease. Thus, while nodular lymphomas are generally indolent and slowly progressive tumours regarded to have a good prognosis, diffuse lymphomas are mostly associated with poorer prognosis in people and dogs (Valli V.E. 2006; Stefanello D. et al., 2011; Flood-Knapik K.E. et al., 2012). Nevertheless, to date there are no accurate and complete works about classification and grading in canine splenic lymphoma.

1.3 MATERIALS AND METHODS

1.3.1 Sampling procedures

In this doctoral thesis the analyses were carried out on dogs suffering from different types of spontaneous hematopoietic malignancies, such as:

- **chronic lymphocytic leukaemia** (T-CLL cells and B-CLL cells)
- **lymph nodes lymphoma** (T cells and B cells)
- **splenic lymphoma**

For all types of tumor we used both fresh samples and stored samples, in particular:

- peripheral blood for CLL and lymph node aspirates for lymph node lymphomas (both in RNA later),
- cytologic glass smears for CLL and lymph nodes lymphomas,
- sections of tissues fixed in formalin and embedded in paraffin (FFPE) for splenic and lymph nodes lymphomas.

The fresh whole blood samples from canine CLL and from healthy dogs were collected in EDTA-coated tubes.

The fresh-frozen lymph node samples were obtained from healthy dogs, or not suffering from neoplastic disease, and dogs with lymphoma by fine-needle biopsy (measure 22) of enlarged lymph nodes.

The formalin-fixed and paraffin-embedded samples were provided by Prof. Paola Roccabianca, Department of Veterinary Sciences and Public Health, University of Milan, to the extent of 4 slices of 20 micron thickness for each sample.

The cytologic glass smears were provided by Dr. Maria Elena Gelain, Department of Veterinary Sciences and Public Health, University of Milan.

The samples were classified on the basis of clinical, haematological and cytological characteristics, and immunophenotyping data.

The lists of all the samples on which the analyzes were performed, divided by type of cancer and type of sample (fresh, FFPE and cytologic glass smears), are shown below.

FRESH-FROZEN LYMPH NODES LYMPHOMAS				
Sample code	**Sample type**	**Phenotype**	**Grade***	**Updated Kiel classification**
F1	Lymphoma	T	L	**Lymphocytic/small clear cell**
F2	Lymphoma	T	L	**Lymphocytic/small clear cell**
F3	Lymphoma	T	H	**Pleomorphic, medium and large cell**
F4	Lymphoma	T	H	**Pleomorphic, medium and large cell**
F5	Lymphoma	T	L	**Lymphocytic/small clear cell**
F6	Lymphoma	T	L	**Lymphocytic/small clear cell**
F7	Lymphoma	T	H	**Pleomorphic, medium and large cell**
F8	Lymphoma	B	H	**Centroblastic**
F9	Lymphoma	B	H	**Centroblastic**
F10	Lymphoma	B	H	**Centroblastic**
F11	Lymphoma	B	H	**Centroblastic**
F12	Lymphoma	B	H	**Centroblastic**
F13	Lymphoma	B	H	**Centroblastic**
F14	Lymphoma	B	H	**Centroblastic**
F15	Lymphoma	B	H	**Centroblastic**
F16	Non-neoplastic			
F17	Non-neoplastic			
F18	Non-neoplastic			

Table 3. Fresh-frozen lymph node lymphomas samples list and classification.

*L=low; H=high.

FFPE LYMPH NODES LYMPHOMAS				
Sample code	**Sample type**	**Phenotype**	**Grade***	**Updated Kiel classification**
P1	Lymphoma	T	H	**Pleomorphic, medium and large cell**
P2	Lymphoma	T	L	**Lymphocytic/small clear cell**
P3	Lymphoma	B	L	**Macronucleolated medium-sized cells**
P4	Lymphoma	B	L	**Macronucleolated medium-sized cells**
P5	Lymphoma	B	H	**Centroblastic**
P6	Lymphoma	B	H	**Lymphoblastic**
P7	Lymphoma	B	H	**Immunoblastic**
P8	Non-neoplastic			
P9	Non-neoplastic			
P10	Non-neoplastic			
P11	Non-neoplastic			
P12	Non-neoplastic			

Table 4. FFPE lymph node lymphomas samples list and classification.
*L=low; H=high.

CYTOLOGIC GLASS SMEARS LYMPH NODES LYMPHOMAS			
Sample code	**Phenotype**	**Grade***	**Update Kiel**
C 1	T lymphoma	L	Lymphocytic (small cells)
C 2	T lymphoma	L	Pro lymphocytic
C 3	T lymphoma	L	Lymphocytic (small cells)
C 4	T lymphoma	H	Pleomorphic (big cells)
C 5	T lymphoma	H	Pleomorphic (medium- big cells)
C 6	B lymphoma	H	Centroblastic
C 7	B lymphoma	H	Centroblastic
C 8	B lymphoma	H	Centroblastic
C 9	B lymphoma	H	Centroblastic
C 10	B lymphoma	H	Centroblastic
C 11	B lymphoma	H	Centroblastic
C 12	B lymphoma	H	Centroblastic
C 13	B lymphoma	H	Centroblastic Pleomorphic
C 14	B lymphoma	H	Centroblastic
C 15	B lymphoma	H	Centroblastic

Table 5. Cytologic glass smears lymph node lymphomas sample, list and classification. *L=low; H=high.

FRESH-FROZEN CLLS		
Sample code	**Sample type**	**Phenotype**
F 19	Non neoplastic blood	
F 20	Non neoplastic blood	
F 21	Non neoplastic blood	
F 22	Non neoplastic blood	
F 23	Non neoplastic blood	
F 24	Non neoplastic blood	
F 25	Peripheral blood	T- CLL
F 26	Peripheral blood	T- CLL
F 27	Peripheral blood	T- CLL
F 28	Peripheral blood	T- CLL
F 29	Peripheral blood	T- CLL
F 30	Peripheral blood	T- CLL
F 31	Peripheral blood	T- CLL
F 32	Peripheral blood	T- CLL
F 33	Peripheral blood	B- CLL
F 34	Peripheral blood	B- CLL
F 35	Peripheral blood	B- CLL
F 36	Peripheral blood	B- CLL
F 37	Peripheral blood	B- CLL
F 38	Peripheral blood	B- CLL
F 39	Peripheral blood	B- CLL
F 40	Peripheral blood	B- CLL

Table 6. Fresh/frozen CLLs samples, list and classification

CYTOLOGIC GLASS SMEARS CLLS	
Samples	**Immunophenotype**
C 16	T CLL
C 17	T CLL
C 18	T CLL
C 19	T CLL
C 20	T CLL
C 21	T CLL
C 22	T CLL
C 23	B CLL
C 24	B CLL
C 25	B CLL
C 26	B CLL
C 27	B CLL
C 28	B CLL
C 29	B CLL

Table 7. Cytologic glass smears CLLs samples, list and classification

A. FFPE NON-NEOPLASTIC SPLEEN			
Sample code	**Sample type**	**Updated Kiel classification**	**Signalling**
P 13	Non-neoplastic spleen		Boxer, F, 5 years
P 14	Non-neoplastic spleen		X, F, 6 months
P 15	Non-neoplastic spleen		X, Fs, 13 years
P 16	Non-neoplastic spleen		King Charles, F, 4 month
P 17	Non-neoplastic spleen		Amstaff, F, 6 months
P 18	Non-neoplastic spleen		X, M, 5 years
P 19	Non-neoplastic spleen		Pomeranian, F, 3 month

B. FFPE SPLENIC LYMPHOMA			
Sample code	**Sample type**	**Updated Kiel classification**	**Signalling**
P 20	Splenic lymphoma	Splenic marginal zone lymphoma- extention	X, F, 12 years
P 21	Splenic lymphoma	Follicular lymphoma grade 1	Boxer, F, 5 years
P 22	Splenic lymphoma	Splenic marginal zone lymphoma focal	Cairn Terrier, M, 8 years
P 23	Splenic lymphoma	Splenic marginal zone lymphoma focal	X, F, 8 years
P 24	Splenic lymphoma	Nodular Mantle cell lymphoma	Fox Terrier, Fc, 8 years
P 25	Splenic lymphoma	Splenic marginal zone lymphoma focal	X, F, adult
P 26	Splenic lymphoma	Splenic marginal zone lymphoma	X, M, 11 years
P 27	Splenic lymphoma	Splenic marginal zone lymphoma focal	X, M, 8 years
P 28	Splenic lymphoma	Splenic marginal zone lymphoma focal	X, Fc, 14 years
P 29	Splenic lymphoma	Splenic marginal zone lymphoma multifocal	X, M, 9 years
P 30	Splenic lymphoma	Splenic marginal zone lymphoma focal	X, M, 7 years
P 31	Splenic lymphoma	Nodular Mantle cell lymphoma	X, M, 9 years
P 32	Splenic lymphoma	Small lymphocytic lymphoma	Cocker, F c
P 33	Splenic lymphoma	Follicular lymphoma grade 2	Medium Schnauzer, F, 10 years
P 34	Splenic lymphoma	Lymphocytic lymphoma	Boxer, M, 7 years
P 35	Splenic lymphoma	Nodular lymphoma almost diffuse in blastic transformation	Rottweiler, F, 8 years
P 36	Splenic lymphoma	Nodular lymphoma almost marginal diffuse	X, F, 6 years
P 37	Splenic lymphoma	Nodular lymphoma almost marginal diffuse	X, F, 10 years
P 38	Splenic lymphoma	Diffuse Mantle cell lymphoma	X, M, 10 years
P 39	Splenic lymphoma	Diffuse lymphoma (medium cells)	Lagotto, M, 9 years
P 40	Splenic lymphoma	Diffuse lymphoma (marginal)	X, F c, 11 years
P 41	Splenic lymphoma	Peripheral T-cell lymphoma (PTCL)	Boxer, F, 10 years
P 42	Splenic lymphoma	Diffuse lymphoma	X, F, 8 years
P 43	Splenic lymphoma	Diffuse lymphoma (medium cells)	German Shepherd, F, 10 years
P 44	Splenic lymphoma	Diffuse lymphoma (big cells)	West Highland White Terrier, F, 7 years
P 45	Splenic lymphoma	Peripheral T-cell lymphoma (PTCL)	X, M, 8 years
P 46	Splenic lymphoma	Hepatosplenic lymphoma	Boxer, M, 7 years
P 47	Splenic lymphoma	Diffuse lymphoma (big cells)	Siberian Husky, M, 11 years
P 48	Splenic lymphoma	Diffuse lymphoma (Plasmacytoma/Myeloma)	Pyrenean mountain dog, F, 11 years

Table 8. FFPE splenic lymphomas, list and classification. 8A) FFPE non-neoplastic spleen samples. 8B) FFPE splenic lymphoma samples Legend: F = Female, M = male, X = mixed race

1.3.2 Cells sorting by flow cytometry

Flow cytometry: technique and instrument

Flow cytometry is a methodic that allows the measurement and characterization of cells suspended in a fluid medium. In particular, this methodic makes possible the measurement of multiple properties (size, graininess, etc. ..) of individual cells at high speed, allowing very detailed cytologic analysis. The appearance of the flow cytometry, around the 70s, resulting in a rapid and intensive development of cytochemical and histological techniques. The flow cytometry, thanks to the use of monoclonal antibodies labeled with fluorescein isothiocyanate (FITC), has brought great impetus to the study of the immune system. The great complexity of the immune system and the presence of different subpopulations that react with the same antibody, have stimulated the development of monoclonal antibodies ever more specific, the search for new fluorescent dyes coniugated to antibodies without altering their capacity of binding the antigen and the creation of multiparameter flow cytometers that using fluorophores with different emission spectra. A turning point in flow cytometry was the development of dyes such as phycobiliproteins; these fluorochromes are natural water-soluble, fluorescent at neutral pH, easily conjugated with monoclonal antibodies and with high quantum yields. The Phycoerythrin (PE), for example, is a fluorochrome which is excited by the same wavelength of FITC (488 nm) but has a different emission spectrum, and for this reason the two fluorochromes can be used together to provide a very sensitive double marking detecting system. The flow cytometry, as well as being a method now essential for cytological analysis qualitative and quantitative, also allows to separate physically, from heterogeneous cell populations, subpopulations of specific cells thanks to specific membrane structures, present on the cells surface, recognized by specific monoclonal antibodies. This procedure is called "cell sorting" and allows to obtain cell populations with a purity greater than 95%. The operating principle of flow cytometry is based on the interaction of each cell with a beam of focused light from a laser or a mercury vapor lamp. The

meeting between the light beam and the cell, previously labeled with an antibody conjugated to a fluorochrome, generates signals that are related to the physical characteristics of the cell and the presence, on the cell surface, of specific fluorescent molecules.

The instrument utilized in flow cytometry is called flow cytometer and it is composed of 5 functional units:

1. fluidic system
2. optical system
3. electronic system
4. mechanical system
5. system software (SW) - data analysis

The fluidic system

The fluidic system brings the sample cells in the area of interaction with the light beam. The main part of the entire system is the flow cell, consisting of a "nozzle" (a cone that contains the needle for the injection) and a capillary. For set up individually the sample cells in columns, is necessary the presence of a laminar type of motion at the center of the capillary, guaranteed by a physiological solution (buffer) that acts as a dragging liquid for the sample. Liquid and sample arrive in the capillary where takes place the interaction with the light.

The optical system

The optical system consists of a series of diaphragms, lenses, filters and dichroic mirrors. All this to convey the beam of light as precisely as possible on the detector. The diaphragms improve the ratio between signal and background noise reducing scattered light; lenses serve to focus the laser beam and the fluorescence light; mirrors and filters are used to select the wavelengths of excitation spectra for emission continues and also the wavelengths that affect detectors.

The electronic system

The electronic system consists of several subsystems:

- Opto-detectors: convert light energy (photons) into electricity (electrons);
- Photodiodes: collect the scattered light intensity, which is the parameter used for the determination of the size and granularity of the cell;
- Photomultiplier tubes: detect the emitted fluorescence.

In practice, the light incise on a photosensitive material (cathode), releasing electrons that are accelerated by different potential differences and a series of electrodes in cascade which increase the flow of electrons, in order to have at the end a easily measurable current. The problem is that the eddy currents generated by background noise it also amplifies. For this reason a filter system is used. Then the electrical signals detected are measured in width, intensity and area. The data obtained are inserted into a channel that collects all the data within a certain range. Finally, a graph that shows the distribution of cells along a series of channels and for each channel (i.e., for a series of values) was made, and it provides a certain number of cells.

The mechanical system

The mechanical system allows to adjust the speed of release of the sample.

The System software (SW) - data analysis

Associated with the instrument there is a computer that stores, processes and presents data. Can be setted a threshold, or a regions (gates), that allows to capture only the parameters for some cell subpopulations or otherwise to exclude debris and impurities. The data already acquired can also be retrieved and reworked.

Cell subset purification:

Peripheral mononuclear cells (PBMC) and polymorphonuclear (PMN) cells from 3 healthy dogs were isolated over ficoll-hypaque discontinuous density gradient. Platelets (PLT) were recovered from plasma through centrifugation. The percentage of purity and the number of recovered cells were evaluated using Sysmex XT2000iV automated hematology analyzer (Sysmex, Kobe, Japan) and microscopically after cytocentrifugation and May Grünwald-Giemsa stain. To isolate lymphocyte subpopulations, PBMC were adjusted at 2 x 106 113 in 200 µl PBS and labelled with 200 µl of lineage specific antibody: anti-canine CD4-FITC and anti-canine CD8pe for T-cells, anti-CD21pe for mature B-cells. CD4, CD8, and CD21 positive cells were sorted using a fluorescent activated cell sorter (BD FACSVantage, BD Biosciences, San Jose, CA, USA). A minimum sorting yield of 1 x 105 cells with more than 95% purity was considered suitable for molecular biologyinvestigation.

1.3.3 Classification of lymphoma and CLL samples

A. Immunophenotyping by flow cytometry

For all the fresh samples (peripheral blood and lymph node aspirates) a Immunophenotyping by flow cytometry of neoplastic cells using a FACSort instrument (Becton Dickinson) (Comazzi S. et al., 2006) was performed. In short, the following canine antigens were analysed using the corresponding antibodies: CD45 (clone mAb YKIX716.13 Serotec, Oxford, UK, all leukocytes), CD18 (clone mAb CA1.4E9, Serotec, all leukocytes), CD3-FITC (mAb clone CA17.2A12, Serotec, T lymphocytes), CD4-FITC, CD8-PE, CD21, CD11b (MAb clone CA163E10, Serotec, granulocytes and monocytes), CD34-PE (clone 1H6 mAb Pharmingen, BD Bioscience, cells blasts), and CD49d (clone mAb Ca4.5B3, PF Moore, Davis, CA, United States of America, T lymphocytes, myeloid cells). For unlabelled primary antibodies, indirect labeling was performed using secondary rabbit anti-mouse FITC-labeled polyclonal antibody (Serotec). Intracytoplasmic staining with anti CD79a-PE (clone HM57 Dako, Glostrup, Denmark, B cells, all stages) was performed after permeabilization using BD FACS permeabilizing solution 2 (Becton Dickinson

B. Immunophenotyping with immunohistochemistry

The tissue samples were embedded in paraffin after formalin fixation. For histology, tissue sections of 5 micron in thickness were put on slides and stained with hematoxylin-eosin. For immunohistochemistry, sections of 5 microns were put on a glass slide coated with polylysine and colored according to the standard technique of peroxidase avidin-biotin. The antibodies used for phenotyping analysis of FFPE samples were: anti-CD18 to identify all leukocytes and used diluted 1:20 (Leukocyte Biology Laboratory, PF Moore, University of California, CA, USA), anti-CD79a and anti-CD20 (Dako) for recognizing the B cells and used diluted 1:40. Anti-CD3-epsilon (Dako) diluted 1:900 was used to identify the chain Y intracellular expressed in the majority of lymphocytes T. Negative controls consist of substitution of specific antibodies with an isotype specific

species, an irrelevant monoclonal antibody, or with the omission of the primary antibody. All samples of lymphoma were then analyzed under a microscope and classified according to the histological classification of hematopoietic tumors of domestic animals (Valli V.E. et al. 2002).

C. Grading classification of FFPE splenic lymphoma samples

For the splenic lymphoma FFPE samples a retrospective cohort study was performed. Dogs with confirmed primary splenic lymphoma were identified through medical record, biopsy and necropsy database search of the electronic archives of the Anatomical Pathology service of the University of Milan, Italy. A total of 29 cases of primary splenic lymphomas were evaluated and tissue from 7 normal spleens from necropsy investigations were included as controls. Clinical data of the dogs were recorded. Tissue samples were fixed in 10% buffered formalin, routinely processed, and 5 micron sections were stained with haematoxylin and eosin for histopathological evaluation. Lymphomas were classified according with the WHO classification (Valli V.E. et al., 2011); as part of the WHO classification, cell size and the number of mitoses were assessed. The pathologists classified the cell size as small (nuclei approximately 1 times the diameter of a red blood cell), intermediate (nuclei approximately 1.5–2 times the diameter of a red blood cell) and large (nuclei approximately 2.0–2.5 times the diameter of a red blood cell). Number of mitoses was evaluated by counting mitoses per 10 representative, artefact free fields at 400X magnification by three pathologists independently. If mitotic index differed among pathologists a mean of the three counts was calculated (Table 9). Grade was determined according with the WHO classification (cell size, diagnosis and mitotic index). On the basis of the grading, the samples were divided into two categories: **Low (L) tumor samples** and **Intermediate/High (I/H) tumor samples**.

SAMPLE	IM	Mitosis counts, 10 fields, 400X										GRADE	P
P 20	0,2	0	0	1	0	0	0	1	0	0	0	L	B
P 21	0,4	0	0	0	1	0	2	1	0	0	1	L	B
P 22	0,1	1	0	0	0	0	0	0	0	0	0	L	B
P 23	0	0	0	0	0	0	0	0	0	0	0	L	B
P 24	0,3	0	0	0	0	0	1	0	2	1	0	L	B
P 25	0,7	2	0	0	0	1	1	1	0	2	0	L	B
P 26	0,3	1	1	0	0	0	0	0	1	0	0	L	B
P 27	0,3	0	1	0	0	1	0	0	1	0	0	L	B
P 28	0,2	1	0	0	0	0	0	1	0	0	0	L	B
P 29	0,2	0	0	1	0	1	0	0	0	0	0	L	B
P 30	0,2	1	0	0	0	0	1	0	0	0	0	L	B
P 31	0,4	0	1	1	2	0	0	0	0	0	0	L	B
P 32	0,3	1	0	0	0	0	0	0	0	2	0	L	T
P 33	0,8	2	1	0	1	0	1	1	2	0	0	L	B
P 34	0,9	0	0	0	1	3	0	2	2	0	1	L	B
P 35	0,9	0	0	6	0	0	1	1	1	0	0	L	B
P 36	0,6	1	1	2	0	1	1	0	0	0	0	L	B
P 37	0,4	0	0	0	0	1	1	0	1	1	0	L	B
P 38	0,2	0	0	0	0	0	0	1	0	1	0	L	B
P 39	1,7	2	1	5	1	3	2	1	2	0	1	L	NK like
P 40	1,5	1	3	2	2	0	0	1	3	2	1	L/I	B
P 41	3,3	10	5	2	7	6	3	0	1	2	2	I	T
P 42	5,3	9	6	3	7	5	4	6	4	3	6	I	B
P 43	7,9	12	5	6	7	1	7	9	14	9	9	I	NK like
P 44	2,3	2	1	0	2	2	4	2	3	2	5	I	B
P 45	3,6	5	3	3	4	4	2	2	4	2	7	I	T
P 46	3,5	4	3	5	4	3	4	6	0	3	3	I/H	NK like
P 47	11,4	13	11	6	14	11	17	8	13	10	11	H	B
P 48	27,3	14	35	33	38	32	28	28	29	22	14	H	B

Table 9. Sample grading of FFPE splenic tissue samples.
IM= mitotic index, L= low, I= intermediate, H= high, P= phenotype

D. Phenotype assessment of FFPE splenic lymphoma samples

For the application of the WHO classification for the tumoral cells, the phenotype was assessed. Briefly, 5 micron tissue sections were glued onto polylisine coated glass slides and were dewaxed and rehydrated before immunostaining. Immunohistochemical staining was performed utilizing monoclonal anti-human CD79a-α (Dako, Glostrup, Denmark) at a 1:100 and polyclonal anti-human CD20 (Neomarkers, Freemont, CA) at 1:400 were utilized for B cells recognition. Polyclonal anti-CD3-ε (Dako, Glostrup, Denmark) was utilized at 1:900 dilution for the identification of the intracellular epsilon chain expressed mostly in T cells. These antibodies recognize epitopes conserved in many species, including dogs (Jubala et al., 2005; Flood-Knapik et al., 2012; Stefanello et al., 2011). Heat induced antigen retrieval was performed by incubation in pH 6,4 citrate buffer and heated in a microwave oven at maximum power for 1 minute and at 750 watt for 3 minutes for two times and cooled for 20 minutes. Negative controls consisted of substitution of specific antibodies with an isotype-matched, irrelevant monoclonal antibody or omission of the primary antibody. Primary antibodies were incubated overnight in a humidified chamber at 4°C. Secondary detection was performed with the Avidin-Biotin enzyme Complex (ABC kit, Vectastain®, Burlingame, CA, U.S.A.) for 30 minutes. The reaction was developed with the peroxidase Amino-9-ethyl-carbazole (AEC) substrate kit (Dako®, Glostrup, Denmark). Smears were counterstained with Mayer's hematoxylin for 3 minutes and cover-slipped with an aqueous mounting media (Glicerine, Sigma-Aldrich®, St. Louis, MO, U.S.A.).

1.3.4 RNA extraction

1. From fresh/frozen samples

The RNA was stabilized immediately after sampling by the addition of a stabilizing solution RNA (RNAlater ®, Ambion Inc., Austin, TX, USA) and storage at -80 ° until the extraction. Total RNA was extracted from whole blood samples with the miRNA Isolation Kit ™ Mirvana of Ambion, adapting the procedure for extraction of total RNA from tissue (whole blood is first centrifuged to remove the RNA later and then the pellet is lysed according to the procedure). The Mirvana ™ miRNA Isolation Kit has been developed for the purification of RNA suitable for studies of miRNA and siRNA. The kit uses organic extraction followed by immobilization of the RNA on a glass fiber filter to purify total RNA or RNA enriched for small species from cells or tissues samples. This extraction method presents considerable differences compared to classical chemical extraction method. In fact, the chemical extraction uses high concentrations of chaotropic salts with acid solutions of phenol or phenol-chloroform, to inactivate RNases and to purify RNA from other biomolecules. These methods lead to the recovery of pure RNA, however, provide an additional step of removal of salts and concentration with precipitation in alcohol. The latter step is not suitable for the recovery of miRNAs. The method of solid phase extraction using high concentrations of salts or salts and alcohol to decrease the affinity of RNA for water and increase it for the support of the solid phase. The Mirvana ™ miRNA Isolation Kit combines the advantages of the two methods, while avoiding their disadvantages.

The kit consists on 2 steps:

- Cells lysis and organic extraction: the sample is broken using a denaturant lysis buffer. Subsequently, the sample is subjected to extraction with phenol-chloroform, which allows a purification also removing most of the DNA.
- RNA final purification on a glass fiber filter: absolute ethanol is added to sample which is then loaded onto the column containing the filter that

immobilizes the RNA. The filter is washed several times with special solutions, and finally the RNA is eluted with 100 µl of water previously heated to 95 ° C.

2. From formalin-fixed and paraffin-embedded samples

The samples of FFPE splenic tissue are extracted with the RecoverAll kit of Ambion, following the procedure for Total RNA. The RecoverAll ™ Total Nucleic Acid Isolation Kit is developed to extract total nucleic acid (RNA, miRNA and DNA) from tissues fixed in formaldehyde or paraformaldehyde or paraffin-embedded (FFPE). In a single reaction sections of more than 20 µm can be processed. The FFPE samples are dewaxed using xylene attended by a series of washes in ethanol. Subsequently, the samples are subjected to digestion with a protease. The nucleic acids are then purified using a rapid methodology with glass fibers filter of which includes a treatment with nuclease directly on the filter, and finally are eluted with 60 µl of water previously heated to 95 ° C.

3. From cytologic glass smears

For cytologic glass smears we performed two different extraction protocols depending on the type of sample: peripheral blood or lymph node aspirate. The lymph node aspirate samples were incubated in xylene for 2-5 days in order to facilitate detachment of the coverslip and, subsequently, are subjected to two ethanol washes, first using 100% ethanol and then 70% ethanol. The smears are air dried and then the samples are retrieved from the surface of the slidse by means of scratching in 400 microliters of a solution of 75:25 RNA later-PBS: each sample is scraped from the coverslip, directly in the solution, in two steps from 200 microliters each, using the blade of a sterile scalpel. The solutions after scratching are placed in an eppendorf. Each sample is then subjected to extraction and quantification of total RNA using miRNA Isolation Kit ™ Mirvana as described in the previous paragraph. On the other hand, on peripheral blood slides samples, given the smallest number of cells and the lowest quality of smears present, the RNA extraction is performed using a TRIzol protocol,

developed for the extraction of miRNAs from plasma (Laterza et al. 2009). In detail, the cytologic glass smears are incubated in xylene for 2-5 days and, subsequently, are subjected to two washings with 100% ethanol and 70% respectively. Then, the cytologic glass smears are air dried and the samples are retrieved from the surface of the slide by scratching in 1 ml of TRIzol: each sample is scraped from the slide, directly in the solution, in four steps from 250 microliters each, using the blade sterile as scalpel. The solutions after scratching are placed in an eppendorf. Each sample is then incubated briefly at room temperature and then are added 200 µl of chloroform. The samples thus obtained are centrifuged at 12000 rpm for 15 minutes at 4 °C in order to facilitate the separation of the three phases: inferior (DNA), interphase (proteins) and upper aqueous phase (RNA). At this point the aqueous phases, containing the RNA, are recovered and 800 µl of isopropanol are added. After a further centrifugation (12000 rpm for 10 minutes at 4 °C) and elimination of the supernatant, 1 ml of 75% ethanol is added. The samples are then incubate at room temperature for 10 minutes and, after a final centrifugation (12000 rpm for 10 minutes at 4 °C), the supernatants are removed and the samples are allowed to dry under chemical hood. Finally the RNAs are resuspended with 25 µl of water.

1.3.5 RNA quantification and quality control

The concentration of RNA extracts was determined, in all cases with the exception of RNA obtained from CLL cytologic glass smears, by using a spectrophotometer ND-100 (NanoDrop® Technologies Inc., Wilmington, DE, USA) which expresses the concentration in terms of nanograms/microliter (ng/µl) accompanied by the ratio between absorbance at 260 nm and absorbance at 280 nm (A260/A280 ratio). For RNA obtained by cytologic glass smears and from the corresponding fresh samples we carried out a quality control using Agilent Bioanalyzer 2100, in combination with the kit "RNA 6000 Nano LabChip ®" and the kit "Agilent Small RNA Chip".

The Agilent Bioanalyzer 2100 is an instrument for the RNA quantitative and qualitative analysis. The quantification is relative because it is based on a comparison with a marker of known molecular weight. Each chip contains a series of tightly interconnected microchannels: the nucleic acid fragments are then separated according to their molecular weight as in a standard electrophoresis in agarose gel. The microchannels of each chip are filled with a matrix and a fluorochrome:

- samples move through the microchannels from the hole of loading
- each sample is inserted into the separation channel
- samples are separated through an electrophoretic run
- at the end of the electrophoresis, samples are read according to their fluorescence and this information is translated into a typical image of gel electrophoresis and electropherograms.

The system, thanks to a dedicated software, is able to measure the quality and quantity of the RNA samples. At the end of the run, the instrument provides an electropherogram for each individual sample, the virtual image of a typical agarose gel and a tabulation with the results of quantification and contamination. In the case of Nano chip the instrument returns a value defined RIN (RNA Integrity Number) that allows to assign a quality index for the total RNA examined. This parameter has a scale that goes from 10, which indicates RNA of

excellent quality, to zero, which indicates that RNA is completely degraded. The Small RNA chips, however, is able to provide the percentage of enrichment of RNA fragments long about 20-40 nt, those corresponding to a population of miRNAs.

1.3.6 Search of miRNAs in miRBASE

Twelve computationally-predicted canine miRNA sequences (cfa-let-7a, cfa-miR-15a, miR-16a-cfa, cfa-miR-17-5p, miR-cfa -21, cfa-miR-26b, miR-29b-cfa, cfa-miR-125b, miR-150-cfa, cfa-miR-155, miR-cfa-181st and cfa-miR-223), known in humans as ubiquitous or typical of hematopoietic cells, were obtained either from miRBase (http://microrna.sanger.ac.uk) or from literature. The sequence identity of the mature miRNA sequence with the corresponding homologous human mature miRNA sequence was confirmed by BLAST alignment (http://blast.ncbi.nlm.nih.gov/bl2seq/wblast2.cgi). The corresponding precursor sequence were also checked to show a minimum 95% identity between the two species. Besides, the small nucleolar gene RNU6B was selected as a non-miRNA candidate EC since its previous use as unique EC gene in canine miRNA expression studies by other researchers (Boggs et al., 2007 and 2008).

1.3.7 Specific gene reverse transcription of miRNAs

For each sample, and for each miRNA of interest, 10 nanograms of RNA (CLLs) and 20 nanograms of RNA (lymphomas) were reverse transcribed to cDNA using the corresponding TaqMan ® MicroRNA Assay kit (Applied Biosystems Inc., Foster City, CA, USA) and TaqMan ® Assay snoRNU6B (Applied Biosystems Inc., Foster City, CA, USA). These kits are marketed specifically for humans but are also valid for the corresponding canine miRNA when the sequence is completely conserved. The RT reactions were performed with specific RT primers stem-loop for each miRNA and contained in the corresponding MicroRNA TaqMan ® Assay.

We used the reverse transcription kit microRNA TaqMan®, following the manufacturer's instructions.

TaqMan MicroRNA Reverse Transcription General Procedure, Kit ABI

The reverse transcription master mix is prepared as follows (amounts for 10 reactions already include a round up of 10% to compensate losses due to pipetting):

Component	1 sample	10 samples
dNTP mix (100 mM)	0.15 µl	1.7 µl
Multiscribe RT enz. (50 U/mcl)	1 µl	11 µl
10x RT Buffer	1.5 µl	16.5 µl
RNase Inhibitor (20 U/mcl)	0.19 µl	2.1 µl
Water RNasi-free	4.16 µl	45.7 µl
Total	**7 µl**	**77 µl**

First, for every 7 µl of retrotranscription master mix, 5 µL of each sample total RNA (that contains 20 or 10 nanograms) are added, except for CLL cytologic glass smears where 5 microliters of the aqueous solution directly obtained after extraction with TRIzol, without prior quantification, are added. Then, an Eppendorf 0.5 µl for each reverse transcription reaction is prepared and 12 µl of master mix, already added of RNA, are aliquoted into each tube. After which, 3 µl of the reverse transcription primers, specific for a given target, are added to each tube. The retrotranscription reaction provides the following thermal protocol: incubation on ice for 5 minutes, followed by 30 minutes at 16 ° C, 30 minutes at 42 ° C and 5 minutes at 85 ° C.

1.3.8 Standard curves construction for absolute quantification

The miRNAs absolute quantification was calculated by interpolation of the corresponding threshold cycle (Ct) values with a reference curves obtained through miRNA-specific RT reaction followed by TaqMan real-time PCR quantification of 1:100 serial diluition points of the mirVana™ miRNA Reference Panel v9.1 (Ambion) following manufacturer's instructions. The miRNA Reference Panel contains hundreds of miRNAs with known concentration. In particular, we used the following points of serial dilution for each miRNA of interest: 1 femtomole, 10^{-2} femtomoles, 10^{-4} femtomoles, 10^{-6} femtomoles. The log ranges of the reference curves were chosen encompassing the putative amount of each target sequence that could be expected in cDNA prepared from our kind of samples.

1.3.9 Standard curves construction for efficiency calculation and relative quantification

To evaluate the efficiency of the MicroRNA TaqMan® Assay, serial amounts (125 ng, 25 ng, 5 ng, 1 ng, 0.2 ng and 0.04 ng) of total RNA from non-neoplastic control tissue samples were used to obtain standard curves. The 125 ng-0.04 ng range was designed to encompass the 20 ng and 10 ng of total RNA that is the amount used for expression profiling. No-template RT reactions were performed as negative control for each target.

Relative expression of each miRNA was calculated using the comparative delta-delta Ct method with the three most stable EC genes selected as described below.

1.3.10 qRT-PCR TaqMan

The real time PCR reactions were performed utilizing the TaqMan MicroRNA Assay (Applied Biosystems) according to the instructions described by the manufacturer in 20 microliter total containing the following reagents quantities:

- ✓ 1.33 microliter RT product,
- ✓ 1X TaqMan® Gene Expression Master Mix, and
- ✓ 1X specific MicroRNA TaqMan® Assay.

Each reaction was assayed in triplicate on a 96-well plate. The real time amplification reactions were run on an iQ™5 Real Time PCR Detection System (Bio-Rad, Hercules, CA, USA) following the thermal protocol recommended for MicroRNA TaqMan® Assays by the manufacturer.

The absolute quantification for each miRNA retrotranscribed is calculated by interpolation of the corresponding threshold values with the straight line obtained from Reference Panel, while the relative quantification was determined by the comparative method ΔΔCT (Giulietti A. et al, 2001).

1.3.11 Cloning of the amplifieds and DNA sequencing

The specificity of each MicroRNA TaqMan® Assay for the corresponding canine target was assessed by amplicon cloning followed by DNA sequencing. The amplicons were run on 2.5 ethidium-bromide agarose gel followed by UV-visualization and gel-purification by QiaquickTM Gel Extraction kit (Qiagen GmbH, Hilden, Germany). The concentration of purified amplicons was spectrofotometrically measured using a ND-100 Spectrophotometer (NanoDrop technology). Each quantitated amplicon was ligated into a P-GEM T-Easy plasmid (Promega Corporation, Madison, WI, USA) following manufacturer's instructions. The constructs thus obtained were used to transform cells of E. coli DH5alpha. The colonies grown on the plate after processing were analyzed for the presence of the plasmid containing the insert by PCR using the primers T7 and SP6 specific for the plasmid. Two positive clones for each target were sequenced using T7

and SP6 primers and the DNA sequencer ABI PRISM 310 (Applied Biosystems). The obtained sequences were aligned with the expected target sequences using ClustalW.

1.3.12 Housekeeping gene's selection using NormFinder and geNorm algorithms

The candidate reference genes Ct values, obtained by real-time qPCR, were analyzed in order to assess the stability of expression in all samples using the software NormFinder (Andersen C.L. et al., 2004), available at http://www.mdl.dk/publicationsnormfinder.htm, and the geNorm software, version 3.5 (Vandesompele J. et al., 2002), available at http://www.medgen.ugent.be/jvdesomp/genorm/.

1.3.13 Calculation of ΔΔCt

The miRNAs threshold cycle (Ct) values, obtained with the qRT-PCR, were analyzed utilizing the comparative ΔΔCT method (Giulietti A. et al, 2001). This method compares the Ct value of the test sample with the Ct value of the reference sample (the corresponding non-neoplastic tissue). The two Ct values are normalized according to the values of one or more endogenous control (EC) genes. The relative expression of the gene of interest in the different samples was calculated according to the following formula:

$$\Delta Ct = Ct\ (\text{target gene}) - Ct\ (\text{housekeeping gene})$$

Ct target gene- indicates the value of the threshold cycle for the gene of interest, Ct housekeeping gene- indicates the value of the threshold cycle for the transcript used as reference.

Subsequently, the relative expression of all samples compared to a sample of non-neoplastic control was calculated as follows:

$$Er = 2^{-\Delta\Delta Ct} \quad ; \quad \Delta\Delta Ct = \Delta Ct\ (sample) - \Delta Ct\ (control)$$

Er indicates the relative expression, ΔCt (sample) indicates the difference of Ct values calculated for the individual sample, ΔCt (control) indicates the difference of Ct values calculated for the sample taken as a reference.
Then, for each miRNA of interest of each sample was calculated the geometric mean of the values of differential expression obtained for each EC.

1.3.14 Statistical analysis

Significance analysis of expression data obtained in the present work were performed using the nonparametric Kruskal-Wallis test and Mann-Whitney test, using SPSS statistical package (version 13, SPSS, Chicago, IL, USA). Furthermore, to compare the extraction method from cytologic glass smears with the extraction method from fresh/frozen sample was used the test Passing-Bablok, which allows to detect the presence of correlations, also non-linear, followed by Bland-Altman test, which provide indications about a possible correlation and allows to detect the presence of errors proportional and / or constants. A p-value less than 0.05 was considered significant.

1.4 RESULTS

1.4.1 Extracted RNA quantification and quality control

The total RNA quantification procedure showed that the RNA extraction methods (miRNA Mirvana Isolation Kit ™ from fresh/frozen samples and Ambion RecoverAll kit from FFPE samples) has provided high quality RNA (ratio generally around 2) and in good concentration, largely sufficient for subsequent analysis. The tables below show the list of total RNA extracts, their concentrations and their A260/A280 ratio.

A. Fresh/frozen lymph node aspirates:

Sample code	Sample type	Concentration	Ratio
F 1	Lymphoma T	3140 ng/µl	2.03
F 2	Lymphoma T	3245 ng/µl	2.04
F 3	Lymphoma T	490 ng/µl	2.00
F 4	Lymphoma T	685 ng/µl	2.06
F 5	Lymphoma T	172 ng/µl	2.07
F 6	Lymphoma B	304 ng/µl	2.02
F 7	Lymphoma B	178 ng/µl	2
F 8	Lymphoma B	2035 ng/µl	2.05
F 9	Lymphoma B	155 ng/µl	1.97
F 10	Lymphoma B	87 ng/µl	2.08
F 11	Lymphoma B	336 ng/µl	2.06
F 12	Lymphoma B	416 ng/µl	2.04
F 13	Lymphoma B	237 ng/µl	2.09
F 14	Lymphoma B	1224 ng/µl	2.03
F 15	Lymphoma B	310 ng/µl	2.01
F 16	Non neoplastic	913 ng/µl	2.01
F 17	Non neoplastic	70 ng/µl	1.97
F 18	Non neoplastic	410 ng/µl	1,97

B. FFPE lymph node aspirates:

Sample code	Sample type	Concentration	Ratio
P 1	Lymphoma T	180 ng/µl	2.01
P 2	Lymphoma T	228 ng/µl	1.98
P 3	Lymphoma B	326 ng/µl	2
P 4	Lymphoma B	63 ng/µl	2.06
P 5	Lymphoma B	64 ng/µl	1.97
P 6	Lymphoma B	1810 ng/µl	2.01
P 7	Lymphoma B	223 ng/µl	1.99
P 8	Non neoplastic	181 ng/µl	1.94
P 9	Non neoplastic	42 ng/µl	2.05
P 10	Non neoplastic	190 ng/µl	2.06
P 11	Non neoplastic	92 ng/µl	2.03
P 12	Non neoplastic	128 ng/µl	1.88

C. Fresh/frozen CLLs:

Sample code	Sample type	Concentration	Ratio
F 19	Non neoplastic blood	10 ng/µl	1.80
F 20	Non neoplastic blood	50 ng/µl	2.02
F 21	Non neoplastic blood	46 ng/µl	2.02
F 22	Non neoplastic blood	123 ng/µl	1.91
F 23	Non neoplastic blood	28 ng/µl	2.01
F 24	Non neoplastic blood	120 ng/µl	1.98
F 25	T- CLL	315 ng/µl	2.06
F 26	T- CLL	740 ng/µl	2.09
F 27	T- CLL	233 ng/µl	2
F 28	T- CLL	275 ng/µl	2.03
F 29	T- CLL	110 ng/µl	1.88
F 30	T- CLL	82 ng/µl	2.07
F 31	T- CLL	67 ng/µl	2.16
F 32	T- CLL	118 ng/µl	2.07
F 33	B- CLL	128 ng/µl	2.07
F 34	B- CLL	71 ng/µl	2.00
F 35	B- CLL	63 ng/µl	2.04
F 36	B- CLL	329 ng/µl	2.08
F 37	B- CLL	63 ng/µl	2.05
F 38	B- CLL	57 ng/µl	2
F 39	B- CLL	37 ng/µl	1.91
F 40	B- CLL	107 ng/µl	2.1

D. FFPE splenic lymphomas:

Sample code	Sample type	Concentration	Ratio
P 13	Non-neoplastic	45 ng/µl	1.93
P 14	Non-neoplastic	91 ng/µl	1.89
P 15	Non-neoplastic	78 ng/µl	1.95
P 16	Non-neoplastic	158 ng/µl	1.99
P 17	Non-neoplastic	157 ng/µl	2.03
P 18	Non-neoplastic	25 ng/µl	2.19
P 19	Non-neoplastic	60 ng/µl	1.99
P 20	Splenic lymphoma	145 ng/µl	1.97
P 21	Splenic lymphoma	313 ng/µl	2.01
P 22	Splenic lymphoma	46 ng/µl	2.00
P 23	Splenic lymphoma	55 ng/µl	1.85
P 24	Splenic lymphoma	135 ng/µl	1.96
P 25	Splenic lymphoma	1320 ng/µl	1.94
P 26	Splenic lymphoma	40 ng/µl	2.05
P 27	Splenic lymphoma	362 ng/µl	2.01
P 28	Splenic lymphoma	130 ng/µl	1.88
P 29	Splenic lymphoma	55 ng/µl	1.90
P 30	Splenic lymphoma	103 ng/µl	1.89
P 31	Splenic lymphoma	113 ng/µl	1.92
P 32	Splenic lymphoma	362 ng/µl	2.02
P 33	Splenic lymphoma	130 ng/µl	1.88
P 34	Splenic lymphoma	55 ng/µl	1.90
P 35	Splenic lymphoma	103 ng/µl	1.89
P 36	Splenic lymphoma	153 ng/µl	1.92
P 37	Splenic lymphoma	342 ng/µl	2.01
P 38	Splenic lymphoma	130 ng/µl	1.88
P 39	Splenic lymphoma	55 ng/µl	1.90
P 30	Splenic lymphoma	103 ng/µl	1.89
P 31	Splenic lymphoma	113 ng/µl	1.92
P 32	Splenic lymphoma	362 ng/µl	2.00
P 33	Splenic lymphoma	130 ng/µl	2.05
P 34	Splenic lymphoma	58 ng/µl	1.90
P 35	Splenic lymphoma	103 ng/µl	1.89
P 36	Splenic lymphoma	113 ng/µl	1.92
P 37	Splenic lymphoma	342 ng/µl	2.01
P 38	Splenic lymphoma	128 ng/µl	1.90
P 39	Splenic lymphoma	99 ng/µl	1.98
P 40	Splenic lymphoma	49 ng/µl	1.89
P 41	Splenic lymphoma	37 ng/µl	1.79
P 42	Splenic lymphoma	65 ng/µl	2.01
P 43	Splenic lymphoma	38 ng/µl	1.88
P 44	Splenic lymphoma	167 ng/µl	1.80
P 45	Splenic lymphoma	29 ng/µl	1.89
P 46	Splenic lymphoma	136 ng/µl	1.92

P 47	Splenic lymphoma	267 ng/µl	2.02
P 48	Splenic lymphoma	145 ng/µl	1.98

Table 10. Results of NanoDrop quantification. List of total RNA extracts, with concentration nanograms/microliter (ng/µl) and ratio 260/280. A) lymph node aspirates fresh/frozen B) lymph node aspirates FFPE, C) Samples peripheral blood fresh/frozen, controls and CLL, D) splenic tissue samples embedded in paraffin, controls and lymphomas.

As shown in Table 11, also the extraction protocols from lymph node aspirated cytologic glass smears were generally able to provide RNA in good concentration, not too far from that obtained from the corresponding frozen samples (which are extracted from an amount of sample significantly higher) and with high quality (the optimal ratio A260/A280 for RNA is between 1.8 and 2.1).

Sample	P	Concentration (ng/µ)		Ratio A260/A280	
		Smear	Fresh/frozen	Smear	Fresh/frozen
C 1/F 1	T	23	155	1,87	1,97
C 2/F 2	T	60	304	2	2,02
C 3/F 3	T	50	510	1,52	2,04
C 4/F 4	T	24	60	1,84	1,61
C 5/F 5	T	132	34	1,96	1,94
C 6/F 6	B	158	3245	2,03	2,04
C 7/F 7	B	55	685	1,97	2,06
C 8/F 8	B	17	178	2	2
C 9/F 9	B	50	2035	1,83	2,05
C 10/F 10	B	66	416	1,91	2,04
C 11/F 11	B	19	237	1,93	2,09
C 12/F 12	B	107	920	1,94	2,03
C 13/F 13	B	55	85	1,97	2,05
C 14/F 14	B	48	1300	1,4	2,07
C 15/F 15	B	55	74	1,78	2,05

Table 11. Concentrations and relative A260/A280 ratios of RNA extracted from lymph node aspirates fresh/frozen and their equivalent cytologic glass smears

The total RNA obtained from peripheral blood cytologic glass smears of leukemic dogs was not sufficiently abundant to be adequately quantified with the micro spectrophotometer. This is not surprising considering the minimum volume of blood (few microliter) that is usually utilized to prepare a cytologic smear, and that this kind of samples naturally contains fewer cells rather than a similar volume of aspirated lymph node lymphoma. So, Agilent Bioanalyzer 2100 instrument was utilized to analyze the total RNA extracted from cytologic glass smears and its corresponding fresh sample. For each sample is provided an electropherogram, the virtual image of an agarose gel, the total RNA quantification, the ratio between the two ribosomal RNA and the RIN (RNA INTEGRITY NUMBER). The value of the ratio between the two ribosomal RNA works as an indicator of the quality of RNA in question. As a result of the relationship existing between the two ribosomal RNA, the optimal value is 2. In the course of our project, unable to obtain RNA of such high quality, we decided to consider of good quality an RNA with a two ribosomal ratio included between 1.2 and 2. In Figure 14 is shown an example of electropherogram and gel image of a lymphoma lymph node sample, both from cytologic glass smears that the respective fresh lymph node aspirate. From the observation of the electropherograms, we can note that the fresh sample (F 6), presents a total RNA of good quality since the 2 peaks representative 18S rRNA and 28S are visible. From the results obtained from the cytologic glass smears of the corresponding sample (C 6) we can note that the RNA is totally degraded because the RIN is N/A. This data is not surprising because the cytologic glass smears are stored in non-RNase free conditions and at room temperature, moreover the nucleic acid may be subject to further degradation during the step of mechanical removal of cells from cytologic glass smears.

F 6

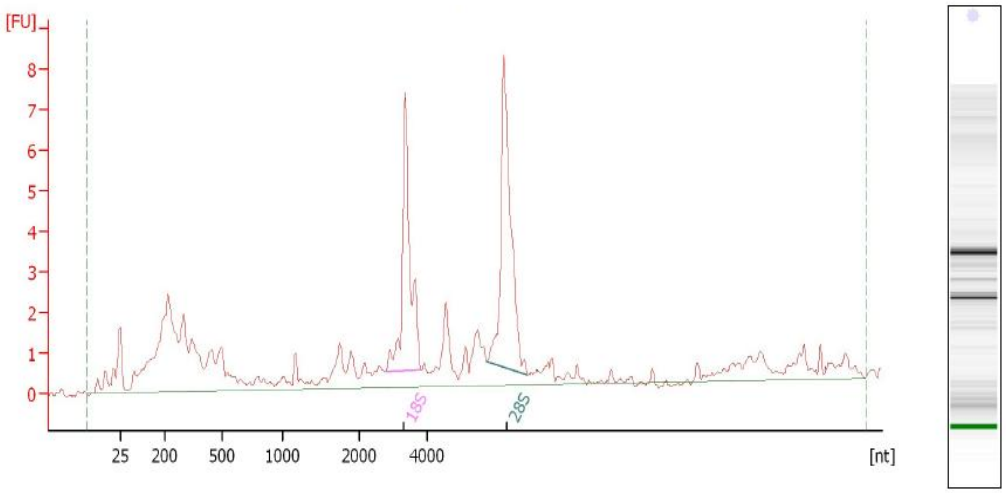

Overall Results for sample 8 : F 6

RNA Area:	78.2	RNA Integrity Number (RIN):	7.9 (B.02.07)
RNA Concentration:	155 ng/µl	Result Flagging Color:	
rRNA Ratio [28s / 18s]:	1.3	Result Flagging Label:	RIN: 7.90

C 6

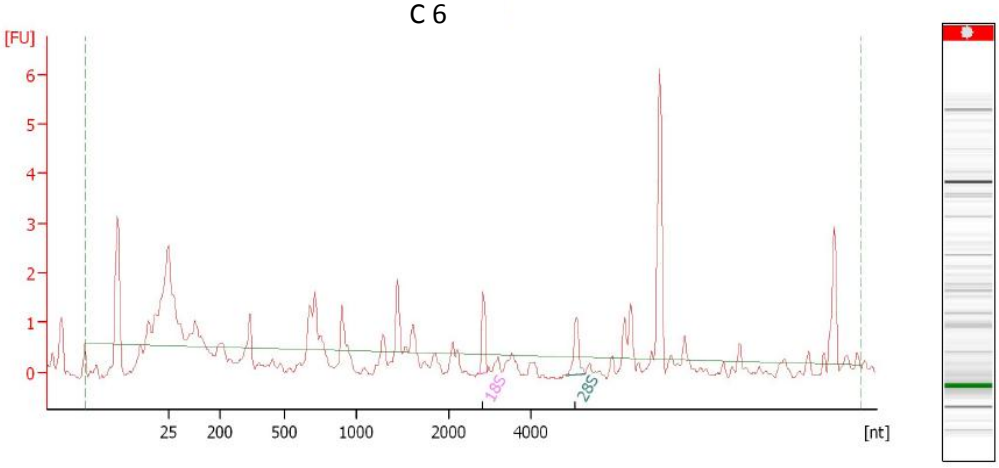

Overall Results for sample 7 : C 6

RNA Area:	16.2	RNA Integrity Number (RIN):	N/A (B.02.07)
RNA Concentration:	20 ng/µl	Result Flagging Color:	
rRNA Ratio [28s / 18s]:	1.0	Result Flagging Label:	RIN N/A

Figure 14. Comparison results Agilent RNA 6000 Nano chip between a fresh lymphoma and its corresponding cytologic glass smears.

By the use of Agilent Bioanalyzer 2100 instrument and the appropriate small RNA chip, the percentage of enrichment of RNA fragments from 20 to 40 nt long (ie those that include miRNA) compared to total RNA, was calculated. From observation of the data shown in Table 12, we can see that the percentage of miRNAs in RNA extracted from cytologic glass smears is almost always higher than the percentage of those in the corresponding RNA extracted from fresh samples, this is probably due to the high chemical stability and to the small size of these molecules, which make them stable to the procedures of handling and preservation of cytologic glass smears with respect to the other nucleic acids.

SAMPLE	PERCENTAGE MIRNA AND CONCENTRATION pg/µl	
	SMEARS	FRESH/FROZEN
C1=F1	36 % miRNA; Concentration: 6686.10 pg/µl	23 % miRNA; Concentration: 3428.80 pg/µl
C2=F2	33 % miRNA; Concentration: 11404.30 pg/µl	27 % miRNA; Concentration:13106.60 pg/µl
C3=F3	22 % miRNA; Concentration: 1266.80 pg/µl	23 % miRNA; Concentration: 7146.40 pg/µl
C6=F6	34 % miRNA; Concentration: 9253.40 pg/µl	30 % miRNA; Concentration:13099.60 pg/µl
	30 % miRNA; Concentration: 3543.50 pg/µl	36 % miRNA; Concentration:186585.70 pg/µl
C7=F7	50 % miRNA; Concentration: 13934.60 pg/µl	35 % miRNA; Concentration: 5200.90 pg/µl
C8=F8	62 % miRNA; Concentration: 8467.30 pg/µl	33 % miRNA; Concentration:17999.60 pg/µl
C9=F9	36 % miRNA; Concentration: 5415.20 pg/µl	22 % miRNA; Concentration:9788.80 pg/µl

Table 12. Results obtained with Agilent small RNA chip. Percentage and miRNA concentrations compared with total RNA extracted from fresh lymph node aspirates and corresponding cytologic glass smears.

1.4.2 Evaluation of the TaqMan assay for the canine miRNAs

The sensitivity of the TaqMan® MicroRNA Assay, designed for human, was evaluated for some canine targets by 6 serial dilutions of cDNA obtained retro transcribing the total RNA extracted from canine lymph node aspirate and amplifyed utilizing the corresponding set of primers and probes. For each miRNA target, the relative straight line was obtained (Figure 15). The result shows that, for each miRNA, there is a linear reverse relationship between RNA input and threshold cycle (Ct), and efficiency values are close to optimal: indeed, the correlation values are in the range 0.997-1.000, and the efficiencies of PCR are included in the range 93.2-105% (Table 13). The dynamic range of each assay includes about four logarithms of concentration.

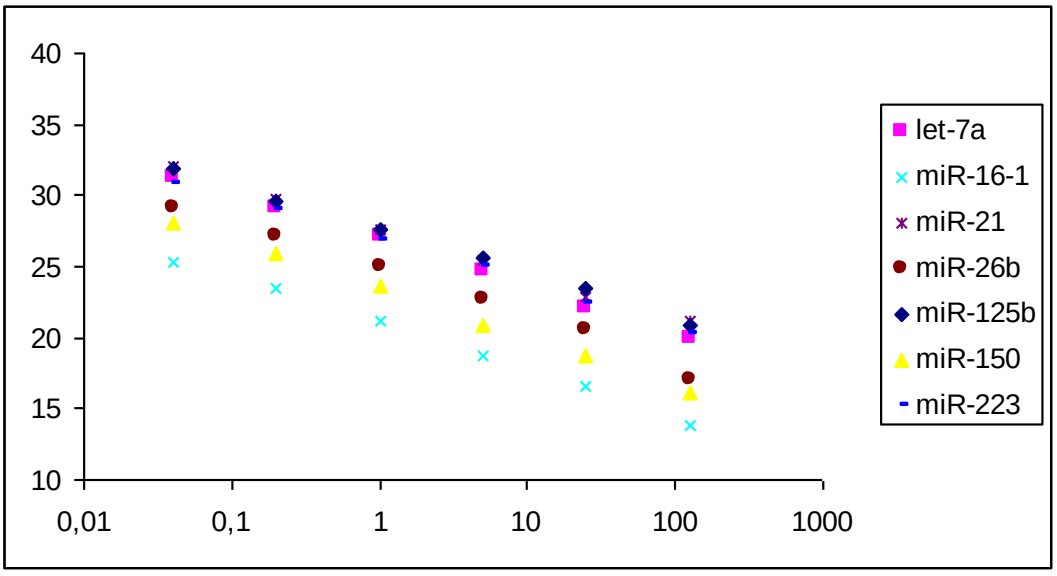

Figure 15. Straight lines obtained from six serial dilutions of some cDNA obtained utilizing the TaqMan® MicroRNA Assay

miRNA	Correlation coefficient	PCR efficiency
let-7a	1.000	101
miR-16	0.999	93.2
miR-17-5p	0.992	98.2
miR-21	0.998	98.9
miR-26b	1.000	99.7
miR-29b	0.997	97.8
miR-125	0.998	95.4
miR-150	0.999	92.9
miR-155	1.000	105
miR-181a	0.999	99
miR-223	0.998	103

Table 13. Dilution curves obtained for some miRNA assays: correlation values and PCR efficiency

The sequencing of the amplicon after cloning, confirmed the amplification specificity for each miRNA target. As representative title, is shown below the clone sequence obtained after amplification with the assay for canine miR-26b (the sequence in bold refers to the sequence of the miRNA, which fully corresponds to the expected sequence, while the flanking sequences belong to the cloning site of the vector and the additional base resulting from the stem-loop system amplification).

CCTGCTCCCGGCCGCCATGGCGGCCGCGGGTAATTCGATTTGCAGGGNAC
CGAGGAACTGGATACG**ACAACCTATCCTGAATTACTTGA**ACGCGCCAATC
ACTAGTGAATTCGCGGCCGCCTGCAGGTCGACCATATGGGAGAGCTCCCA
ACGCGTTGGATGCATAGCTTGAGTATT

1.4.3 qRT-PCR TaqMan

For each type of sample and neoplasia studied we proceeded to an accurate analysis and selection of suitable endogenous control (EC) genes in order to perform a correct normalization of target miRNA. The threshold cycles (CT) of the reference genes tested, obtained by real time, were analyzed using the algorithms geNorm, version 3.5 (Vandesompele J. et al. 2002), and NormFinder (Andersen C.L. et al. 2004). In all lymphoid malignancies studied, and for each miRNA target, after selecting the best housekeeping genes was performed a **relative quantification**, by calculating the delta-delta Ct to the endogenous control gene selected, and an **absolute quantification**, interpolating its Ct on standard curves obtained from serial dilutions of an equimolar pool of synthetic miRNAs (Mirvana ™ miRNA Reference Panel v9.1, Ambion).

1.4.4 Selection of the best endogenous control (EC) genes

A. <u>Lymph nodes lymphomas</u>

In lymph nodes lymphomas, for choosing the best endogenous control (EC) gene, 7 miRNA (cfa-let-7a, miR-16-cfa, cfa-miR-21, miR-26b-cfa, cfa-miR-125b, miR-150-cfa, cfa-miR-223) and RNU6B were analyzed. The analysis were carried out on non-neoplastic lymph nodes and nodal lymphomas, both frozen and paraffin-embedded. The candidate miRNA and RNU6B EC genes showed a wide expression range in non-neoplastic and neoplastic lymph node samples. Figure 16 shows the arithmetic average of the threshold cycles obtained after amplification of each miRNA EC candidate for each sample (A non-neoplastic lymph nodes, B lymph node lymphomas), both frozen and paraffin-embedded. From the results obtained it was possible to distinguish two categories of expression: highly expressed genes had median Ct values below cycle 25, and lowly expressed genes had median Ct values below cycle 25. Although it

highlighted some general variability, it can be noted that some miRNAs (let-7a, miR-16-1, miR-26b) show a more constant level of expression in different types of samples.

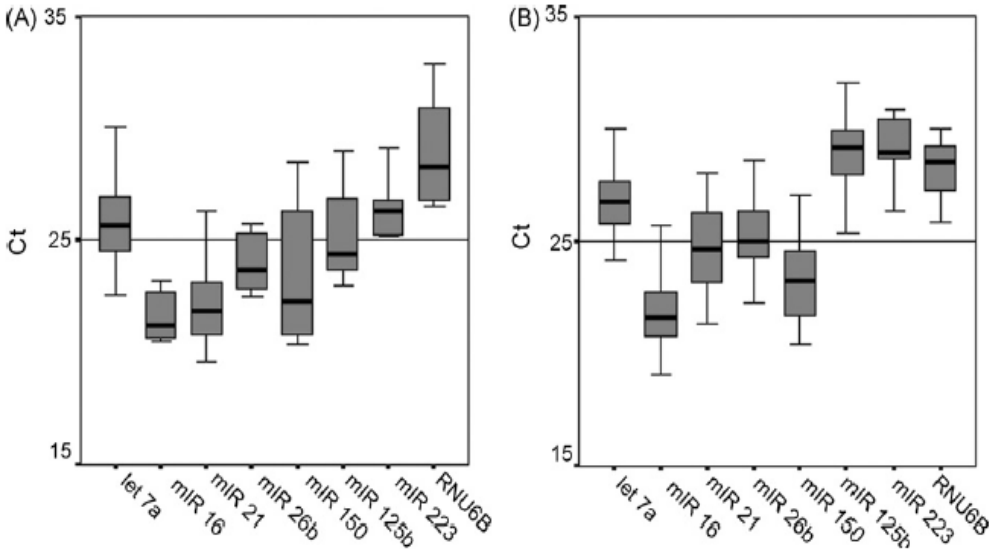

Figure 16. Median and range of Ct values of candidate genes as endogenous controls: (A) non-neoplastic lymph node samples and (B) lymph node samples with cancer. The arbitrary line drawn at 25 Ct defines two groups of candidate genes EC.

In Table 14 are reported the results obtained by analyzing the data referring to the average of the threshold cycles of each miRNA both with the algorithm NormFinder that, for purposes of comparison and possible confirmation, with the algorithm geNorm. The samples were analyzed separately by type, or all together. From the general point of view, it can be deduced that, for the different types of samples, the rankings obtained with the two different statistical approaches coincide in absolute or almost absolute, confirming the validity of the experimental data. From a specific point of view, it should be noted that the samples of lymphoma, both frozen and embedded in paraffin, show an high stability of miR-16 and miR-26b and an high instability of miR-21 and RNU6B, while in samples of lymph node control non-neoplastic, on the contrary, miR-21 is characterized by high stability of expression. Taking into account the totality of the samples, both control and neoplastic, both frozen and

embedded in paraffin, it appears that the best housekeeping gene is the miR-26b, followed by let-7a and miR-16, while the genes characterized by greater instability of expression are the miR-150 and RNU6B (Figure 17). This latter fact has relevant importance, since the gene RNU6B was frequently used as housekeeping gene for the normalization in miRNAs quantification experiment (Boggs et al., 2007).

Fresh-frozen	NormFinder		GeNorm	
Rank	Gene	Stability	Gene	Stability (*M*)
A				
1	miR-26b	0.453	miR-26b	1.507
2	let-7a	0.509	miR-16	1.642
3	miR-21	0.609	miR-223	1.766
4	miR-16	0.832	let-7a	1.785
5	miR-223	0.873	miR-125b	1.852
6	miR-125b	1.026	RNU6B	1.995
7	miR-150	1.191	miR-21	2.036
8	RNU6B	1.241	miR-150	2.230
FFPE	NormFinder		GeNorm	
Rank	Gene	Stability	Gene	Stability (*M*)
B				
1	let-7a	0.264	let-7a	1.345
2	miR-21	0.355	miR-21	1.396
3	miR-16	0.533	miR-26b	1.474
4	miR-26b	0.640	miR-16	1.584
5	miR-150	0.681	miR-150	1.667
6	miR-125b	0.844	miR-125b	1.714
7	RNU6B	1.018	miR-223	2.054
8	miR-223	1.082	RNU6B	2.114
All samples	NormFinder		GeNorm	
Rank	Gene	Stability	Gene	Stability (*M*)
C				
1	let-7a	0.347	miR-26b	1.691
2	miR-26b	0.495	let-7a	1.805
3	miR-21	0.666	miR-16	1.886
4	miR-16	0.710	miR-223	1.992
5	miR-150	0.841	miR-125b	2.080
6	miR-223	0.897	miR-21	2.131
7	RNU6B	0.984	miR-150	2.153
8	miR-125b	1.016	RNU6B	2.160

Table 14. Ranking candidate genes EC obtained with the algorithms NormFinder and geNorm from lymph nodes neoplastic and non-neoplastic of dog: (A) fresh/frozen samples, (B) FFPE samples, and (C) fresh/frozen and FFPE samples. The values of stability of NormFinder shown are representative of both the intragroup variations which those of intergroup (control vs. tumors). GeNorm M values reported were calculated for the 8 candidates EC before the process of stepwise exclusion.

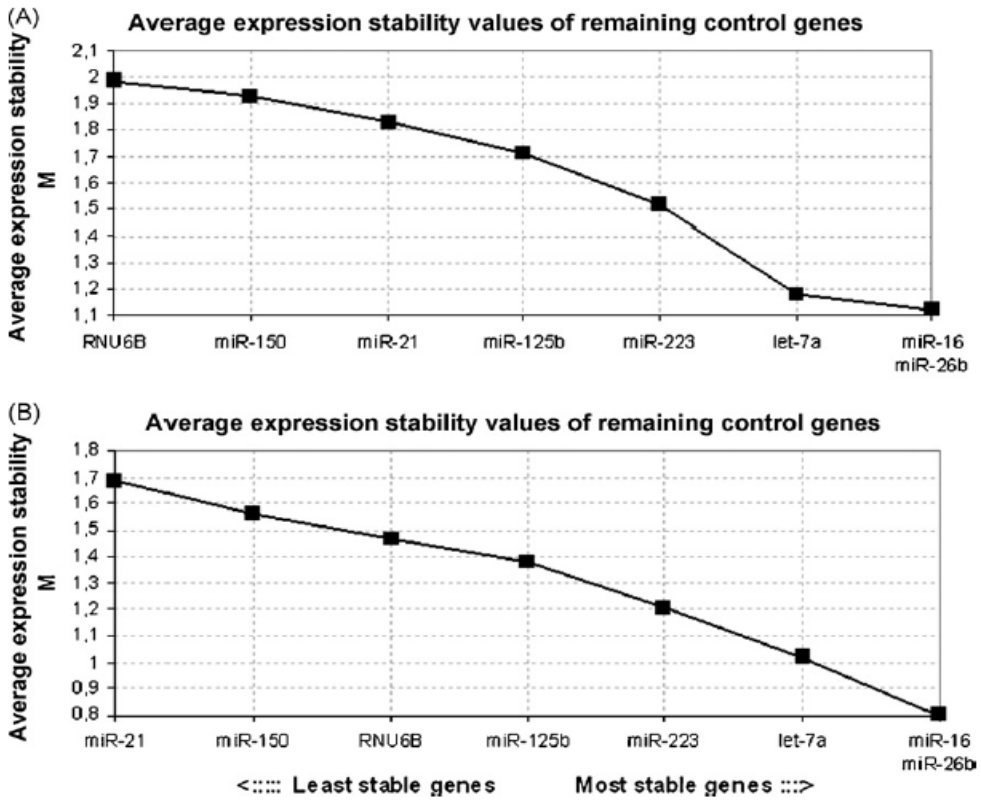

Figure 17. Average of stability expression of the endogenous control candidates obtained by geNorm. Gradual exclusion of the least stable gene in samples fresh/frozen and FFPE. (A) Controls and Lymphomas, (B) Only Lymphomas

An important confirmation of the RNA extraction comparability from cytologic glass smears sample rather than from fresh/frozen samples was provided by the analysis in parallel of the 7 miRNA candidates EC using ranking algorithms geNorm and NormFinder, that classify miRNAs on the basis of their expression stability in order to select the best control gene endogenous. Table 15 shows the results obtained by analyzing the data referring to the average of the threshold cycles of each miRNAs with the algorithm NormFinder (both for fresh samples and cytologic glass smears). The rankings of stability between the two different kinds of samples is comparable, and in particular let-7a is the best candidate CEs in both cases, while miR-125b is revealed as the candidate EC less stable both for the cytologic glass smears that for frozen. In Figure 18 is shown the high level of correlation between the stability values obtained for each miRNAs from the analysis of two different kinds of samples (cytologic glass smears and fresh/frozen).

Gene name	Stability value	
	Smears	Fresh/frozen
let-7a	0,338	0,421
miR-16	0,526	0,629
miR-26b	0,436	0,663
miR-125b	1,478	2,042

Table 15. Stability values of the candidates genes of endogenous control in the two kinds of samples.

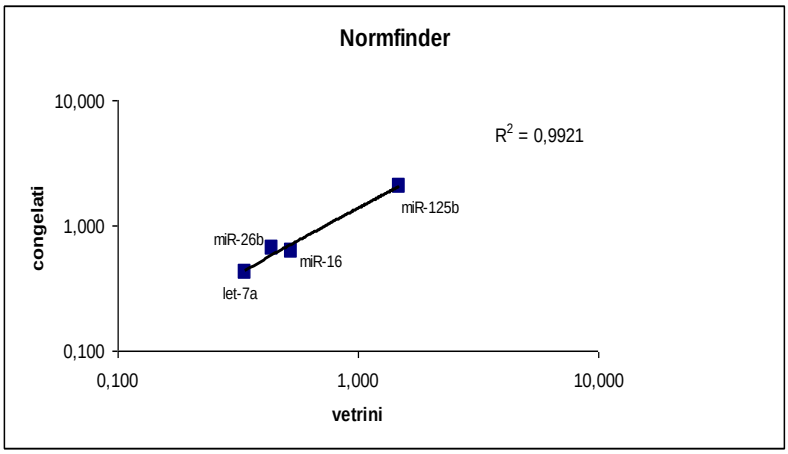

Figure 18. Correlation degree between the stability values obtained for each candidate EC in the two kinds of samples.

The miRNAs stability values obtained by cytologic glass smears samples show a quite similar stability compared to the corresponding fresh/frozen samples (Table 15). This result confirms that the intrinsic variability of the amplification yield obtained from cytologic glass smears samples is not greater than other kind of archive's sample. In this regard, it should be noted that the stability ranking of the different candidates EC genes is similar for both kind of samples (Table 15), with an inversion between miR-16 and miR-26b, presumably due to the oscillation of stability values very close to each other. Furthermore, the linearity degree between the two kind of samples is very high (Figure 18). This confirms the validity of the extraction procedure from cytologic glass smears sample with respect to the extraction from samples of conventional archive, and finally the possibility of using lymph node aspirate cytologic glass smears for miRNAs expression analysis as a supplement or replacement of fresh/frozen samples.

B. Chronic lymphocytic leukemia (CLL)

In CLL, to choose the best candidate EC gene, were analyzed 12 miRNAs (let-7a-cfa, cfa-miR-15, miR-16-cfa, cfa-miR-17-5p, cfa -miR-21, miR-26b-cfa, cfa-miR-29, miR-125b-cfa, cfa-miR-150, miR-155-cfa, cfa-miR-223) and RNU6B. Analyses were carried out on non-neoplastic peripheral blood samples and blood samples of subjects suffering from CLL with different immunophenotype. Initially, the analysis for the evaluation of miRNAs expression levels have been carried out only on fresh/frozen samples, later the same investigations were made also in peripheral blood cytologic glass smears of leukemic dogs. As in the nodal lymphomas, even in CLL the analyzed miRNAs and the gene nucleolar RNU6B showed variable levels of expression between neoplastic samples and control samples (Figure 19).

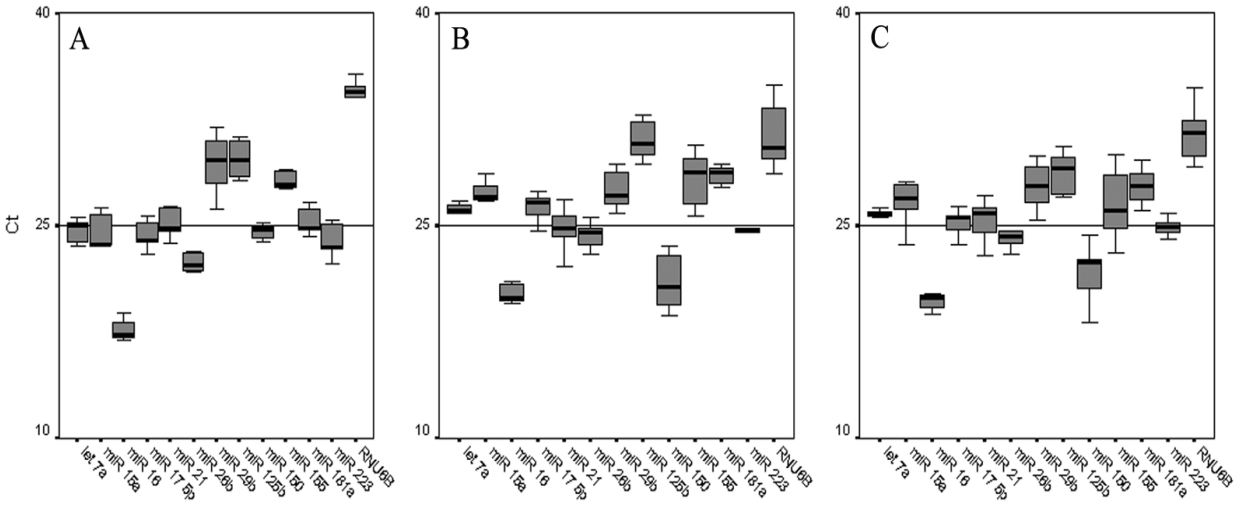

Figure 19. Median and range of Ct values of candidate EC genes in: (A) non-neoplastic peripheral blood samples, (B) T-CLL samples, (C) B-CLL samples. The arbitrary line drawn at 25 Ct defines two groups of candidate EC genes.

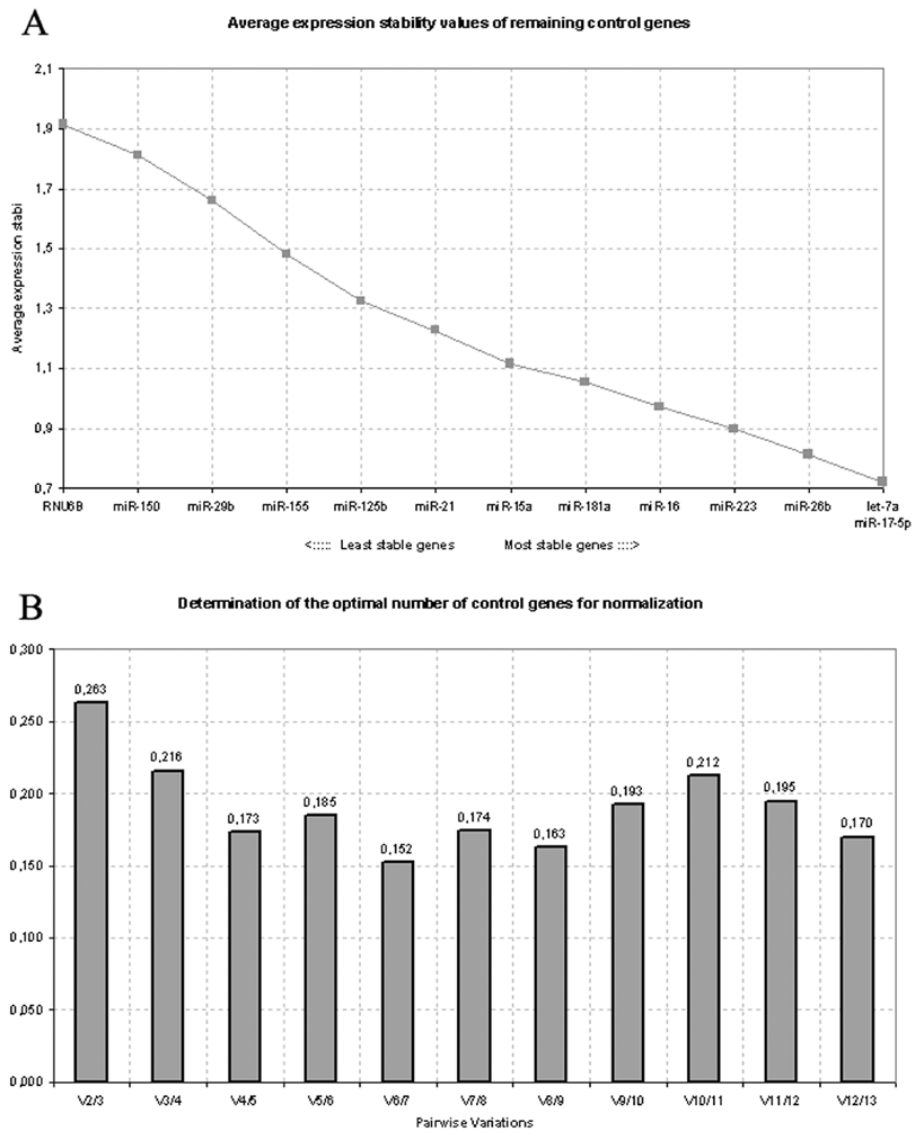

Figure 20. Best EC gene selection in peripheral blood samples with geNorm. (A) The average value of stability of expression (M) was calculated for each candidate EC. Comparison comparative two by two, which in turn eliminates the less stable miRNA and recalculates the stability among the remaining miRNA, thus giving as result a single pair of miRNA reference (the most stable). (B) Determination of the optimal number number of EC genes for normalization. Is calculated the value of systematic variation (v) between two normalization factors in a sequential manner. V 4/5 shows the variation of the normalization factor with 4 vs 5 EC genes

GeNorm analysis of the whole sample set identified let-7a and miR-17-5p as the most stable pair of candidate EC genes, followed by miR-26b and miR-223 (Figure 20A). Noticeably, RNU6B was the least stable candidate EC. Pairwise variation analysis showed that a value (0.173) close to the recommended threshold value (0.15) was achieved when the top 4 candidate EC genes were selected as normalizers, and that the observed trend of V values did not change significantly after inclusion of additional genes (Figure 20B).

Based on geNorm analysis results, four EC genes (let-7a, miR-17-5p, miR-26b and miR-223) were selected for optimal normalization of miRNA expression in canine normal and leukemic whole blood samples. The remaining eight miRNAs have been studied as target miRNA in CLL.

C. Splenic lymphomas

In splenic lymphoma, to choose the best endogenous control (EC) gene, we analyzed the 6 miRNAs (let-7a-cfa, cfa-miR-16, cfa-miR-21, cfa-miR-26b, cfa-miR-150, cfa-miR-223) resulting as better endogenous control genes in lymph nodes lymphomas. The assayed miRNA genes showed a wide expression range in normal and neoplastic spleen samples. According to NormFinder algorithm (Table 16) the most stable gene is miR-16 in both sample types, followed by let-7a, miR-26b, miR-150, miR-223 and miR-21. According to geNorm algorithm (Figure 21) the most stable pair of miRNAs result to be let-7a and miR-16 while the less stable is, once again, miR-21.

RANK	miRNA	Stability value
1	miR-16	0.108
2	let-7a	0.242
3	miR-26b	0.310
4	miR-150	0,485
5	miR-223	0.623
6	miR-21	0.686

Table 16. Stability values of the candidates genes of endogenous control obtained with NormFinder algorithm.

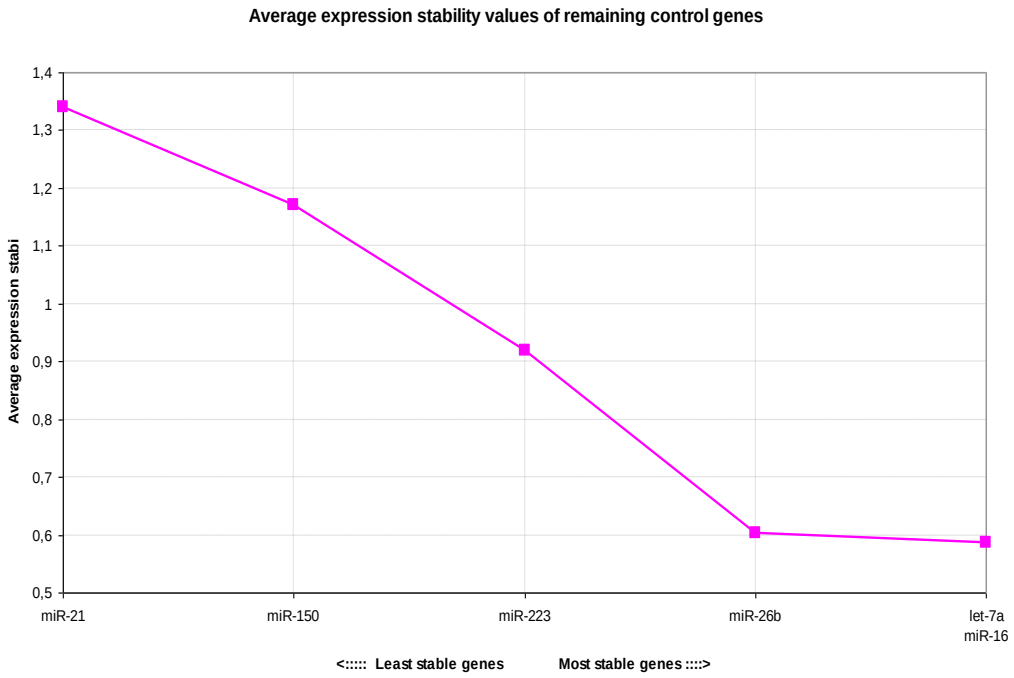

Figure 21. Average of stability expression of the endogenous control candidates obtained by geNorm. Gradual exclusion of the least stable gene in splenic lymphoma samples.

Based on these results, we chosed miR-16 as endogenous control gene as it shows the more stable expression levels in both algorithms. It can be noted that some miRNAs (let-7a, miR-16, miR-26b) show a greater stability of the level of expression in various samples, regardless of their type.

1.4.5 Assessment of miRNAs levels in canine blood cell subpopulations

Analysis of miR-15a, miR-16, miR-29b, miR-150, miR-155 and miR-181a expression was performed in canine CD4+ and CD8+ T cells, CD21+ B cells, PMN cells, PMBC and PLTs purified from three healthy subjects. The presence of all tested miRNAs was confirmed based on the amplification results. The expression data of blood line subpopulations were normalized to the miR-26b because it has comparable levels of expression in different cell subpopulations. Indeed, miR-26b was found to be the most suitable housekeeping miRNAs for the lymphoid tissues.

Absolute quantification of each miRNA was performed through interpolation of the CT values, obtained with the qRT-PCR, on the corresponding Reference Panel curve. The expression ratio (molar ratio) between femtomoles of the single miRNA and miR-26b (normalization gene) was then calculated for each sample, including platelets, and the corresponding mean and standard deviation gene ratios for each dog were calculated (Table 17).

A cell-type specific expression in peripheral blood cells was clearly detected, and each cell lineage was characterized by a specific miRNA expression pattern with a predominantly expressed gene. MiR-150 showed the maximal expression in T-lymphocytes, and especially in CD4+ cells compared to CD8+ cells, and a low expression in PMN. The same was detected, on a lesser extent, for miR-29b and miR-155. The most expressed miRNAs in B-lymphocytes were miR-29b and miR-150. Within lymphoid cell subpopulations, the expression level of miR-150 in B-lymphocytes was appreciably lower compared to T-lymphocytes, whereas miR-29b, miR-155 and miR-181a expression was rather similar in both cell types. Mir-181a expression in lymphocytes was comparable to expression in PMN. MiR-15a showed preferential expression in PMN, whereas miR-16-1 was expressed in all cell types at a comparable level. MiR-15a was also the only miRNA showing higher expression in B-lymphocytes compared to T-lymphocytes. PBMC showed an intermediate expression profile between lymphocyte and PMN. PLT showed

the lowest expression level of miR-29b, miR-150, miR-155 and miR-181a, whereas miR-15a and miR-16-1 were expressed in a way comparable to other cell subpopulations.

A

Sample	N	15a/26b		16-1/26b		29b/26b		150/26b		155/26b		181a/26b	
		m	sd	m	sd	m	Sd	m	sd	m	sd	m	sd
CD4+	3	0.24	±0.10	1.04	±0.02	2.13	±0.72	11.22	±2.71	1.01	±0.63	0.70	±0.34
CD8+	3	0.29	±0.17	0.88	±0.16	2.58	±0.30	5.13	±0.65	0.69	±0.11	1.00	±0.38
CD21+	3	0.49	±0.25	0.42	±0.11	1.57	±1.23	1.66	±0.91	0.49	±0.24	0.42	±0.24
PMN	3	4.12	±0.69	2.28	±1.52	0.34	±0.06	0.14	±0.02	0.05	±0.01	0.76	±0.27
PBMC	3	0.62	±0.16	0.62	±0.15	0.37	±0.07	0.29	±0.17	0.13	±0.07	0.20	±0.02
PLT	3	0.53	±0.05	0.60	±0.05	0.03	±0.003	0.01	±0.002	0.01	±0.004	0.12	±0.02

B

Sample	N	150/223		150/15a		150/181a	
		M	sd	m	sd	m	Sd
CD4+	3	229.74	±210.05	48.17	±8.47	17.48	±4.94
CD8+	3	59.12	±51.66	26.63	±23.03	5.50	±1.47
CD21+	3	3.55	±1.03	3.31	±1.07	4.02	±1.23
PMN	3	0.005	±0.0037	0.03	±0.01	0.20	±0.07
PBMC	3	0.32	±0.25	0.52	±0.35	1.43	±0.43
PLT	3	0.02	±0.008	0.01	±0.002	0.05	±0.01

Table 17. Comparison of the expression levels of miRNA target, expressed as mean and standard deviation A) ratio of the number of copies of the target miRNA and miRNA housekeeping cfa-mir-26b B) ratio of the number of copies of two different target genes, calculated in canine leukocyte subpopulations purified from three healthy subjects. PMN: polymorphonuclear PBMC: peripheral blood mononuclear cells; PLT: platelets.

1.4.6 Expression of targets miRNA in canine hematological malignancies

A. Lymph nodes lymphomas

1. Fresh/Frozen and FFPE samples

Relative quantification of four miRNAs (miR-17-5p, miR-29b, miR-155 and miR-181a), selected as target, was performed for all lymphoma samples (both in fresh/frozen samples than in FFPE samples) with reference to a representative non-neoplastic fresh-frozen (sample code F16) and FFPE (sample code P12) lymph node respectively (Table 18). Besides, based on the results obtained with NormFinder and geNorm analysis, let-7a, miR-16 and miR-26b were choosed as normalizing genes.

	miR-17-5p			miR-29b			miR-155			miR-181a		
	F	P	Mean	F	P	Mean	F	P	Mean	F	P	Mean
T-cell lymphoma	1.4	1.2	1.3	0.3	1.4	0.8	0.8	0.5	0.7	27.7	41.5	34.6
B-cell lymphoma	6.6	5.7	6.1	0.7	1.9	2.8	1.1	0.8	1	0.7	1	0.8

Table 18. Relative quantification of the four miRNA target in all lymph nodes lymphomas. F= fresh/frozen, P= FFPE

The relative expression (RE) values obtained for each miRNA versus F16 and P12 reference samples showed excellent correlation, with the exception of those relative to miR-155 (Figure 22).

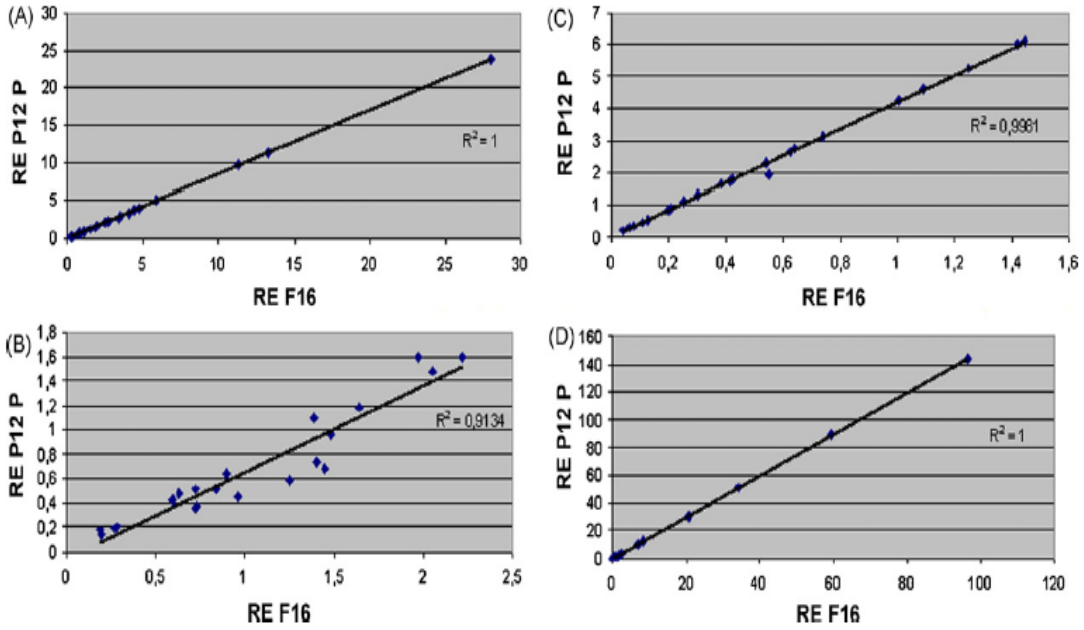

Figure 22. Correlation between the relative expression data of miRNAs target normalized to the let-7a, miR-16 and miR-26b and with reference to the control sample F16 (non-neoplastic lymph node aspirate fresh) and P12 (non-neoplastic lymph node embedded in paraffin). (A) miR-17-5p, (B) miR-155, (C) miR-29b, and (D) miR-181a.

Non-parametric Kruskal-Wallis test of relative expression data, using either fresh-frozen or FFPE non-neoplastic lymph node as reference sample, showed significant overexpression of miR-181a (p-value < 0.01) and downregulation of miR-29b (p-value < 0.05) in T-cell lymphoma cases compared to B-cell lymphomas, and significant (p-value < 0.01) overexpression of miR-17-5p in B-cell lymphomas compared to T-cell lymphomas. No significant ($p > 0.05$) difference in expression between T-cell lymphomas and B-cell lymphomas was detected for miR-155 (Figure 23).

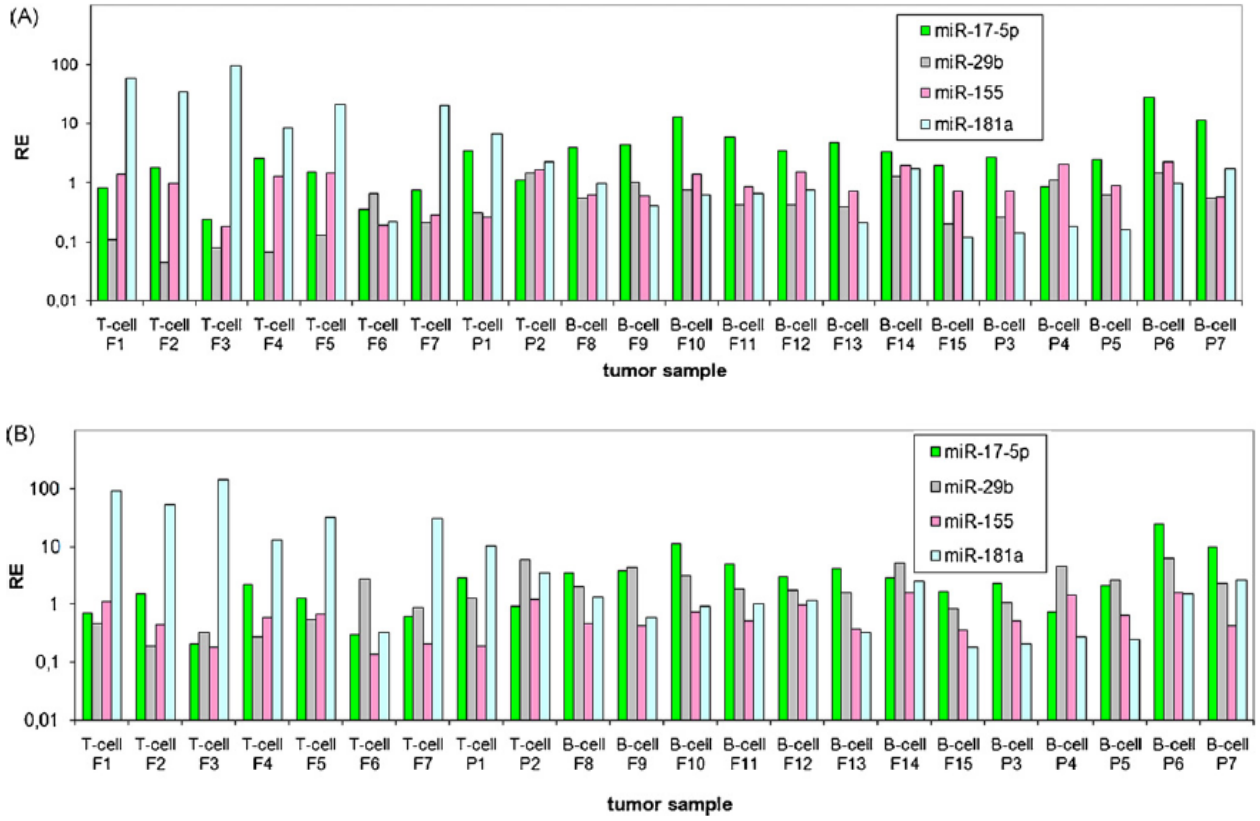

Figure 23. Relative expression of target miRNAs (miR-17-5p, miR-29b. miR-155 and miR-181a) in fresh/froze and paraffin-embedded samples of canine lymphoma, normalized to the EC genes miR-16, miR-26b and let-7a. The expression values were calculated in relation to the average of the lymph nodes of non-neoplastic control. (A) fresh/frozen control, (B) FFPE control.

Absolute quantification of miR-181a and miR-17-5p in femtomoles was then performed for each sample through interpolation of the obtained Ct values on the corresponding Reference Panel curve. In order to derive a molecular parameter useful for the differentiation of B-cell lymphomas compared to T-cell lymphomas, the gene ratio between absolute quantities of miR-181a and miR-17-5p was then calculated for each lymphoma sample (Figure 24). Non-parametric Mann-Withney test showed significant (p-value <0.01) difference of mean miR-181a/miR-17-5p gene ratio between T-cell lymphomas and B-cell lymphomas. No statistical differences were found between high and low grade lymphomas either when all samples were analysed or considering different phenotypes.

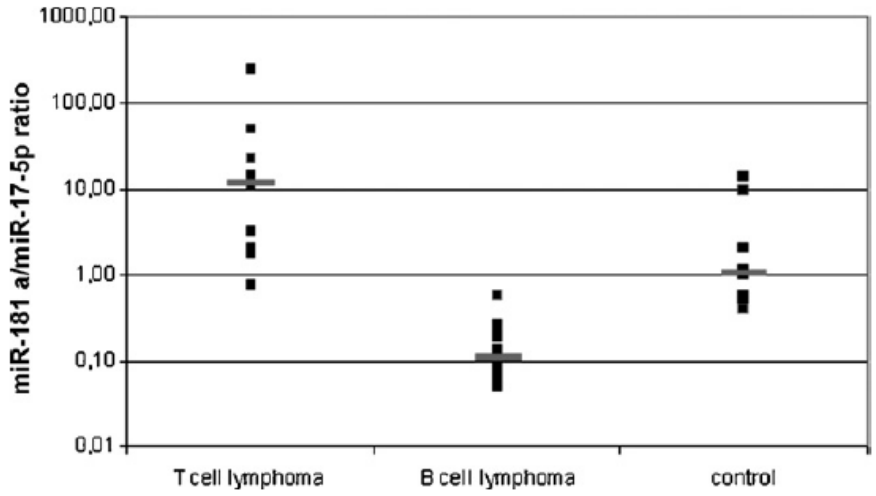

Figure 24. Analysis of Ratio miR-181a/miR-17-5p in canine neoplastic lymph node sample divided by immunophenotype.

2. Cytologic glass smears samples

In order to highlight the usefulness of the miRNAs analysis from cytologic glass smears and to derive a molecular parameter useful for the differentiation of B-cell lymphomas compared to T lymphomas, the absolute expression of miR-181a and let-7a was calculated even in this type of sample. After that, the ratio of expression (molar ratio) between the absolute quantities of miR-181a and the let-7a, for each cytologic glass smears sample, was calculated. The result is a clear distinction of molar ratio values between T lymphoma compared with B-cell lymphomas, with an average ratio of 9.11 in lymphoma type T and 3.4 in lymphoma type B (Figure 25).

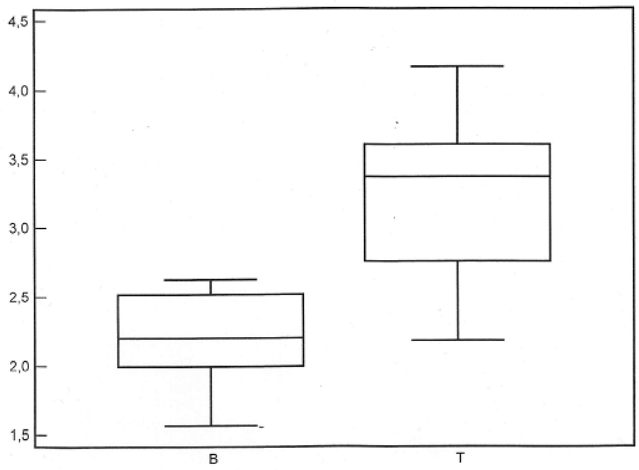

Figure 25. Ratio miR-181a/miR-17-5p in B-cell lymphomas and T lymphomas from cytologic glass smears

Non-parametric Mann-Withney test showed significant (p-value = 0.008) difference of mean miR-181a/miR-17-5p gene ratio between T-cell lymphomas and B-cell lymphomas from cytologic glass smears samples. Figure 26 shows the Bland-Altman test result regarding the molar ratio miR-181a/let-7a of the two types of samples (cytologic glass smears and frozen). Based on this test, it should be noted that the results of the two methods of extraction are sufficiently concordant despite a minimum constant error next to the proportional error.

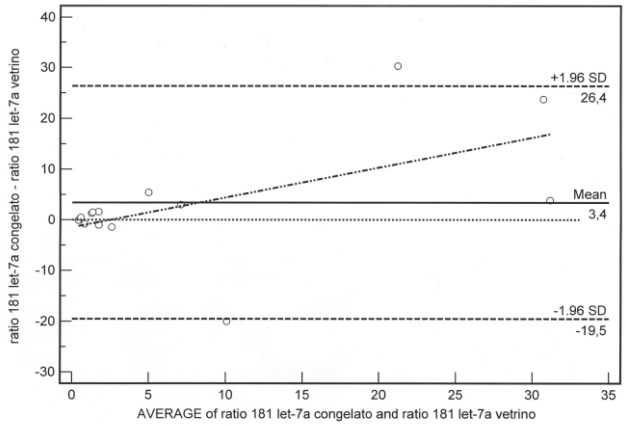

Figure 26. Results of the Bland-Altman test for the ratio miR-181a/let-7a in lymphomas samples.

Figure 27 shows similarly the result of the Passing-Bablok test regarding the molar ratio miR-181a/let-7a of the two types of samples. Based on this test, it should be noted that the two methods of extraction show sufficiently concordant results despite a moderate error of proportional type about the frozen samples (relatively to the cytologic glass smears samples) with a higher value of molar ratio. In particular, the results of the statistical analysis show an intercept very close to the expected value of zero (-0.14) and a slope of the straight estimated at 1.87 (ideal value equal to 1), however in the range of confidence between 0.69 and 3.51.

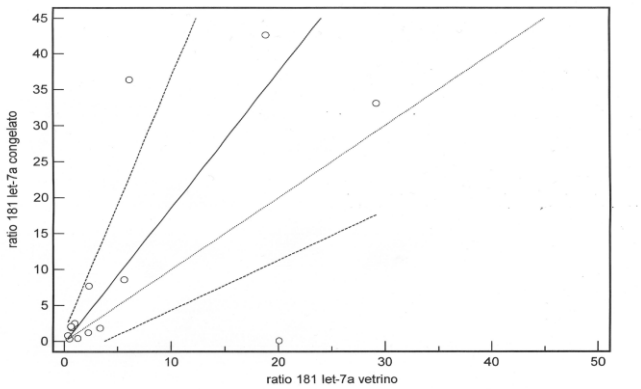

Figure 27. Results of Passing-Bablok test for the ratio miR-181a/let-7a in lymphomas samples.

B. Chronic lymphocytic leukemia (CLL)

1. Fresh/Frozen and FFPE samples

Relative expression (RE) of the eight miRNA not selected as ECs was calculated in the CLL whole blood sample set after normalization with the four EC genes, and expressed as fold change (FC) with reference to a representative normal whole blood sample (Figure 28).

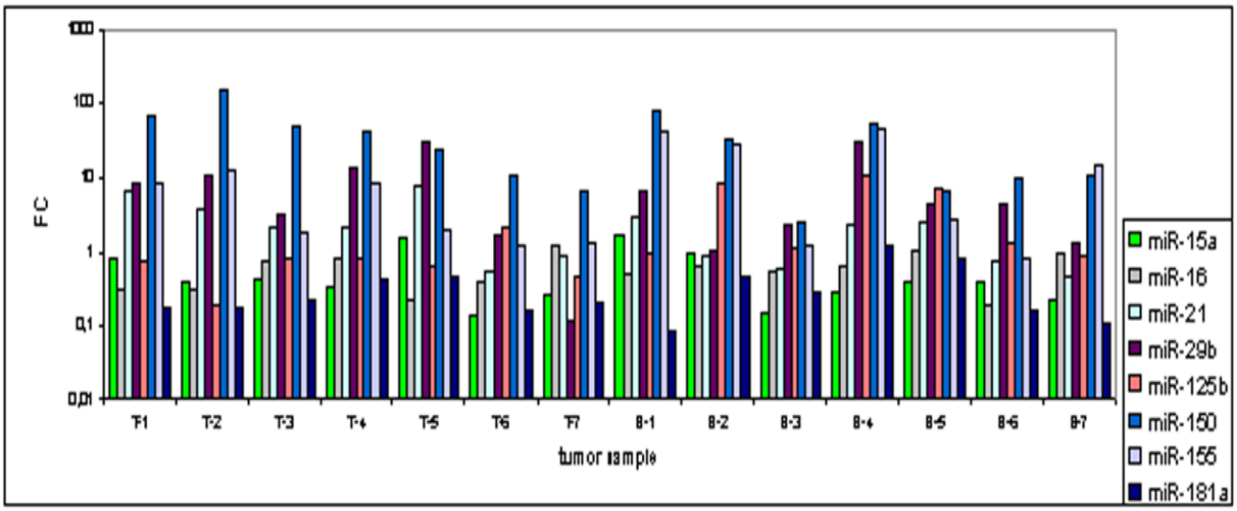

Fig 28. Relative expression of miRNA target in fresh/frozen samples of canine CLL, normalized to the genes miR-17-5p, miR-26b, miR-223 and let-7a. The expression values were calculated compared to the average of non-neoplastic blood samples. FC values of each miRNA were plotted on a log scale. T-1 to T-7: T-CLL whole blood samples. B-1 to B-7: B-CLL whole blood samples.

The histogram above shows that miR-21 and miR-150 were overexpressed in T-CLL while miR-125b and miR-155 were overexpressed in B-CLL (Table 19).
Analysis of RE data by non-parametric Kruskal-Wallis test showed a significant (p-value=0.007) overexpression of miR-125b in B-CLL compared to T-CLL (Table 19).

	Av. FC T-CLL	Av. FC B-CLL	KW test, p-value
miR-15a	0.57	0.70	0.902
miR-16	0.53	0.71	0.318
miR-21	3.42	1.63	0.318
miR-29b	9.83	7.36	0.620
miR-125b	0.79	4.63	0.007
miR-150	48.78	32.30	0.535
miR-155	4.93	21.46	0.209
miR-181a	0.26	0.47	0.805

Table 19. Average fold change (av. FC) of target miRNAs in canine CLL whole blood samples with reference to normal whole blood, calculated from the data reported in Figure 24. KW, non-parametric Kruskal-Wallis test.

Absolute quantification of the eight targets miRNA was then performed for each normal and neoplastic whole blood sample through interpolation of the obtained Ct values on the corresponding Reference Panel curve. In order to obtain a molecular parameter useful for immunophenotyping of CLL in dog, the gene ratio between absolute quantities of each miRNA pair was then calculated for each normal and CLL sample. Statistical analysis performed through non-parametric Kruskal-Wallis and Mann-Whitney tests showed significant difference of mean miR-150/miR-125b and miR-150/miR-155 gene ratios among samples of different leukemic status (Table 20). No statistical differences were found regarding gene ratios of the remaining miRNA pairs (data not shown).

	miR-150/miR-125b	miR-150/miR-155
Normal samples (N)	5.3	4.6
T-CLL samples (T)	318,7	60.1
B-CLL samples (B)	43.2	17.3
N vs B vs T (KW test, p-value)	0.004	0.002
N vs T (MW test, p-value)	0.003	0.003
N vs B (MW test, p-value)	0.048	0.018
T vs B (MW test, p-value)	0.038	0.017

Table 20. Averages of the ratio miR-150/miR-125b and miR-150/miR-155 in samples with different stages of leukemia. p-value calculated using the nonparametric Kruskal-Wallis (KW) for all independent samples and the nonparametric Mann-Whitney (MW) for two independent samples.

2. Cytologic glass smears samples

As though for fresh/frozen samples, the molar ratio between miR-150 (more expressed in CLL T-type) and miR125b (more expressed in CLL B-type) was calculated also for cytologic glass smears CLL samples. The result is a clear distinction, also in cytologic glass smears, of molar ratio in T- CLL compared to B-CLL (average ratio miR-150/miR-125b: 15788 in CLL T-type, and 145 in CLL B-type) (Figure 29).

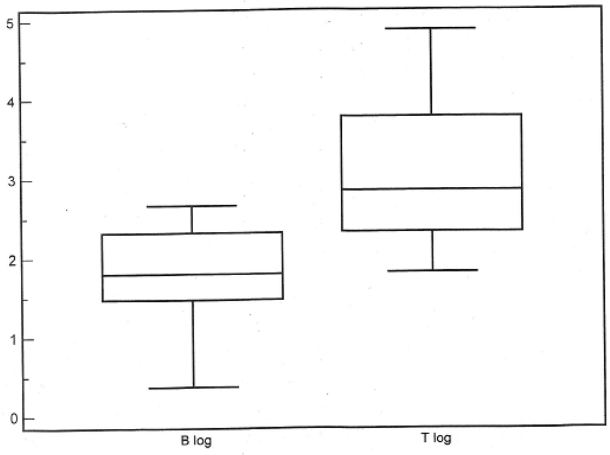

Figure 29. Ratio miR-150/miR-125b in B-CLL and in T-CLL

Non-parametric Mann-Withney test showed significant (p-value = 0.015) difference of mean miR-150/miR-125b gene ratio between T-CLL and B-CLL from cytologic glass smears samples.

As a control of the actual specificity of the target amplification from CLL cytologic glass smears (in the absence of the possibility of properly quantify the total RNA subjected to reverse transcription, and then extract information about the RNA purity from the ratio of absorbance), the retrotranscription for miR-125b and miR-150 of a RNA sample from CLL cytologic glass smears, in the absence of the reverse transcriptase enzyme, was carried out. This control samples had not amplified, and so it was possible to exclude any nonspecific amplification due to genomic DNA contaminating.

C. Splenic lymphomas

On the basis of the grading, the samples were divided into two categories: Low (L) tumor samples and Intermediate/High (I/H) tumor samples. Relative quantification of the four target miRNAs (miR-17-5p, miR-29b, miR-155 and miR-181a) was performed for all splenic lymphoma samples, to analyze the expression levels of the above miRNAs in L and I/H splenic tumor samples with reference to a representative non-neoplastic spleen FFPE sample, code P15 (Figure 30). The normalization was performed using miR-16, previously identified as the best endogenous control.

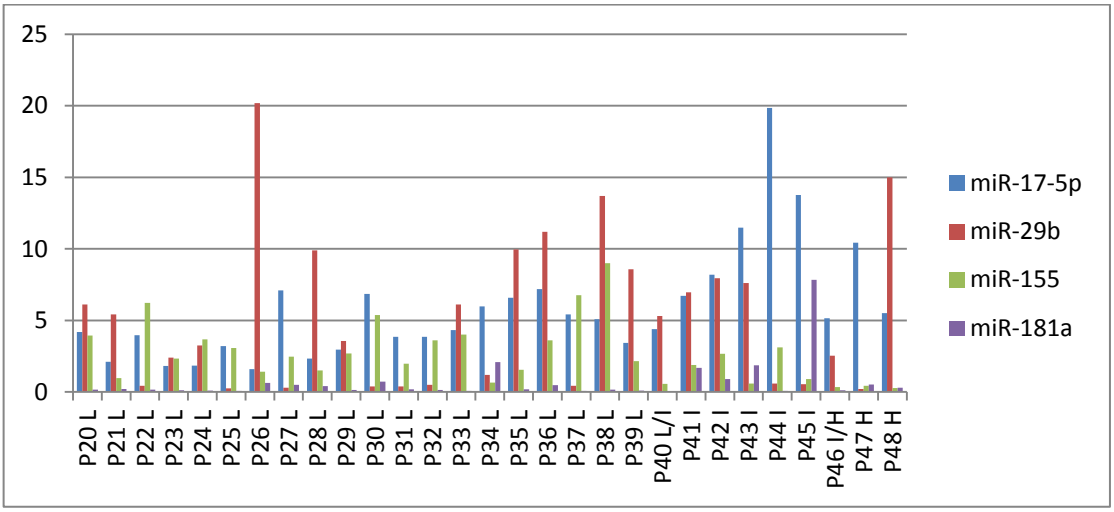

Figure 30. Relative expression of miRNA target in FFPE samples of canine splenic lymphoma (y-axis), normalized to the miR-16 gene. X-axis, miRNA relative expression (fold changes) compared to non-neoplastic spleen.

Analysis of relative expression (RE) data by non-parametric Kruskal-Wallis test showed a significant (p-value=0.0015, two-tailed test) overexpression of miR-17-5p and a non-significant (p-value=0.22, two-tailed test) overexpression of miR-181a in the I/H samples compared to the L samples. Furthermore, a significant (p-value= 0.0025, two-tailed test) downregulation of miR-155 was shown in I/H samples compared to the L samples. Finally, a stable expression of miR-29b in the two types of samples was detected (Figure 31).

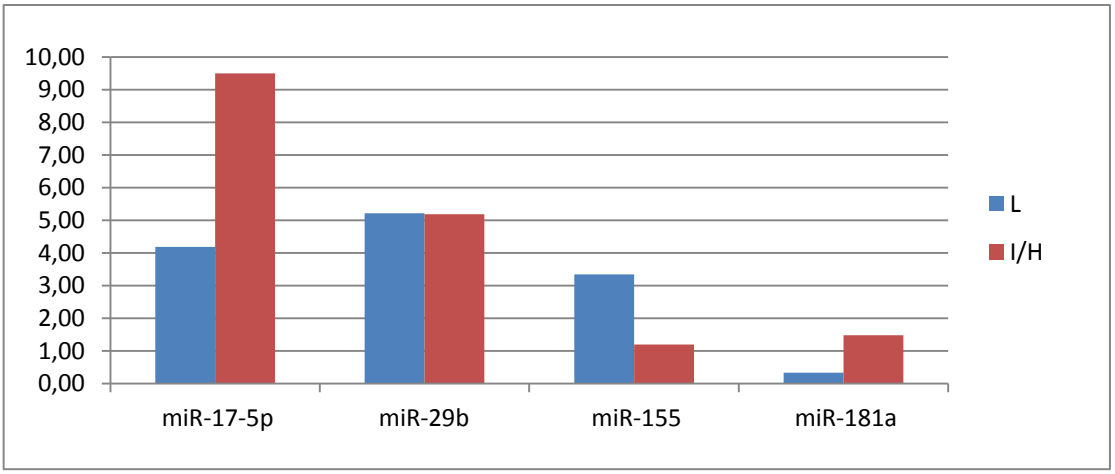

Figure 31. Mean differential expression (fold changes, y-axis) of the four miRNAs in Low grade (L) samples compared to Intermediate (I)/High (H) grade samples.

Absolute quantification of miR-17-5p and miR-155 was then performed for each sample through interpolation of the obtained Ct values on the corresponding Reference curve. In order to validate a new molecular parameter useful to support the grading of canine splenic lymphoma samples, the gene ratio between absolute quantities of miR-17-5p and miR-155 was then calculated for each lymphoma sample (Figure 32 and 33). As we can see in figure 33, non-neoplastic samples have the lowest ratio, followed by L samples, while the I/H samples have the highest ratio.

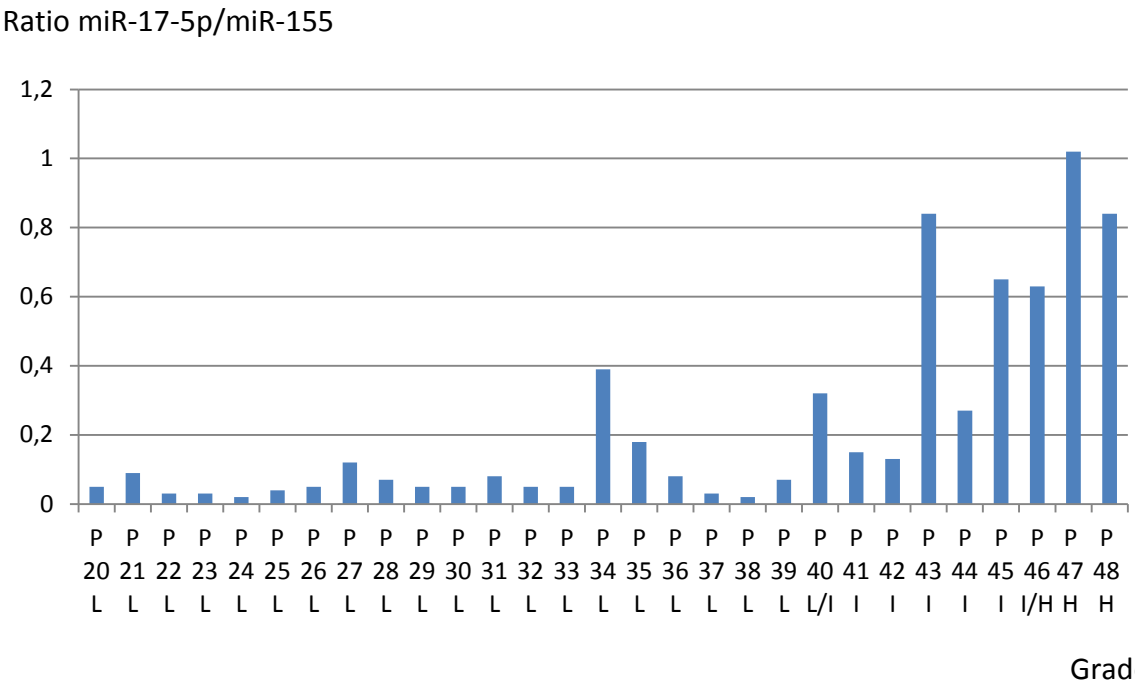

Figure 32. Ratio miR-17-5p/miR-155 obtained with absolute quantification in L and I/H splenic lymphomas samples.

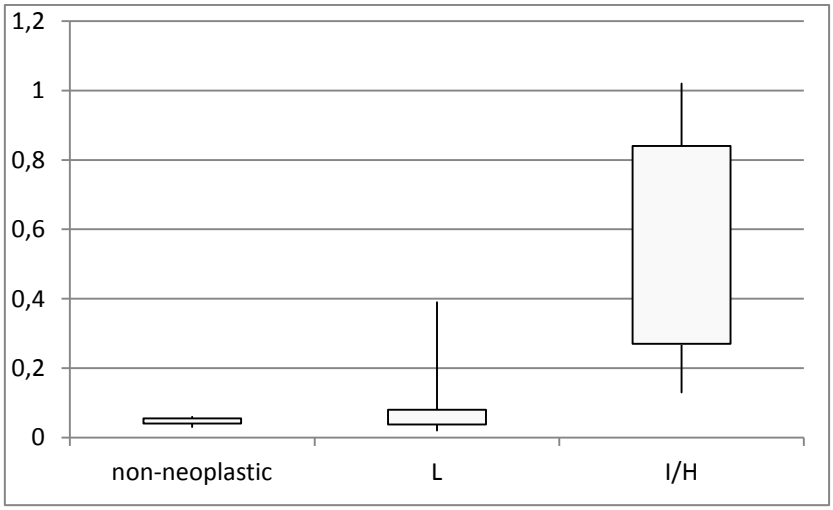

Figure 33. Mean miR-17-5p/miR-155 ratio in the non-neoplastic samples (controlli), the Low grade (L) samples and the Intermediate/High grade (I/H) samples.

Non-parametric Mann-Withney test showed significant (p-value <0.001) difference of mean miR-17-5p/miR-155 gene ratio between L and I/H tumoral samples.

Finally, we performed a correlation between the ratio miR-17-5p/miR-155 and the mitotic index of the same tumoral samples (Table 21). This correlation was statistically significant (Pearson's coefficient= 0,74).

SAMPLE CODE	GRADING	IM	RATIO 17-5p/155
P 20	L	0,2	0,05
P 21	L	0,4	0,09
P 22	L	0,1	0,03
P 23	L	0	0,03
P 24	L	0,3	0,02
P 25	L	0,7	0,04
P 26	L	0,3	0,05
P 27	L	0,3	0,12
P 28	L	0,2	0,07
P 29	L	0,2	0,05
P 30	L	0,2	0,05
P 31	L	0,4	0,08
P 32	L	0,3	0,05
P 33	L	0,8	0,05
P 34	L	0,9	0,39
P 35	L	0,9	0,18
P 36	L	0,6	0,08
P 37	L	0,4	0,03
P 38	L	0,2	0,02
P 39	L	1,7	0,07
P 40	L	1,5	0,32
P 41	I	3,3	0,15
P 42	I	5,3	0,13
P 43	I	7,9	0,84
P 44	I	2,3	0,27
P 45	I	3,6	0,65
P 46	I/H	3,5	0,63
P 47	H	11,4	1,02
P 48	H	27,3	0,84

Table 21. Correlation between the ratio miR-17-5p/miR-155 and the mitotic index (IM) of the tumoral samples.

1.5 DISCUSSION AND CONCLUSIONS

The main results obtained in this thesis are:

1. The detection of a panel of miRNAs expressed in canine hematological malignancies

In the recent years, bioinformatic studies on dog genome predicted a large number of canine miRNAs, but expression studies are still lacking of almost all of them. In particular, accurate expression data regarding normal and neoplastic canine lymph node samples, canine splenic lymphoma samples and normal and leukemic whole blood samples were still missing at the time of this study. The present work provided basic information regarding the expression in these canine haematological malignancies of some miRNAs that are used for diagnosis and prognosis of human hematopoietic tumors. Furthermore, the analysis was extended from fresh-frozen samples to FFPE samples and cytologic glass smears in order to increase sample size and to compare three different tissue sources procured independently by one another.

The MicroRNA TaqMan® Assays originally designed for human miRNAs let-7a, miR-16, miR-17-5p, miR-21, miR-26b, miR-29b, miR-125a, miR-150, miR-155, miR-181a and miR-223 were successful in the amplification of the corresponding canine mature miRNAs extracted from normal lymph node with high sensitivity and specificity over a four-logs diluition range, from normal and leukemic whole blood samples, and from normal and neoplastic canine spleen samples. This result is a further confirmation of the outcome of previous studies where the MicroRNA TaqMan® Assays originally designed for several human miRNAs were validated for the corresponding canine miRNAs (Boggs et al., 2007; Boggs et al., 2008). The accumulating evidence that the stem-loop TaqMan® assay is suitable for investigation of heterologous miRNA expression, provided perfect sequence identity with the concerning human mature miRNAs, opens interesting perspectives for comparative expression studies in organisms, especially mammals, for which dedicated commercial miRNA assays are not available.

2. The identification and validation of suitable ECs for miRNA analysis in canine lymph node and splenic lymphoma and in canine CLL

A very important issue for qRT-PCR expression experiments is the variability associated with the various steps of the procedure: different amounts and quality of starting material, variable extraction and retrotranscription efficiencies, or differencies between tissues or cells in bulk transcriptional activities (Ginzinger D.G. 2002). The identification of proper internal normalization genes is considered a valid strategy to remove as much technical and biological variation as possible between samples except for that difference that is consequence of a disease status. To be considered as reliable controls for a defined sample type, the genes should exhibit stable expression across all samples under investigation as empirically evaluated within a panel of candidate normalizers from a representative number of the sample population if not the entire sample set. Moreover, having a gene that is stable in one tissue type or disease state does not necessarily mean that the same gene will be stable enough in a different tissue type or disease to represent suitable EC. Various softwares are now available to assess the degree of variation in candidate reference genes and identify the most stable one(s) for the tissue(s) of interest. Expression studies on a new molecular class like miRNAs with peculiar properties should include the careful selection of appropriate normalization gene(s) in the tissue of interest. It is well recognized that empirical validation of ECs is the optimal strategy for ensuring accurate quantification of miRNAs by RT-qPCR. Recently, the few studies that have been published regarding the selection of miRNA reference genes in human normal and cancerous samples using geNorm and NormFinder applets (Xi Y. et al, 2006; Davoren P.A. et al, 2008). To our knowledge, no information have been published until now on the selection of suitable ECs for qRT-PCR analysis of miRNAs in any canine tissues. The two pivotal studies in canine miRNA analysis employed the non-miRNA gene RNU6B as a single EC gene, without any validation of its expression stability (Boggs et al., 2007; Boggs et al., 2008).

- **lymph node lymphoma samples**

With the present work we provided experimental justification for the selection of three suitable ECs, such as let-7a, miR-16 and miR-26b, for miRNA analysis in canine lymphoma samples from three different archival sources using the two more widely used, complementary algorithms NormFinder and geNorm. The wide range in stability values observed in the non-neoplastic and neoplastic lymph node sample sets reflects the high variability detected in candidate ECs gene stability. This could be partly due to the different tissue source and preparation method of the analysed samples (fresh-frozen, FFPE and cytologic glass smears samples). On the other hand, the observed overall conservation in miRNA stability across the three kind of samples confirmed the possibility to effectively normalize RT-qPCR miRNA expression data using very different tissue preparation methods. This finding was consistent with recent studies suggesting miRNA stability is less affected by FFPE or cytologic glass smears sample preparation compared to mRNA, due to the smaller size (Xi Y. et al, 2006; Peltier H.J. et al, 2008). Another relevant finding of the present study was that RNU6B turned out to be an unstably expressed candidate EC with both algorithms. This was consistent with a recent miRNA expression study performed in normal and cancerous human solid tissues, where RNU6B was among the least stable candidate ECs evaluated [27]. Taken together, these results strongly suggest that the default use of non-miRNA EC genes for miRNA expression studies should be carefully evaluated.

- **CLL samples**

In this study let-7a, miR-17-5p, miR-26b and miR-223 were ranked as the best candidate ECs for normal blood and CLL samples and again, RNU6B was the least stable, consistently with a study performed in normal and cancerous human solid tissues (Peltier H.J. et al, 2008). Taken together, these results strongly suggest that let-7a and miR-26b should always be included in the panel of candidate ECs when dealing with miRNA analysis in canine lymphoid cancer, and the use of non miRNA EC genes, like RNU6B, should be carefully evaluated.

- **splenic lymphoma samples**

In this work, to choose the best endogenous control (EC) gene were analyzed, using the complementary algorithms NormFinder and geNorm, the 6 miRNAs that result as better EC genes in lymph nodes lymphomas. The assayed miRNA genes showed a wide expression range in normal and neoplastic spleen samples. For both algorithms the most stable pair of miRNAs result to be let-7a and miR-16 while the less stable is miR-21. It can be noted that some miRNAs (let-7a, miR-16, miR-26b) show a greater stability of the level of expression in various samples, regardless of their type.

3. Identification of differentially expressed miRNAs that can be used as potential new molecular targets for diagnosis and prognosis in canine leukemias and lymphomas

The quantification of miRNAs expression in canine lymphoma and leukemia profiling and progression is an attractive perspective for veterinary clinical oncology and also, from a comparative point of view, since the similarities in both genetics and physiology and considerable overlap in treatment regimens, make dog an ideal model for many human diseases (Boggs R.M. et al, 2008; Paoloni M. and Khanna C. 2008). Moreover dogs share the same environment with human beings, being cronically and sequentially exposed to outdoor pollutants, yet they do not indulge in occupational activities or lifestyles which can confound interpretation of epidemiological studies (Marconato L. et al, 2009).

In humans, miRNA analysis has provided new possibilities in hematopoietic tumor classification, disease prognosis, early cancer detection and therapeutic decision making: for instance altered miRNA expression associated to ZAP-70 and IgH mutations reflect the survival or proliferation of neoplastic cells in B-CLL (Cummins J.M. and Velculescu V.E. 2006; Calin G.A. et al, 2005). Identification of valid targets in canine cancers with direct association with human tumor targets could provide significant rationale for the study of new diagnostic and therapeutic approaches both in dogs and humans.

- **Ratio miR-181a/miR-17-5p as a marker for the immunophenotype in canine lymph node lymphomas**

Normalization of the expression data to the three most stable miRNA and to fresh-frozen and FFPE non-neoplastic lymph node both supported the statistically significant identification of **miR-181a upregulation** in canine **T-cell lymphoma** and **miR-17-5p upregulation** in canine **B-cell lymphoma**. When absolute quantification was performed, the molar ratio between miR-181a and miR-17-5p clearly distinguished between T-cell and B-cell lymphoma samples, but not between high grade and low grade tumors. The correlation of miR-181a and miR-17-5p transcript disregulation to tumor immunophenotype, and not to tumor grade, directs future research toward hypothetical correlations with particular pathogenetic features or cancer biomarkers at the phenotypic level in neoplastic lymph nodes. Noteworthly, in other canine hematopoietic tumors like chronic lymphocytic leukaemia (CLL) and splenic lymphoma the expression pattern of miR-17-5 and miR-181a is not related to the immunophenotype. The results of the present study are in accordance with what already performed in humans, that described very different miRNA expression patterns in a variety of hematopoietic tumors. In particular, the miR-181 family is generally considered to be oncogenic, with observed overexpression in breast, pancreas and prostate cancers (Calin G.A. and Croce C.M. 2006). Besides, miR-181a shows enhanced expression in leukaemia cell lines, and miR-181 family is upregulated in cytogenetically normal, molecular high risk acute myeloid leukaemia (Ramkissoon S.H. et al, 2005; Marcucci G. Et al, 2008). On the other hand, the miR-181 family has reported to be a tumor suppressor in human B-CLL and glioma (Pekarsky Y. Et al, 2006; Marton S. Et al, 2008; Shi L. Et al, 2008). In particular, both miR-181b and miR-29b regulate the expression of the oncogene *TCL1* and are downregulated in human aggressive B-CLL with high Tcl1 expression (Pekarsky Y. Et al, 2006). The dual nature of miR-181 family (oncogenic/tumor suppressor) could depend on the specific cellular context (Fabbri M. et al, 2008). MiR-17-5p is encoded within the miR-17-92 polycistron, a cluster of seven miRNAs associated with a broad range of human tumors

including lymphoma (Lawrie C.H. et al, 2009). Due to its capability to interact with a number of known promoters of cellular proliferation, miR-17-5p is able to act as both an oncogene and a tumor suppressor in different cellular contexts, dependant on the expression of other transcriptional regulators (Cloonan N. Et al, 2008).

There are a number of limitations in the present study that can be addressed in future work. One relates to the functional verification of the observed differences in miRNA levels affecting any specific outcomes in canine lymphoma, for example, modulation of target genes. Further studies should also be performed on purified neoplastic cells, since in clinical samples as lymph node aspirates the relative abundance of each cell subpopulations in neoplastic cases is usually different from normal range and this could affect a precise evaluation of miRNA expression status. However, even if the percentage of purity of neoplastic cells was difficult to evaluate in our samples, canine lymphomas are mostly characterized by a diffuse pattern in contrast with human medicine in which follicular or mixed pattern are often recognized. For this reason the population of neoplastic cells was considered almost pure in our samples as also shown in flow cytometry by the limited (less than 10%) percentage of residual non-neoplastic cells in most samples. Finally, large scale studies including long-term follow-up monitoring after diagnosis are needed in order to obtain a proper evaluation of the potential utility of miR-181a and miR-17-5p as new molecular tools for the clinical monitoring of canine T- and B- cell lymphoma.

- **Ratio miR-150/miR-125b as a marker for the immunophenotype in canine CLL**

The utility of immunophenotyping to predict survival in CLL affected dogs has been recently reported (Comazzi S. et al., 2010) and analysis of relevant miRNAs should also allow to detect immunophenotype in archival samples problematic for standard immunophenotyping methods, like cytologic glass smears (Comazzi S. et al., 2010). In this study the least stable miRNAs in canine CLL were miR-29b, miR-125b, miR150 and miR-155. In particular, statistically significant

disregulation of **miR-125b** was shown depending on CLL immunophenotype. This findings could direct future research toward hypothetical correlations of miR-125b with particular pathogenetic features or cancer biomarkers at the phenotypic level in canine B-CLL. Notewhorty, in humans miR-125b influences B-cell differentiation in germinal center lymphocytes, and is upregulated in acute myeloid leukemia with t(2;11)(p21;q23) chromosomal traslocation and PML/RARA rearrangement (Bousquet M. et al., 2008; Malumbres R. et al., 2009; Zhang H. et al., 2009). In this work, **miR-155** was upregulated in 4/7 B-CLL without reaching statistical significance. In humans, miR-155 is upregulated in diffuse large B-cell lymphoma and in CLL with differential expression linked to chromosome 17p deletion status (Lawrie C.H. 2007; Garzon R. and Croce C.M. 2008; Visone R. et al., 2009; Rossi S. et al., 2010). The analysis of purified blood cell subpopulations showed that miR-155 is basically a lymphoid miRNA with preferential expression in normal T-lymphocytes. This finding enforce the hypothesis that the observed increase expression in some B-CLL cases compared to T-CLL may not be an accidental result and could imply pathogenetic significance in canine B-CLL similarly to human CLL. Further analysis of larger sample sets could clarify if a real disregulation of miR-155 with any diagnostic and prognostic significance exists in (sub)population of canine B-CLL. The highest fold changes in canine CLL samples compared to normal blood were observed for **miR-150**, followed by **miR-29b**. MiR-150 is highly expressed in mature B- and T-cells, controls B lymphopoiesis in mice and is overexpressed in human CLL (Fulci V. et al., 2007; Zhou B. et al., 2007). In canine blood cell subpopulations, miR-150 is strongly expressed in lymphoid cells, with preferential expression in T cells compared to B-cells. This result could justify the hypothesis that the observed upregulation of miR-150 in T-CLL samples compared to B-CLL, without statistical significance, could be at least partly linked to a biased T vs B cellular ratio in the leukemic samples. The same could apply, on a lesser extent, to the observed miR-29b upregulation in T-CLL.

The oncosuppressive miR-15a and miR-16, that target the antiapoptotic gene Bcl-2, in humans are cotranscribed from the same cluster and are frequently

downregulated in CLL due to a deletion of the corresponding 13q14 genomic region (Calin G.A. et al., 2002; Calin G.A. et al., 2008). Deletion of the corresponding CFA 22q11.2 genomic region was reported in one case of canine CLL, but no extensive studies are available at this regard. The comparable deletion in canine CLL, in which T-cell phenotype is prevalent compared to human CLL, that are almost B-cell, suggested that miR-15a and miR-16-1 could be essential factors in the pathogenesis of the CLL regardless the immunophenotype (Breen M. and Modiano J.F. 2008). In this thesis work, it was not detected any significant variation of miR-15a and miR-16 in leukemic samples compared to normal blood. The analysis of canine blood cell subpopulations showed that miR-15a, and on a lesser extent miR-16, are strongly expressed in PMNs compared to lymphoid cells. In CLL samples at least 80% of leukocytes were found to be lymphocytes but it can't be excluded that even slighty differences in PMN abundance could have masked disregulation of these two miRNAs in leukemic cells. Finally, the expression pattern of miR-17-5 and miR-181a, that can distinguish between T-cell and B-cell lymphoma in lymph nodal lymphoma samples, in CLL is not related to the immunophenotype.

The limitations of the present study, which can be addressed in future work, are mainly relate to the functional verification of the observed differences in miRNA levels affecting any specific outcomes in canine CLL, for example, modulation of target genes. Moreover, definitive evaluation of leukemia-specific miRNA expression status should be performed on purified neoplastic cells, even if leukemic cells in CLL whole blood samples are usually overrepresented and they could be considered almost pure in our samples as also shown in flow cytometry by the limited percentage of residual non-neoplastic cells in most samples. Finally, large scale studies including long-term follow-up monitoring after diagnosis are needed to obtain a proper evaluation of the potential utility of miR-125b, miR-150 and miR-155 as new molecular tools for the possible clinical monitoring of canine T- and B- CLL.

- **Ratio miR-17-5p/miR-155 correlates with grading in canine splenic lymphoma**

To date there are no accurate and complete works about classification and grading in canine splenic lymphoma. We performed for the first time a comprehensive grading as follows. Splenic lymphoma samples were classified according with the WHO classification (Valli et al., 2011). Grade was determined according with the WHO classification (cell size, diagnosis and mitotic index).

On the basis of the grading, we divided our samples into two categories: Low (L) tumor samples and Intermediate/High (I/H) tumor samples. Relative quantification of the four target miRNAs (miR-17-5p, miR-29b, miR-155 and miR-181a) was used to analyze the expression levels of the miRNAs target in L and I/H splenic tumor samples. **miR-17-5p** is significantly overexpressed in I/H samples compared to L samples. **miR-155** is significantly downregulated in I/H samples compared to L samples. miR-181a is upregulated in I/H samples compared to L samples but this up-regulation is not statistically significant. Finally, miR-29b doesn't vary appreciably its expression profile in the two types of samples.

Absolute quantification of miR-17-5p and miR-155 was then performed and the molar ratio miR-17-5p/miR-155 was obtained for each sample. The miR-17-5p/miR-155 ratio clearly distinguished between low and high-grade tumors. Finally, marked correlation between the ratio miR-17-5p/miR-155 and the mitotic index of the same tumoral samples was evidenced. The molar ratio miR-17-5p/miR-155, then, was validated as a new grading marker for L/H canine splenic lymphoma (since the two types of neoplasms have a different course and prognosis) and can be considered a useful research product of this thesis complementing the corrently used classification tools.

4. Development and validation of methods for extraction and analysis of miRNAs from archive's samples, such as formalin-fixed and paraffin-embedded (FFPE) tissue and cytologic glass smears

This goal of the thesis has a significant importance because the techniques classically used for the determination of the phenotype and expression analysis

(flow cytometry, immunohistochemistry, RT-PCR and related techniques) often require fresh material in abundance, or biopsy. Therefore, it would be very useful to achieve the same result by analyzing miRNA from small amounts of archival material deposited on glass slides as cytological smears, or embedded in paraffin after formalin fixation. Furthermore, compared to human oncology, in veterinary medicine the availability of a sufficient number of fresh samples for validation studies of molecular markers is often very limiting. This is because of the smaller number of cases and the difficulty to obtain material suitable for subsequent studies. Hence the importance of being able to use different types of archive's samples that can be normally available for clinical types such as lymphoma and leukemia. In general, it is known that miRNAs are characterized by high chemical stability such as to remain virtually unaffected, even in case of procedures for handling and storage of the biological material that irreparably damage other types of nucleic acids (eg. messenger RNA). In addition, fixed and stained cytologic glass smears are frequently prepared in veterinary clinics and can be easily stored for many years after preparation.

In lymph nodal lymphoma, yield and stability of some representative miRNAs from smears and FFPE samples was comparable to the standard sample type that is currently used for expression studies, i.e. the frozen sample. Furthermore, for both lymphoma and CLL, it was possible to establish the immunophenotype, i.e. an information of diagnostic and prognostic relevance, by monitoring the expression of certain miRNAs from cytologic glass smears and FFPE samples, with the same result compared to frozen samples. This validation procedure for the expression data obtained by the miRNA extracted from the smear is an undoubted progress in the technology of analysis of these important cancer markers. The possibility to use material from smears allows to implement the number of cases for retrospective studies of dog's hematological malignancies (and even neoplasms of different origin). It also allows to manage and maintain, in a simple and affordable way for every veterinarian, the material on which to perform analysis for diagnosis and prognosis.

Chapter 2:

High Resolution Melting Analysis (HRMA) of genic polymorphisms for diagnostic purposes

2.1 High Resolution Melting Analysis (HRMA)

High Resolution Melting Analysis (HRM or HRMA) is a recently developed technique for fast, high-throughput post-PCR analysis of genetic mutations or variance in nucleic acid sequences. It enables researchers to rapidly detect and categorize genetic mutations (e.g. single nucleotide polymorphisms (SNPs)), identify new genetic variants without sequencing (gene scanning) or determine the genetic variation in a population (e.g. bacterial diversity) prior to sequencing. The first step of the HRM protocol is the amplification of the region of interest, using standard PCR techniques, in the presence of a specialized double-stranded DNA (dsDNA) binding dye. This specialized dye is highly fluorescent when bound to dsDNA and poorly fluorescent in the unbound state. This change allows to monitor the DNA amplification during PCR (as in quantitative PCR). After completion of the PCR step, the amplified target is gradually denatured by increasing the temperature in small increments, in order to produce a characteristic melting profile; this is termed melting analysis. The amplified target denatures gradually, releasing the dye, which results in a drop in fluorescence. When set up correctly, HRM is sensitive enough to allow the detection of a single base change between otherwise identical nucleotide sequences. HRM uses low-cost dyes and requires less optimization than similar systems based on TaqManR and fluorescence resonance energy transfer (FRET) probes. Compared to these methods HRM is a simpler and more cost-effective way to characterize multiple samples (High Resolution Melt Analysis, Application Guide, www.kapabiosystem.com).

Overview of the Melting Profile Principle

Amplification product melting analysis is not a novel concept and exploits a fundamental property of DNA, called melting: the separation of the two strands of DNA with heat. PCR product melting analysis in combination with real-time PCR was first introduced with the LightCyclers and the stability of DNA duplexes was monitored using SYBRR Green I dsDNA intercalating dye to detect primer-dimers or other non-specific products (Wittwer et al., 1997). This procedure, called Low Resolution Melting has been performed for over a decade. A Low Resolution Melt curve is produced by increasing the temperature, typically in 0.5 °C increments, thereby gradually denaturing an amplified DNA target. Since SYBRR Green I is only fluorescent when bound to dsDNA, fluorescence decreases as duplex DNA is denatured. The melting profile depends on the length, GC content, sequence and heterozygosity of the amplified target. The highest rate of fluorescence decrease is generally at the melting temperature of the DNA sample (Tm). The Tm is defined as the temperature at which 50% of the DNA sample is doublestranded and 50% is single-stranded. The Tm is typically higher for DNA fragments that are longer and/or have a high GC content. The fluorescence data from low resolution melting curves can easily be used to derive the Tm by plotting the derivative of fluorescence vs. temperature (-dF/dT against T) as shown in Figure 34 (High Resolution Melt Analysis, Application Guide, www.kapabiosystem.com).

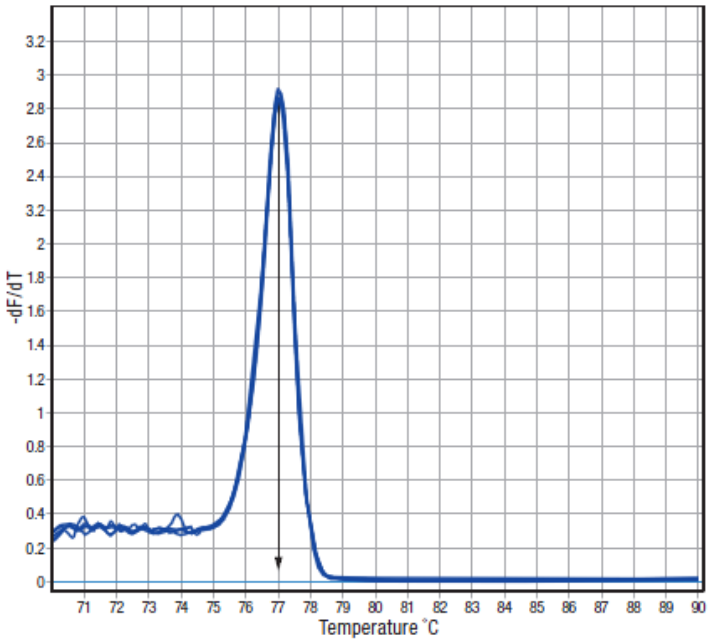

Figure 34. Low Resolution Melt profile derivative plot (-dF/dT against T). The steepest slope is easily visualized as a melt peak. In this example the Tm of the amplicon is 77 °C (High Resolution Melt Analysis, Application Guide, www.kapabiosystem.com).

The principle of HRM is the same as a Low Resolution Melt, except that the temperature difference between each fluorescence reading is reduced. During a Low Resolution Melt curve analysis, the temperature increases are typically in 0.5 °C steps, but for HRM this is reduced to 0.008 - 0.2 °C increments, depending on the instrument. This allows a much more detailed analysis of the melting behavior. HRM sensitivity and reliability has been improved with the use of a variety of new dsDNA intercalating dyes and the availability of new instruments and more sophisticated analysis' software.

The introduction of HRM has revived the use of DNA melting for a wide range of applications, including: SNP genotyping, mutation discovery (gene scanning), heterozygosity screening, DNA fingerprinting, haplotype blocks characterization, DNA methylation analysis, DNA mapping, species identification, viral/bacterial population diversity investigation, HLA compatibility typing, association study (case/control).

The Intercalating Dyes

There are various types of dsDNA intercalating dyes, which have distinctly different properties. The requirements of the dyes used for HRM are different from dyes typically used for standard quantitative PCR (qPCR) assays. Factors critical in qPCR, such as the signal-to-noise ratio and amplification efficiency, are not essential requirements for HRM. Instead, the dye must provide detailed information on the melting behavior of an amplified target. Ideally the dye should not bind preferentially to pyrimidines or purines, change the Tm of the amplicon, or inhibit DNA amplification (High Resolution Melt Analysis, Application Guide, www.kapabiosystem.com). The three main classes of dsDNA binding dyes currently available are:

- **Non-saturating dyes.** SYBR® Green I is the most common non-saturating dsDNA intercalating dye. It is generally unsuitable for most HRM applications. At high concentrations, SYBR® Green I stabilizes the duplex DNA and inhibits the DNA polymerase. To allow reliable amplification, low concentrations of SYBR® Green I must therefore be used. At lower concentrations, SYBR® Green I is able to redistribute from the melted regions of single-stranded DNA back to the regions of dsDNA, which results in poor base-difference discrimination, as detailed in Figure 35. To overcome this limitation, saturating dyes have been developed.
- **Saturating dyes.** A new class of dsDNA intercalating dyes that do not inhibit DNA polymerases, or alter the Tm of the product, have recently been developed; these dyes can be added at higher concentrations than non-saturating dyes, ensuring more complete intercalation of the amplicon. The dye is not able to redistribute during melting because the dsDNA is saturated. More precise examination of the melting behavior is therefore possible, as indicated in Figure 35. Dyes such as SYTO9® and LCGreen® can be used at the saturating concentrations required for HRM.

- **Release-on-demand dyes.** The “release-on-demand” class of dyes, which include EvaGreen®, can be added at non-saturating concentrations. This is due to the novel method of fluorescence emission, where the fluorescent signal is quenched when the dye is free in solution. Upon binding to duplex DNA, the quenching factor is released and the dye emits high fluorescent signal. This allows non-saturating concentrations of the dye to be used, ensuring that there is no PCR inhibition, whilst the unique dye chemistry provides highly sensitive HRM analysis.

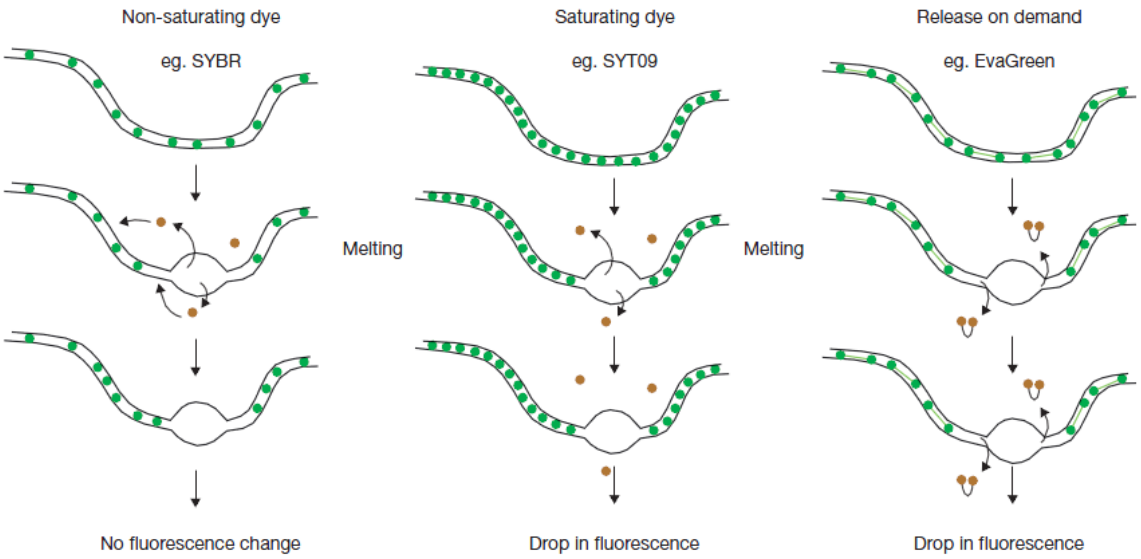

Figure 35. Non-saturating, saturating and ‘release-on-demand’ dsDNA intercalating dyes (High Resolution Melt Analysis, Application Guide, www.kapabiosystem.com). Melting of the duplex as the temperature increases releases the intercalated dyes. At non-saturating concentrations the dye rapidly rebinds to regions that remain double stranded; consequently there is no drop in fluorescence. Saturating and ‘releaseon-demand’ dyes do not redistribute from the melted regions of single-stranded DNA back to dsDNA, resulting in a reduction of fluorescence. This difference gives dyes such as EvaGreenR the high sensitivity required for HRM analysis.

Instruments and software

The power of any HRM analysis depends upon the sensitivity of the instrument and the nature of the PCR reagents used. Certain instruments have been designed specifically for HRM analysis. These can be summarized into two distinct classes:

1. Block based instruments – Samples are placed in a block for cycling and a scanning head or stationary camera is used for detection.

2. Rotary – Samples reside in a single chamber and spin past an optical detector.

There are advantages and disadvantages with each class, and the user should choose the type of instrument that best suits their needs. As a general rule, for high sensitivity and reproducibility a rotarybased instrument should be used, whilst for high-throughput and ease-of-handling, block-type instruments are optimal. The HRM run can vary considerably between instruments; some take considerably longer than others. Every instrument should be calibrated regularly (as recommended by the manufacturer, typically every 6 months), kept in a clean area on a secure and stable benchtop, and checked daily for dust buildup around the optics. The computer hardware and software must be capable of handling the large quantities of data usually generated during a HRM experiment. Analysis of the data is relatively easy with the appropriate software. HRM specific software uses various algorithms to analyze the data and display the results in easily accessible formats to help discriminate between sequence variants. Additional software packages, designed for more detailed analysis, are available from the instrument manufacturer (High Resolution Melt Analysis, Application Guide, www.kapabiosystem.com).

In this work of thesis we used the Eco™ Real-Time PCR System instrument, Illumina Inc. (9885 Towne Centre Drive San Diego, CA 92121 USA), a block based instrument whose technical characteristics are shown in Table 22. The main instrument specifications are:

- Thermal system: silver block with Peltier-based system
- Block format: 48-well block
- Samples volumes: validated for 5-20 µl

- Average ramp rate: 5.5°C/sec
- Temperature range: 40-100°C
- Temperature uniformity : ± 0.1°C
- Optical system: dual LED excitation ($%”-486 nm and 542-582 nm), four emission filters (505-545 nm, 562-596 nm, 604-644 nm, and 665-705 nm) and CCD camera
- Calibrated dyes at shipment: SYBR Green, FAM, HEX, ROX, Cy5.
- Passive reference dyes: use of ROX is supported, but optional
- Data collection: data collection in all four filters for all wells regardless of plate setup; plate setup for data analysis can be altered after run completion.
- Melt curve analysis supports continuous data acquisition in a single filter to provide increased data point collection and reduced run times
- Real-Time PCR run time (40 cycles): less than 40 minutes

Optical	Light Source	Two sets of 48 LEDs (452-486 nm and 542-582 nm)
	Detector	CCD camera (4 filters) (505-545 nm, 562-596 nm, 604-644 nm, and 665-705 nm)
Thermal	Thermal Cycling	Proprietary hollow silver block with Peltier-based system
	Thermal Uniformity	± 0.1°C
Operational	Sample Format	48-well plate
	Reaction Volume	5–20 µl
	Warmup Time	~ 20 minutes
	Typical PCR Run Time	Less than 40 minutes for 40 cycles
	Sensitivity of Detection	1 copy
	High Resolution Melt	Supported resolution to 0.1°C
	Multiplexing	Detection of up to four targets simultaneously (four-plex)
	Passive Reference	Optional (ROX)
Physical	Dimensions	34.5 cm W x 31 cm D x 32 cm H (13.6 in. W x 12.2 in. D x 12.6 in. H)
	Weight	13.6 kg (30 lb) including power supply
Environmental	Electrical	100–240 VAC, 50/60 Hz, 5A
	Temperature Range	Operating: 15°C to 30°C (59° F to 86° F) Storage: 10°C to 100°C (50° F to 212° F)
	Humidity Range	Operating: 15–90% Relative Humidity Storage: 5–95% Relative Humidity

Table 22. Specifications and Environmental Requirements of Eco™ Real-Time PCR System, Illumina.

HRM assay and reagent optimization

Due to the highly sensitive nature of HRM analysis, proper assay design is critical. Factors such as genomic DNA (gDNA) quality, primer design, MgCl2 concentration and carryover of inhibitors will all affect the melting behavior. Small differences in the initial setup can greatly affect the final results. Achieving specific amplification is critical to the success of an assay, since any non-specific amplification will greatly impair the melt analysis. Some important aspects to consider are (High Resolution Melt Analysis, Application Guide, www.kapabiosystem.com):

1. DNA quality and quantity

One of the major factors that can detract from the quality of results is the carryover of buffer from template DNA samples/preparations. Unsuitable DNA purification techniques can exacerbate this problem. Salt carryover can subtly change the melting behavior of the PCR product, and can result in low sensitivity, poor reproducibility and incorrect genotype calls. Buffer carryover from the template DNA will not only modify the Tm and melting behavior during the HRM, but can also encourage nonspecific amplification during the PCR. For optimum results the following is recommended:

- ideally, all DNA samples to be analyzed (including genotype controls) should be extracted using the same DNA extraction method or kit.
- some kits use high concentrations of salt for elution of DNA from columns. All template samples should be eluted with low salt buffers, ideally 10 mM Tris-HCl, pH 8.5.
- the DNA sample should be as concentrated as possible after purification. This helps to reduce buffer variation between samples.
- addition of a low volume of template DNA will reduce the carryover salt in the reaction; ideally the lowest volume of template that can be accurately added should be used (1 - 2 µl).
- all samples should have a similar final concentration of DNA in each assay. Table 23 details the recommended concentration of DNA for different types of

template. At low template concentrations, there is a greater chance of incorporating a mutation early in the PCR which will affect the melting behavior; high concentrations of DNA will result in high background fluorescence due to increased intercalation of dye into dsDNA.

- positive control(s) for all genotypes should be included where possible, preferably at the same concentration as their corresponding test samples. Control DNA should also be eluted and/or diluted in the same buffer as the samples.

Type of DNA	Recommended amount for HRM analysis/reaction
Genomic DNA (gDNA)	10 ng - 100 pg
Plasmid DNA (1 – 10 kb)	1 ng - 10 fg
Amplicon DNA	10 pg - 1 fg

Table 23. Recommended concentration of DNA for different types of template (High Resolution Melt Analysis, Application Guide, www.kapabiosystem.com)

2. Primer design

The design of primers for HRM analysis can be a challenge, due to the fact that small amplicon sizes are required for maximum sensitivity. The short amplicon lengths required for HRM restricts the number of potential primer locations; well-designed primer sets will improve the quality of the final result. Potential primer sets and full-length amplicons can then be tested for specificity using a BLAST search. Factors such as the position of the primer, the need for a GC region on the 3' end, the presence of any secondary structures in the primers or target, and the predicted specificity of amplification should be carefully considered. Some commercial primer design software program such as Primer3 or Primer3Plus may be helpful. This software assists in positioning primers such that specific regions are included or excluded, and amplicon size can be

specified. Figure 36 shows an example of the input page of the Primer 3 design package, when used to design primers for amplification of a human SNP.

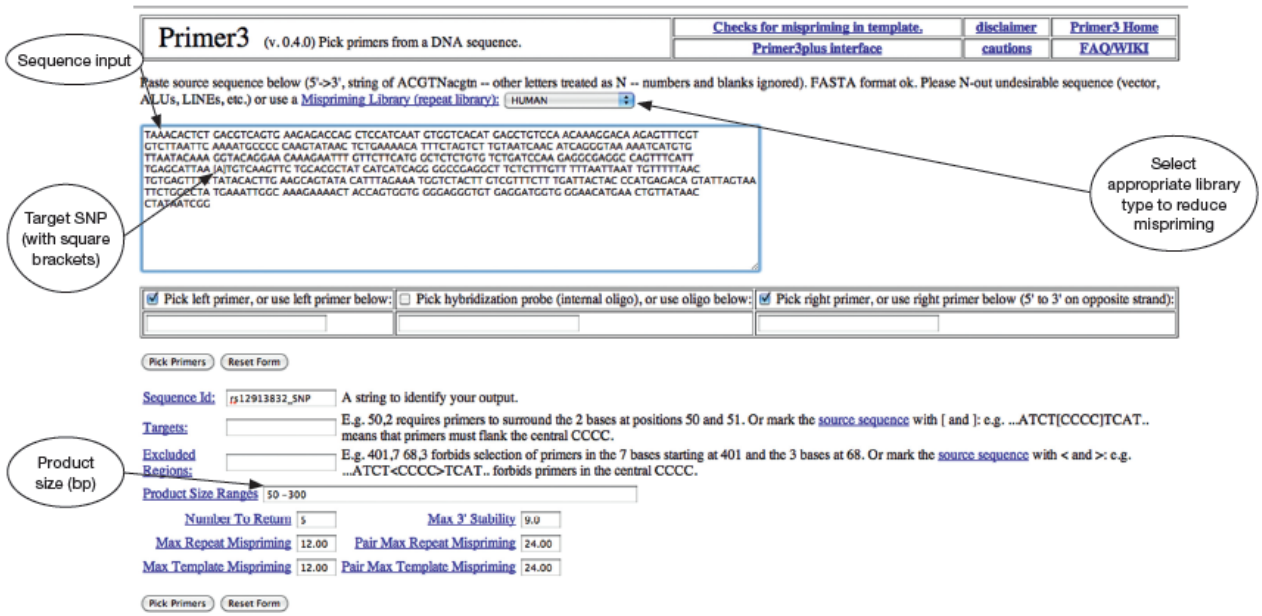

Figure 36. Design of primers for amplification of a human SNP using Primer 3 (http://frodo.wi.mit.edu/primer3/). The target SNP is shown in square brackets (e.g. ... TTAA[A]TGTC...) and the product size is set to 50 – 300 (bp). Selection of the mispriming library 'HUMAN' helps reduce the chances of non-specific amplification (High Resolution Melt Analysis, Application Guide, www.kapabiosystem.com).

After the primers have been designed, the following factors must be checked:

• The presence of a GC 'clamp' on the 3' end. This is not essential, but usually improves amplification.

• The specificity of the primers and the presence of known sequence variations. A BLAST search with both primer sets and the expected amplification product should be performed. If possible, sequence variations should also be checked.

• The secondary structure of the primers and the expected amplification product. This should be examined using appropriate software for example, m-fold, http://mfold.rna.albany.edu/?q=mfold/dna-folding-form, or operon, http://www.operon.com/tools/oligo-analysis-tool.aspx. Amplification of any secondary structure within the product may result in unusual melting profiles. Primers may need to be redesigned to avoid areas of secondary structure.

• Amplicon size. This must be optimal for the specific application, typically between 100 - 300 bp.

3. Primer concentration and purification

The primer concentration should not greatly affect the overall HRM result. Minor changes are possible, but are likely to be amplicon specific. The recommended primer concentration to avoid nonspecific amplification is between 0.05 and 0.5 µM final. We used the final concentration of 0.3 µM as recommended by the Evagreen's manufacturers.

4. Effect of MgCl2 on HRM analysis

The concentration of MgCl2 in PCR is known to greatly affect amplification efficiency. For some targets, adjusting the MgCl2 concentration will result in reduced non-specific amplification, allowing clearer distinction of sequence variations; however, MgCl2 concentration has other, notable effects on HRM. It is important to realize that the optimum MgCl2 concentration for amplification efficiency is not necessarily optimal for HRM sensitivity. The effect of MgCl2 is shown in Figure 37. As the MgCl2 concentration is increased, the HRM difference graphs change distinctively.

5. Amplicon length

The optimal length of an amplicon is dependent upon the nature of the assay. The longer the amplicon, the more difficult it is to obtain clear discrimination between sequence variants. For single base changes or SNPs, and for single base insertions/deletions, it is recommended that amplicons be 50 – 300 bp. The clearest discrimination is usually seen with the shortest amplicons. As the amplicon size increases, a more complex melting pattern can develop, making it more difficult to distinguish between single nucleotide variants. The use of smaller amplicons may result in low fluorescence values, presumably due to reduced dye incorporation. However, this is usually not a problem unless the assay is run alongside a longer amplicon assay. When screening for unknown

sequence differences, longer amplicons (typically 200 – 500 bp) can be used. This is useful in gene scanning or determining the variation within a population (e.g. viral) and reduces the number of primer sets required. Furthermore, too short amplicons are difficult to sequence.

6. Effect of PCR enhancers on HRM analysis

PCR enhancers are commonly added to end-point PCR in order to help reduce non-specific amplification, reduce the number of required cycles and increase yield. These enhancers function by assisting the melting and annealing of primers and templates, and can affect HRM performance. For GC-rich amplicons, the addition of DMSO appears not to affect the HRM significantly, and is recommended if amplification is difficult. Overall, the addition of PCR enhancers is not recommended as they usually detract from HRM performance.

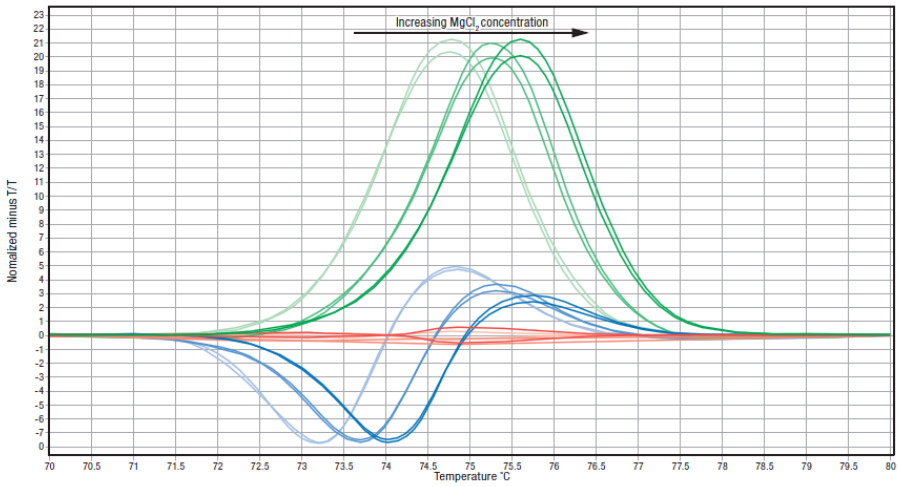

Figure 37. Effect of increasing MgCl2 on melting behavior. Three Difference Graphs are overlayed to demonstrate the dependence of amplicon melting on MgCl2 concentration. The effect of MgCl2 is most pronounced in the heterozygote samples (blue), a result of the magnesium stabilizing the annealing of mispairs. The MgCl2 concentrations are 1.5 mM, 2.5 mM and 3.5 mM final. G/G = green, G/A = blue, and A/A = red (High Resolution Melt Analysis, Application Guide, www.kapabiosystem.com).

Analysis of results

With the correct software, data analysis is typically straightforward, allowing multiple samples to be analyzed simultaneously. It is important to know what to look for when interrogating results; unforeseen errors made during setup can be identified at this point. Low resolution melt plots are often viewed as a derivative plot (−dF/dT against T); however, HRM raw melting curves must be analyzed differently. This section concerns how to analyze the HRM results; a 124 bp product covering a Type IV SNP (rs641805) is used as an example (High Resolution Melt Analysis, Application Guide, www.kapabiosystem.com).

Amplification plots. Reproducibility of amplification is more important for HRM analysis than the efficiency of amplification (as compared to qPCR). For example, HRM analysis can still be performed if the product amplifies later than expected (i.e. due to limitations in primer design), provided that all the samples are consistent, the no template control (NTC) does not amplify and the product is specific.

Raw data melt curve. The data collected during the HRM analysis has a range of initial (pre-melt) fluorescence readings. This variance makes it difficult to properly analyze results, even though different genotype groups may be visible. Figure 38A illustrates how the selection of pre-and post-melt regions is used to align data. Pre- and post-melt regions must be selected for each primer set, by positioning the parallel double-bars as shown. It is important to adjust these bars so that the melt region is not selected. If the preor post-melt regions are not clearly defined, it is possible to repeat the HRM run only (without repeating the amplification step), and adjust the temperature range as required.

Normalization data. If the data is normalized correctly, it will appear as shown in Figure 38B. This is termed ‘Normalization Data’. Here the fluorescence variance seen in Figure 38A has been eliminated, and only the temperature range between the outer bars of the pre- and post-melt regions is shown. The genotypes are now more distinct, but the two homozygote samples (in red and blue) are still difficult to distinguish.

Difference graph. Some HRM software applications allow calculation of the difference plot. This is achieved by subtracting the normalized fluorescence data of a user-defined genotype from that of each of the other samples in the HRM analysis. In Figure 38C, the A/A genotype has been selected as a baseline (any genotype can be selected, but usually one of the homozygotes is used). The position of each sample relative to the baseline is plotted against the temperature. This form of HRM analysis is an aid for visualizing the Normalization Data. Automatic calling of genotypes of sequence variants can usually be performed with the software; sometimes confidence ratings are given. However, checking the difference to confirm the genotype is recommended.

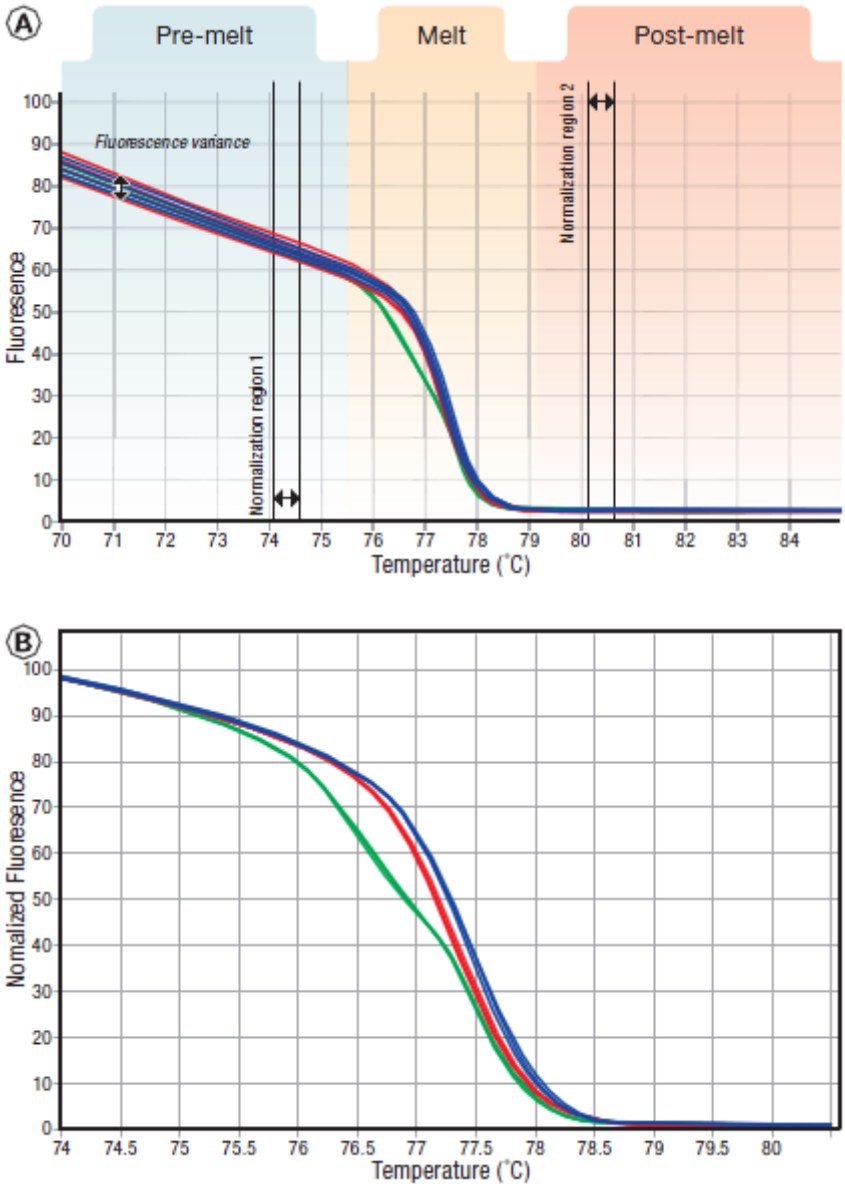

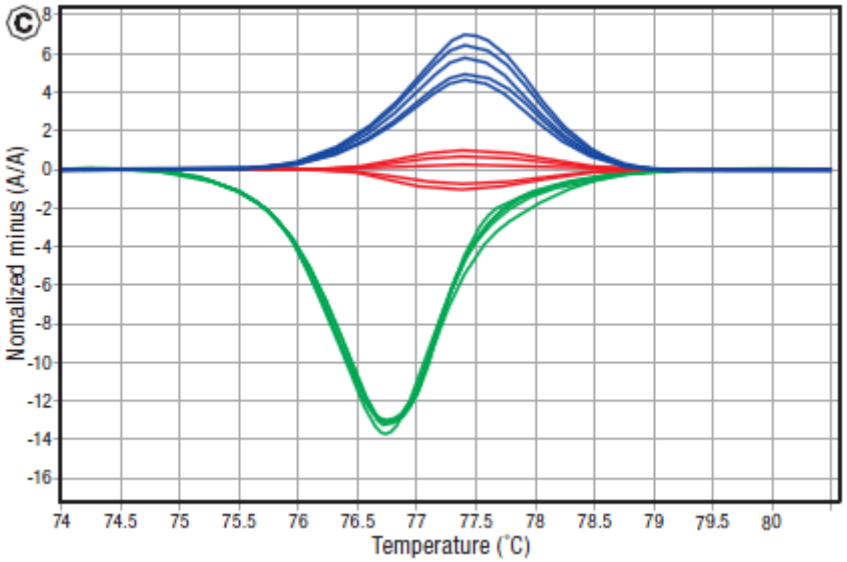

Figure 38. Analysis of HRM data from a type 4 SNP (A/T). Different genotypes are highlighted in different colors. A/A = red, A/T = green, and T/T = blue. **A.** Raw data showing the pre-melt, melt and post-melt regions. Notice the fluorescence variance and the positioning of the pre- and post-melt identification bars. **B.** Normalization Data derived from the raw data plots in A. Positioning of the pre-melt, and post-melt bars provides a more detailed view of the melt region. **C.** Difference Graph derived from the Normalization Data (High Resolution Melt Analysis, Application Guide, www.kapabiosystem.com).

2.2 HRMA of gyrA Ser84Leu mutation conferring resistance to fluoroquinolones in *Staphylococcus pseudintermedius* isolates from canine clinical samples

2.2.1 Introduction

Staphylococci: General information and Taxonomy

The genus *Staphylococcus* belongs to the family of *Micrococcaceae*, and is the only of its kind that includes pathogens with medical and veterinary concern. It is Gram-positive, spherical in shape (cocci), a diameter of about 0.5-1,5 μm aerobic and facultative anaerobic, motionless, catalase-positive and oxidase-negative (Poli G. And Cocilovo A., 2005). The taxonomic classification of staphylococci has changed a lot over the years thanks to improvements in microbiological and enzymatic techniques but especially in molecular methods. We can then identify the different species on the basis of different criteria:

- Phenotype (colony morphology, cell wall composition, molecular structure and activity of various enzymes, nutritional and oxygen requirements, composition of cellular fatty acids, products of the fermentation of carbohydrates, products of glucose metabolism, electron transport system, sensitivity to bacteriophages, resistance to specific antibiotics such as novobiocin)
- Genotype (chromosome size, composition and homology of the DNA, ribotype)

Staphylococci are now classified into forty different species on the basis of genotype, habitat, and the pathological process caused (Martino P.A. et al., 2005). A good criterion to classify staphylococci is the production of coagulase. In fact the various species can be divided, according to their ability to coagulate

rabbit plasma, in coagulase-positive and coagulase-negative. Coagulase is an enzyme considered by many authors as a factor closely related to pathogenicity, as it promotes the spread and survival of the bacteria in the body. It is present in many staphylococci and its main action is to coagulate the plasma resulting in activation of fibrinogen and its subsequent transformation into fibrin. The formed clot protects the bacteria from the immune system that fails to reach, for which bacteria who develop this enzyme are more resistant to the immune defenses of the host (Cox H.U. 2006). The coagulase is also defined free coagulase to distinguish it from clumping factor, an enzyme that bound to the bacterial cells and which has the same function.

Staphylococci are ubiquitous bacteria widely distributed in the environment. They can be found in water, air, soil, dust, and a wide variety of inanimate objects (Martino P.A. et al., 2005). They can also be considered the most common saprophytic of humans and animals skin. As well as on the skin, Staphylococci can be isolated from mucous membranes of various apparatuses, including the respiratory, gastrointestinal and urogenital tracts. Many people can be healthy carriers which are then considered a likely source of infection for themselves and for others (Cox H.U. 2006). Moreover, given their strong environmental resistance, they can survive the toughest conditions, persisting for months outdoors (protected from sunlight), and in the laboratory after transplantation in fresh medium or freezing. They are also relatively resistant to heat (about thirty minutes at 60 °C), drying and also to the common disinfectants if properly protected from organic material (pus, mucus, milk, serum, debris) (Martino P.A. et al., 2005; Cox H.U. 2006). In addition to being very resistant these bacteria have developed several factors which allow the colonization and infection of host tissues. Each species of staphylococcus can therefore be considered as potentially pathogenic, although each shows a wide and varied spectrum of virulence as well as host and seat preference. These bacteria then act as opportunistic pathogens (except *Staphylococcus aureus* a real pathogen). They in fact, after a decrease in immune function, invade the epithelium. This colonization can be stimulated by various conditions such as: mechanical insults

of the skin (eg., wounds, abrasions, etc.), other infections / infestations (eg., demodicosis, dermatophytosis, pyoderma, etc.) or even particular changes (eg., seborrhea, hypothyroidism, Cushing's disease and Addison's disease). In addition, subjects persistently immunosuppressed are more affected and develop more violent and persistent clinical forms. When bacteria invade the skin may cause local infections, from light (acne, impetigo) to severe (furunculosis) or, as a result of colonization of the bloodstream with bacteremia, develop purulent processes of various kinds (especially abscesses) in different locations: liver, kidneys, lungs, joints. In dogs they can be attributed to specific diseases such as otitis, pyoderma and metritis (Cox H.U. 2006).

Staphylococcus pseudintermedius

Staphylococcus pseudintermedius is a bacterium that is commonly found on the skin or in the nose or intestinal tract of 50% of more of healthy dogs, and a smaller percentage of healthy cats. Typically it causes no problems at all, but it is an opportunistic pathogen. This bacterium can infect almost any tissue, but skin and soft tissue infections are more common, particularly when the skin has been damaged by something else (e.g. allergies, scratching, chronic wetness, wounds, surgery). Ear infections are also very commonly caused by *S. pseudintermedius.* Infections of other body sites and organs are much less common, but can be very severe. *Staphylococcus pseudintermedius* can also be found in the nose of up to 4% of healthy pet owners. MRSP stands for methicillin-resistant *S. pseudintermedius*, which is highly resistant to many antibiotics, including most of the drugs that are commonly used to treat bacterial infections in dogs and cats. Non-MRSP strains of *S. pseudintermedius* are methicillin-susceptible (MSSP). People and animals that carry MRSP without any signs of infection at all are said to be colonized. When infection with *S. pseudintermedius* (either MRSP or MSSP) occurs, this causes signs of inflammation (e.g. heat, pain, swelling, discharge, fever) (www.wormsandgermsblog.com).

Staphylococci: classical methods of isolation and identification

Staphylococci easily grow on common growth media, without the need of particular substances or pH indicators; they form colonies with color from gray to yellow to orange (Figure 39) (Cox H.U. 2006).

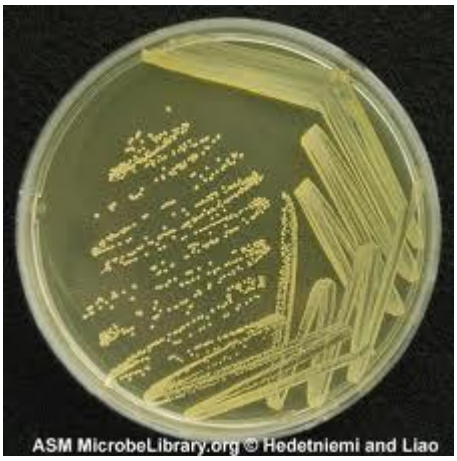

Figure 39. Colonies of *Staphylococcus aureus* in a growth medium common Agar (ASM Microbel library.org®)

However, due to the great resistance of these bacteria, specific selective media to disadvantage the growth of contaminants and promote the purity of the colony are often used. In particular, since staphylococci are halophilic, they are able to withstand high concentrations of sodium chloride (up to 10%), and they can grow on culture medium (MSA-Mannitol Salt Agar-) that contains a large percentage of this salt (approximately 7.5%). Being staphylococci mesophilic bacteria, their growth temperature is between 18 and 40 ° C with an optimum at 37 ° C, and also being aerobic-anaerobic facultative, they can grow both under normal oxygen conditions and in modified atmosphere (10% of carbon dioxide) (Martino P.A. et al., 2005; Cox H.U. 2006).

With regard to the macroscopic appearance of the colonies, in liquid media a uniform turbidity is obtained, while in solid media, after incubation for 24 hours at 37 ° C, are present as large colonies roundish of about 2-3 mm in diameter, opaque, smooth and convex; encapsulated strains can form colonies of mucoid appearance (Martino P.A. et al., 2005). The staining of these colonies may vary as

already mentioned from gray to yellowish, to orange depending on the pigmentation of the cell membrane, being the colour not associated with pathogenicity. Isolation of the bacterium on soil Agar-blood can be useful for identification, because some staphylococci, according also to the type of red blood cells used for the ground, show a well clear halo of hemolysis (Figure 40).

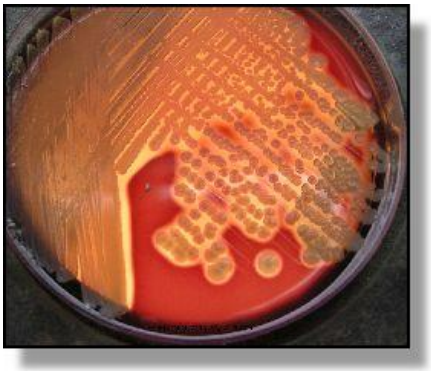

Figure 40. Clear area of hemolysis around the colonies of *S. aureus* on blood-Agar (ASM Microbel library.org®)

After isolation of blood-Agar colonies, identification by various cultural and biochemical methods can be done:

- Examination of the morphology. The morphological characteristics (size, shape, color, odor, presence of hemolysis, etc.) of the colonies already provide some important information useful for a first partial identification. Staphylococci tend to aggregate in irregular clusters, but occasionally can be found arranged individually, in pairs (diplococci) or in groups of four (tetrads) (Figure 41) (Martino P.A. et al., 2005).

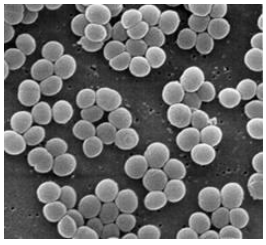

Figure 41. Staphylococci in electron microscopy arranged in small clusters of several subjects. (ASM Microbel library.org®)

- Bacterioscopic examination of stained preparations. This test provides further information on the morphological characteristics of the isolated bacteria and also on how they react to certain differentials colors (eg, Gram, Ziehl-Neelsen). In the case of staphylococci the examination with an optical microscope is preceded by Gram stain, which, for Gram-positive bacteria, allows detection of blue-violet microorganisms (Figure 42).

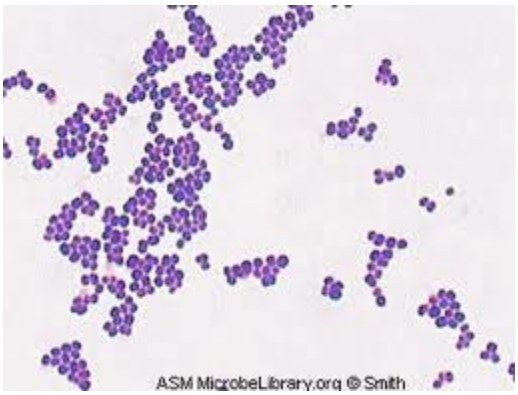

Figure 42. Staphylococci with Gram stain

- Proof of the catalase. This test is used to highlight the presence or absence of this enzyme and to easily distinguish staphylococci (catalase-positive) from streptococci (catalase negative). There are several commercial kits but more simply is to dissolve a colony in one drop of water 3% hydrogen peroxide placed on a glass slide. In case of positivity we note the presence of bubbles due to the formation of free oxygen, within a few seconds (Poli G. and Cocilovo A., 2005).
- Proof of the oxidase. For this test a colony of the bacteria in question is dissolved in a drop of saline placed on a glass slide; the suspension is subsequently immersed in a disk of paper, impregnated with a solution of tetramethyl-p-phenylenediamine dihydrochloride (the disks are commercially available). In case of positive reaction, within 10-20 seconds is observed the appearance of an intense purple color. There are also commercial kits, which allow the simultaneous execution, in vitro, of the

catalase and oxidase tests. Obviously, in the presence of colonies of staphylococci, this test must be negative (Figure 43) (Poli G. and Cocilovo A., 2005).

Figure 43. Outcome of the catalase test: on the right a positive sample, on the left a negative sample (www.mesacc.edu)

- Proof of coagulase. For the determination of the coagulase presence several techniquescan be used: the test in a single tube, for the detection of free and bound coagulase, performed on colonies from selective and differential media, for example MSA. A sub-culture of the strain in question is prepared in a generic liquid medium, like BHI Broth (Brain-Hearth Infusion Broth), for the cultivation and maintenance of a wide variety of microorganisms. After approximately 6-12 hours of incubation, when appreciates microbial growth, the test is carried out, taking 0.05 ml of culture broth and adding 0.5 ml of rabbit plasma. The anticoagulant used in commercial preparations of rabbit plasma can be lyophilized citrate or EDTA, we must remember that the citrate can be metabolized, with consequent risk of false positives caused by nonspecific plasma coagulation, when free calcium ions previously chelates. After incubation at 37 ° C, the observation is carried out at 1, 2, 4, 8 and 24 hours. If the bacteria is coagulase-positive, coagulation is observed within 24 hours. Beyond this time, there may be a spontaneous fibrinolysis, with the risk of false negatives. The test slide (for the detection of bound coagulase or clumping factor) is presumptive and the negative result must be

confirmed by the test tube. A drop of rabbit plasma is deposited on a glass slide and a colony is dissolved; the occurrence, within 5 seconds, of microscopic flakes is a sign of positivity (Poli G. and Cocilovo A., 2005).

- Biochemical tests and API-System®. The microorganisms differ from each other for the differential ability to use certain substrates or to produce certain substances. It is possible to identify and classify them according to the final products or intermediates of various biochemical reactions of which they are capable. API-System® (bioMérieux) is a miniaturized and standardized system for the identification of microorganisms by biochemical tests. It is used when the first phase of identification has narrowed down the possibilities to a few genera or it only remains to identify the species. It consists of a gallery with 20 wells, each containing a different soil and appropriate chromogenic indicators; therefore allows the simultaneous execution of 20 biochemical tests. Some reactions are read immediately, according to the spontaneous color changes of the substrates used in the individual well; in other cases, only after the addition of specific reagents. Is thus possible to detect simultaneously the ability of the microorganism to metabolize various sugars to produce acids or gas, to liquefy the gelatine, to use citrate, to reduce nitrate, etc. There is a version of this identification system, called API-Staph® specifically targeted to the genera Staphylococcus and Micrococcus.

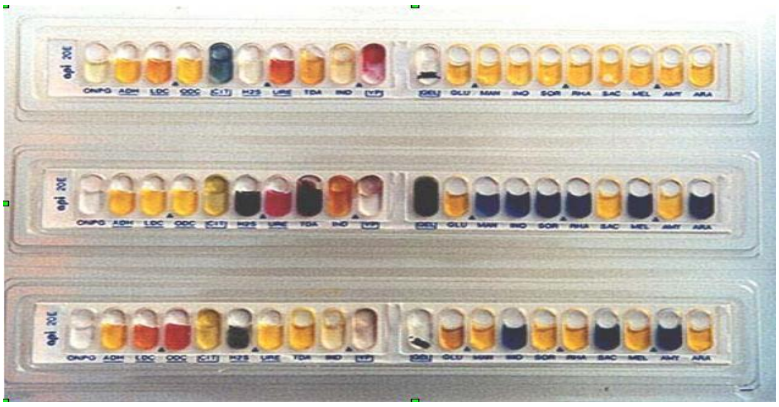

Figure 44. Example of a biochemical test API-System ®
(www.jlindquist.net)

Antibiotic resistance

Antibiotic resistance is a phenomenon by which a bacterium is immune to the effects of one or more antimicrobial drugs. This phenomenon can be considered as an evolutionary and adaptive biological process that bacteria carry out to escape the selection (Levin B.R. et al., 2000). The selection pressures reach maximum levels when bacteria are exposed to sub-optimal doses of the drug. The resistance may be natural or acquired: the first is determined by the innate characteristics of the microorganism, for example a Gram-negative bacterium is naturally resistant, thanks to the porosity characteristics of their membrane, to glycopeptide antibiotics such as vancomycin. The second appears when occurring genetic modifications that allow to changed subjects the survival and transmission of the modifications (Levin B.R. et al., 2000).

The changes are divided into chromosomal and plasmidic. The chromosomal mutations, also known as endogenous, occur primarily at the level of nuclear DNA by spontaneous phenomena of substitution, insertion and deletion of base pairs (point mutations) or more pairs of bases repeated (mutations for repeated sequences) within the colony to each replication cycle with a frequency of 1:103 - 1:109 for cell division. This type of mutation occurs more slowly and rarely compared to plasmid-mediated mutations but usually gives to the changed population a permanent resistance to antimicrobial agents. Obviously, being this mutation spontaneous and random, it does not mean that, once completed, a mutation affects exactly the portion of DNA that contains sequences related to molecules or structures that are antibiotic targets. The genic modifications mediated by plasmids, however, are caused by fragments of double-stranded circular cytoplasmic DNA. This type of filament is common in bacteria and promotes the exchange of genetic information between phylogenetically related micro-organisms. The plasmids are small DNA fragments of different size: the smaller ones (approximately 10kb) are generally present in large number in the cytoplasm (10-20); those more bulky (100-150kb) are usually present in single or double copy. The plasmids replicate with the aim of specific proteins and are divided among the daughter cells during binary fission. They are able to transmit

genetic information that are used to develop new features dangerous for the host: virulence factors, the production of new proteins or enzymes for the survival, detoxification, antibiotic-resistance (Smillie C. et al., 2010).

There are mainly three other mechanisms that bacteria can use for the exchange of genetic material, with both chromosomal and plasmid nature:

- Conjugation: it is a process in which takes place the direct exchange of genetic material from a donor cell to a recipient through the formation of a particular structure called pilo sexual, which allows the horizontal passage of chromosomal DNA or, more frequently, plasmid.
- Transformation: during this process the genes are acquired by the recipient cell in the form of naked extracellular DNA. Basic assumption is the death of another microorganism which, after analysis of their structures, releases the DNA into the surrounding environment. The recipient cell adsorbs the free DNA through the cell wall and, as a result of recombination with a homologous segment, it incorporates into its DNA acquiring new characters.
- Transduction: in this process, the gene transfer is mediated by bacteriophages (or phages), i.e. from viruses that infect bacteria. A phage infects a bacterium, basically, and takes control of the genetic processes of the bacteria to replicate. During this process, inadvertently, bacterial DNA (genomic or plasmid) can replace and/or become incorporated into the newly formed phage DNA, a phenomenon called transduction (only the phages characterized by dsDNA can be transducing). After bacterial death, which follows the lysis, the new phages are released and go on to infect other bacteria, carrying to them genetic material from previously infected bacteria (an example of transfer by transduction regards the plasmid carrying the gene for β-lactamase in S. aureus).

In any cases the appearance of antibiotic resistance is linked to three main categories of mechanisms: alteration of the binding site between the target protein and antibiotic; production of enzymes that destroy the drug; decrease in

the concentration of the antibiotic in the cytoplasm (Walsh C. 2000). The alteration of the binding site occurs via genetic mutations both chromosomal ande plasmid-mediated, which alter the affinity for the drug by changing the nucleotide sequence of a certain protein. In this way even if the antibiotic reaches the cytoplasm, it fails to exert its bacteriostatic action or bactericidal activity. Examples of this mechanism are provided by PBPs (Penicillin Binding Proteins), that are target enzymes of β-lactam antibiotics. The production of enzymes that break down the drug is definitely one of the most studied and known mechanisms of antimicrobial resistance. The best known case is undoubtedly that of beta-lactamase enzymes produced by many microorganisms that destroy the antibiotic belonging to the group of β-lactam (penicillins and cephalosporins). These enzymes are encoded both by plasmids, such as the R plasmid which also contains the TEM-lactamase, and by chromosomal sequences such as AmpC, characteristic of many Gram-negative bacteria (Nikaido H. 2009). The beta-lactamases cause hydrolysis and subsequent destruction of antibiotics and have become increasingly refined and perfected by the great use of β-lactam antibiotics. These antibiotics are increasingly improved over the years to escape the enzymes produced by bacteria, but inexorably microorganisms develop resistance by producing and adapting their defense mechanisms. The production of pumps for the cytoplasmic efflux is a very refined mechanism of resistance whose transmission to other bacteria is quite difficult because of the complexity of the genes that encode them. Antibiotics enter into the cell through pores of the membrane, but can be extruded from the cytoplasm due to the presence of these pumps which are nothing more than transmembrane proteins that actively expel the drug. This system, developed by both Gram-positive and Gram-negative bacteria, has been particularly studied in E. coli, but also in staphylococci, especially *S. aureus*, and is responsible for resistance to multiple antibiotics, especially the fluoroquinolones (NorA), tetracyclines, macrolides and β-lactam antibiotics (Nikaido H. 2009).

Evaluation of antibiotic susceptibility

All chemoantibiotics compounds are effective only towards certain bacterial species while have no effect on others species. Furthermore, the emergence of resistance makes immune some bacterial strains that commonly fall in the spectrum of action of the antimicrobial. For this reason when infection by a pathogenic micro-organism is suspected, before embarking on empirical therapy, at least one antibiogram should be performed since it gives not only information about the involved strain, but also general information about the antibiotic resistance. The antibiogram, performed according to the Kirby-Bauer technique, is certainly one of the most used techniques in clinical practice and is a standardized method regarding the amount of bacteria seeded (using a bacterial inoculum equal to Section 0.5 of the McFarland scale, i.e. to 5 x 108 CFU / ml) and the type of media used (Mueller-Hinton, devoid of para-amino acid -benzoic acid). The inoculums are seeded for inclusion in agar or slithered on the surface by swab. Then a number of cellulose diskettes impregnated with known amounts of antibacterial drugs are deposited on the surface of theplates. Since the chemoantibiotics spread by disks into the surrounding media and, if effective, inhibit bacterial replication in a much larger area, after the incubation period of the plates (typically 37 ° C for 24 hours) it is thus observed the appearance of zones of inhibition of growth around the diskette antibiotic, whose diameter is proportional to the antibacterial activity of the antibiotic content (the greater is the halo, the greater is the antibiotic activity). The absence of a halo is, instead, a sign of ineffectiveness of the drug. With this technique it is therefore possible to classify the bacteria as susceptible, intermediate or resistant to several antibiotics tested (Figure 45).

Figure 45. Antibiogram performed according to the Kirby-Bauer technique (www.wikipedia.org)

MIC (Minimum Inhibiting Concentration), is the minimum concentration of antibiotic capable of inhibiting bacterial growth. The most common technique of execution involves dilution in liquid media (or broth): the technique can be performed in a test tube (macromethod) or in 96-well plates (micromethod). It starts from a bacterial inoculum with a concentration equal to 100 CFU/ml, which is mixed at scalar concentrations of antibiotic. The technique performed in a test tube provides the twofold serial dilution, starting from 128 micrograms/ml of the antibiotic, in volumes of 1 ml. The micromethod instead is performed by mixing 100 µl of BHI for growth of the bacterium, 100 µl of bacterial suspension and, in the first tube, 100 µl of stock solution of antibiotic (equal to 1 mg/ml, obtained by dilution of the powder of the principles active in distilled water and filtration), or two-fold serial dilutions of the same antibiotic solution for the remaining tubes. Following incubation at 37 ° C for 18-24-48 hours, the MIC is obtained as the highest dilution, i.e. the smallest amount of antibiotic, capable of visibly inhibiting bacterial growth.

Fluoroquinolones: Historical background and generality

Quinolones are a class of chemotherapy (i.e. generated by chemical synthesis) antibiotics discovered at the end of the Fifties of the last century, whose progenitor may be considered the nalidixic acid. Given their spectrum of activity, i.e. Gram-negative aerobes and anaerobes, their rapid renal excretion and the achievement of high urinary concentrations, they were usually used to treat infections of the genito-urinary tract. However, given their narrow spectrum of activity and the emergence of significant resistance phenomena, they have slowly fallen into disuse. In more recent years, starting from quinolones, novel compounds called fluoroquinolones have been synthesized that, due to the presence in their structure of a fluorine atom, have a broader spectrum of action and smaller phenomena of resistance. These drugs have a good intestinal absorption, good tissue distribution and prolonged half-life of elimination (Carli et al., 2009). Lately there is a growing series of antibiotic resistance even against this class. Currently, in Italy, some fluoroquinolones are registered for use in veterinary medicine (i.e. enrofloxacin, danafloxacin, difloxacin, flumequine, marbofloxacin and norfloxacin).

Fluoroquinolones: Chemistry and mechanism of action

The fluoroquinolones are synthesized starting from the same chinolonic structure, from time to time amended with different chemical substituents (such as fluorine) and side chains. These modifications, as a rule, do not change the spectrum of action of fluoroquinolones but instead affect the kinetic characteristics, in particular the bioavailability, the ability of tissue distribution and excretion rhythms (Carli et al., 2009). The mechanism of action of these chemotherapeutic type is bactericidal, very rapid and dose-dependent. It is carried out at the level of two enzymes of the class of topoisomerase: DNA gyrase and topoisomerase IV. The DNA gyrase, an enzyme composed of two GyrA subunit and two GyrB subunits transcribed respectively by gyrA and gyrB genes, is crucial as it is the only enzyme able to rotate the DNA windings negative; this ability is important during the step of replication and synthesis of

the DNA (Drlica K. and Malik M. 2003). The topoisomerase IV is an isomerase type II and is the main enzyme responsible to the separation of DNA strands at the end of the replication process. It also consists of two subunits ParC (calls grlA in *Staphylococcus aureus*) and two subunits ParE. The main targets of fluoroquinolones are GyrA and parC; the bond with these molecules hampers the separation and rejoining of DNA strands and this results in inhibition of DNA synthesis, poor reparative ability of the genetic material and cell death (Drlica K. and Malik M. 2003). More precisely, the link between drug, enzyme and open DNA, called ternary complex, prevents the progression of replication and transcription, and causes fragmentation of the chromosome which will lead to cell lysis. The high selective toxicity that these compounds have towards prokaryotic cells is justified by the fact that the eukaryote DNA-gyrase is inhibited at much higher concentrations than those of the bacterial cell (about 100-1000 micrograms/ml against 0.1-10 micrograms/ml) (Carli et al., 2009). For Gram-negative the primary target of fluoroquinolones is the DNA gyrase enzyme, while for the Gram-positive is the topoisomerase IV enzyme.

Fluoroquinolones: Resistance

The resistance against these drugs is predominantly chromosome-linked, then stable, and its appearance is directly related to the concentrations of the chemotherapeutic in the site of infection. A repeated exposure to sublethal concentrations of fluoroquinolones can then produce a dangerous and stable resistance; which usually, being of cross-type, makes ineffective the other drugs of the same class (Carli et al., 2009). The onset of this phenomenon assumes the appearance of defensive mechanisms against the quinolone by the bacterial cell, which can implement two main strategies: the formation of transmembrane pumps that actively expel the drug outside of the cytoplasm, and the modification of target enzymes of the antibiotic. The first resistance mechanism is provided by several efflux systems associated to genes with chromosomal and extra-chromosomal localization coding for transmembrane proteins that are able to reduce the cytoplasmic concentration of the drug (Table 24).

Antibiotic drug	Working	Resistance genes	Genes location	Bacteria
Tetracyclines	Outflow	*tet*	P, T, C	Gram-positive Gram-negative
Macrolides	Outflow	*mefA*	P, T, C	*Salmonella spp* *E.coli*
Chloramphenicol, Fluoroquinolones	Outflow	*blt, norA*	C	*Bacillus spp.* *Staphylococcus spp.*
Chloramphenicol, Fluoroquinolones, β-lactams, Macrolides, Tetracyclines	Outflow	*MexA, MexB AcrA, AcrB, oprM, tolC*	C	*Pseudomonas spp.* *E.coli* *Salmonella spp.*

Table 24. Examples of microbial resistance through development of transmembrane pumps. P= Plasmids, T= Transposons, C= Chromosomes. (Carli et al., 2009).

Over the years, many bacteria have also developed a tenacious resistance to these chemotherapeutic thanks to the modification of the target enzymes of these antibiotics. Obviously, the microorganisms have not followed a single common process but have adapted their strategy according to their features. As remembered above, the resistance is usually linked to stable modifications in the chromosomal genome, and its appearance is directly proportional to the concentrations of the drug in the site of infection. This occurs more frequently when the microorganism is exposed to sub-lethal concentrations of the drug for a long time. Typically the resistance is of cross-type, for which its appearance makes the bacterial strain immune, or at least not very sensitive, to all drugs in the same category.

Fluoroquinolone resistance in *S. pseudintermedius* and other Staphylococci is predominantly mediated by a mutation located at position 84 of the gyrA subunit of DNA gyrase enzyme (Ser84Leu), together with a mutation located at position 80 of the grlA subunit of topoisomerase IV enzyme (Intorre L. et al., 2007;

Descloux S. et al., 2008). All these amino acid substitutions are caused by point mutations (substitution of a single nucleotide) on particular chromosomal genes, gyrA and parC, which encode for the production of these enzymes. This causes a different reading of the nucleotide triplet and then the change in the aminoacid sequence of the enzyme. The modification of the enzyme structure decreases the binding affinity between target enzyme and quinolone that fails to form the ternary complex and thus to cause cell death (Intorre L. et al., 2007; Descloux S. et al., 2008).

2.2.2 Application of the HRMA

Since the standard methods for determining FQ resistance based on the CLSI guidelines (www.clsi.org) are tedious and time consuming, and the molecular techniques currently used to characterize FQ resistance usually require sequence-specific probes or post-amplification processing such as gel electrophoresis and DNA sequencing (Kaltenboeck B. and Wang C., 2005) which are expensive, there is a need for reliable and accurate methods allowing fast identification of gyrA-mediated FQ resistance in S. pseudintermedius strains isolated during clinical routine. Furthermore, since the appearance of resistance to fluoroquinolones in staphylococci is mediated primarily by a point mutation, we decided to use the HRM technique to detect single nucleotide polymorphisms in the *gyrA* gene, related to the antibiotic resistance, in strains of *Staphylococcus pseudintermedius* isolated from dogs with pyoderma.

Materials and methods

1. Samples isolation, species identification and evaluation of fluoroquinolones resistance

In this study, 16 *S. pseudintermedius* strains were screened for the presence of *gyrA* Ser84Leu mutation through a specific real time PCR-HRMA protocol. The strains were obtained as the unique or prevalent bacterial isolate from canine

skin, external ear and conjunctive clinical samples submitted for microbiological examination to our Department during 2009. Isolation was performed through cultivation on tryptone soy agar plates containing 5% sheep blood (Oxoid S.p.A, Rodano, Italy) for 24 h at 37°C under aerobical conditions. Isolates were identified as *S. pseudintermedius* by morphology, Gram staining, catalase activity, growth in mannitol salt agar selective medium, and API-Staph® analysis. The strains were tested for FQ susceptibility to enrofloxacin and marbofloxacin by the disc diffusion method on Muller Hinton agar (Oxoid).

2. Design of primer set

Coding sequence of *S. pseudintermedius gyrA* gene was obtained from NCBI (http://www.ncbi.nlm.nih.gov; accession number: NC_014925.1). Since nucleotide polymorphisms not related to resistance status can affect interpretation of HRMA results, we choose as target a portion of *gyrA* gene that is reported to undergo only mutations causing amino acid substitutions in FQ-resistant *S. pseudintermedius,* and no silent mutations or mutations causing amino acid substitutions in both FQ-resistant and FQ-susceptible strains (Descloux S. et al., 2008). Degenerate primer sequences available in literature for *gyrA* amplification in Staphylococci (Intorre L. et al., 2007) were adapted to *S. pseudintermedius* as follows: GyrAsmod forward primer 5'-ATGAGTGTTATCGTATCTCGTGC-3' and GyrAasmod reverse primer 5'-CCATCGAACCGAAGTTACCTTG-3', for the amplification of a *gyrA* 262 bp fragment.

3. Sample processing and DNA extraction

For *gyrA* sequence analysis, each *S. pseudintermedius* isolate was tip-sampled from a single colony and placed in an 0,5 ml Eppendorf containing 50 microl of water. Samples were then subjected to three alternate cicles of 5' at 95 °C and 5' at -80°C to obtain bacterial cell lysis and DNA extrusion.

4. Conventional PCR and sequencing

The bacterial lysates were then subjected to PCR amplification in a Mastercycler® Gradient thermal cycler (Eppendorf AG, Hamburg, Germany). The PCR reactions were carried out in duplicate in a total volume of 20µl containing 1µl of bacterial lysate, 1X Taq buffer containing 1.5mM $MgCl_2$ and 0.2mM dNTPs, 1.25 U Taq Promega and 0.5µM of GyrAsmod forward and GyrAasmod reverse primers. The thermal profile for the amplification was 94 ◦C for 90 sec; 35 cycles of 94 ◦C for 45sec, 51 ◦C for 30sec, 72 ◦C for 90sec and final elongation step at 72 ◦C for 300sec. Amplification products were run on 2% agarose gel and purified using Qiaquick™ Gel Extraction kit (Qiagen GmbH, Hilden, Germany). The purified amplicons were then sequenced using standard Applied Biosystems technology.

5. Real-time PCR amplification and HRM analysis

The same primer pair used for conventional PCR was then used for real time PCR-HRMA on an Eco™ Real-Time PCR System (Illumina, Inc., San Diego, CA, USA) carrying out each amplification reaction with 1µl of bacterial lysate, 7.5µl Supermix SsoFast EvaGreen Biorad, 0.3µM of each primer and H_2O to reach a total volume of 15µl. The thermal protocol for the PCR was 95 °C for 10min, 40 cycles of 95 °C for 5sec and 60°C for 5sec. The melting protocol was 95 °C for 15sec, 55 °C for 15sec, ramping to 95 °C with fluorescence data acquisition each 0.1 °C and a final step at 95 °C for 15sec. Sample melt curves were subjected to normalization and temperature shifting. The difference plot for each sample was generated for subsequent grouping analysis. A *S. capitis* strain of human origin, conserving the primer annealing sequences, was used to generate a *gyrA* external control curve, in order to check sequence specificity of the melting profile.

Results and discussion

1. Evaluation of fluoroquinolones resistance by antibiogram

The disc diffusion method on Muller Hinton agar showed that 5 *S. pseudintermedius* isolates were resistant to enrofloxacin and marbofloxacin, while the remaining 11 isolates resulted sensitive to both FQs.

2. Sequencing results

After conventional PCR, the purified amplicons were then sequenced using standard Applied Biosystems technology. The obtained sequences were aligned to the expected sequence for *gyrA* gene of *S. pseudintermedius* using ClustalW (http://www.ebi.ac.uk/clustalw). The 5 FQ-resistant strains showed a C to T transition at position 251 leading to substitution from Ser to Leu at codon 84, whereas all the 11 FQ-sensitive strains showed no mutation at the same position. None of the strains showed any other mutations in the amplification target.

3. Real-time PCR amplification and HRM analysis

The HRMA, with the protocol we developed, has been proven to be able to discriminate two sequences that differ by a single nucleotide, thus allowing to recognize strains of *S. pseudintermedius* presenting the single nucleotide mutation (fluoroquinolones resistant) than wild-type (fluoroquinolones sensible). Furthermore, the results obtained through HRMA coincide perfectly with those obtained with the classical microbiology and with the sequencing.

Figure 46 shows the results obtained with HRMA: the 11 *S. pseudintermedius* that have gyrA wild-type (sensitive to fluoroquinolones), contain a codon TCG and are highlighted in blue. The 5 *S. pseudintermedius* that have gyrA mutant (resistant to fluoroquinolones) contain a codon TTG and are highlighted in red. A strain of S. capitis (gray) was analyzed as a control. The three different curves are clearly distinguishable.

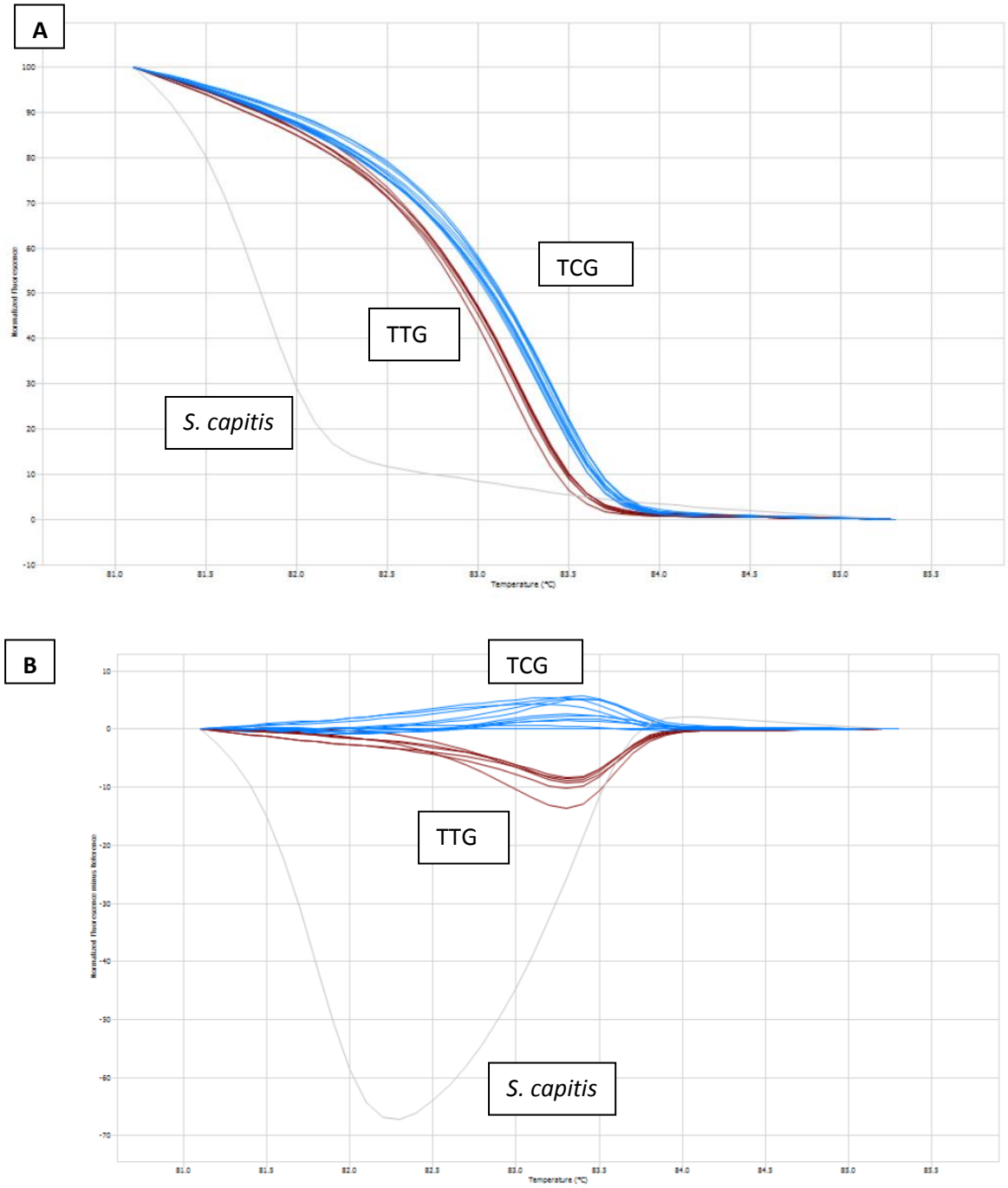

Figure 46. Results of HRMA shown in normalized mode (46.A) and in differential mode (46.B). The strains of *S. pseudintermedius* susceptible to fluoroquinolones (in blue) and the strains resistant to fluoroquinolones (in red) are clearly distinguishable. In gray the strain of *S. capitis* analyzed as control.

Conclusions

The real time PCR-HRMA protocol was able to discriminate among FQ-sensitive and FQ-resistant strains on the basis of the corresponding melt curves, with complete agreement with data obtained by DNA sequencing of the same gene as a reference technique and by FQ susceptibility testing (Figure 45). In this study we validated as proof of concept a HRM analysis-based approach for rapid identification of *gyrA*-linked FQ resistance in *S. pseudintermedius* clinical isolates at molecular level without the need to perform DNA sequencing or to use mutation-specific probes. We also confirmed previous reports that in *S. pseudintermedius*, the main mutation site associated to FQ resistance is at position 251 (Ser84Leu) of *gyrA* as detected in all the five resistant strains.

2.3 HRMA for detection and discrimination of *Dirofilaria immitis* and *Dirofilaria repens* in canine peripheral blood

2.3.1 Introduction

Filariasis: General information and Taxonomy

The etiological agents of disease defined generally "filariasis" fall into two subfamilies of parasites belonging to the *Onchocercidae* family and to the *Filarioidea* superfamily (Table 25). These subfamilies are represented by: *Dirofilarinae*, which includes *Dirofilaria immitis* and *Dirofilaria repens* (*Nochtiella repens*), and *Onchocercinae*, which includes *Dipetalonema reconditum* (*Acanthocheilonema reconditum*), *Dipetalonema dracunculoides* (*Acanthocheilonema dracunculoides*) and *Dipetalonema grassii* (*Cercopithifilaria grassii*) (Chauve C.M., 1990; Euzeby J., 1990; Urquhart G.M. et al., 1996).

Kingdom	*Animalia*
Phylum	*Nemathelmintes*
Class	*Nematoda*
Order	*Spirurida*
Suborder	*Spirurina*
Superfamily	*Filarioidea*
Family	*Onchocercidae*
Subfamily	*Dirofilarinae*
Gender	*Dirofilaria*
Species	*Immitis e Repens*

Table 25. Classification of *D. immitis* and *D. repens*.
(Urquhart G.M. et al., 1996)

Morphology of the parasite

The present study deals only with parasites belonging to the subfamily of *Dirofilarinae.* Here below the morphology of both the adult parasites and microfilariae, which is of great diagnostic value, is described.

Morphology of adult parasites

Dirofilaria immitis (Figure 47) is a filiform parasite that measures approximately 20-30 cm in length and 1 mm in diameter; the male can be distinguished by the female for the smaller size and the caudal ends wound in a spiral. The mouth is surrounded by eight median and two lateral papillae. The caudal area of the male presents 4 to 6 pairs of voluminous, pedunculated and ovoid papillae, of which 2-4 are pre-cloacal and 2 post-cloacal and fingerlike, and 3-4 pairs of conical small papillae, located in terminal position. The spicules measure respectively 315 and 200 microns. In the caudal edge of the female, in sub-ventral position, there is a conical and papilliforme structure facing backwards (Euzeby J., 1990).

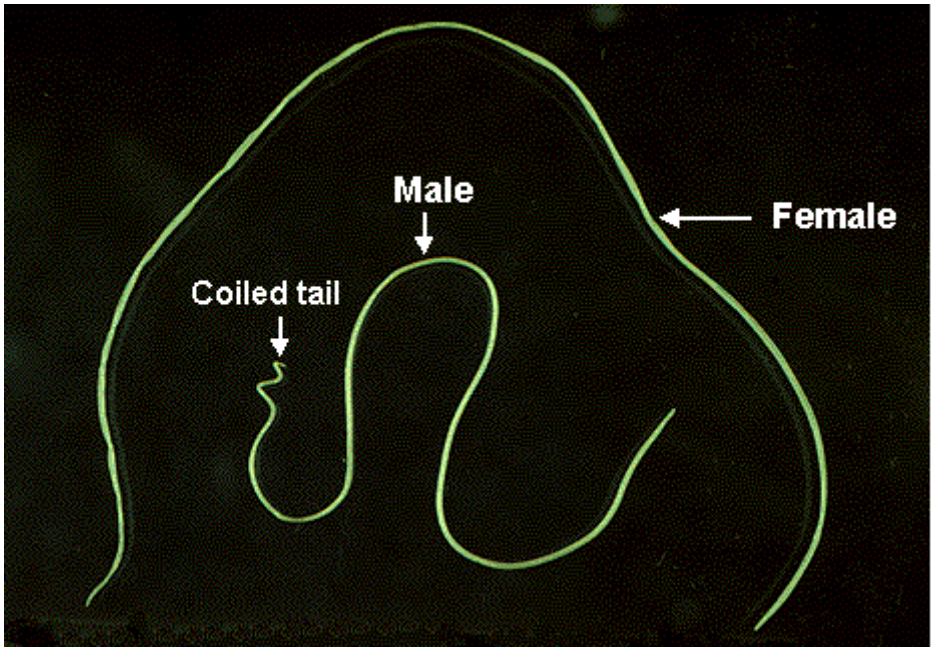

Figure 47. Adult specimens of *D. immitis*
(cal.vet.upenn.edu/merial/hrtworm/hw_1a.htm)

Dirofilaria (Nochtiella) repens has smaller dimension than D. immitis: in fact the female measures 10-17 cm long and 460-650 microns wide, while the male measures 5-7 cm long and 370-450 microns wide. The male has 2 to 4 pre-anal papillae on one side (with spicules measuring 465 to 590 microns) and 5 or 6 on the other (with spicules which measuring 185 to 206 microns). In the female the vulva is distant 1.15 to 1.60 mm from the front end (Chauve C.M., 1990).

Morphology of microfilariae

The larval forms of the parasite are represented by the microfilariae (L1): these are found in the circulating blood of the definitive host and, like the adult parasites, their characterization is necessary to reach a proper etiologic diagnosis. The morphological elements that allow the identification of microfilariae are the length and the shape of the cephalic and caudal end.

The microfilariae of ***Dirofilaria immitis*** (Figure 48) measure 300-330 x 5-7 microns and are not equipped with sheath: the caudal part is straight and sharp while the cephalic end is tapered and blunt-ended (Figure 49) (Chauve C.M, 1990; Euzeby J., 1990; Manfredi M.T., 1998; Urquhart G.M. et al., 1996).

The microfilariae of ***Dirofilaria (Nochtiella) repens*** (Figure 48) measure 207-360 microns in length and 5-8 microns in width; they do not exhibit sheath, the cephalic end is rounded and the caudal end has a shape similar to an umbrella handle (Figure 50) (Chauve C.M., 1990; Manfredi M.T., 1998).

The microfilariae are identified, as well as on the basis of morphology, also with histochemical and immunological methods; such investigation method are described later in this thesis work.

Figure 48. Microfilaria of *D. immitis* (left) and *D. repens* (right). (Photo kindly provided by Dr. Marco Genchi).

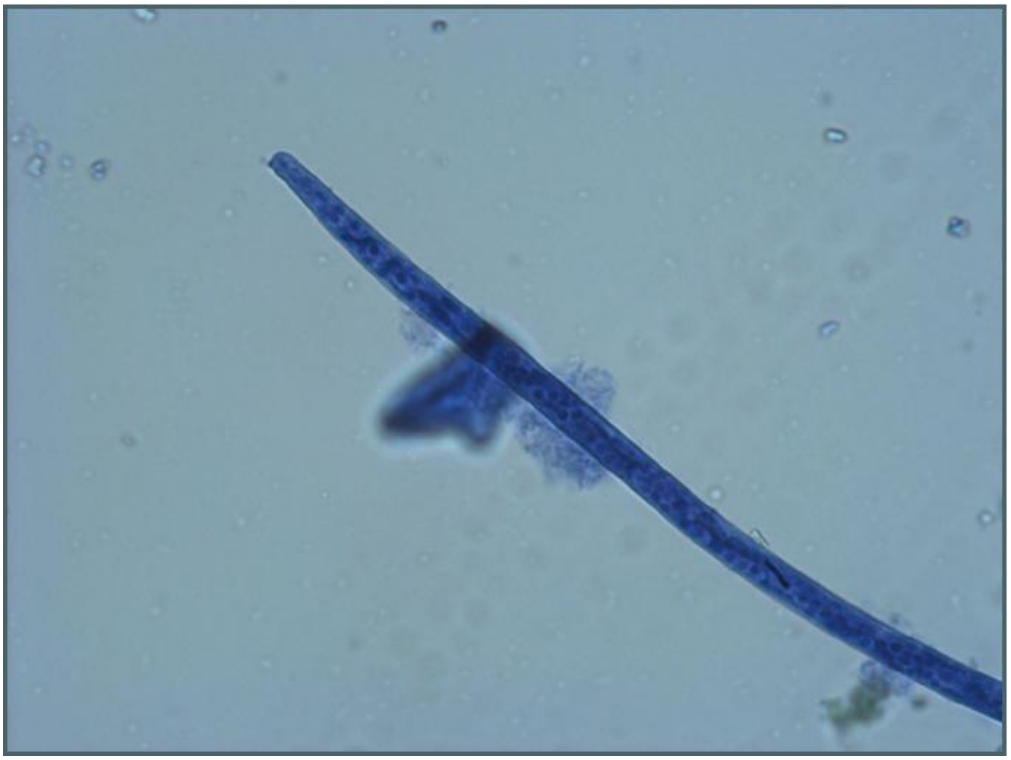

Figure 49. Tapered cephalic-end of *D. immitis*.
(Photo kindly provided by Dr. Marco Genchi).

Figure 50. Caudal ends with shape of umbrella handle of D. repens.
(http://www.personalweb.unito.it/ezio.ferroglio/atlante/parassiti_cane/dirofilaria/d_repens/foto/coda_rep1.jpg)

Biological cycle of the parasite

Dirofilaria immitis, like the other members of the superfamily Filarioidea, is a dixenic parasite, and it depends on insect vectors for the completion of the cycle, for transmission to the definitive hosts and for its dissemination (Euzeby J., 1990; Urquhart G.M. et al., 1996). *D. immitis* is a hematophagous parasite that can remain for years within the definitive host, continuing to produce microfilariae (Euzeby J., 1990). It is a viviparous parasite: the female lays the microfilariae that circulate in the blood of the host. The microfilariemia has a monthly and seasonal circadian periodicity that is highest in July and August and lowest in winter. To become adult, the larvae make various moults and part of their evolutionary cycle takes place in a hematophagous Diptera (mosquitoes of the genera Aedes, Anopheles, Coquillettidia, Culex, Culiseta and Mansonia) which acts as carrier and as intermediate host (Cancrini G., 1998). The first stage larvae (L1, microfilariae) are taken from the Diptera during the blood meal and remain viable in its gut. Subsequently, they migrate towards the Malpighian tubules and are transformed, through two moults, into larvae of the second stage (L2) and third stage (L3). These become infesting in two weeks, after reaching the cephalic space and the *labium*. The infesting ability depends on the temperature: if this is too low, larval development stops and may then resume in more favorable climatic conditions. The cycle in the final host begins when L3 are inoculated by the mosquito during a blood meal. The L3 remain in the skin for about six days, then moults in the fourth stage larva (L4) that is localized in the capillaries of the abdominal wall (about 20 days after the bite of the insect) and thoracic wall (after about 40 days from inoculation of L3). Within 60-80 days, it moults into the fifth stage larva (L5) that migrates through the venous system to localize in the pulmonary artery (between 70 and 120 days after infestation). It persists in this location up to a length of 8-11 cm and subsequently performs, about 110 days after infestation, a retrograde migration into the right ventricle, where it becomes an adult individual (Euzeby J., 1990; Urquhart G.M. et al., 1996). The prepatent period, i.e. the interval between infection of a host by a parasitic organism and the first ability to detect a diagnostic stage of the

organism from that host, is about 6 months, after which the adult females begin to produce the microfilariae. The infestation of the final host (mostly dogs) can take place between June and October; during the first infestation, usually L5 reach the pulmonary artery in late August and persist here until December, and then migrate into the right ventricle and start producing microfilariae. In an already parasitized subject, however, the larvae can be found in the blood throughout the year. In the pregnant dog, microfilariae can cross the placenta and reach the fetus (in this case microfilariae are not able to evolve because it must spend part of their cycle in the mosquito) , while the infesting larvae (L3) are not able to perform this migration (Euzeby J., 1990) (Figure 51).

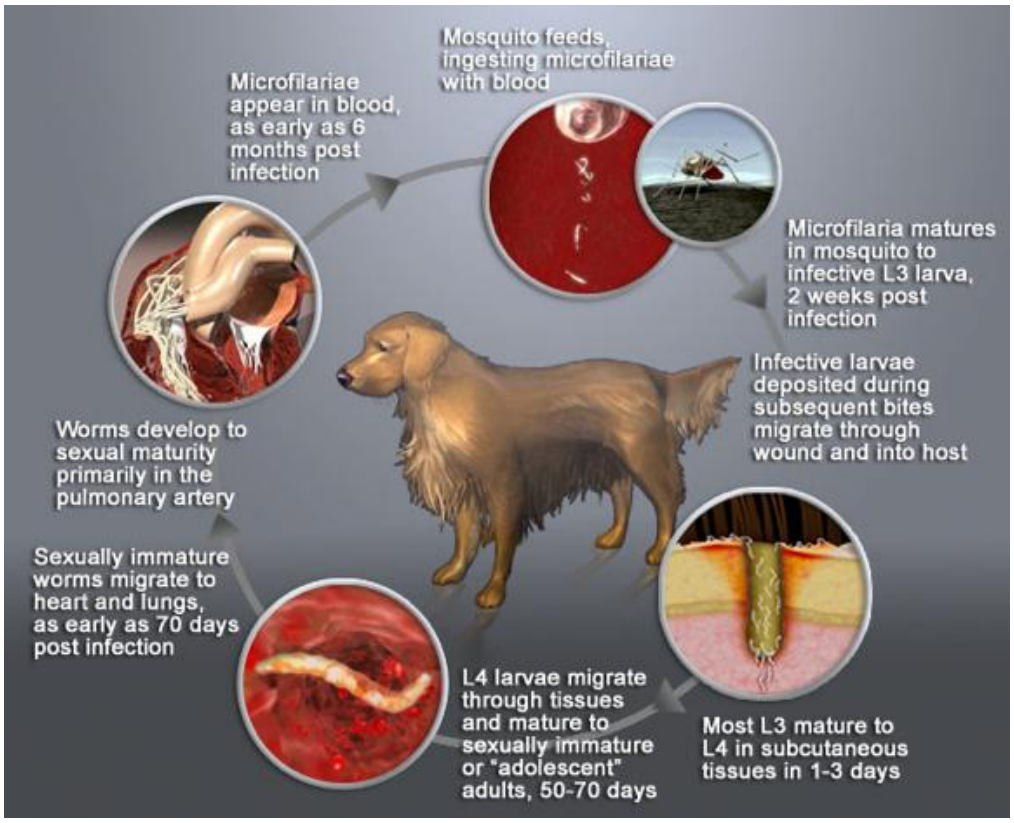

Figure 50. Biological cycle of *D. immitis.* (http://www.capcvet.org/capc-recommendations/canine-heartworm)

Dirofilaria (Nochtiella) repens, like *D. immitis*, to evolve to adult parasite needs a phase of development in an intermediate host (the mosquito) in which parasite development takes place from L1 to L3. This is followed by the final inoculation

into the final host (dog, cat, man, other canids and wild felines) where the parasite is localized in the subcutaneous connective tissue and connective bands of skeletal muscle. In these locations it makes two moults, becoming first L4 and subsequently L5 and reaching then the sexual maturity (Chauve C.M., 1990).

Epidemiology and geographical spread

The epidemiology of canine heartworm, and in particular the cardiopulmonary pathology by D. immitis, is a complex problem because there are several factors involved, which interact with each other, that lead to the spread of the disease in dogs, the main reservoir of the parasite, and increase the risk of human infections. Although the number of dogs subjected to specific prevention is more and more increasing, the prevalence of this disease is still high (Vayna de Pava M., 2002).

The areas which best allow the diffusion of heartworm have a climate characterized by high temperatures for a few months of the year, with high humidity and poor oxygenation. All these conditions are, in fact, favorable to the development of the intermediate host and in particular, are to be considered at high risk especially the river areas. Dirofilariasis is an endemic disease in the United States of America, Japan and north eastern Australia. *D. immitis* has also been reported in Asia, Africa and in South America (Figure 52). The situation in Europe shows that the most involved species are *D. immitis* and *D. repens*. In Spain, the south-central area is characterized by a high prevalence of infection with *D. immitis* and a low prevalence of that by *D. repens*; distribution is sporadic, and prevalence rates vary widely, ranging from 0 to 5% in northern areas to over 37% in the western regions and the Canary Islands. In France, *D. immitis* is present in the west and *D. repens* occupies the same territory as well as the central part of the nation; the infestation is found mostly along the coasts of the Mediterranean, and dogs positive for the parasite are mainly found at the mouth of the Rhone, Vaucluse, Haute-Garonne, Dordogne, Pyrenees Atlantiques , Gard, Var, Alpes-Maritimes and in Corsica. In Portugal, the disease is reported mainly in the southern regions, with prevalence rates between 10% and 30% of

the canine population. In Greece there are both species of heartworm (Cancrini G. et al., 2000; Chauve C.M., 1997; Muro A. et al., 1999). With regard to Eastern Europe, few data are available, which show that the prevalence ranges between 2% and 17% in Slovenia, Bulgaria and Turkey, while more than 65% in Romania, where some regions are considered endemic for heartworm (Leuterer G. and Goethe R., 1993). Finally, in northern Europe, particularly in Germany, Austria and Switzerland, there have been some cases of dirofilariasis, but they are considered imported, i.e. are attributed, according to available anamnestical information, to infestations contracted in countries where the disease is endemic (Figure 52) (Leuterer G. and Gothe R., 1993).

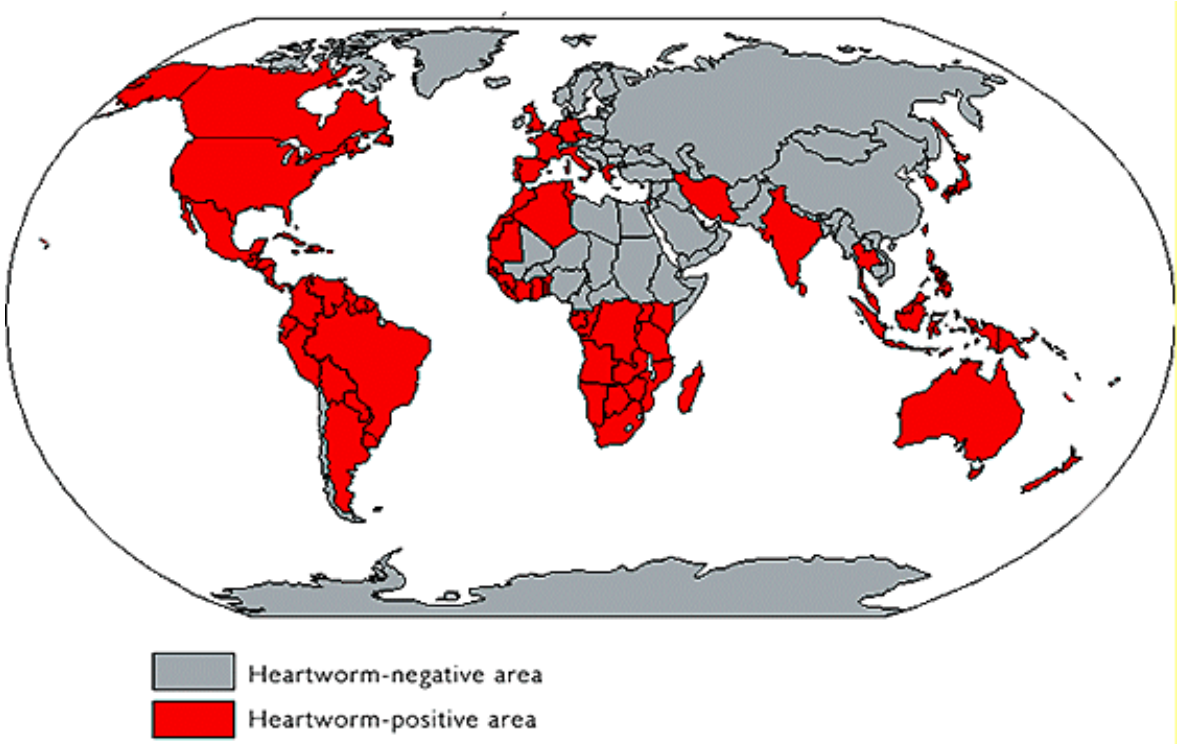

Figure 52. Geographic distribution of heartworm disease in the world. (http://www.stanford.edu/group/parasites/ParaSites2005/Dirofilariasis/Pages/Epidemiology.htm)

The largest endemic area of Europe is along the middle and lower course of the Po river and Oglio river, in the Po Valley, between 45 and 46 degrees North Latitude. It has, in fact, the more favorable characteristics to the development of the carrier: it is surrounded and protected by the Alps and Apennines, characterized by abundant rainfall, high relative humidity and extensive

monoculture cropping systems (Maffi S. et al. 1999). It would sound restrictive to consider dirofilariasis as a parasitic infection "confined" in certain areas with special environmental characteristics and climate. The infestation, in fact, has a tendency to stabilize in canine populations where the presence of the parasite was in the past considered sporadic, and to spread into areas once considered to be free. The expansion of areas at risk for the parasitosis can be considered, in part, as a consequence of the ability of the vector to adapt to various situations. The expansion occurs in the foothill areas surrounding the Po Valley to the south, also, to the northeastern edge, localized in the provinces of Veneto and Friuli Venezia Giulia, where the infection can now be considered endemic with reports of prevalence of medium-high level (28%). Filariasis is rising almost everywhere in Italy, colonizing new habitats substantially, such as hilly areas and foothills (up to a height of about 900 meters above sea level), Maremma, the upper valley of the Arno River and other areas of Central Italy. In southern Italy most cases of dirofilariasis are due to parasites different from D. immitis: in Campania showed a high prevalence of infections with D. reconditum, while in Sicily the parasite is more involved D. repens (Giannetto S. et al., 1997) (Figure 53).

In recent years several epidemiological studies to establish the prevalence and spread of heartworm disease in the dog population in Italy have been performed. The infection is spreading from endemic areas in the Po Valley to peripheral areas once considered to be free. It should be emphasized that there is an interaction between the two species of Dirofilaria (D*. immitis* and *D. repens)* in dogs and this may hinder the spread of D. immitis to areas where D. repens is extremely widespread and vice versa. In this regard, the mosquito species involved in the transmission, their biology, and competence as vectors of Dirofilaria species should be considered. The introduction in Europe of a new species of mosquito as *Aedes albopictus*, and the recent highlighting of its role as a vector for heartworm, may influence the risk and spread of infection (Cancrini G. et al., 2003; Cancrini G. et al., 2007). This species of mosquito could spread from south to north European countries in the near future, changing the epidemiological models of heartworm disease in both humans and animals

(Genchi C. et al., 2005). It was stated that the prevalence of heartworm infection is increasing in dogs non treated with preventive drugs, and that there is a risk that infested host from outside will trigger cycles in indigenous regions previously free, as reported about several regions of the United States. In this regard, climate change can be considered a key factor responsible for the spread of vectors to the north and their ability to transmit pathogens. In addition to climate change and global warming, it is also important to consider the effects of the global movement of animals, as an important factor for the spread of vector-borne diseases (Genchi C. et al., 2009)

Figure 53. Distribution of Dirofilaria immitis in Italy. Outbreaks of canine heartworm disease by Dirofilaria immitis in the area until 1990 endemic of the Po Valley (blue dots) and outside the endemic area (blue symbol). New outbreaks (red points) reported in non-endemic areas, after 1990, until 2009. (www.parasitesandvectors.com/content/2/S1/S2)

Pathogenesis and clinical signs

The principal location of *D. immitis* are pulmonary arteries and heartworm must be considered as a pulmonary disease, that during the last stage also affects the heart chambers (Figure 54). A few days after the arrival of the parasite in the caudal pulmonary arteries, the endothelial cells become swollen, the intercellular junctions become dilated in response to trauma and activated neutrophils adhere in the space between endothelial cells. Adhesion and platelet activation are also found. The damaged arterial wall allows albumins, fluid plasma and blood-cells to reach the perivascular space inducing a persistent perivascular inflammatory edema. After the endothelial changes, the tunica intima thickens and leukocytes invade the smooth muscular wall; the smooth muscle cells multiply within the tunica media and migrate to the surface endovascular as a response to the growth factor released from platelets. The proliferation and migration of smooth muscle cells determines the presence, on the inner surface of the arteries, of villi and collagen lined by endothelial cells. The surface of the arteries of infected dogs and cats appear to be strongly rough and smooth and the lumen of the pulmonary arteries is decreased. Lung disease is secondary to vascular changes; the leakage of liquids and proteins through the wall of the affected arteries produces an edema in the parenchyma. Moreover, the spontaneous death of some filariae is capable of producing pulmonary thromboembolism and severe inflammatory reactions. The reduction of conformation and caliber of the pulmonary arteries, which may also be occluded by a thromboembolism or severe villous proliferation, causes a state of pulmonary hypertension and, consequently, an increase of the post load in the right ventricle, which can induce the cor pulmonale syndrome and congestive heart failure. The leaking of fluid and proteins through the wall of the affected arteries produces further swelling and inflammation in the lung parenchyma.

The clinical evolution of heartworm disease in dogs is usually chronic. Most infected dogs have no symptoms of the disease for a long time, months or years, depending on the amount of heartworms, the individual reactivity and physical exercise, as there is more serious damage in dogs that perform strenuous

exercise compared to other dogs. The disease can begin with occasional coughing and develops gradually. The cough may be followed by dyspnea, moderate to severe, weakness, and sometimes fainting after exercise or excitement. Sound of crackling can be found at lung auscultation. Later, when congestive heart failure is developing occur: swelling of the abdomen and legs, fluid accumulation, anorexia, weight loss and dehydration. At this stage, there is a cardiac murmur on the right side of the chest, because of insufficiency of the tricuspid valve, and the heart rhythm is altered because of atrial fibrillation. Sudden death occurs rarely and usually as a result of respiratory distress or cachexia. In the course of this chronic disease, sometimes there is an acute symptomatology due to a severe thromboembolism following the natural death of heartworms, and dogs may show acute dyspnea and hemoptysis (Genchi C. et al., 2007). In small dogs, the movement of adult worms from the pulmonary artery to the right chambers of the heart due to pulmonary hypertension and a sudden drop in right cardiac output is also common. In this case, the affected dogs show the so-called *superior vena cava syndrome*. This syndrome shows dyspnea and cardiac murmur due to the presence of microfilariae in the vicinity of the tricuspid valve. This syndrome is also called *intravascular hemolytic*, being accompanied by hemolytic anemia and hemoglobinuria due to mechanical intravascular hemolysis (red blood cell fragmentation occurs due to the continuous movement between atrium and ventricle of filarial intertwined). This implies a systemic hemodynamic decompensation and shock with consequent death of the affected animal (Venco L., 1993). Disseminated intravascular coagulopathy often accompanies the superior vena cava syndrome, being secondary to hemolysis and metabolic acidosis. In addition, the dog may experience liver lesions characterized by hepatomegaly, with expansion venous thrombosis, centrilobular necrosis and fibrosis. Finally, there may be a serious kidney disease, resulting from the hemoglobinuria with renal tubular necrosis and cylindruria.

In subcutaneous filariasis, caused by D. repens, the adult parasite is localized in the subcutaneous tissues of the dog and cat. This disease presents with minor

clinical signs such as itching, swelling of the skin, subcutaneous nodules or remains asymptomatic (Genchi C. et al., 2007).

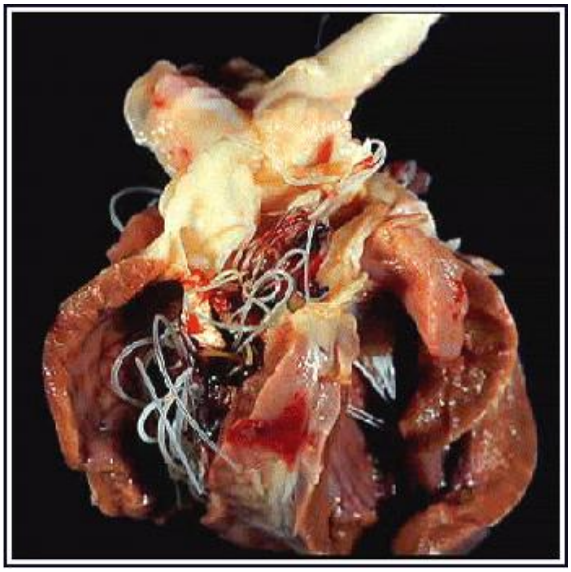

Figure 54. Adult of *Dirofilaria immitis* in dog heart. (http://www.stanford.edu/group/parasites/ParaSites2001/dirofilariasis/Synonyms.html)

Diagnosis

Knott test to microfilariae search in the peripheral blood

The circulating microfilariae can be detected with the Knott test. The microfilariae are detected and identified under the microscope on the basis of morphological criteria, and this is considered as a definitive proof of infection (specificity 100%). However up to 30% of dogs may be oligo-or amicrofilaremic, despite presenting adult worms, for the presence of worms only of the same sex (quite unusual in dogs), for a host immune reactivity towards microfilariae or for administration of microfilaricidal drugs. So, the sensitivity of the test for microfilariae is not considered sufficient to rule out infection in the event of a negative result. Furthermore, in certain cases the identification based on morphology may be made more difficult by the presence of artifacts and/or intermediate morphologies, especially if the operator is not very experienced or if they are not put in place perfectly reproducible procedures of sampling and analysis (Genchi C. et al., 2007).

Blood test for antigen research of adult females of D. immitis

Different ELISA kits for detection of circulating antigens of Dirofilaria immitis adult female in serum, plasma or whole blood of a dog are commercially available. Most are very specific, sensitive, rapid and easy to perform. The sensitivity is actually very high, but false negatives may occur during the prepatent period, very light infestations or when there are only males in the host (male filariae are not detectable by this test). Most kits are intended for the clinical diagnosis of a single sample, but multi-test ELISA plates are also available. Manufacturers claim that for a positive result parasite is sufficient 1 female adult, although many factors may influence the sensitivity of the test as the age of the parasite, the ratio between parasite females and males, and the size of the dog. Reliable and reproducible results can be obtained when there are 2-3 or more adult female worms. A detectable antigenemia develops after 5 to 6.5 months from the infestation. After the death of adult parasites, circulating antigens disappear rather quickly; for this reason, this technique can be used to evaluate the efficacy of a therapy adulticide. To confirm the success of adulticide therapy in dogs, the antigenemia must be reassessed at 5 and 9 months after treatment. If the test is negative at 5 months, the test at 9 months can be avoided (Genchi C. et al., 2007).

Chest radiographs

Chest radiographs may show, in an advanced stage, the enlargement of the pulmonary arteries, abnormal lung pattern and, in the worst cases, right cardiomegaly. In the event of congestive heart failure right payments and peritoneal effusions are found. Radiographs are useful for assessing the severity of lung injury, but not for assessing the parasite. The radiographic signs of pulmonary vascular disease in advanced stages may persist long after the infestation has run its course and some of the most severely ill dogs may have a low number of parasites. In contrast, some dogs can host large parasites but remaining clinically asymptomatic with light or absent radiographic lesions (Genchi C. et al., 2007).

Electrocardiography

Only at the last stage of the disease, when the heart chambers are seriously damaged, the ECG may show a deviation to the right of the axis cardiac and / or atrial fibrillation (Genchi C. et al., 2007).

Echocardiography

Echocardiography allows direct visualization of the cardiac chambers and of communicating vessels. It can also allow the visualization of parasites in the cardiac chambers, the caudal vena cava, the main pulmonary artery and in the proximal portion of both pulmonary caudal arteries. The heartworms are highlighted as floating objects in the right cardiac chambers or in the lumen of the vessels. It is performed mainly in cases where the clinical and radiographic results suggest a severe form of the disease. The cardiac ultrasound can increase the accuracy in the staging of the disease and in the estimation of filarial influencing the treatment plan and prognosis (Genchi C. et al., 2007).

Polymerase chain reaction (PCR)

The polymerase chain reaction (PCR) is a sensitive and specific technique that allows to detect the presence of DNA belonging to a given organism, and as such can be used to identify the different species of heartworm. During the last years several researchers have developed different molecular protocols with diagnostic and epidemiological purposes. In particular, specie-specific PCR assays for single species identification, and multiplex PCR and PCR-RFLP assays, single and multistep, for simultaneous detection of the different Dirofilaria species either in the vector or in peripheral blood of infected dog have been designed (Favia G. et al., 1996; Mar P.H. et al., 2002; Casiraghi M. et al., 2006; Rishniw M. et al., 2006; Gioia G. et al., 2010). For diagnostic purposes, protocols applicable to the identification of microfilariae in the peripheral blood are particularly useful, especially in cases where the morphological recognition of microfilariae proves to be difficult, or even in the case of mixed infections (Genchi C. et al., 2007). In addition, for clinical diagnostics use, it is critical to perform fast procedures getting simple and clear results, and including a precise assessment of the level of sensitivity and specificity in the peripheral blood.

2.3.2 Application of the HRMA

The purpose of this work was to develop a HRM analysis, fast and relatively inexpensive, able to simultaneously detect and unambiguously identify D. immitis and D. repens in the peripheral dog blood samples, targeting nucleotide differences existing between the sequences of a target gene in the two different species.

Materials and methods

1. Sampling procedures and microfilarial phenotyping

D. immitis and *D. repens* microfilariae were collected from anticoagulated canine peripheral blood samples referred to the Faculty of Veterinary Medicine of the University of Milan (Italy). Blood samples were tested by a modified Knott's test, and circulating microfilariae were identified based on morphology and morphometry (Knott, 1939; Euzeby, 1981; Soulsby, 1982; Genchi 2007), and counted in 20 microliters of blood. In total, 3 *D. immitis* blood samples, 8 *D. repens* positive blood samples and 3 blood samples with natural mixed infection were selected for the HRM analysis. Furthermore, a Knott's test-negative blood sample was included as negative controls and single adults of *D. immitis* and *D. repens* were used as positive controls. Also, positive blood samples from dogs with different filarial loads (i.e., 4 mf/ml and 32250 mf/ml for *D. immitis*; 4 mf/ml and 100000 mf/ml for *D. repens*) were examined to test the range of sensivity of the method.

2. DNA extraction

Genomic DNA was isolated from 300 µl of each mf-positive peripheral blood sample and from isolated *D. immitis* and *D. repens* worms by adding 900 µl of TNNT lysis buffer (0.5% Tween 20, 0.5% Nonidet P-40, 10mM NaOH, 10mM Tris [pH 7.2]) and 50 µl of 20mg/ml proteinase K (Lachaud L. et al., 2002). Samples

were then incubated at 56 °C for 18 h. Proteinase K was inactivated by incubation at 95 °C for 10 min. DNA was isolated by standard basic phenol chloroform extraction followed by ethanol precipitation. The extracted DNA was resuspended in 30 µl of PCR-grade water and then stored at −20 ◦C until tested by real-time PCR. For each sample, 2 µl of resuspended DNA was used as template in the multiplex PCR assay.

3. Design of primer set

Dirofilaria mitochondrial gene for cytochrome oxidase, subunit I, was chosen as gene target. The gene sequences of *D. immitis* (AM749226.1, AM749228.1, HQ540424.1, EU169124.1) and *D. repens* (AM749234.1, AM749231.1) were obtained from GenBank and aligned automatically using the CLUSTALW program. The primer pair was designed by us in a region where there is no variability intra-species (the sequence is conserved), while the interspecies variability is maximized. In addition, the primer set for the Q-PCR mixture containing the fluorescent binding dye was designed to have no misprimings and no dimers. Also, the primer sequence was proved to be unique for Dirofilaria species through a homology search using Basic Local Alignment Search Tool (BLAST; NCBI, NIH. The forward primer (COXdirHRMF): 5' –AGTATGTTTGTTTGAACTTC- 3' and reverse primer (COXdirHRMR): 5' –AACGATCCTTATCAGTCAA- 3' have an annealing temperature of 52 ° C to give an amplicon of 256 bp.

4. Real-time PCR amplification and HRM analysis

Each amplification reaction was carried out in a mixture containing the following reagents: 7,5 µl Supermix SsoFast EvaGreen mix Biorad, 0.3 µM of each primer, 2 µl of resuspended DNA and H_2O to reach a total volume of 15 µl. The real time PCR-HRM amplification reactions were performed on a Eco^{TM} Real-Time PCR System (Illumina, Inc., San Diego, CA, USA). The thermal protocol started with a denaturation-activation step at 95°C for 8 min, followed by a 40 cycle program (denaturation at 95 °C for 30 s, annealing at 52 °C for 1 min). The melting program comprised 3 steps: denaturation at 95 °C for 15 s, renaturation at 55 °C

for 15 s, and finally melting with continuous fluorescence measurement (ramping 0.1 °C/s) to 95 °C, kept for 15 s. The HRM curve was analyzed using the Eco_v4.0 software. Raw melting-curve data was normalized by setting the pre-melt (initial fluorescence) and post-melt (final fluorescence) signals of all samples to uniform values. Pre-melt signals were uniformly set to a relative value of 100%, while post-melt signals were set to a relative value of 0%. Genotypes were defined by selecting a sample from each standard species as a reference control to identify unknown samples. As a blank control double distilled water was the used in parallel with each experiment.

5. Sequencing

To confirm the results of HRM analysis, after the HRM analysis the samples were run on 2 ethidium-bromide agarose gel followed by UV-visualization and gel-purification by Qiaquick™ Gel Extraction kit (Qiagen GmbH, Hilden, Germany). The concentration of purified amplicons was spectrofotometrically measured using a ND-100 Spectrophotometer. The purified amplification products were then sequenced using standard Applied Biosystems technology on ABI Prism 310 DNA sequencer (Applied Biosystems). The obtained sequences were aligned to expected target sequences using ClustalW (http://www.ebi.ac.uk/clustalw).

Results and discussion

All samples showed a robust and reproducible amplification signal, this allowing an optimal HRM analysis. The amplicons were of the expected size (256 bp), nor any nonspecific amplicons or primer dimers were detected (Figure 55). No amplification was obtained from Knott's-negative samples, confirming the specificity of the procedure. Sensivity range was confirmed for the two species by successful amplification of the highest (naturally infected blood samples of 32250 mf/ml for *D. immitis* and 100000 mf/ml for *D. repens*) and the lowest (reconstructed blood samples of 4 mf/ml for each single Dirofilaria species) mf load.

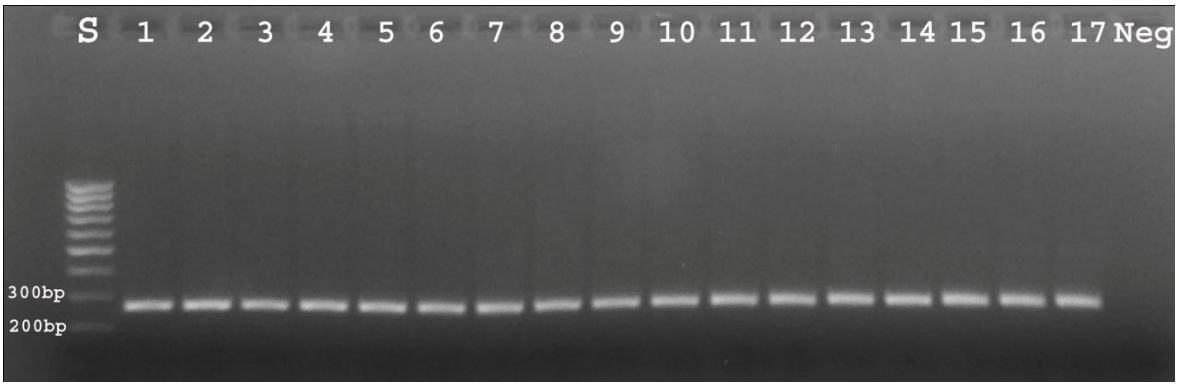

Figure 55. Results of the gel electrophoresis performed after real time PCR-HRMA. The amplicons are of the expected size (256 bp) and the amplification is robust, reproducible and don't show nonspecific or dimers of primers.

HRM analysis allowed to discriminate clearly the two species according to the different melting temperature of the two sequences. Figure 56 shows the normalized graph of *D. immitis* samples (bunch of curves to the right), the *D. repens* samples (bunch of curves to the left) and the three mixed samples in the centre (asterisk). Figure 57 shows the difference plot curve, that allows further analysis of the differences in melting-curve shapes by subtracting the curves from a reference curve (in this case repens 4 mf/ml), which helps to cluster samples into groups that have similar melting curves.

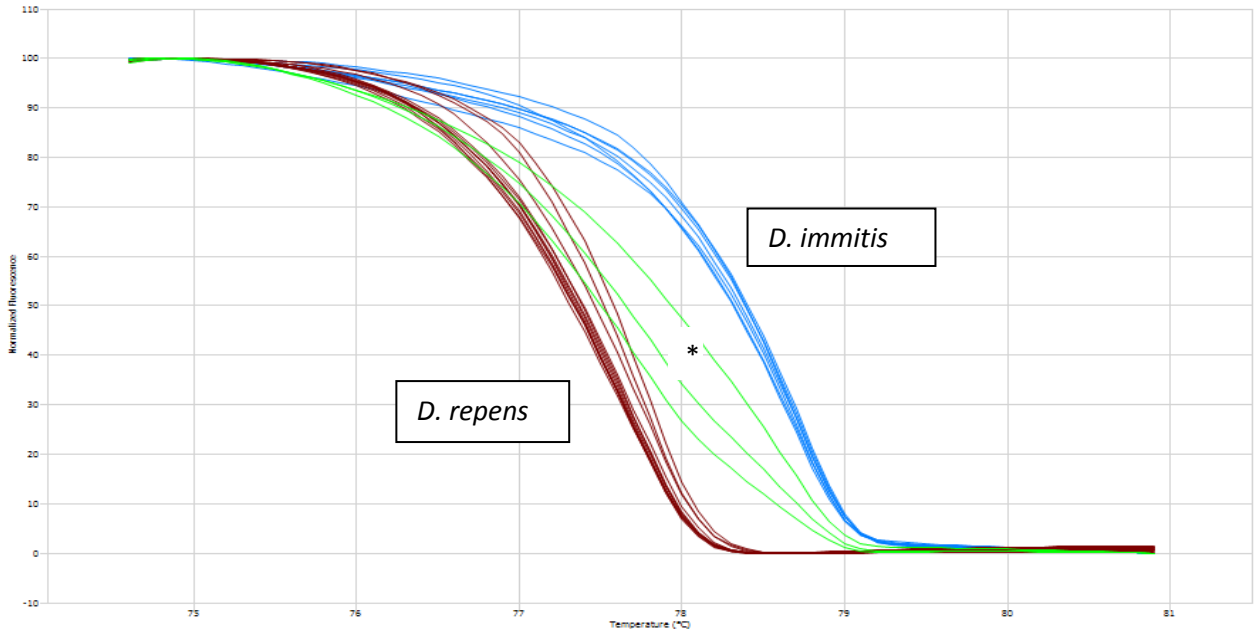

Figure 56. Normalized graph of the melting curves obtained with the HRMA. Are clearly distinguishable the *D. immitis* samples (in blue on the right), from the *D. repens* samples (in red on the left) from samples with mixed infestation (in green in the center, indicated by an asterisk).

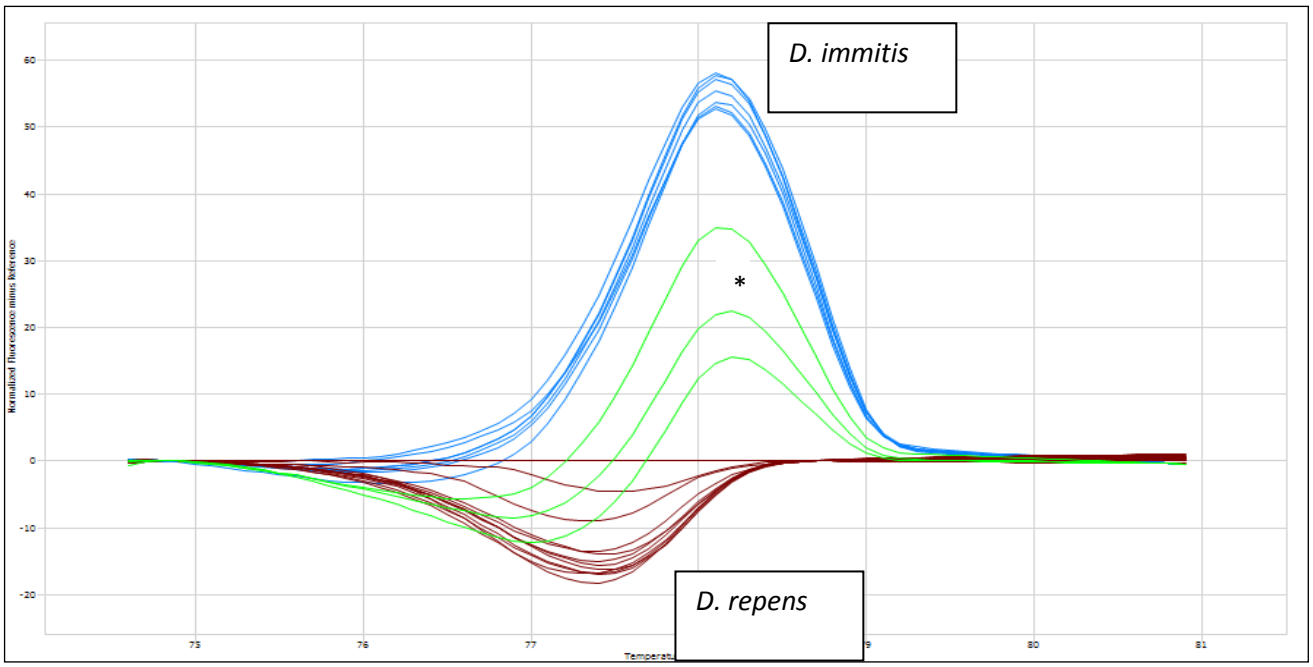

Figure 57. Differential graph of the melting curves obtained with the HRMA. The three different types of sample are easily distinguishable: in blue *D. immitis* samples, in red *D. repens* samples and green (indicated by an asterisk) samples with mixed infestation.

Conclusions

In this work we report a new molecular method based on real-time PCR and HRM analysis to detect and differentiate simultaneously and unequivocally *D. immitis* and *D. repens* on DNA extracted from canine peripheral blood. The availability of a HRM assay reduces the reagent cost, the labor time, and the contamination risk. This quick, sensitive and specific single step assay able to discriminate the two most common filarial parasite in dogs represents an additional tool for epidemiological studies and routine disease assessment in co-endemic areas for the two species.

BIBLIOGRAPHY

- Alvarez-Garcia I., Miska E.A. (2005) MicroRNA functions in animal development and human disease. Development 132: 4653–4662.
- Adam F., Villiers E., Watson S., Coyne K., Blackwood L. (2009) Clinical pathological and epidemiological assessment of morphologically and immunologically confirmed canine leukemia. Vet Comp Oncol. 7(3):181-19
- Ambros V. (2004) The functions of animal microRNAs. Nature 431:350–355.
- Andersen C.L., Jensen J.L., Ørntoft T.F. (2004) Normalization of real-time quantitative reverse transcription-PCR data: a model-based variance estimation approach to identify genes suited for normalization, applied to bladder and colon cancer data sets. Cancer Res. 64(15):5245-50.
- Aravin A.A., Hannon G.J., Brennecke J. (2007) The Piwi-piRNA pathway provides an adaptive defense in the transposon arms race. Science 318:761–764.
- Bhatia K., Sahdev A., Reznek R.H. (2007) Lymphoma of the spleen. Semin Ultrasound CT MR. 28(1):12-20.
- Bartel D.P. (2004) MicroRNAs: genomics, biogenesis, mechanism, and function. Cell 23(116):281–97.
- Bartel D.P. (2009) MicroRNAs: target recognition and regulatory functions. Cell 136: 215–233.
- Bentwich I. (2005) Prediction and validation of microRNAs and their targets. FEBS Lett. 579(26):5904-10. Review.
- Bissels U., Bosio A., Wagner W. (2011) MicroRNAs are shaping the hematopoietic landscape. Haematologica. 97(2):160-7.
- Boggs R.M., Moody J.A., Long C.R., Tsai K.L., Murphy K.E. (2007) Identification, amplification and characterization of miR-17-92 from canine tissue. Gene. 404(1-2):25-30.
- Boggs R.M., Wright Z.M., Stickney M.J., Porter W.W., Murphy K.E. (2008) MicroRNA expression in canine mammary cancer.. Mamm Genome. 19(7-8):561-9.
- Bohnsack M.T., Czaplinski K., Gorlich D. (2004) Exportin 5 is a RanGTP-dependent dsRNA-binding protein that mediates nuclear export of pre-miRNAs. RNA 10, 185–191.
- Bousquet M., Quelen C., Rosati R., Mansat-De Mas V., La Starza R., Bastard C., Lippert E., Talmant P., Lafage-Pochitaloff M., Leroux D., Gervais C., Viguié F., Lai J.L., Terre C., Beverlo B., Sambani C., Hagemeijer A., Marynen P., Delsol G., Dastugue N., Mecucci C., Brousset P. (2008) Myeloid cell differentiation arrest by miR-125b-1 in myelodysplastic syndrome and acute myeloid leukemia with the t(2;11)(p21;q23) translocation. J Exp Med. 205(11):2499-506.
- Breen M., Modiano J.F. (2008) Evolutionarily conserved cytogenetic changes in hematological malignancies of dogs and humans--man and his best friend share more than companionship. Chromosome Res. 16(1):145-154.
- Brennecke J., Stark A., Russell R.B., Cohen S.M. (2005) Principles of microRNA-target recognition. PLoS Biol 3:e85.
- Bruchova H., Yoon D., Agarwal A.M., Mendell J., Prchal J.T. (2007) Regulated expression of microRNAs in normal and polycythemia vera erythropoiesis. Exp Hematol. 35(11):1657-67.
- Byrd J.C., Stilgenbauer S., Flinn I.W. (2004) Chronic lymphocytic leukemia. Hematology Am Soc Hematol Educ Program 163–83.
- Cai X., Hagedorn C.H., Cullen B.R. (2004) Human microRNAs are processed from capped, polyadenylated transcripts that can also function as mRNAs. RNA 10:1957–1966.

- Calin G.A., Dumitru C.D., Shimizu M., et al. (2002) Frequent deletions and down-regulation of microRNA genes miR15 and miR16 at 13q14 in chronic lymphocytic leukemia. Proc Natl Acad Sci U S A 99: 15524–15529.
- Calin GA, Croce CM. Chronic lymphocytic leukemia: interplay between noncoding RNAs and protein-coding genes. Blood. 2009;114(23):4761-70.
- Calin G.A., Liu C.G., Sevignani C., et al. (2004) MicroRNA profiling reveals distinct signatures in B cell chronic lymphocytic leukemias. Proc Natl Acad Sci USA 101:11755–60.
- Calin G.A., Sevignani C., Dumitru C.D., et al. (2004) Human microRNA genes are frequently located at fragile sites and genomic regions involved in cancers. Proc Natl Acad Sci U S A 101: 2999–3004.
- Calin G.A., Ferracin M., Cimmino A., et al. (2005) A MicroRNA signature associated with prognosis and progression in chronic lymphocytic leukemia. N Engl J Med 353: 1793–801.
- Calin G.A., Croce C.M. (2006) MicroRNA signatures in human cancers. Nat Rev Cancer 6: 857–866.
- Calvo K. R., Traverse-Glehen A., Pittaluga S. and Jaffe E. S. (2004) Molecular profiling provides evidence of primary mediastinal large B-cell lymphoma as a distinct entity related to classic Hodgkin lymphoma. Adv. Anat. Pathol. 11, 227–238.
- Cancrini G. (1998): Il vettore, in Genchi C., Venco L., Vezzoni A. (eds): Filariosi cardiopolmonare del cane e del gatto, Edizioni Scivac, Cremona, p.13.
- Cancrini G., Allende E., Favia G., Bornay F., Anton F., Simon F. (2000): Canine Dirofilariosis in two Cities of South-eastern Spain, in «Veterinary Parasitology», 39, p. 395.
- Cancrini G., Frangipane DI Regalbono A., Ricci I., Tessarin C., Gabrielli S., Pietrobelli M. (2003). Aedes albopictus is a natural vector of Dirofilaria immitis in Italy. Vet Parasitol. 2003, 118,p. 195.
- Cancrini G., Scaramozzino P., Gabrielli S., DI Paolo M., Toma L., Romi R. (2007) Aedes albopictus and Culex pipiens implicated as natural vectors of Dirofilaria repens in central Italy. J Med Entomol. 44, 1064.
- Carmell M.A., Xuan Z., Zhang M.Q., Hannon G.J. (2002) The Argonaute family: tentacles that reach into RNAi, developmental control, stem cell maintenance, and tumorigenesis. Genes Dev 16:2733–2742.
- Carli, Ormas, Re, Soldani (2009) Farmacologia Veterinaria , Idelson Gnocchi 771-778.
- Carter R.F., Valli V.E. and Lumsden J.H. (1986) The cytology, histology and prevalence of cell types in canine lymphoma classified according to the National Cancer InstituteWorking Formulation. Canadian Journal of Veterinary Research 50: 154–164.
- Casiraghi M., Bazzocchi C., Mortarino M., Ottina E., Genchi C. (2006): A simple molecular method for discriminating common filarial nematodes of dogs (Canis familiaris). Vet Parasitol 141, 368.
- Castoldi M., Schmidt S., Benes V., Noerholm M., Kulozik A.E., Hentze M.W., Muckenthaler M.U. (2006) A sensitive array for microRNA expression profiling (miChip) based on locked nucleic acids (LNA). RNA 12:913–920
- Chauve C.M. (1990): Dirofilaria repens, Dipetalonema reconditum, Dipetalonema dracunculoides et Dipetalonema grassii: quatre filaires méconnues du chien, in «Pratique médicale et chirurgicale de l'animal de compagnie», (numéro spécial Dirofilariose canine), p.293.
- Chauve C.M. (1997): Importance in France of the Infestation by Dirofilaria (Nochtiella) repens in Dogs, in «Parassitologia», 39, p. 395.

- Chen C., Ridzon D.A., Broomer A.J., Zhou Z., Lee D.H., Nguyen J.T. et al. (2005) Real-time quantification of microRNAs by stem-loop T-PCR. Nucleic Acids Res 33: e179.
- Chen C., Ridzon D.A., Broomer A.J., Zhou Z., Lee D.H., Nguyen J.T., Barbisin M., Xu N.L., Mahuvakar V.R., Andersen M.R., Lao K.Q., Livak K.J., Guegler K.J. (2005) Real-time quantification of microRNAs by stem-loop RT-PCR. Nucleic Acids Res. 27;33(20):e179
- Chang-Zheng C. (2005) MicroRNAs as Oncogenes and Tumor Suppressors. N Engl J Med 2005; 353:1768-1771.
- Chen C.Z., Li L., Lodish H.F., Bartel D.P. (2004) MicroRNAs modulate hematopoietic lineage differentiation. Science. 303 (5654):83-6.
- Chen R.W., Bemis L.T., Amato C.M., Myint H., Tran H., Birks D.K., Eckhardt S.G., Robinson W.A. (2008) Truncation in CCND1 mRNA alters miR-16-1 regulation in mantle cell lymphoma. Blood 112:822–9.
- Christensen N., Canfield P., Martin P., Krockenberger M., Spielman D., Bosward K. (2009) Cytopathological and histopathological diagnosis of canine splenic disorders. Aust Vet J 87(5):175-181.
- Cienava E.A., Barnhart K.F., Brown R., Mansell J., Dunstan R., Credille K. (2004) Morphologic, immunohistochemical, and molecular characterization of hepatosplenic T-cell lymphoma in a dog. Vet Clin Pathol. 33(2):105-10.
- Cimmino A., Calin G.A., Fabbri M., et al. (2005) miR-15 and miR-16 induce apoptosis by targeting BCL2. Proc Natl Acad Sci USA 102:13944–9.
- Cloonan N., Brown M.K., Steptoe A.L., Wani S., Chan W.L., Forrest A.R., Kolle G., Gabrielli B., Grimmond S.M. (2008) The miR-17-5p microRNA is a key regulator of the G1/S phase cell cycle transition. Genome Biol. 9:R127.
- Comazzi S., Gelain M.E., Riondato F., Paltrinieri S. (2006) Flow cytometric expression of common antigens CD18/CD45 in blood from dogs with lymphoid malignancies: a semi-quantitative study. Vet Immunol Immunopathol. 112(3-4):243-52.
- Comazzi S., Gioia G., Gelain M.E., Mortarino M. (2010) Extraction of nucleic acids from stained blood and lymph node smears: a tool for retrospective studies on clonality and microRNA. Proceedings ESVONC congress, Turin, March 18th-20th 2010.
- Comazzi S., Gelain M.E., Martini V., Riondato F., Miniscalco B., Marconato L., Stefanello D., Mortarino M. (2011) Immunophenotype predicts survival time in dogs with chronic lymphocytic leukemia. J Vet Intern Med. 25(1):100-6.
- Costinean S., Zanesi N., Pekarsky Y., Tili E., Volinia S., Heerema N., Croce C.M. (2006) Pre-B cell proliferation and lymphoblastic leukemia ⁄ high-grade lymphoma in E(mu)-miR155 transgenic mice. Proc Natl Acad Sci USA 103:7024–9.
- Costinean S., Sandhu S.K., Pedersen I.M., et al. (2009) Ship and C⁄ebp{beta} are targeted by miR-155 in B cells of E{micro}-miR-155 transgenic mice. Blood 114:1374–82.
- Cox H.U. (2006) Staphylococcal infections. In: Greene C.E.: Infectious diseases of the dog and cat, 3rd edition. Saunders-Elsevier – St. Louis, Missouri, 316-320.
- Cummins J.M., Velculescu V.E. (2006) Implications of micro-RNA profiling for cancer diagnosis. Oncogene 25:6220-7.
- Day M.J., Lucke V.M., Pearson H. (1995) A review of pathological diagnoses made from 87 canine splenic biopsies. J Small Anim Pract 36(10):426-433.
- Davoren P.A., McNeill R.E., Lowery A.J., Kerin M.J., Miller N. (2008) Identification of suitable endogenous control genes for microRNA gene expression analysis in human breast cancer. BMC Mol Biol 9:76.
- Debernardi S., Skoulakis S., Molloy G., Chaplin T., Dixon-McIver A., Young B.D. (2007) MicroRNA miR-181a correlates with morphological sub-class of acute myeloid leukaemia and the expression of its target genes in global genome-wide analysis. Leukemia 21:912–6.

- Denli A.M., Tops B.B., Plasterk R.H., Ketting R.F., Hannon G.J. (2004) Processing of primary microRNAs by the Microprocessor complex. Nature 432:231–235.
- Descloux S., Rossano A., Perreten V. (2008) Characterization of new staphylococcal cassette chromosome mec (SCCmec) and topoisomerase genes in fluoroquinolone- and methicillin-resistant Staphylococcus pseudintermedius. Journal of Clinical Microbiology 46, 1818-1823.
- Doench J.G., Sharp P.A. (2004) Specificity of microRNA target selection in translational repression. Genes Dev 18:504–511.
- Dohner H., Stilgenbaue S., Benner A., Leupolt E., Krober A., Bullinger L., Dohner K., Bentz M., Lichter P. (2000) Genomic aberrations and survival in chronic lymphocytic leukemia. N Engl J Med 343:1910–6.
- Dore L.C., Amigo J.D., Dos Santos C.O., Zhang Z., Gai X., Tobias J.W., et al. (2008) A GATA-1-regulated microRNA locus essential for erythropoiesis. Proc Natl Acad Sci USA. 105(9):3333-8.
- Drlica K., Malik M. (2003) Fluoroquinolones: action and resistance. Curr Top Med Chem. 3(3):249-82. Review.
- Dugas D.V., Bartel B. (2004) MicroRNA regulation of gene expression in plants. Curr Opin Plant Biol 7:512–520.
- Eberle N., von Babo V., Nolte I., Baumgärtner W., Betz D. (2012) Splenic masses in dogs. Part 1: Epidemiologic, clinical characteristics as well as histopathologic diagnosis in 249 cases (2000-2011). Tierarztl Prax Ausg K Kleintiere Heimtiere. 40(4):250-260.
- Eis P.S., Tam W., Sun L., Chadburn A., Li Z., Gomez M.F., Lund E., Dahlberg J.E. (2005) Accumulation of miR-155 and BIC RNA in human B cell lymphomas. Proc Natl Acad Sci USA 102:3627–32.
- Elbashir S.M., Lendeckel W., Tuschl T. (2001) RNA interference is mediated by 21- and 22-nucleotide RNAs. Genes Dev 15:188–200.
- Erson A.E., Petty E.M. (2008) MicroRNAs in development and disease. Clin Genet. 74(4):296-306. Review.
- Euzeby J. (1990): Dirofilaria immitis, in «Pratique médicale et chirurgicale de l'animal de compagnie», 25 (numéro spécial Dirofilariose canine), p.283.
- Fabbri M., Garzon R., Andreeff M., Kantarjian H.M., Garcia-Manero G., Calin G.A. (2008) MicroRNAs and noncoding RNAs in hematological malignancies: molecular, clinical and therapeutic implications. Leukemia 22:1095–105.
- Fabbri M., Croce C.M., Calin G.A. (2009) MicroRNAs in the ontogeny of leukemias and lymphomas. Leuk Lymphoma 50:160–70.
- Favia G., Lanfrancotti A., Della Torre A., Cancrini G., Coluzzi M. (1996): Polymerase chain reaction identification of Dirofilaria repens and Dirofilaria immitis, in Parasitology 113, 567.
- Fazi F., Rosa A., Fatica A., Gelmetti V., De Marchis M.L., Nervi C., Bozzoni I. (2005) A minicircuitry comprised of micro-RNA-223 and transcription factors NFI-A and C⁄ EBPalpha regulates human granulopoiesis. Cell 123:819–31.
- Felli N., Fontana L., Pelosi E., Botta R., Bonci D., Facchiano F., et al. (2005) MicroRNAs 221 and 222 inhibit normal erythropoiesis and erythroleukemic cell growth via kit receptor down-modulation. Proc Natl Acad Sci USA. 102(50):18081-6.
- Felli N., Pedini F., Romania P., et al. (2009) MicroRNA 223-dependent expression of LMO2 regulates normal erythropoiesis. Haematologica 94:479–86.
- Filipowicz W., Jaskiewicz L., Kolb F.A., Pillai R.S. (2005) Post-transcriptional gene silencing by siRNAs and miRNAs. Curr Opin Struct Biol 15:331–341.

- Flood-Knapik K.E., Durham A.C., Gregor T.P., Sánchez M.D., Durney M.E., Sorenmo K.U. (2012) Clinical, histopathological and immunohistochemical characterization of canine indolent lymphoma. Vet Comp Oncol.
- Fontana L., Pelosi E., Greco P., Racanicchi S., Testa U., Liuzzi F., et al. (2007) MicroRNAs 17-5p-20a-106a control monocytopoiesis through AML1 targeting and M-CSF receptor upregulation. Nat Cell Biol. 9(7):775-87.
- Fournel-Fleury C., Magnol J., Bricaire P., Marchal T., Chabanne L., Delverdier A., Bryon P.A. and Felman P. (1997) Cytohistological and immunological classification of canine malignant lymphomas: comparison with human non-hodgkin's lymphomas. Journal of Comparative Pathology 117: 35–59.
- Frey A.J., Betts C.W. (1977) A retrospective survey of splenectomy in the dog. J Am Anim Hosp Assoc 13:730-734.
- Fry M.M., Vernau W., Pesavento P.A., Brömel C., Moore P.F. (2003) Hepatosplenic lymphoma in a dog. Vet Pathol. 40(5):556-62.
- Fukao T., Fukuda Y., Kiga K., Sharif J., Hino K., Enomoto Y., Kawamura A., Nakamura K., Takeuchi T., Tanabe M. (2007) An evolutionarily conserved mechanism for microRNA-223 expression revealed by microRNA gene profiling. Cell 129:617–31.
- Fulci V., Chiaretti S., Goldoni M., et al. (2007) Quantitative technologies establish a novel microRNA profile of chronic lymphocytic leukemia. Blood 109:4944–51.
- Garzon R., Pichiorri F., Palumbo T., et al. (2006) MicroRNA fingerprints during human megakaryocytopoiesis. Proc Natl Acad Sci USA 103:5078–83.
- Garzon R., Pichiorri F., Palumbo T., et al. (2007) MicroRNA gene expression during retinoic acid-induced differentiation of human acute promyeloctic leukemia. Oncogene 26:4148–57.
- Garzon R., Croce C.M. (2008) MicroRNAs in normal and malignant hematopoiesis. Curr Opin Hematol 15:352–8.
- Garzon R., Garofalo M., Martelli M.P., et al. (2008) Distinctive microRNA signature of acute myeloid leukemia bearing cytoplasmic mutated nucleophosmin. Proc Natl Acad Sci USA 105:3945–50.
- Garzon R., Volinia S., Liu C.G., et al. (2008) MicroRNA signatures associated with cytogenetics and prognosis in acute myeloid leukemia. Blood 111:3183–9.
- Gaur A., Jewell D.A., Liang Y., et al. (2007) Characterization of microRNA expression levels and their biological correlates in human cancer cell lines. Cancer Res 67: 2456–2468.
- Genchi C., Rinaldi L., Cascone C., Mortarino M., Cringoli G. (2005): Is heartworm disease really spreading in Europe?, in «Veterinary parasitology» 133, p.137
- Genchi C., Rinaldi L., Cringoli G. (2007): Dirofilaria immitis and D. repens in dog and cat and human infections, in «Mappe parassitologiche» n.8, p.117.
- Genchi C., Rinaldi L., Mortarino M., Genchi M., Cringoli G. (2009): Climate and Dirofilaria infection in Europe, in «Veterinary parasitology» 163, p.286
- Georgantas R.W. III, Hildreth R., Morisot S., Alder J., Liu C.G., Heimfeld S., Calin G.A., Croce C.M., Civin C.I. (2007) CD34+ hematopoietic stem-progenitor cell microRNA expression and function: a circuit diagram of differentiation control. Proc Natl Acad Sci USA 104:2750–5.
- Giannetto S., Pampiglione S., Santoro V., Virga A. (1997): Research of canine filariosis in Trapani province (Western Sicily). Morphology on SEM of male Dirofilaria repens, in «Parassitologia», 39, p.403.
- Ginzinger D.G. (2002) Gene quantification using real-time quantitative PCR: an emerging technology hits the mainstream. Exp Hematol 30:503-12.

- Gioia G., Lecová L., Genchi M., Ferri E., Genchi C., Mortarino M. (2010) Highly sensitive multiplex PCR for simultaneous detection and discrimination of Dirofilaria immitis and Dirofilaria repens in canine peripheral blood. Vet Parasitol. 172(1-2):160-3.
- Giulietti A., Overbergh L., Valckx D., Decallonne B., Bouillon R., Mathieu C. (2001) An overview of real-time quantitative PCR: applications to quantify cytokine gene expression. Methods 25, 386-401.
- Gregory R.I., Yan K.P., Amuthan G., Chendrimada T., Doratotaj B., Cooch N. et al (2004) The Microprocessor complex mediates the genesis of microRNAs. Nature 432:235–240.
- Han J., Lee Y., Yeom K.H., Kim Y.K., Jin H., Kim V.N. (2004) The Drosha-DGCR8 complex in primary microRNA processing. Genes Dev 18:3016–3027.
- Han J., Lee Y., Yeom K.H., Nam J.W., Heo I., Rhee J.K. et al (2006) Molecular basis for the recognition of primary microRNAs by the Drosha-DGCR8 complex. Cell 125:887–901.
- He L., Thomson J.M., Hemann M.T., Hernando-Monge E., Mu D., Goodson S. et al. (2005) A microRNA polycistron as a potential human oncogene. Nature 435: 828–833.
- Hutvagner G., Zamore P.D. (2002) A microRNA in a multiple-turnover RNAi enzyme complex. Science 297:2056–2060.
- Hutvagner G., Simard M.J., Mello C.C., Zamore P.D. (2004) Sequence-specific inhibition of small RNA function. PLoS Biol 2:E98.
- Hwang H.W., Wentzel E.A., Mendell J.T. (2007) A hexanucleotide element directs microRNA nuclear import. Science 315, 97–100.
- Intorre L., Vanni M., Di Bello D., Pretti C., Meucci V., Tognetti R., Soldani G., Cardini G., Jousson O. (2007) Antimicrobial susceptibility and mechanism of resistance to fluoroquinolones in Staphylococcus intermedius and Staphylococcus schleiferi. Journal of Veterinary Pharmacology and Therapeutics 30, 464-469.
- Isaacson P.G. (1996) Splenic marginal zone lymphoma. Blood 88:751–752.
- John B., Enright A.J., Aravin A., Tuschl T., Sander C., Marks D.S. (2004) Human MicroRNA targets. PLoS Biol 2:e363.
- Johnnidis J.B., Harris M.H., Wheeler R.T., Stehling-Sun S., Lam M.H., Kirak O., Brummelkamp T.R., Fleming M.D., Camargo F.D. (2008) Regulation of progenitor cell proliferation and granulocyte function by microRNA-223. Nature 451:1125–9.
- Johnson S.M., Grosshans H., Shingara J., Byrom M., Jarvis R., Cheng A. et al. (2005) RAS is regulated by the let-7 microRNA family. Cell 120: 635–647.
- Kaltenboeck B., Wang C. (2005) Advances in real-time PCR: application to clinical laboratory diagnostics. Advances in Clinical Chemistry 40, 219-259.
- Kaza R.K., Azar S., Al-Hawary M.M., Francis I.R. (2010) Primary and secondary neoplasms of the spleen. Cancer Imaging. 10:173-82.
- Keller S.M., Vernau W., Hodges J., Kass P.H., Vilches-Moure J.G., McElliot V., Moore P.F. (2012) Hepatosplenic and Hepatocytotropic T-Cell Lymphoma: Two Distinct Types of T-Cell Lymphoma in Dogs. Vet Pathol.
- Kim V.N. (2006) Small RNAs just got bigger: Piwi-interacting RNAs (piRNAs) in mammalian testes. Genes Dev 20:1993–1997.
- Kiriakidou M., Nelson P.T., Kouranov A., Fitziev P., Bouyioukos C., Mourelatos Z. et al (2004) A combined computational-experimental approach predicts human microRNA targets. Genes Dev 18:1165–1178.
- Kisseberth W.C., Nadella M.V., Breen M., Thomas R., Duke S.E., Murahari S., Kosarek C.E., Vernau W., Avery A.C., Burkhard M.J.., Rosol T.J. (2007) A novel canine lymphoma cell line: a translational and comparative model for lymphoma research. Leuk Res. 31(12):1709-20.
- Kloosterman W.P., Plasterk R.H. (2006) The diverse functions of microRNAs in animal development and disease. Dev Cell 11: 441–450.

- Kluiver J., Poppema S., de Jong D., Blokzijl T., Harms G., Jacobs S., Kroesen B.J., van den Berg A. (2005) BIC and miR-155 are highly expressed in Hodgkin, primary mediastinal and diffuse large B cell lymphomas. J Pathol 207:243–9.
- Kluiver J., Kroesen B.J., Poppema S., Van den Berg A. (2006) The role of microRNAs in normal hematopoiesis and hematopoietic malignancies. Leukemia. 20(11):1931-6.
- Kluiver J., Haralambieva E., de Jong D., Blokzijl T., Jacobs S., Kroesen B.J., Poppema S., Van den Berg A. (2006) Lack of BIC and microRNA miR-155 expression in primary cases of Burkitt lymphoma. Genes Chromosomes Cancer 45:147–53.
- Kuppers R. (2009) The biology of Hodgkin's lymphoma. Nat. Rev. Cancer 9, 15–27.
- Kurtin P.J. (2009) Indolent lymphomas of mature B lymphocytes. Hematol Oncol Clin North Am. 23(4):769-90.
- Labbaye C., Spinello I., Quaranta M.T., et al. (2008) A three-step pathway comprising PLZF⁄ miR-146a ⁄CXCR4 controls megakaryopoiesis. Nat Cell Biol 10:788–801.
- Lachaud L., Chabbert E., Dubessay P., Dereure J., Lamothe J., Dedet J.P., Bastien P. (2002) Value of two PCR methods for the diagnosis of canine visceral leishmaniasis and the detection of asymptomatic carriers. Parasitology. 125(Pt 3):197-207.
- Lages E., Ipas H., Guttin A., Nesr H., Berger F., Issartel J.P. (2012) MicroRNAs: molecular features and role in cancer. Front Biosci. 17:2508-40.
- Lagos-Quintana M., Rauhut R., Meyer J., et al. (2003) New microRNAs from mouse and human. RNA 9:175–179.
- Lai E.C. (2002) Micro RNAs are complementary to 3' UTR sequence motifs that mediate negative post-transcriptional regulation. Nat Genet 30:363–364.
- Landais S., Landry S., Legault P., Rassart E. (2007) Oncogenic potential of the miR-106-363 cluster and its implication in human T-cell leukemia. Cancer Res 67:5699–707.
- Lawrie C.H. (2007) MicroRNA expression in lymphoma. Expert Opin Biol Ther 7:1363–74.
- Lawrie C.H., Soneji S., Marafioti T., et al. (2007) MicroRNA expression distinguishes between germinal center B celllike and activated B cell-like subtypes of diffuse large B cell lymphoma. Int J Cancer 121:1156–61.
- Lawrie C.H., Gal S., Dunlop H.M., et al. (2008) Detection of elevated levels of tumour-associated microRNAs in serum of patients with diffuse large B-cell lymphoma. Br J Haematol 141:672–5.
- Lawrie C.H., Chi J., Taylor S., et al. (2009) Expression of Micro-RNAs in diffuse large B cell lymphoma is associated with immunophenotype, survival, and transformation from follicular lymphoma. J Cell Mol Med 13:1248–60.
- Laterza O.F., Lim L., Garrett-Engele P.W., Vlasakova K., Muniappa N., Tanaka W.K., Johnson J.M., Sina J.F., Fare T.L., Sistare F.D., Glaab W.E. (2009) Plasma MicroRNAs as sensitive and specific biomarkers of tissue injury. Clin Chem. 55(11):1977-83.
- Lee R.C., Feinbaum R.L., Ambros V. (1993) The C. elegans heterochronic gene lin-4 encodes small RNAs with antisense complementarity to lin-14. Cell. 75(5):843-54.
- Lee Y., Jeon K., Lee J.T., Kim S., Kim V.N. (2002) MicroRNA maturation: stepwise processing and subcellular localization. EMBO J 21: 4663–4670.
- Lee Y., Ahn C., Han J., Choi H., Kim .J, Yim J. et al (2003) The nuclear RNase III Drosha initiates microRNA processing. Nature 425:415–419.
- Lee Y., Kim M., Han J., Yeom K.H., Lee S., Baek S.H., Kim V.N. (2004) MicroRNA genes are transcribed by RNA polymerase II. EMBO J. 23(20):4051-60.
- Leuterer G., Gothe R. (1993): Die Herzwurmkrankheit des Hundes: Erregerbiologie und-öcologie, Pathogenese, Klinik, Diagnose, Therapie und Profylaxe, in «Kleintierpraxix», 38 (10), p.633.
- Levin B.R., Perrot V., Walker N. (2000) Compensatory mutations, antibiotic resistance and the population genetics of adaptive evolution in bacteria. Genetics 154, 985–997.

- Lewis B.P., Shih I.H., Jones-Rhoades M.W., Bartel D.P., Burge C.B. (2003) Prediction of mammalian microRNA targets. Cell 115:787-98.
- Lewis B.P., Burge C.B., Bartel D.P. (2005) Conserved seed pairing, often flanked by adenosines, indicates that thousands of human genes are microRNA targets. Cell 120:15-20.
- Liu J., Carmell M.A., Rivas F.V., Marsden C.G., Thomson J.M., Song J.J. et al (2004) Argonaute2 is the catalytic engine of mammalian RNAi. Science 305:1437–1441.
- Liu J., Zheng M., Tang Y.L., Liang X.H., Yang Q. (2011) MicroRNAs, an active and versatile group in cancers. Int J Oral Sci. 3(4):165-75. Review.
- Liu X., Fortin K., Mourelatos Z.(2008) MicroRNAs: biogenesis and molecular functions. Brain Pathol. 18(1):113-21. Review.
- Llave C., Xie Z., Kasschau K.D., Carrington J.C. (2002) Cleavage of Scarecrow-like mRNA targets directed by a class of Arabidopsis iRNA. Science 297:2053–2056.
- Lu J., Getz G., Miska E.A., Alvarez-Saavedra E., Lamb J., Peck D., Sweet-Cordero A., Ebert B.L., Mak R.H., Ferrando A.A., Downing J.R., Jacks T., Horvitz H.R., Golub T.R. (2005) MicroRNA expression profiles classify human cancers. Nature 435:834–838
- Lu J., Getz G., Miska E.A., et al. (2005) MicroRNA expression profiles classify human cancers. Nature 435: 834–838.
- Lu J., Guo S., Ebert B.L., Zhang H., Peng X., Bosco J., et al. (2008) MicroRNA-mediated control of cell fate in megakaryocyte-erythrocyte progenitors. Dev Cell. 14(6):843-53.
- Lum A.M., Wang B.B., Li L., Channa N., Bartha G., Wabl M. (2007) Retroviral activation of the mir-106a microRNA cistron in T lymphoma. Retrovirology 4:5.
- Lund E., Guttinger S., Calado A., Dahlberg J.E., Kutay U. (2004) Nuclear export of microRNA precursors. Science 303, 95–98.
- Maffil S., Marella M., Genchi C. (1999): Indagine sulla diffusione della filariosi cardiopolmonare del cane lungo il medio corso del fiume Oglio, in «Veterinaria», 13 (4), p.63.
- Malumbres R., Sarosiek K.A., Cubedo E., Ruiz J.W., Jiang X., Gascoyne R.D., Tibshirani R., Lossos I.S. (2009) Differentiation stage-specific expression of microRNAs in B lymphocytes and diffuse large B-cell lymphomas. Blood. 113:3754-64.
- Manfredi M.T. (1998): Diagnosi di laboratorio, in Genchi C., Venco L., Vezzoni A. (eds): Filariosi cardiopolmonare del cane e del gatto, Edizioni Scivac, Cremona, p. 80.
- Mar P.H., Yang I.C., Chang G.N., Fei A.C. (2002): Specific polymerase chain reaction for differential diagnosis of Dirofilaria immitis and Dipetalonema reconditum using primers derived from internal transcribed spacer region 2 (ITS2). Vet. Parasitol. 106, p.243.
- Marconato L., Leo C., Girelli R., Salvi S., Abramo F., Bettini G., Comazzi S., Nardi P., Albanese F., Zini E. (2009) Association between Waste Management and cancer in companion animals.
- Marcucci G., Radmacher M.D., Maharry K., et al. (2008) Micro-RNA expression in cytogenetically normal acute myeloid leukemia. N Engl J Med 358:1919–28.
- Marcucci G., Maharry K., Radmacher M.D., Mrózek K., Vukosavljevic T., Paschka P., Whitman S.P., Langer C., Baldus C.D., Liu C.G., Ruppert A.S., Powell B.L., Carroll A.J., Caligiuri M.A., Kolitz J.E., Larson R.A., Bloomfield C.D. (2008) Prognostic significance of, and gene and microRNA expression signatures associated with, CEBPA mutations in cytogenetically normal acute myeloid leukemia with high-risk molecular features: a cancer and leukemia Group B study. J Clin Oncol.
- Martinez J., Tuschl T. (2004) RISC is a 5′ phosphomonoester-producing RNA endonuclease. Genes Dev 18:975–980.

- Martino P.A., Caldora C., Cocilovo A., Dall'Ara P. (2005) Classificazione dei batteri e batteriologia speciale. In: Poli G., Cocilovo A.: Microbiologia e immunologia veterinaria 2a edizione. UTET-Torino, 199-266
- Marton S., Garcia M.R., Robello C., Persson H., Trajtenberg F., Pritsch O., Rovira C., Naya H., Dighiero G., Cayota A. (2008) Small RNAs analysis in CLL reveals a deregulation of miRNA expression and novel miRNA candidates of putative relevance in CLL pathogenesis. Leukemia. 22(2):330-8.
- Meister G., Landthaler M., Patkaniowska A., Dorsett Y., Teng G., Tuschl T. (2004) Human Argonaute2 mediates RNA cleavage targeted by miRNAs and siRNAs. Mol Cell. 15(2):185-97.
- Mendell J.T. (2005) MicroRNAs: critical regulators of development, cellular physiology and malignancy. Cell Cycle. 4(9):1179-84. Review.
- Metzler M., Wilda M., Busch K., Viehmann S., Borkhardt A. (2004) High expression of precursor microRNA-155 / BIC RNA in children with Burkitt Lymphoma. Genes Chromosomes Cancer 39:167–9.
- Mi S., Lu J., Sun M., et al. (2007) MicroRNA expression signatures accurately discriminate acute lymphoblastic leukemia from acute myeloid leukemia. Proc Natl Acad Sci USA 104:19971–6.
- Miska E.A., Alvarez-Saavedra E., Townsend M., Yoshii A., Sestan N., Rakic P., Constantine-Paton M., Horvitz H.R. (2004) Microarray analysis of microRNA expression in the developing mammalian brain. Genome Biol 5:R68.
- Mollejo M., Rodríguez-Pinilla M.S., Montes-Moreno S., Algara P., Dogan A., Cigudosa J.C., Juarez R., Flores T., Forteza J., Arribas A., Piris M.A. (2009) Splenic follicular lymphoma: clinicopathologic characteristics of a series of 32 cases. Am J Surg Pathol. 33(5):730-8.
- Monticelli S., Ansel K.M., Xiao C., et al. (2005) MicroRNA profiling of the murine hematopoietic system. Genome Biol 6:R71.
- Mourelatos Z., Dostie J., Paushkin S., Sharma A., Charroux B., Abel L. et al (2002) miRNPs: a novel class of ribonucleoproteins containing numerous microRNAs. Genes Dev 16:720–728.
- Munker R., Calin G.A. (2011) MicroRNA profiling in cancer. Clin Sci (Lond). 121(4):141-58. Review.
- Muro A., Genchi C., Cordero M., Simon F. (1999): Human Dirofilariasis in the European Union in «Parasitology Today», 15 (9), p.386.
- Navarro A., Gaya A., Martinez A., et al. (2008) MicroRNA expression profiling in classic Hodgkin lymphoma. Blood 111:2825–32.
- Navarro A., Diaz T., Martinez A., Gaya A., Pons A., Gel B., Codony C., Ferrer G., Martinez C., Montserrat E., Monzo M. (2009) Regulation of JAK2 by miR-135a: prognostic impact in classic Hodgkin lymphoma. Blood 114, 2945–2951
- Nelson P.T., Baldwin D.A., Scearce L.M., Oberholtzer J.C., Tobias J.W., ourelatos Z. (2004) Microarray-based, high-throughput gene expression profiling of microRNAs. Nat Methods 1:155–161
- Nicoloso M.S., Kipps T.J., Croce C.M., Calin G.A. (2007) Micro-RNAs in the pathogeny of chronic lymphocytic leukaemia. Br J Haematol 139:709–16.
- Nie K., Gomez M., Landgraf P., Garcia J.F., Liu Y., Tan L.H., Chadburn A., Tuschl T., Knowles D.M., Tam W. (2008) MicroRNA-mediated down-regulation of PRDM1/Blimp-1 in Hodgkin / Reed-Sternberg cells: a potential pathogenetic lesion in Hodgkin lymphomas. Am J Pathol 173:242–52.
- Nikaido H. (2009) Multidrug resistance in bacteria. Annu Rev Biochem. 78:119-46. doi: 10.1146/annurev.biochem.78.082907.145923. Review.

- O' Connell R.M.., Rao D.S., Chaudhuri A.A., Boldin M.P., Taganov K.D., Nicoll J., Paquette R.L., Baltimore D. (2008) Sustained expression of microRNA-155 in hematopoietic stem cells causes a myeloproliferative disorder. J Exp Med 205:585–94.
- O' Connell R.M., Chaudhuri A.A., Rao D.S., Baltimore D. (2009) Inositol phosphatase SHIP1 is a primary target of miR-155. Proc Natl Acad Sci USA 106:7113–8.
- O' Donnell K.A., Wentzel E.A., Zeller K.I., Dang C.V., Mendell J.T. (2005) c-Myc-regulated microRNAs modulate E2F1 expression. Nature 435:839–43.
- O' Hara A.J., Vahrson W., Dittmer D.P. (2008) Gene alteration and precursor and mature microRNA transcription changes contribute to the miRNA signature of primary effusion lymphoma. Blood 111:2347–53.
- Orkin S.H., Zon L.I. (2008) Hematopoiesis: an evolving paradigm for stem cell biology. Cell. 132(4):631-44.
- Paoloni M., Khanna C. (2008) Translation of new cancer treatments from pet dogs to humans. Nat Rev Cancer. 8:147-56.
- Pasquinelli A.E., Reinhart B.J., Slack F., Martindale M.Q., Kuroda M.I., Maller B., Hayward D.C., Ball E.E., Degnan B., Müller P., Spring J., Srinivasan A., Fishman M., Finnerty J., Corbo J., Levine M., Leahy P., Davidson E., Ruvkun G. (2000) Conservation of the sequence and temporal expression of let-7 heterochronic regulatory RNA. Nature 408 (6808): 86–9.
- Pekarsky Y., Santanam U., Cimmino A., et al. (2006) Tcl1 expression in chronic lymphocytic leukemia is regulated by miR-29 and miR-181. Cancer Res 66:11590–3.
- Peltier H.J., Latham G.J. (2008) Normalization of microRNA expression levels in quantitative RT-PCR assays: identification of suitable reference RNA targets in normal and cancerous human solid tissues. RNA 14:844-52.
- Pfeffer S., Sewer A., Lagos-Quintana M., Sheridan R., Sander C., Grasser F.A., van Dyk L.F., Ho C.K., Shuman S., Chien M., Russo J.J., Ju J., Randall G., Lindenbach B.D., Rice C.M., Simon V., Ho D.D., Zavolan M., Tuschl T. (2005) Identification of microRNAs of the herpesvirus family. Nat Methods 2:269-76.
- Pittaluga S., Verhoef G., Criel A., Wlodarska I., Dierlamm J., Mecucci C., Van den Berghe H., De Wolf-Peeters C. (1996) ''Small'' B-cell non-Hodgkin's lymphomas with splenomegaly at presentation are either mantle cell lymphoma or marginal zone cell lymphoma. A study based on histology, cytology, immunohistochemistry, and cytogenetic analysis. Am J Surg Pathol 20:211–223.
- Poli G., Cocilovo A. (2005) Microbiologia e immunologia veterinaria, 2a edizione UTET-Torino, 169-197.
- Ponce F., Marhal T., Magnol J., Turinelli V., Ledieu D.,Bonnefont C., Pastor M., Delignette M.L. and Fournel-Fleury C. (2010) A morphological study of 608 cases of canine malignant lymphoma in France with a focus on comparative similarities between canine and human lymphoma morphology. Veterinary Pathology 43: 414–433.
- Rai D., Karanti S., Jung I., Dahia P.L., Aguiar R.C. (2008) Coordinated expression of microRNA-155 and predicted target genes in diffuse large B-cell lymphoma. Cancer Genet Cytogenet 181:8–15.
- Rajewsky N., Socci N.D. (2004) Computational identification of microRNA targets. Dev Biol 267:529–535.
- Ramkinssoon S.H., Mainwaring L.A., Ogasawara Y., Keyvanfar K., Philip McCoy J. Jr, Sloand E.M., Kajigaya S., Young N.S. (2005) Hematopoietic-specific microRNA expression in human cells. Leuk Res 30:643–7.
- Reinhart B.J., Slack F.J., Basson M., Pasquinelli A.E., Bettinger J.C., Rougvie A.E., Horvitz H.R., Ruvkun G. (2000) The 21-nucleotide let-7 RNA regulates developmental timing in Caenorhabditis elegans. Nature 403 (6772): 901–6.

- Rishniw M., Barr S.C., Simpson K.W., Frongillo M.F., Franz M., Alpizar J.L.D. (2006) Discrimination between six species of canine microfilariae by a single polymerase chain reaction. Vet. Parasitol. 135, p.305.
- Ro S., Park C., Young D., Sanders K.M., Yan W. (2007) Tissue-dependent paired expression of miRNAs. Nucleic Acids Res 35, 5944–5953.
- Rodriguez A., Griffiths-Jones S., Ashurst J.L., Bradley A. (2004) identification of mammalian microRNA host genes and transcription units. Genome Res 14:1902–1910.
- Rodriguez A., Vigorito E., Clare S., Warren M.V., Couttet .P, Soond D.R., et al. (2007) Requirement of bic/microRNA-155 for normal immune function. Science. 316 (5824):608-11.
- Roehle A., Hoefig K.P., Repsilber D. et al. (2008) MicroRNA signatures characterize diffuse large B-cell lymphomas and follicular lymphomas. Br J Haematol 142:732–44.
- Rossi S., Shimizu M., Barbarotto E., Nicoloso M.S., Dimitri F., Sampath D., Fabbri M., Lerner S., Barron L.L., Rassenti L.Z., Jiang L., Xiao L., Hu J., Secchiero P., Zauli G., Volinia S., Negrini M., Wierda W., Kipps T.J., Plunkett W., Coombes K.R., Abruzzo L.V., Keating M.J., Calin G.A. (2010) MicroRNA fingerprinting of CLL patients with chromosome 17p deletion identify a miR-21 score that stratifies early survival. Blood. 116(6):945-52.
- Sassen S., Miska E.A., Caldas C. (2008) MicroRNA—implications for cancer. Virchow Archiv 452: 1–10.
- Schwarz D.S., Hutvagner G., Du T., Xu Z., Aronin N., Zamore P.D. (2003) Asymmetry in the assembly of the RNAi enzyme complex. Cell 115, 199–208.
- Schwarz D.S., Tomari Y., Zamore P.D. (2004) The RNA-induced silencing complex is a Mg2+-dependent endonuclease. Curr Biol 14:787–791.
- Seitz H. and Zamore P.D. (2006) Rethinking the microprocessor. Cell 125, 827–829.
- Shahi P., Loukianiouk S., Bohne-Lang A., Kenzelmann M., Küffer S., Maertens S., Eils R., Gröne H.J., Gretz N., Brors B. (2006) Argonaute--a database for gene regulation by mammalian microRNAs. Nucleic Acids Res. 34(Database issue):D115-8.
- Shi L., Cheng Z., Zhang J., Li R., Zhao P., Fu Z., You Y. (2008) hsa-mir-181a and hsa-mir-181b function as tumor suppressors in human glioma cells. Brain Res. 1236:185-193.
- Shimizu-Kohno K., Kimura Y., Kiyasu J., Miyoshi H., Yoshida M., Ichikawa R., Niino D., Ohshima K. (2012) Malignant lymphoma of the spleen in Japan: A clinicopathological analysis of 115 cases. Pathol Int. 62(9):577-82.
- Singh S.K., Pal Bhadra M., Girschick H.J., (2008) Bhadra U. MicroRNAs--micro in size but macro in function. FEBS J. 275(20):4929-44. Review.
- Smillie C., Garcillán-Barcia M.P., Francia M.V., Rocha E.P., de la Cruz F. (2010) Mobility of plasmids. Microbiol Mol Biol Rev. 74(3):434-52.
- Spangler W.L., Culbertson M.R. (1992) Prevalence, type, and importance of splenic diseases in dogs: 1,480 cases (1985-1989). J Am Vet Med Assoc 200(6):829-834.
- Stark A., Brennecke J., Russell R.B., Cohen S.M. (2003) Identification of Drosophila MicroRNA targets. PLoS Biol. 1(3):E60.
- Stefanello D., Valenti P., Zini E., Comazzi S., Gelain M.E., Roccabianca P., Avallone G., Caniatti M., Marconato L. (2011) Splenic marginal zone lymphoma in 5 dogs (2001-2008). J Vet Intern Med 25(1):90-93.
- Surdziel E., Cabanski M., Dallmann I., Lyszkiewicz M., Krueger A., Ganser A., et al. (2011) Enforced expression of miR-125b affects myelopoiesis by targeting multiple signaling pathways. Blood. 117(16):4338- 48.
- Swerdlow S.H., Campo E., Harris N.L. et al. (2008) WHO Classification of Tumors of Haematopoietic and Lymphoid Tissues. Lyon, France: IARC Press.
- Tagawa H., Seto M. (2005) A microRNA cluster as a target of genomic amplification in malignant lymphoma. Leukemia 19: 2013–2016.

- Tam W., Ben-Yehuda D., Hayward W.S. (1997) bic, a novel gene activated by proviral insertions in avian leukosis virusinduced lymphomas, is likely to function through its noncoding RNA. Mol Cell Biol 17:1490–502.
- Tang F., Hajkova P., Barton S.C., O' Carroll D., Lee C., Lao K., Surani M.A. (2006) 220-plex microRNA expression profile of a single cell. Nat Protoc 1:1154–1159
- Tasca S., Carli E., Caldin M., Menegazzo L., Furlanello T., Gallego L.S. (2009) Hematologic abnormalities and flow cytometric immunophenotyping results in dogs with hematopoietic neoplasia: 210 cases (2002-2006). Vet Clin Pathol. 38(1):2-12.
- Teixeira D., Sheth U., Valencia-Sanchez M.A., Brengues M. and Parker R. (2005) Processing bodies require RNA for assembly and contain nontranslating mRNAs. RNA 11, 371–382.
- Thai T.H., Calado D.P., Casola S., Ansel K.M., Xiao C., Xue Y., et al. (2007) Regulation of the germinal center response by microRNA-155. Science. 316(5824):604-8.
- Thieblemont C., Felman P., Berger .F, et al. (2002) Treatment of splenic marginal zone B-cell lymphoma : An analysis of 81 patients. Clin Lymphoma 3:41-47.
- Thieblemont C., Felman P., Callet-Bauchu E., et al. (2003) Splenic marginal-zone lymphoma: A distinct clinical and pathological entity. Lancet Oncol 4:95-103.
- Thomson J.M., Parker J., Perou C.M., Hammond S.M. (2004) A custom microarray platform for analysis of microRNA gene expression. Nat Methods 1:47–53.
- Urquart G.M., Armour J., Duncan J.L., Dunn A.M., JenningsS F.W. (1996): Parassitologia veterinaria, Seconda edizione, edizione italiana a cura di Genchi C., UTET, Torino
- Vail D.M., MacEwen E.G. (2000) Spontaneously occurring tumors of companion animals as models for human cancer. Cancer Invest 18:781–92.
- Vail D.M., Young K.M. (2007) Canine lymphoma and lymphoid leukemia. In: Withrow SJ, MacEwen EG, eds. Small Animal Clinical Oncology, 4th ed. Philadelphia, PA: WB Saunders Co 699-733.
- Vajna De Pava M. (2002): Filariosi: sempre più presente, sempre più combattuta in «La Settimana Veterinaria» 338 (supplemento), p.5.
- Valli V.E., Jacobs R. M., Parodi A. L., Vernau W., Moore P. F. (2002) Histological classification of Hematopoiecic tumors of domestic animals. World Health Organization, Vol. III, 2002.
- Valli V.E., Vernau W., de Lorimier L.P., Graham P.S., Moore P.F. (2006) Canine indolent nodular lymphoma. Vet Pathol. 43(3):241-56.
- Valli V.E. (2007) Veterinary Comparative Hematopathology, 1st edn., Ames, Iowa, Blackwell Publishing.
- Valli V.E., San Myint M, Barthel A., Bienzle D., Caswell J., Colbatzky F., Durham A., Ehrhart E.J., Johnson Y., Jones C., Kiupel M., Labelle P., Lester S., Miller M., Moore P., Moroff S., Roccabianca P., Ramos-Vara J., Ross A., Scase T., Tvedten H., Vernau W. (2011) Classification of canine malignant lymphomas according to the World Health Organization criteria. Vet Pathol. 48(1):198-211.
- Valoczi A., Hornyik C., Varga N., Burgyan J., Kauppinen S., Havelda Z. (2004) Sensitive and specific detection of microRNAs by Northern blot analysis using LNA-modified oligonucleotide probes. Nucleic Acids Res 32:e175
- Van Vlierberghe P., DeWeer A., Mestdagh P., Feys T., De Preter K., De Paepe P., Lambein, K., Vandesompele J., Van Roy N., Verhasselt B. et al. (2009) Comparison of miRNA profiles of microdissected Hodgkin/Reed–Sternberg cells and Hodgkin cell lines versus CD77+ B-cells reveals a distinct subset of differentially expressed miRNAs. Br. J. Haematol. 147, 686–690.

- Vandesompele J., De Preter K., Pattyn F., Poppe B., Van Roy N., De Paepe A., Speleman F. (2002) Accurate normalization of real-time quantitative RT-PCR data by geometric averaging of multiple internal control genes. Genome Biol. 3(7):RESEARCH0034.
- Vasilatou D., Papageorgiou S., Pappa V., Papageorgiou E., Dervenoulas J. (2010) The role of microRNAs in normal and malignant hematopoiesis. Eur J Haematol. 84(1):1-16.
- Vernau W., Moore P.F. (1999) An immunophenotypic study of canine leukemias and preliminary assessment of clonality by polymerase chain reaction. Vet Immunol Immunopathol. 69(2-4):145-164.
- Venco L. (1993): Approccio diagnostico alla sindrome della vena cava. Veterinaria, SCIVAC Ed. Cremona p.1-18.
- Ventura A., Young A.G., Winslow M.M., et al. (2008) Targeted deletion reveals essential and overlapping functions of the miR-17 through 92 family of miRNA clusters. Cell 132:875–86.
- Visone R., Rassenti L.Z., Veronese A., Taccioli C., Costinean S., Aguda B.D., Volinia S., Ferracin M., Palatini J., Balatti V., Alder H., Negrini M., Kipps T.J., Croce C.M. (2009) Karyotype-specific microRNA signature in chronic lymphocytic leukemia. Blood. 114(18):3872-9.
- Xi Y., Nakajima G., Gavin E., Morris C.G., Kudo K., Hayashi K., Ju J. (2006) Systematic analysis of microRNA expression of RNA extracted from fresh-frozen and formalin-fixed paraffin-embedded samples. RNA 13:1668-1674.
- Xiao C., Calado D.P., Galler G., Thai T.H., Patterson H.C., Wang J. et al. (2007) MiR-150 controls B cell differentiation by targeting the transcription factor c-Myb. Cell. 131(1):146-59.
- Xie X., Lu J., Kulbokas E.J., Golub T.R., Mootha V., Lindblad-Toh K., Lander E.S., Kellis M.
- Walsh, C. (2000) Molecular mechanisms that confer antibacterial drug resistance. Nature 406, 775–781 .
- Warrington J.A., Nair A., Mahadevappa M., Tsyganskaya M. (2000) Comparison of human adult and fetal expression and identification of 535 housekeeping/maintenance genes. Physiol Genomics 2:143-147.
- Weidmann E. (2000) Hepatosplenic T cell lymphoma. A review on 45 cases since the first report describing the disease as a distinct lymphoma entity in 1990. Leukemia. 14(6):991-7.
- Wiemer E.A. (2007) The role of microRNAs in cancer: no small matter. Eur J Cancer 43: 1529–1544.
- Wiestner A., Tehrani M., Chiorazzi M., et al. (2007) Point mutations and genomic deletions in CCND1 create stable truncated cyclin D1 mRNAs that are associated with increased proliferation rate and shorter survival. Blood 109:4599–606.
- Williams M.J., Avery A.C., Lana S.E., Hillers K.R., Bachand A.M., Avery P.R. (2008) Canine lymphoproliferative disease characterized by lymphocytosis: immunophenotypic markers of prognosis. J Vet Intern Med. 22(3):596-601.
- Wittwer C.T., Herrmann M.G., Moss A.A., Rasmussen R.P. (1997) Continuous fluorescence monitoring of rapid cycle DNA amplification. Biotechniques 22:130–131, 134–138. Systematic discovery of regulatory motifs in human promoters and 3’ UTRs by comparison of several mammals. Nature 2005; 434:338-45.
- Workman H.C., Vernau W. (2003) Chronic lymphocytic leukemia in dogs and cats: the veterinary perspective. Vet Clin North Am Small Anim Pract **33**:1379-1399.
- Yekta S., Shih I.H., Bartel D.P. (2004) MicroRNA-directed cleavage of HOXB8 mRNA. Science 304:594–596.

- Zanette D.L., Rivadavia F., Molfetta G.A., Barbuzano F.G., Proto-Siqueira R., Silva- W.A. Jr, Falcao R.P., Zago M.A. (2007) miRNA expression profiles in chronic lymphocytic and acute lymphocytic leukemia. Braz J Med Biol Res 40:1435–40.
- Zhang B., Pan X., Cobb G.P., Anderson T.A. (2007) MicroRNAs as oncogenes and tumor suppressors. Dev Biol 302:1–12.
- Zhang H., Luo X.Q., Zhang P., Huang L.B., Zheng Y.S., Wu J., Zhou H., Qu L.H., Xu L., Chen Y.Q. (2009) MicroRNA patterns associated with clinical prognostic parameters and CNS relapse prediction in pediatric acute leukemia. PLoS One. 4(11):e7826.
- Zhou B., Wang S., Mayr C., Bartel D.P., Lodish H.F. (2007) miR-150, a microRNA expressed in mature B and T cells, blocks early B cell development when expressed prematurely. Proc Natl Acad Sci USA. 104(17): 7080-5.
- Zhou D., Li S., Wen J., Gong X., Xu L., Luo Y. (2008) Genome-wide computational analyses of microRNAs and their targets from Canis familiaris. Comput Biol Chem. 32(1):60-5.

ACKNOWLEDGEMENTS

I first thank my supervisor, Dr. Michele Mortarino, for the support and the leading figure, with great wisdom and professionalism, during this experience. Despite various commitments has always found time to listen me and solve problems. I also thank all my colleagues, with whom I shared this experience, without them it would not be the same.

I thank my family and all my friends, for the support and the help that always you gave me, you are very important to me.

Finally, I thank Giuliano for everything, you're special.